Fungal susceptibility of bio-based building materials

Liselotte De Ligne

GHENT UNIVERSITY

FACULTY OF BIOSCIENCE ENGINEERING

Promoters

Prof. dr. ir. Joris Van Acker
Department of Environment
UGent-Woodlab, Ghent University

Prof. dr. ir. Jan Van den Bulcke
Department of Environment
UGent-Woodlab, Ghent University

Prof. dr. Bernard De Baets
Department of Data Analysis and Mathematical Modelling
KERMIT, Ghent University

Prof. dr. ir. Jan M. Baetens
Department of Data Analysis and Mathematical Modelling
KERMIT, Ghent University

Examination committee

Chairman

Prof. dr. ir. Kathy Steppe
Department of Plants and Crops
Laboratory of Plant Ecology, Ghent University

Secretary

Prof. dr. ir. Monica Höfte
Department of Plants and Crops
Laboratory of Phytopathology, Ghent University

Prof. dr. Veerle Cnudde
Department of Geology, Ghent University

Dr. Magdalena Kutnik
FCBA Biology Lab, Bordeaux, France

Prof. dr. ir. arch. Marijke Steeman
Department of Architecture and Urban Planning, Ghent University

Prof. dr. Lisbeth Garbrecht Thygesen
Department of Geosciences and Natural Resource Management, University of Copenhagen, Denmark

Dean

Prof. dr. ir. Marc Van Meirvenne

Rector

Prof. dr. ir. Rik Van de Walle

Fungal susceptibility of bio-based building materials

ir. Liselotte De Ligne

Thesis submitted in fulfilment of the requirements for the degree of Doctor of Bioscience Engineering: Natural Resources

Dutch translation of the title
Schimmelgevoeligheid van hernieuwbare bouwmaterialen

Cover
Metropol Parasol, Sevilla, Spain
Also known as Las Setas de la Encarnación (Incarnation's mushrooms)
The six large timber parasols shade the Plaza de la Encarnación and protect its archaeological site. The mushroom-shaped timber lattice is made from laminated veneer lumber, connected with steel bars.
Architect: J. MAYER H. and Partner, Architekten mbB

The present research was possible thanks to a PhD Fellowship of the Research Foundation – Flanders FWO (FWO SB grant 1S53417N).

ISBN
978-94-6357-396-2

Citation
De Ligne, L. (2021) Fungal susceptibility of bio-based building materials. PhD Thesis, Ghent University, Belgium

Acknowledgements

"Science is by no means a solitary business. Scientists build on the knowledge gathered by their predecessors. They collaborate with their colleagues, call each other's hypotheses into question, have discussions and keep each other on their toes." GUM – Ghent University Museum

Teamwork is a fundamental part of scientific research. I would therefore like to thank all the people who contributed to this research, either directly, through collaboration and guidance, or indirectly, by giving me the energy and confidence I need to pursue my passions and research interests.

First of all, I would like to acknowledge my PhD supervisors, Joris, Jan, Jan and Bernard for their excellent guidance and support. I very much enjoyed the energetic brainstorms and am very grateful for all the advice - scientific and career-wise - you shared. I really loved that you encouraged me to attend (many) international workshops and conferences, introduced me to interesting research collaborations and that you involved me with the organisation of the IRG conference, the NSABS symposium and the Biowiskundedagen. Thank you for all the time and effort you put in improving the PhD manuscript and journal articles and, of course, for helping me to obtain the FWO-SB scholarship, where it all began. My gratitude also goes to my jury members, who's complementary input and feedback greatly improved the manuscript. I have looked up to you for many years and am very honoured that you agreed to be part of this work.

Going back to where it began, thank you so much Guillermo, for hiring me as a research assistant on your PhD project and getting the ball rolling. You made me fall in love with research and the PhD life. I very much enjoyed working with you and absolutely loved that you took me along on all the activities and parties (many of which you organized). I have been very fortunate these last four years to be well surrounded by great colleagues, from both the dept. of Environment and dept. of Data Analysis and Mathematical Modelling, as well as from the UGCT-group. My thanks go to Imke, Nele, Piet, Stijn and Toon, for immerging me in the world of wood science, training me, helping me out with experiments, welcoming me to UGent-Woodlab and for all the great talks. To my fellow PhD students at UGent-Woodlab, Michiel V., Victor D., Pierre, Chadrack, Xiuping, Hanna, Marlies, Emmanuel, Bhély, Jasper and Victor M., thanks for the great times (picknicks outside, birthday drinks, yoga sessions, games,…) and for being there for me. I would also like to thank Julie, Romain and Tom, as well as Aisling and Michiel S., for making me dream about an (international) post-doc career and giving excellent advice on how to go about it (and of course, for their amazing company). The same goes for my colleagues at the Dept. of Mathematical modelling, many of you who became good friends, through all the Friday night drinks at Walrus, beer clubs, dinners and game nights. Though some of you have graduated and moved on to exiting new careers over the past years, I am really happy that we still hear each

other every once in a while. Know that you will always have a place to stay in whichever city I live in! I also really enjoyed the nice atmosphere, lunch breaks and BBQs at UGCT and would especially like to thank Amélie, Ivan, Sander and Matthieu for all their help with the X-ray CT scanning and image processing.

I am also very grateful to my master thesis students for their energy and dedication and their contributions to this work. Many thanks as well to Judith, Johanna and Tamara for making the summer periods so lively and interesting. I remember your internships with great fondness and hope our paths cross again sometime in the future.

To the friends I met in Ghent, most of you whom I have known a (really) long time, others who I met in later years, thanks for turning regular evenings into unforgettable moments. When I am with you, life just makes sense. The same goes for my parents, Annick and Paul, and my sisters, Marjolein and Hannelore, who are always there for a good talk and a delicious dinner. Thanks for coaching and supporting me, and helping me out with the final touches on the PhD thesis. And of course, to Jens, for being my biggest supporter of all.

English summary

Bio-based building materials are made from renewable resources and produced with considerably less energy and associated carbon emissions than many traditional building materials. This makes them essential building elements in the much needed transition towards a more sustainable building industry. Many bio-based building materials are (to some extent) biodegradable, an excellent quality at the end of a material's service life as it solves waste issues, but a less desirable feature during use. When an organic material is exposed to favourable moisture and temperature conditions as well as to degrading organisms, its functional and aesthetic service life can decrease. The risk of fungal decay depends on the environmental conditions and the material resistance. It should be noted however that, depending on the application of the material, risk of decay does not equal the consequences of potential failure, which are for example much higher in load-bearing applications then in non-structural uses, such as cladding.

A material's resistance to fungal decay depends on the material's natural durability and its hygroscopicity. Wood protection used to focus mainly on naturally durable wood species, often from tropical regions, or applying non-durable wood species that are treated with fungicidal wood preservatives. General awareness of the negative impact of biocidal products on the environment initiated a new way of thinking about wood protection. Other material characteristics that could extend service life, such as a material's moisture dynamics and structure, have been gaining importance. These are especially interesting when it comes to bio-based building materials, as there are many opportunities to alter material structure and moisture dynamics of engineered wood products and bio-based insulation materials. Unfortunately, in-depth knowledge on the intricate relationship between material characteristics and fungal behaviour is still lacking.

The risk of fungal decay depends on the environment in which a material is applied and the material resistance. A key aspect is how specific environmental conditions affect mycelial growth itself. Therefore, a semi-automated image analysis method developed by Vidal-Diez de Ulzurrun *et al.* (2015) was adopted in Chapter 2 to assess the impact of temperature and relative humidity (RH) on mycelial growth dynamics of *C. puteana* and *R. solani*. The method effectively provided an objective and in-depth analysis of the effect of environmental conditions on various fungal growth characteristics (including the mycelial area, number of tips and branching angle), in a rather short period of time (62 h) and by making use of low-cost imaging devices.

To determine how different material characteristics affect the decay risk of bio-based building materials, several methods were developed and applied to assess the influence of material chemistry, moisture dynamics and structure on fungal susceptibility.

In Chapter 3, a test method was developed to assess the influence of material chemistry on fungal susceptibility, which proved to be useful to assess the impact of fungicidal compounds in 10 wood species and a selection of 18 bio-based building materials, including wood-based panels and insulation materials based on woof fibre, cellulose fibre, flax, cotton or cork. While several of the tested wood species clearly contained fungicidal components, none of the tested bio-based building materials proved to be fungicidal against brown-rot fungus *C. puteana*, with the exception of cellulose fibre insulation which contained boric acid. However, we found that fungicidal components are not always of major importance for the durability of a material. Wood species such as *Aucoumea klaineana* and *Entandrophragma cylindricum* mainly seem to rely on moisture-regulating components while the specific wood anatomical structure of *Pterocarpus soyauxii* likely increased its durability. It is important to recognise that material moisture dynamics and structure can have a (major) influence on durability, especially as there are many opportunities to optimize the structural design and to alter the material's moisture dynamics of bio-based building materials.

In chapter 4, a test method was proposed to assess the influence of RH on fungal decay in function of time, in the presence of a moisture source. Previous methods described in literature, either assessed the influence of RH on decay, without a moisture source, or assessed the level of decay in function of a moisture gradient at a RH of 100%. The brown-rot fungus *C. puteana* experienced difficulties to overgrow and moisten wood specimens at low RH conditions (11-22% RH). An RH of 43% and higher seemed no longer to inhibit fungal growth thus enabling the fungus to moisten and decay non-durable wood specimens. As the RH is often higher than 43% outdoors and in certain indoor spaces (such as bathrooms and swimming pools), water accumulation should be prevented as much as possible, which has been reported before.

The material moisture dynamics of a selection of wood-based panels and wood-fibre insulation materials were assessed as well. The samples were exposed to liquid water in a so-called floating test, and water absorption and desorption were measured over time to compare the materials' moisture dynamics. Three state-of-the-art techniques were used to better understand the differences in moisture dynamics: Low-Field Nuclear Magnetic Resonance (LNFMR) spectroscopy, X-ray CT and Attenuated Total Reflectance Fourier Transform Infrared (ATR-FTIR) spectroscopy. We found that hydrophobic additives, wood modification and production process have a major impact on the material moisture dynamics of bio-based building materials. The samples of thermally modified wood, wood fibre board with bitumen and one of the wood fibre insulation boards (type 2) had excellent moisture dynamics and would be expected to have an extended service life in outdoor exposure conditions.

In chapter 5, a method was developed to assess the influence of material structure on the degradation process in function of time non-destructively, hence X-ray CT

scanning was used. In that way, we were able to temporally monitor decay of individual wood specimens, which each have a unique anatomy. For non-durable wood species, such as beech and spruce, the fungus could easily access the samples in the longitudinal direction (=vessels/tracheid direction) and decay occurred homogenously along the wood specimens. For Scots pine, decay progressed more slowly.

As material moisture dynamics and structure have a (major) influence on durability and decay risk, there is a need for better defined use classes. Although the current use classes differentiate between different moisture risks, the impact of climate, building design and material properties on the time of wetness should be incorporated to better estimate fungal decay risk in practice.

With better defined use classes comes the need for bio-based products that are tailored to these diversified end uses and moisture conditions. As bio-based materials are tailorable, producers should embrace a fit-for-purpose strategy when developing and marketing bio-based building products. Research on improving moisture dynamics should be continued, both fundamental research on understanding moisture dynamics as well as more applied research on optimizing production processes and additives. Also, the influence of material structure on decay and moisture dynamics should be investigated further, as there are many opportunities to alter material structure in engineered wood products and bio-based insulation materials.

Nederlandstalige samenvatting

Hernieuwbare bouwmaterialen zijn vooral gebaseerd op grondstoffen met een biologische oorsprong, zoals hout, vlas en katoen. De CO2 uitstoot bij het produceren ervan ligt aanzienlijk lager dan voor klassieke bouwmaterialen, zoals staal en beton. Dit maakt ze essentieel voor de hoognodige transitie naar een duurzamere bouwindustrie. Hernieuwbare bouwmaterialen zijn vaak ook biologisch afbreekbaar, een uitstekende eigenschap, aangezien dit de hoeveelheid bouwafval kan beperken. Wanneer tijdens de gebruiksfase van hernieuwbare bouwmaterialen optimale condities optreden voor schimmelgroei, kan dit echter een negatieve invloed hebben op de levensduur, zowel naar esthetische waarde als naar structurele integriteit. Twee cruciale factoren voor degradatie van bouwmaterialen zijn de gebruiksomstandigheden – vochtgehalte en temperatuur - en de natuurlijke duurzaamheid van het bouwmateriaal. De gevolgen van een mogelijk falen van de structurele integriteit van een bouwmateriaal zijn veel groter voor structurele toepassingen, zoals gewichtdragende bouwelementen, dan voor niet-structurele toepassingen, zoals gevelbekleding.

De schimmelgevoeligheid van een materiaal hangt af van de natuurlijke duurzaamheid en van de hygroscopiciteit (mate waarin een materiaal water absorbeert). Vroeger was houtbescherming voornamelijk gericht op het toepassen van houtsoorten met een hoge natuurlijke duurzaamheid, meestal afkomstig uit tropische gebieden, of op het toepassen van niet-duurzame houtsoorten die met schimmelwerende houtverduurzamingsmiddelen werden behandeld. De negatieve impact van biociden op het milieu bracht echter een nieuwe opvatting rond houtbescherming teweeg. Andere materiaaleigenschappen die de levensduur kunnen verlengen, zoals de vochtdynamiek en de structuur van een materiaal, winnen aan belang. Onderzoek naar de invloed van zulke materiaaleigenschappen op de duurzaamheid is vooral interessant als het gaat om hernieuwbare bouwmaterialen, aangezien er veel mogelijkheden zijn om de materiaalstructuur en de vochtdynamiek van verwerkte houtproducten en hernieuwbare isolatiematerialen te optimaliseren. Er is echter onvoldoende kennis over hoe materiaaleigenschappen schimmelaantasting beïnvloeden.

Het risico op schimmelaantasting is afhankelijk van de omgeving waarin een materiaal wordt toegepast en van de weerstand van het materiaal. Een belangrijk aspect is hoe specifieke omgevingscondities mycelium ontwikkeling beïnvloeden. In hoofdstuk 2 werd daarom een semi-geautomatiseerde beeldanalysemethode toegepast om de impact van temperatuur en relatieve vochtigheid (RV) op de groeidynamiek van *C. puteana* en *R. solani* te beoordelen. Deze methode werd gebaseerd op de methode van Vidal-Diez de Ulzurrun *et al.* (2015) en leverde een objectieve en diepgaande analyse op van het effect van omgevingscondities op verschillende schimmelgroeikarakteristieken (waaronder de oppervlakte van het mycelium, het

aantal groeitippen en de vertakkingshoek), in een vrij korte periode (62 uur) en met gebruik van goedkope beeldvormingsapparatuur.

Om de invloed van de chemische samenstelling, vochtdynamiek en structuur van een materiaal op schimmelgevoeligheid te beoordelen, werden verschillende methodes ontwikkeld en toegepast.

In hoofdstuk 3 werd een testmethode ontwikkeld om de invloed van de chemische samenstelling op de schimmelgevoeligheid van een materiaal te beoordelen. De testmethode werd succesvol toegepast op 10 houtsoorten en een selectie van 18 hernieuwbare bouwmaterialen, waaronder houtgebaseerde panelen en isolatiematerialen op basis van houtvezel, cellulosevezel, vlas, katoen of kurk. Hoewel verschillende van de geteste houtsoorten duidelijk schimmelwerende stoffen bevatten, bleek geen van de geteste hernieuwbare bouwmaterialen schimmelwerend te zijn tegen de bruinrotschimmel *C. puteana*, met uitzondering van cellulose isolatie. Schimmelwerende componenten zijn echter niet altijd van groot belang voor een hoge duurzaamheid. Houtsoorten zoals *Aucoumea klaineana* en *Entandrophragma cylindricum* lijken hun duurzaamheid vooral te danken aan vochtregulerende componenten, en de houtanatomie van *Pterocarpus soyauxii* draagt vermoedelijk ook bij aan haar duurzaamheid. Het is dus belangrijk om te erkennen dat de vochtdynamiek en structuur van een materiaal een (grote) invloed kunnen hebben op de duurzaamheid, vooral omdat er veel mogelijkheden zijn om de structuur en vochtdynamiek van hernieuwbare materialen te optimaliseren.

In hoofdstuk 4 werd een testmethode voorgesteld om de invloed van relatieve vochtigheid (RV) op schimmelaantasting te bepalen in functie van de tijd en in aanwezigheid van een vochtbron. Eerdere methoden die in de literatuur beschreven staan, bepalen ofwel de invloed van RV op schimmelaantasting in afwezigheid van een vochtbron, ofwel bepalen ze het niveau van schimmelaantasting in functie van een vochtgradiënt bij 100% RV. Bij lage RV (11-22% RV) had bruinrotschimmel *C. puteana* moeite om de houtstalen te overwoekeren. Een RV van 43% en hoger leek hyfe groei niet te belemmeren en de schimmel was in staat om de blokjes te bevochtigen en te degraderen. Aangezien de RV buiten en in bepaalde ruimtes binnenin een gebouw vaak hoger is dan 43% (zoals in badkamers en zwembaden), is het belangrijk dat wateraccumulatie zoveel mogelijk voorkomen wordt.

De hygroscopiciteit van een materiaal beïnvloedt het risico op schimmelaantasting. Daarom werd eveneens de vochtdynamiek van een aantal houtgebaseerde platen en isolatiematerialen onderzocht. In de zogenaamde drijftest werden de stalen in contact gebracht met vloeibaar water. Waterabsorptie en -desorptie werd bepaald van elk materiaal om de vochtdynamieken te vergelijken. Daarnaast werden drie geavanceerde technieken gebruikt om de waargenomen verschillen in vochtdynamiek te onderzoeken: 'Low-Field Nuclear Magnetic Resonance' (LNFMR) spectroscopie, X-

stralen CT en ‘Attenuated Total Reflectance Fourier Transform Infrared’ (ATR-FTIR) spectroscopie. Hieruit bleek dat hydrofobe toeslagstoffen, houtmodificatie en het productieproces een grote invloed hebben op de vochtdynamiek van hernieuwbare bouwmaterialen. Thermisch gemodificeerd hout, houtisolatie met bitumen en houtvezelisolatie type 2 hadden een uitstekende vochtdynamiek en zouden vermoedelijk een langere levensduur hebben in buitencondities.

In hoofdstuk 5 werd een methode ontwikkeld om de invloed van de structuur van een materiaal op het degradatieproces in functie van de tijd niet-destructief te beoordelen. Daarvoor werd gebruik gemaakt van X-stralen CT-scans. Zo konden we het degradatieproces van individuele houtstalen, die elk een unieke anatomie hebben, volgen over de tijd. Bij niet-duurzame houtsoorten, zoals beukenhout en hout van de fijnspar, kon de schimmel gemakkelijk aantasten in de lengterichting (=vaten/tracheide-richting) en degradatie gebeurde homogeen over de lengte van de stalen. Bij stalen van grove den verliep de degradatie langzamer. Het midden van de blokjes werd pas later aangetast dan de zijden en de degradatie gebeurde dus niet homogeen.

Aangezien de vochtdynamiek en de structuur van een materiaal een (grote) invloed hebben op het risico voor schimmelaantasting, is er behoefte aan beter gedefinieerde gebruiksklassen. Hoewel de huidige gebruiksklassen onderscheid maken tussen verschillende vochtrisico's, moet het effect van klimaat, bouwkundig ontwerp en de materiaaleigenschappen op de mate en duur dat een materiaal nat is en blijft worden meegenomen zodat het risico op schimmelaantasting in de praktijk beter kan ingeschat worden.

Met beter gedefinieerde gebruiksklassen komt ook de behoefte aan hernieuwbare producten die zijn afgestemd op deze gediversifieerde eindtoepassingen en vochtomstandigheden naar voor. Producenten zouden bij de ontwikkeling en marketing van hernieuwbare bouwproducten een "fit-for-purpose"-strategie moeten hanteren. Onderzoek naar de optimalisering van vochtdynamiek voor verschillende materialen moet worden voortgezet, zowel fundamenteel onderzoek naar het begrijpen van de vochtdynamiek als meer toegepast onderzoek naar de optimalisering van productieprocessen en toeslagstoffen. Ook de invloed van materiaalstructuur op schimmelaantasting en vochtdynamiek moet verder worden onderzocht, aangezien er veel mogelijkheden zijn om de materiaalstructuur in houtproducten en hernieuwbare isolatiematerialen te optimaliseren.

Table of contents

List of Abbreviations

AIWF	Air-Injected Wood Fibre insulation
ATR-FTIR	Attenuated Total Reflectance Fourier Transform Infrared
BREEAM	Building Research Establishment Environmental Assessment Method
CCA	Chromated Copper Arsenate
CLT	Cross-Laminated Timber
CPMG	Carr-Purcell-Meiboom-Gill
DGNB	Deutsche Gesellschaft für Nachhaltiges Bauen
DIY	Do It Yourself
DTW	Dynamic Time Warping
ECB	Expanded Cork Board
EMC	Equilibrium Moisture Content
GCT	Granger Causality Test
HQE	Haute Qualité Environnementale
IPBC	Iodopropynyl Butyl Carbamate
LCA	Life Cycle Analysis
LEED	Leadership in Energy and Environmental Design
LNFMR	Low-Field Nuclear Magnetic Resonance
LVL	Laminated Veneer Lumber
MC	Moisture content
ML	Mass Loss
MWT	Mann Whitney Test
NECG	Non-Expanded Cork Granules
OSB	Oriented Strand Board
PCP	Pentachlorophenol
PLY	Radiata Pine Plywood
RH	Relative Humidity
RM	Residual Moisture content
TMT	Thermally Modified spruce
TOTEM	Tool to Optimise the Total Environmental impact of Materials
ToW	Time of Wetness
UC	Use Class
WFIB	Wood Fibre Insulation Board

Chapter 1

Introduction

1.1 The conventional building industry and its impact on society

1.2 Bio-based building materials as alternative resources

1.3 Common bio-based building materials and their applications

Mjøstårnet
Brumunddal, Norway
The World's tallest load-bearing wooden building
Architects: Voll Arkitekter

1.1 The conventional building industry and its impact on society

Human activity is putting increasing pressure on the Earth's life support systems. Without drastic measures regarding global emissions in the coming decades, continued global warming will increase the likelihood of severe, pervasive and irreversible consequences such as the collapse of natural ecosystems, the erosion of global food security and displacement of people at unprecedented scales (EEA, 2019). Worldwide, policies are implemented to mitigate climate change and all sectors are being challenged to work towards a more sustainable future.

The construction sector has a major impact on our society. It provides the buildings and infrastructure that surround us, accounts for 29% of industrial employment and makes up 9% of the EU-28 GDP (FIEC, 2019). The housing sector faces huge challenges when it comes to mitigating climate change, as it is responsible for 30-40% of the worldwide energy consumption, in the form of heating, cooling and light (Santamouris 2016). Significant progress has been made regarding the energy performance of buildings. In the EU, all new houses are required to become 'zero energy' by 2021 and thus produce as much energy as they use (EEA, 2019). The energy performance of existing buildings remains a challenge, as retrofitting requires a substantial investment from homeowners.

Besides energy, the construction sector also consumes large quantities of water and raw materials and is responsible for 50% of landfill waste (Melchert, 2007; Santamouris, 2016). Between 1.200 and 1.800 million tons of construction materials per year were consumed by the EU-28 for new buildings and refurbishment from 2003-2011. Furthermore, around 65% of all aggregates (sand, gravel and crushed rock) and approximately 20% of all metals in Europe are used in the construction sector (Herczeg *et al.*, 2014). However, the Earth's raw material resources are finite (minerals, fossil fuel) or limited (biomass) and getting increasingly depleted (Speirs *et al.*, 2015). If we want

to ensure a 'good life for all' within our planetary boundaries[1], material extraction should remain beneath a maximal sustainable level (O'Neill *et al.*, 2018). During extraction, transport, manufacturing, assembly and installation of building materials, as well as during their disassembly, deconstruction and decomposition, energy is consumed as well. This consumption of energy is referred to as the 'embodied energy' of a building material (Dixit *et al.*, 2010). In parallel to the progress being made in the EU with regard to energy performance of buildings, there is need for a holistic approach to tackle the challenges of resource efficiency and embodied energy of building materials (EEA, 2019). The policies that are already in place, directly or indirectly related to resource efficiency, mostly concern waste management, standards on material performance and standards and taxes on aggregates and raw materials on country level (Herczeg *et al.,* 2014). Assessing the sustainability and environmental impact of building materials and buildings has become more common, but is usually not a requirement (Giama and Papadopoulos, 2012). The most commonly used certification schemes are Building Research Establishment Environmental Assessment Method (BREEAM), Haute Qualité Environnementale (HQE), Deutsche Gesellschaft für Nachhaltiges Bauen (DGNB) and Leadership in Energy and Environmental Design (LEED). While these certification schemes contain a wide array of criteria (such as water efficiency, mobility, health and wellbeing), they also include the concept of Life Cycle Analysis (LCA), in which the environmental impact of building materials is assessed over the entire life cycle (Giama and Papadopoulos, 2012; Herczeg *et al.,* 2014). The life cycle of a building product usually includes the extraction and processing of raw materials, manufacturing, transport, use, recycling and waste management of the material (Ortiz *et al.*, 2009). In order for a sustainability assessment of buildings and building materials to become a more integral part of the building industry, it is

[1] Rockstrom *et al*. (2009) defined nine planetary boundaries associated with the Earth's biophysical processes, which should not be exceeded if the Earth is to remain in the stable environmental state of the Holocene.

essential to achieve greater compatibility and transparency between different certification schemes, while leaving room for improvement (Giama and Papadopoulos, 2012). In the Netherlands, the environmental impact of material choices is part of the environmental permits necessary for building (RVO, 2020). In Belgium, this is not yet the case. However, a 'Tool to Optimise the Total Environmental impact of Materials' (TOTEM) has been designed to raise awareness on the environmental impact of building components and to stimulate project designers to take these factors into account when carrying out building projects (TOTEM, 2020).

The environmental impact of buildings and building elements could be greatly reduced by transitioning towards a (more) circular building industry, which focuses on maintenance, reuse and recycling of materials (Bilal *et al.*, 2020). Transformable building, an innovative design and construction strategy which encourages building adaptability and efficient resource management of building components, is essential in the circular building context. Transformable building designs facilitate renovation and reuse of building components, for instance by applying reversible connections to building elements, such as bolts and screws, instead of mortar and glue (Galle, 2016).

1.2 Bio-based building materials as alternative resources

A *bio-based building material* is a building material or product derived from renewable resources from a biological origin, with the requirement that the renewable resource recovers faster than it is drained (Jones and Brischke, 2017). Common bio-based building materials are wood, wood-engineered products and insulation materials from flax, hemp, cotton, etc. Since bio-based building materials are made from renewable resources, they are key in the sustainable building context described above and provide a valid alternative for resource depletion.

Another major advantage is that bio-based building materials are produced with considerably less energy and associated carbon emissions than aluminium, steel and concrete (Sathre and O'Connor, 2008). For instance, for 1 ton of material, the mean carbon emission related to the production of cement and steel is, respectively, 30% and 450% higher than that of timber materials (Churkina *et al.,* 2020). These higher carbon emissions are not only related to the amount of fossil fuel used, but also to the emissions emanated during chemical reactions that are part of the manufacturing process (Davis *et al.,* 2018). For instance, about 60% of the emissions of cement production stem from calcination, i.e. the conversion of $CaCO_3$ in CaO and CO_2 (Andrew, 2018). For the manufacturing of steel, carbon is used to reduce iron oxide, resulting in 1.6-3.1 tons of production process related CO_2 per ton crude steel (Davis *et al.,* 2018). Do note that when it comes to other environmental indicators, such as transport and land use, bio-based building materials do not perform necessarily better than traditional ones (Peñaloza, 2017).

Plant-based bio-based materials are carbon sinks, as CO_2 is stored as biomass during photosynthesis (Sathre and O'Connor, 2008). In a recent study in *Nature Sustainability*, Churkina *et al.* (2020) advocate for a transition towards mass timber usage in the building industry to reduce atmospheric CO_2 concentrations (Figure 1-1). Depending on the percentage of new buildings designed with timber, 0.25-2.3 Gt (10% timber), 1-11 Gt (50% timber) or 2-20 Gt (90% timber) of carbon could be stored in new buildings over the next thirty years, while simultaneously reducing carbon emissions from construction materials by replacing mineral-based by bio-based building materials. Sustainable forest management and continuous re-forestation, as well as re-direction of wood from use as fuel to long-lived products, would be essential (Sathre and O'Connor, 2008; Churkina *et al.,* 2020). Brunet-Navarro *et al.* (2017) also showed that elongating the life span and increasing recycling of wood products are key to the carbon storage context.

A weakness of new bio-based building materials is that the production costs are often high. The scale of production for new products and processes is generally lower than for established products, affecting the price per unit of a product. This makes it more difficult to compete with established products. Additionally, new bio-based products often differ significantly from the original raw materials for which standard assessment methods and certification were designed, requiring considerable adaptations of the standard assessment methods or even new ones (Jones and Brischke, 2017).

This is, for instance, the case for assessing durability of new bio-based building materials against Basidiomycetes in comparison with solid wood (section 1.5.4). A lack in common standards and regulations also hinders large-scale deployment of wood and engineered wood products in high-rise buildings (Hetemäki *et al.*, 2017). Table 1-1 gives an overview of the main strengths and weaknesses associated with bio-based building materials in general, as well as the main opportunities and threats for their increased use.

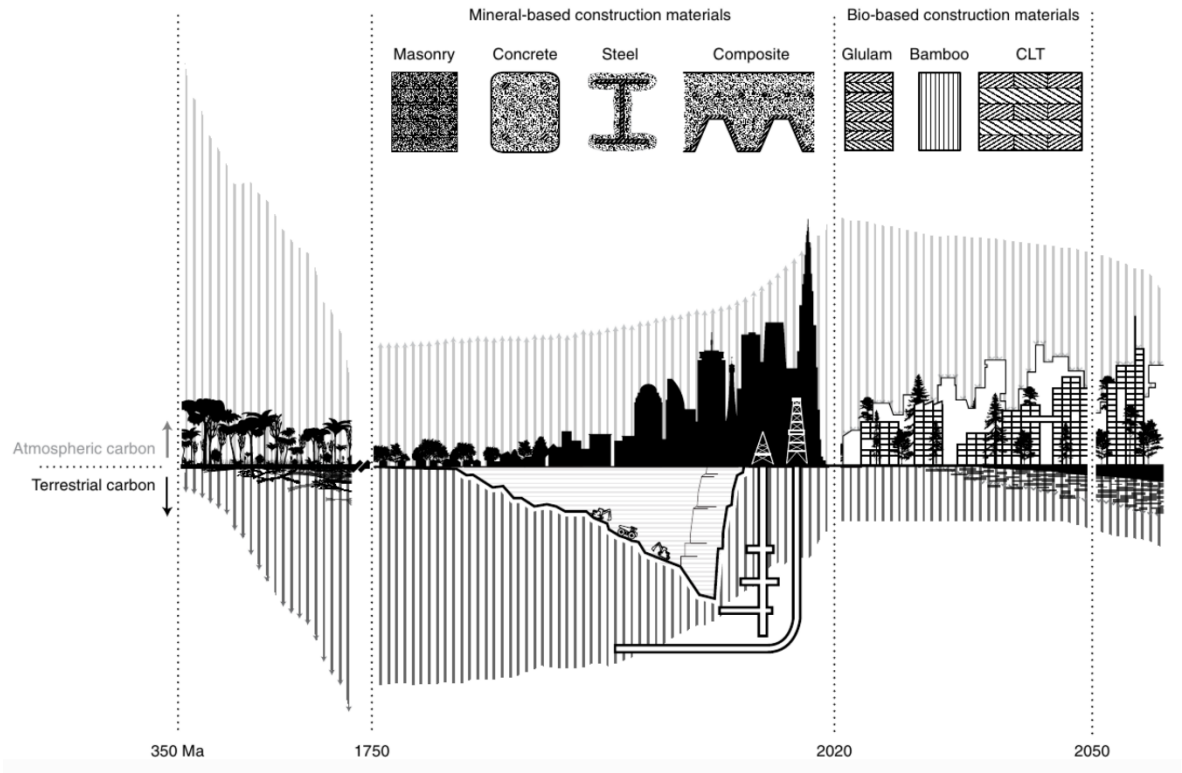

Figure 1-1 Processes responsible for formation, depletion and potential replenishment of land carbon pool, as well as changes in atmospheric CO_2 concentrations over time. Left panel: over millions of years the carbon pool on land was formed and CO_2 concentrations in the atmosphere slowly declined because of various processes including organic carbon burial, rock weathering and so on. Middle panel: urban and industrial growth prompted by the industrial revolution have gradually depleted land-based carbon pools and increased atmospheric CO_2 concentrations. High-reaching and heavy-load-bearing urban buildings constructed from concrete and steel, produced with raw materials and fuels extracted from ever deeper layers of the Earth's crust, were intensive in both energy consumption and greenhouse gas emissions. Right panel: cities built from bio-based materials such as engineered timber and bamboo can serve as constructed carbon sinks. Storing and maintaining carbon in these densely constructed carbon pools will help replenish the terrestrial carbon storage, thereby reducing current atmospheric CO_2 levels and offsetting future emissions. Ma, million years ago. Cited from Churkina *et al.* (2020).

Table 1-1 SWOT analysis of bio-based materials in construction. Adapted from Jones and Brischke (2017).

Strengths	Weaknesses
• Ease of supply • Renewable • Recognised carbon storage option	• Production costs • Intrinsic biological properties impacting performance • Perceived as low technology
Opportunities	**Threats**
• Easily modified to improve performance • Compatible with other building materials • Increasing popularity with architects and designers	• Resource competition (fuel, furniture, …) • Land use competitions (for food and infrastructure) • Aggressive marketing from established building product industries • Lack of common standards and regulations

1.3 Common bio-based building materials and their applications

1.3.1 Solid wood and engineered wood products

Wood in the tree trunk is typically divided in two zones, each of which has its distinct function. The *sapwood* is the metabolically active part of the stem, which is responsible for sap conduction and for the storage and synthesis of bio-chemicals. The *heartwood* is located at the interior of the stem and its cells are no longer active. For many tree species, the heartwood has a distinctly darker colour due to the presence of secondary metabolites (Figure 1-2) and the heartwood is often more durable than the sapwood (Hart, 1989; Hillis, 2012). Note that the term *heartwood* should not be confused with *hardwood,* which indicates wood originating from angiosperms (flowering plants), such as beech (*Fagus*) and oak (*Quercus*). Wood originating from gymnosperms (mostly conifers), such as pine (*Pinus*) and spruce (*Picea*), is referred to as s*oftwood*. Not all parts of the tree provide the same quality of wood. The lower part of the tree stem usually has the widest diameter and the least defects, making it most suitable for sawn timber and for production of veneer sheets. Logs from the upper parts of the stem, which are smaller in diameter and often have branches and more juvenile wood, are generally used for pulping, chipping or flaking (Mazela and Popescu, 2017).

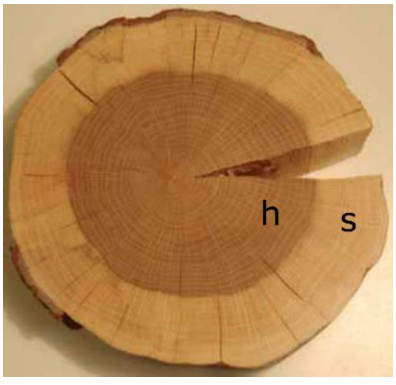

Figure 1-2 Indication of sapwood (s) and heartwood (h) in oak. Adapted from Sass-Klaassen *et al.* (2010).

Solid wood (sawn timber) is a well-established building material for houses across the world. It is used in a wide range of building applications, such as in light-frame construction (Figure 1-3a), roofs, floors, decking, façade cladding, foundations and bridges. Until the late 1980s, wood-framed buildings with more than two stories were prohibited by building regulations in most of the EU, due to the negative perceptions originating from historic city fires (Mazela and Popescu, 2017). After a revision of the Constructive Products Directive in 1988, coinciding with new technical solutions, solid wood has been used to create multi-story buildings with three stories or more, primarily in Nordic countries, the Alpine regions and the British Isles (Hurmekoski *et al.*, 2015). Nowadays, actual skyscrapers are being made from timber, usually with Glulam and Cross-Laminated Timber (CLT).

Glulam is produced by jointing and laminating smaller pieces of timber together, with the grain of all the layers running parallel to the length (Figure 1-3b). The resulting increase in length, depth and width enables large building elements for structural applications to be manufactured, with the possibility to demand specific dimensions (Ong, 2015; Figure 1-3c). CLT is composed of an uneven number of layers (in general three, five, seven or more) of side-by-side placed wooden boards (or beams), arranged crosswise to each other at an angle of 90° and connected by adhesive bonding (Brandner, 2013; Figure 1-3d). This technique greatly increases the strength and dimensional stability, and allows for the creation of building elements that are not limited by the length of the tree (Figure 1-3e). The tallest load-bearing timber building today is the 85,4 meters tall Mjøstårnet in Norway, made with Glulam and CLT (GWR, 2019).

Figure 1-3 a) Wall construction with poplar wood, b) Glulam, c) Glulam applied in an overhang, d) beam alignment in Cross-Laminated Timber (CLT) and e) CLT applied in a multi-storey building. Adapted from TRADA (2015).

Far better known, are the engineered wood products composed of strands, particles, fibres and veneers (Van Acker, 2020). Plywood (Figure 1-4a), for instance, is made from laminated wood veneers that are dried and coated with glue and are pressed together with veneers positioned crosswise to form a flat wood-based panel (Hughes, 2015). As a building material, plywood is applied in the lining and panelling of houses, roof elements, facades and flooring. Veneers can also be glued and pressed with the grain of all veneers orientated in the same direction, forming a beam-like product called laminated veneer lumber (LVL) that is mainly used in load-bearing structures (Figure 1-4b). Low-quality wood and wood residue from saw-mills can also be converted to strands, sprayed with adhesive and hot pressed into wood-based panels or beams, such as Oriented Strand Board (OSB) (Nishimura, 2015; Figure 1-4c). OSB is used as a structural wood-based panel for floors, walls and ceilings. It is also used in the production of I-joists, where it forms the web or support between two flanges of solid wood or LVL (Figure 1-4d). Due to its design, the I-joist is highly resistant against shearing and therefore often applied for covering long spans, for instance, in roof framing.

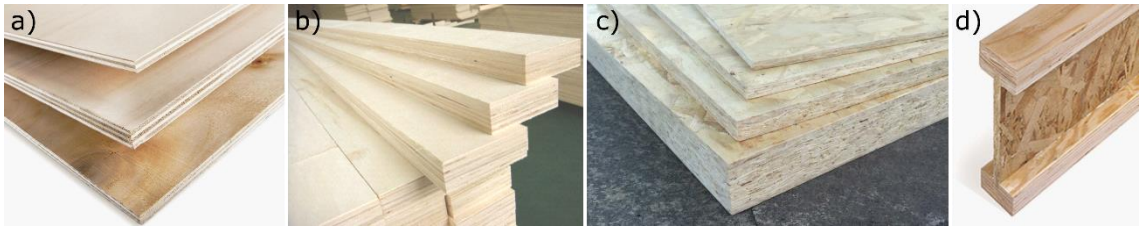

Figure 1-4 a) Plywood, b) laminated veneer lumber (LVL), c) OSB and d) I-beam. Adapted from APAWOOD (2020).

1.3.2 Insulation materials

Bio-based insulation materials include all loose wood fibre insulation, insulation mats and insulation boards made from natural fibres, as well as cork and cork board (Figure 1-5). While insulation materials based on cork, cellulose and wood fibres are perceived as conventional, insulation materials based on other fibre sources such as flax, hemp, kenaf and sheep wool are still perceived as alternative materials (Schiavoni *et al.*, 2016). The thermal performance is the feature of main importance for an insulation material, but fire performance, acoustic performance and interaction with water vapour are important characteristics as well.

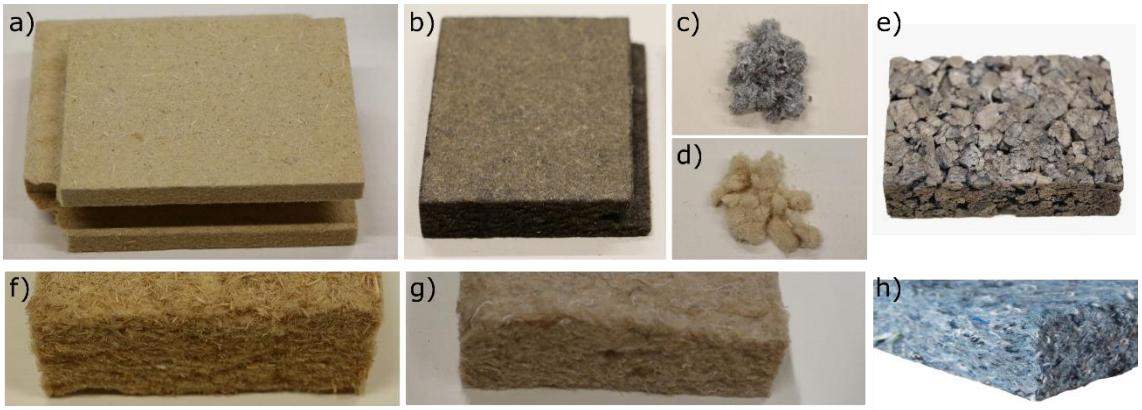

Figure 1-5 a) Wood fibre insulation board, b) wood-fibre insulation board with bitumen emulsion, c) cellulose fibre insulation, d) air-injected wood-fibre insulation, e) cork board, f) flexible wood fibre insulation mat, g) flax fibre insulation mat and h) cotton fibre insulation mat.

By varying material density and additives, a broad range of bio-based insulation materials can be obtained, with specific application purposes in mind. For instance, wood fibre insulation boards applied as roof insulation or next to the cavity wall often contain hydrophobic agents, such as paraffin and bitumen (Figure 1-5b), to decrease water absorption. This is useful in such applications with higher risk of wetting (Figure 1-6, applications 1 and 5). Thick, flexible wood fibre insulation mats, flax mats, air-injected wood fibre and cellulose fibre insulation are usually applied as cavity insulation between the exterior wall and the cavity wall and in roof elements (Figure 1-6, applications 2 and 3). Cotton mats are applied as cavity insulation as well, but not between the exterior wall and the cavity wall, as there is a higher moisture risk in that application. Floor insulation, such as cork or wood-fibre boards, are specifically designed for improvement of acoustics (Figure 1-6, application 7), while the main purpose of floor insulation at the ground floor is thermal performance. Thicker cork boards and cork granules are applied as insulation in walls and roofs as well.

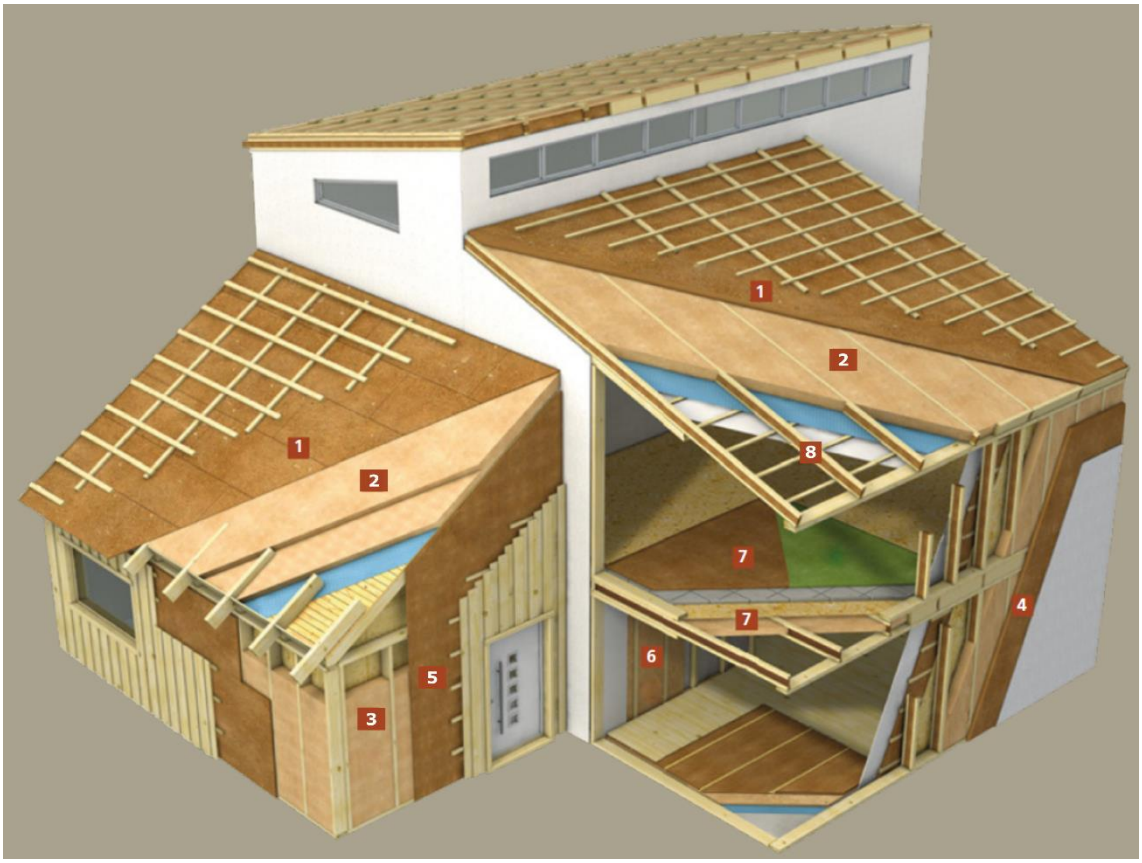

Figure 1-6 Applications of bio-based insulation materials: 1) wind barrier, 2) insulation between rafters, 3) cavity insulation, 4) external wall insulation system, 5) wall insulation panels applied between exterior wall and cavity wall or cladding, 6) insulation of lightweight partition walls and 7) floor insulation. Application of I-joists as rafters (8). Adapted from Dederich *et al.* (2019).

1.4 Performance of bio-based building materials

The *performance* of a material means the minimal capabilities necessary to satisfy the criteria of certain standards or user expectations. For bio-based building materials, the following properties are of interest according to Jones and Brischke (2017): functional performance, durability, moisture dynamics, aesthetics, thermal properties and fire resistance.

Functional performance

Bio-based materials can be applied for structural or non-structural purposes. When used as a structural (i.e. load-bearing) element in a building, the probability of failure needs to be very low and well controlled, in order to guarantee human safety. Variability in strength and stiffness should be considered and control systems must be implemented in practice. The latter is usually more challenging for bio-based materials compared to more conventional structural materials such as steel and concrete, for which systems to safeguard structural performance are already well developed (Brischke *et al.*, 2017). The functional performance of structural bio-based building materials can, for instance, be jeopardized by climatic exposure or fire.

For non-structural applications, other properties besides strength are important. Depending on the application, functionality based on aesthetics, dimensional and shape stability, stiffness and hardness, slip resistance, thermal insulation, acoustics and well-being need to be considered as well (Jones and Brischke, 2017).

Durability

The *durability* of wood or bio-based materials, which is the resistance to destruction by material-destroying organisms, is one of the most important factors affecting functional performance of bio-based materials (Van Acker and Palanti, 2017). Wood-destroying organisms can be categorized into bacteria, fungi, wood-destroying insects (e.g. beetles and termites) and marine borers (Figure 1-7). Each of these organisms have certain requirements to grow and thrive, which limits the risk of them occurring. The risk of occurrence and infestation is mostly related to the exposure conditions and geographical position of the bio-based material (Brischke and Thelandersson, 2014). For instance, termites mainly occur in Southern-European countries, while marine borers are present in sea water with a certain salinity only. In temperate climates, fungi are the most important organisms that cause damage to wood (Morris, 1998). The risk of fungal infestation mainly depends on the exposure conditions and, more specifically, the presence of moisture, which is one of the main factors determining fungal damage and occurrence.

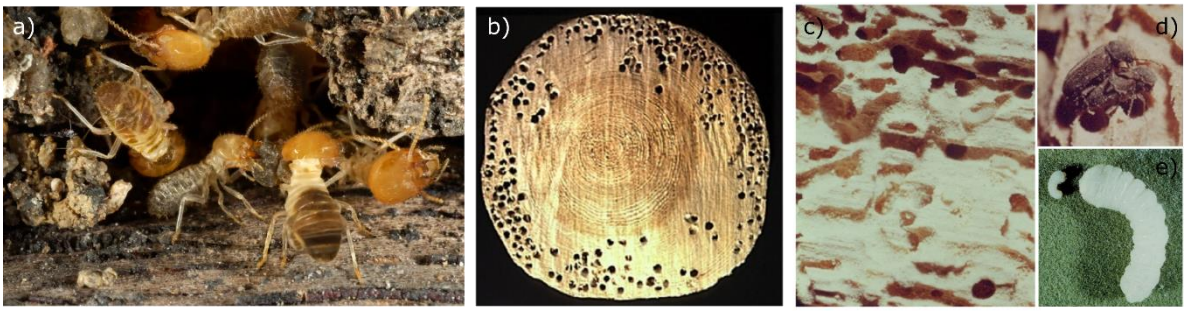

Figure 1-7 a) Termites © Getty / jeridu b) softwood pole attacked by shipworm *Teredo navalis* (Guerreiro *et al.,* 2016), and c) wood damage, d) adult beetles and e) larvae of *Anobium punctatum* (Van Acker and Palanti, 2017).

The European Committee of standardisation has derived five 'use classes' for applications of wood, with corresponding harmful organisms that can occur in those application types (CEN EN 335 standard, 2013; Table 1-2). Before applying a bio-based product, the durability of the product and the risk of occurrence of a certain pest need to be considered. Ideally, materials with a low durability are applied in applications with low risk, while materials with a high intrinsic durability or an enhanced durability are applied in applications with a high risk of infestation (fit-for-purpose). For instance, in indoor applications (use class 1), no or limited fungal protection is necessary due to the lack of moisture (Brischke, 2014).

Table 1-2 Use classes and the organisms that can occur in wood and wood products in the respective use class, according to CEN EN 335 standard (2013).

Use class	**General service conditions**	Wood-disfiguring fungi	Wood-destroying fungi	Beetles	Termites	Marine organisms
1	Interior, dry	–	–	U	L	–
2	Interior or under roof, not exposed to weather, possibility of condensation	U	U	U	L	–
3	Exterior, without soil contact, exposed to weather:					
	3.1 limited moist conditions	U	U	U	L	–
	3.2 persistently moist conditions	U	U	U	L	–
4	Exterior, in contact with soil or freshwater	U	U	U	L	–
5	Permanently or regularly immersed in salt water	U	U	U	L	U

U = spread all over EU, L = occurs locally in Europe

Moisture dynamics

Most bio-based materials are hygroscopic in nature and absorb water molecules from the surrounding atmosphere and from liquid moisture sources. Moisture affects the strength of structural bio-based materials. Although strength increases with lower moisture content, maximal strength properties occur around 4-10% MC, when wood is not completely dry (Ross, 2010). Moisture uptake and release also cause dimensional changes due to swelling and shrinking. Nevertheless, the hygroscopic nature of wood and other bio-based building materials is also a major advantage, as they can act as moisture-buffering materials (Li *et al.*, 2012; Rode *et al.*, 2006). In the hygroscopic moisture range, generally from 0 to about 95-98% relative humidity (RH), moisture from the interior climate is absorbed by the wood cell walls and bound to the wood cell wall polymers through hydrogen bounding (Fredriksson, 2019). This is an excellent characteristic, as a more constant air humidity reduces the energy needed for heating and cooling of an interior space and improves the air quality (Osanyintola and Simonson, 2006; Lozhechnikova *et al.*, 2015). However, when liquid water is present, for instance due to condensation or leakage or in outdoor exposure applications, hygroscopic materials take up water in cell lumen, pits and macro voids (such as the space between strands in oriented strand board) and the risk of fungal decay increases (CEN EN 335 standard, 2013; Brischke and Alfredsen, 2020). For many wood-based products and bio-based materials, the moisture dynamics are a key element in the product's performance. Moisture risk is included as a factor in the use classes (Table 1-2), but these do not consider the time of wetness, which is a key factor for fungal development and should not be neglected (Kutnik *et al.*, 2014). The importance of the latter has been acknowledged and a standardized method was developed to determine the wetting ability of wood and wood products (CEN TS 16818 standard, 2018). The laboratory method proposed in standard CEN TS 16818 standard was found to be a promising tool to estimate the outdoor moisture performance of solid wood (Brischke *et al.*, 2014). In 2018, De Windt *et al.* presented their extensive research on

the moisture dynamics of uncoated plywood, and found good correlations between laboratory tests and outdoor exposure tests. Furthermore, Kržišnik *et al.* (2020) showed there was a clear correlation between the laboratory test values and outdoor moisture performance of wood applied vertically and as decking. A similar approach should be taken to investigate the moisture dynamics of different types of bio-based building materials, besides plywood and solid wood. Furthermore, wood-water relations and the physiological needs of wood-decaying fungi are still not fully understood (Brischke and Alfredsen, 2020).

Aesthetics

Many abiotic and biotic factors affect the appearance of material surfaces. Abiotic factors, such as water, solar radiation and pollutants cause changes in appearance. Biotic factors affecting material appearance are bacteria, moulds and decay fungi, algal growth and insects (Sandak *et al.*, 2019). However, whether the appearance of bio-based materials is perceived as aesthetically pleasing or not, is based on personal preference, which is subject to social influences (Sandak and Sandak, 2017).

Figure 1-8 Colour changes in wood due to weathering, with the amount of weathering increasing from left to right (Sandak and Sandak, 2017).

Thermal performance

Thermal performance is usually expressed by the thermal conductivity λ (W/m K), which is a measure of the rate of heat flow (W/m^2) that passes through a material with a certain thickness (m) due to a temperature gradient (K) (Ross, 2010). The thermal conductivity of solid wood is usually low and two to four times that of insulation materials, due to its porous structure (Ross, 2010). Thermal performance is an important factor for the functional use of bio-based insulation materials, and long-term stability of the thermal performance needs to be ensured. For instance, loose cellulose fibre insulation, which is blown into the cavities between the walls, might collapse and compact within the 50-year period as expected service life. When becoming wet, the loose and fluffy fibre insulation materials can collapse as well, decreasing the insulating functionality (Jones and Brischke, 2017). However, bio-based insulation materials used in applications with a moisture risk usually contain hydrophobic agents, such as bitumen or paraffin (Dederich *et al.*, 2019).

Fire performance

Since wood is commonly used as a fuel, it is often associated with a low fire performance. While this is generally the case for timber with a small cross-section, the opposite is true for structural wooden beams with a large cross section, CLT and Glulam (Jones and Brischke, 2017). When structural wood beams are exposed to fire, a

charring layer is formed. This charring layer has an insulating effect and protects the inner part of the wooden beam from burning, thus retaining the structural integrity and preventing collapse. No structural building material is inherently better at withstanding exposure to fire (Churkina *et. al*, 2020). For instance, while structural steel is very strong, plastic failure occurs in case of fire (Wong, 2001). Wood and bio-based insulation materials are often treated with fire retardants, which reduce the ignitability, heat release and flame spread (Jones and Brischke, 2017). Note that although the fire performance of building components is important, the fire resistance of a building can also be greatly reduced by proper building design and maintenance. For instance, implementing area and height limitations, fire stops, draft stops, sufficient doors and other exits, automatic sprinklers, and fire detectors greatly improve fire safety (Ross, 2010). The past has taught us that building failure is due to system engineering failure first, and then material failure (Churkina *et al.*, 2020).

1.5 Appraising durability of building materials – considering fungal decay

1.5.1 Mould growth and fungal decay

While some fungi cause aesthetic damage, such as moulds and stain fungi, decay fungi are able to degrade bio-based building elements and cause severe structural damage (Schmidt, 2006; Jones and Brischke, 2017). An overview of surface moulds, staining fungi and decay fungi that are known to attack wood and bio-based materials is given in Table 1-3. Surface moulds, staining fungi and soft-rot fungi usually belong to the phyla Ascomycota. The former are known to form an a*scus* or sac containing ascospores (Figure 1-9a) during the sexual reproduction cycle. Brown- and white-rot fungi usually belong to the phylum Basidiomycota, which are filamentous fungi that are composed of hyphae (Figure 1-9c) and form *basidia*, specialized end cells containing basidiospores (Figure 1-9b). Fungi that only have an asexual stage are classified within their corresponding taxonomic groups in the Ascomycota or Basidiomycota based on molecular data (Shenoy *et al.*, 2007).

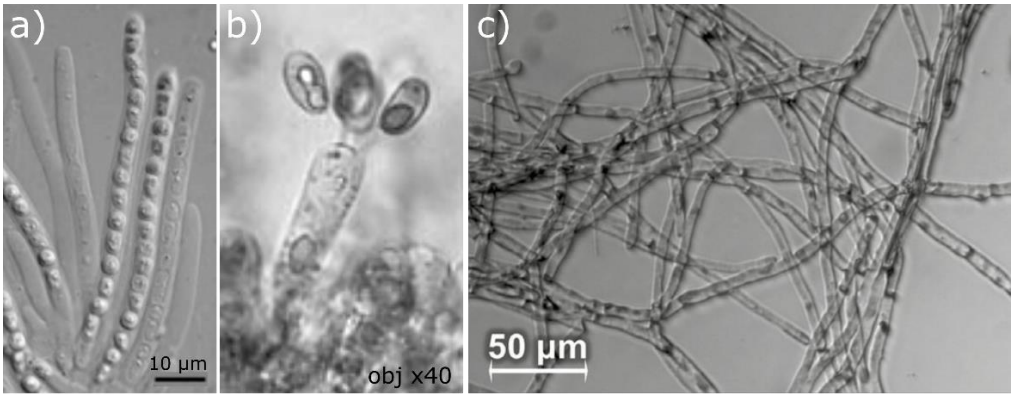

Figure 1-9 a) Ascus with ascospores of *Trichoderma koningiopsis* (Samuels *et al.*, 2006), b) basidia with basidiospores of *Coniophora puteana* © Leif Goodwin and c) hyphae of *Aspergillus aculeatus* (Kubo *et al.*, 2018).

Table 1-3 Overview of surface moulds, staining fungi and decay fungi that are known to attack wood and other bio-based building materials, with examples of commonly occurring fungal species. Adapted from Brischke and Unger (2017).

Surface moulds	Staining fungi	Decay fungi		
		Soft-rot fungi	Brown-rot fungi	White-rot fungi
Ascomycota Order: Eurotiales *Paecilomyces variotii,* *Aspergillus niger,* *Penicillium* spp. Order: Hypocreales *Trichoderma* spp.	**Ascomycota** Blue stain fungi: Order: Dothideales *Aureobasidium pullulans* Order: Microascales *Ceratocystis* spp. Order: Ophiostomatales *Ophiostoma* spp., *Ceratocystiopsis* spp. Other stain fungi: Order: Diaporthales *Discula* spp. Order: Helotiales *Chlorociboria aeruginosa*	**Ascomycota** Order: Sordariales *Chaetomium globosum,* *Humicola grisea* Order: Chaetothyriales *Phialophora* spp. Order: Microascales *Petriella setifera,* *Trichurus spiralis* Order: Coniochaetales *Lecythophora mutabilis*	**Basidiomycota** Order: Boletales *Coniophora puteana,* *Serpula lacrymans,* Order: Polyporales *Rhodonia placenta* Order: Gloeophyllales *Gloeophyllum trabeum*	**Basidiomycota** Order: Polyporales *Trametes versicolor,* *Donkioporia expansa,* *Phanerochaete chrysosporium* Order: Agaricales *Schizophyllum commune,* *Pleurotus ostreatus*

Surface moulds and staining fungi

Moulds and staining fungi grow on the surface of wood and bio-based materials and live on sugar, starch and protein in parenchyma cells (Schmidt, 2006). The strength properties of the material remain unchanged, as moulds and staining fungi cause little or no damage to the cell wall structure (Brischke and Unger, 2017). Moulds can cause aesthetic damage due to discoloration of the material surface (Figure 1-10a) and may cause health problems, usually in the form of respiratory allergies (Schmidt, 2006). Blue stain, a blue to black discoloration caused by blue stain fungi (Figure 1-10,b-d), can superficially occur or penetrate deeply into the wood, as the hyphae of blue stain fungi can grow from cell to cell through the pits (Figure 1-10e).

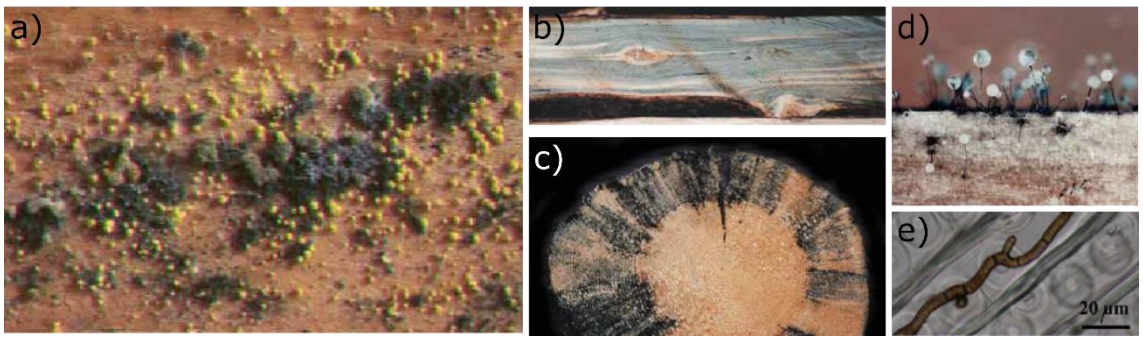

Figure 1-10 a) Mix of mould species on wood surface, b) blue stain affecting the sapwood of a log, c) blue stain affecting the sapwood of a log, as seen from the log cross section, d) blue stain spore structures at 20x magnification and e) hyphae of blue stain fungus growing in tracheid lumen. Images adapted from Uzunovic *et al.* (2008) and Schmidt (2006).

Decay fungi

Wood-decay fungi are traditionally grouped into brown-, white- and soft-rot fungi. Brown- and white-rot fungi are strictly speaking not actual distinct groups from a genetic point of view, as some brown-rot fungi also contain genes associated with decay mechanisms typical for white-rot fungi and *vice versa* (Riley *et al.*, 2014). Nevertheless, the terms are still widely used because they refer to general decay mechanisms.

Brown-rot fungi predominantly use hemicellulose and cellulose as a nutrient source, while only modifying the lignin (Floudas, 2012). Rapid strength loss occurs as cellulose chains are degraded. Due to the cellulose removal, wood shrinks during brown rot and a typical cubical cracking pattern appears (Morris, 1998; Figure 1-11a). Most brown-rot fungi preferably attack softwoods species and are the most economically important agent of decay in wood buildings in temperate climates (Morris, 1998; Schmidt, 2006). White-rot fungi degrade hemicelluloses, cellulose and lignin, either simultaneously or successively (Schmidt, 2006). In simultaneous white rot (for instance *Trametes versicolor)*, carbohydrates and lignin are nearly uniformly degraded at the same time. In successive white rot, lignin and hemicellulose are degraded faster than cellulose, at least in the earlier stages of attack. Lignocellulose attacked by white-rot fungi looks bleached and whitish (Brischke and Unger, 2017; Figure 1-11b and c). White rot also reduces the strength properties of wood, but to a lesser extent than brown rot, since for the same amount of mass loss, less cellulose is consumed, and no cracking or cubical rot occurs (Schmidt, 2006). White-rot fungi predominantly attack hardwoods.

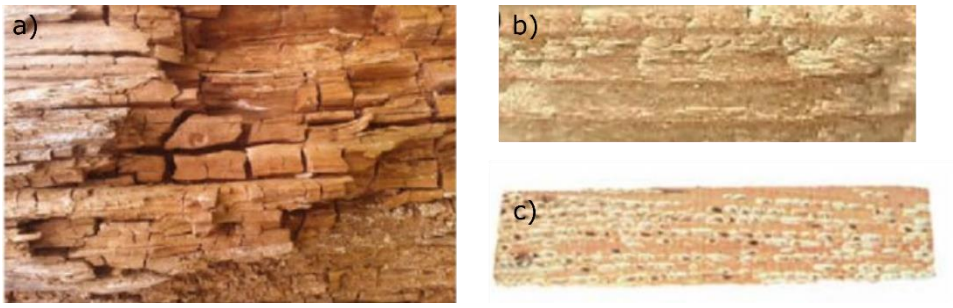

Figure 1-11 a) Cubic pattern due to brown rot, b) bleached appearance after white-rot decay and c) white rot in maple wood. Images adapted from Sandak *et al.* (2019) and Owens (2015).

Soft-rot fungi predominantly degrade hemicellulose and cellulose. Lignin is not or little attacked, at least in the initial stage. Soft-rot fungi differ from brown-rot and white-rot Basidiomycetes by growing mainly inside the woody cell wall. They are able to degrade at very high moisture conditions and are known to cause damage in conditions that are less suited to Basidiomycetes, such as wood in ground contact and wood that is constantly wet but not permanently submerged (like cooling tower timber and in harbour construction and ships) (Schmidt, 2006).

1.5.2 Environmental conditions required for decay

Fungi are ubiquitous and grow even in the most extreme environments (Cooke, 1968). Nevertheless, each fungal species has its particular range of environmental conditions at which it thrives (Mislivec and Tuite, 1970). Environmental factors influencing fungal growth are nutrients, oxygen, temperature, moisture and pH (Schmidt, 2006). The optimal pH for Basidiomycetes ranges from pH 4–6, while growth is possible between 2.5 and 9 (Schmidt, 2006). Although several fungal species, among which *Coniophora puteana*, can survive without oxygen for a week, a lack of oxygen does limit decay. However, in most applications, oxygen levels are sufficiently high for decay to occur. Minimal, maximal and optimal temperature ranges are species- and even isolate-specific. However, some general temperature indications that apply to most wood decay fungi can be given (Schmidt, 2006). Generally, fungal growth does not occur below freezing point, because liquid water is unavailable, which is necessary for the fungal metabolism. Usually, fungal enzymes become inactive and chemical reactions are reduced at temperatures below 5°C (Deacon, 2013). The maximum temperature for mycelial growth and wood damage by most wood fungi is often found at 40–50°C, because at those temperatures protein (enzyme) denaturing takes place. The optimum temperature of decay fungi usually lies between 20-40°C. Moisture is an important factor for fungal growth, as hyphae consist for 90% out of water and need it to take up, transport and metabolise nutrients. The influence of temperature and moisture on fungal growth is usually assessed separately. However, it is very likely that there is a combined effect of temperature and relative humidity on mycelial development. Moisture also plays an important role in degradation, as degradation enzymes require an aqueous environment to perform their function. Moisture is therefore essential to fungal decay and keeping bio-based materials dry and preventing water accumulation in building structures is the most effective way to protect them from wood degradation (Brischke and Alfredsen, 2020).

1.5.3 Material protection

The service life of a bio-based building material is the period of time after application during which the product meets its minimal performance requirements and no replacement is needed (Kutnik *et al.*, 2020). This depends on the durability of the material and the environmental conditions (Brischke and Rapp, 2010).

Protection by (building) design

In general, moisture is responsible for more than 50% of all building damage, either directly or indirectly. Damage due to moisture can be avoided by implementing good building practice (Langmans *et al.*, 2012; Van den Bossche *et al.*, 2016; Van Linden *et al.*, 2019). The presence of liquid water should be avoided, and water should be removed as fast and effectively as possible (Jones and Brischke, 2017). These principles can also be applied to increase the service life of wood and bio-based building materials in practice. However, the importance of design details and the role they play in enhancing service life, especially in the case of outdoor applications, is often

neglected and should not be underestimated. For instance, in an experiment on different designs for outdoor exposure, non-durable wood was able to withstand decay over a period of 10 years in applications designed to avoid water trapping (Kutnik *et al.*, 2020). Some examples of design rules that should be considered are the following (Figure 1-12):

- Avoid water accumulation by providing drainage
- Avoid ground contact
- Avoid direct contact with wet walls
- Provide end grain protection (liquid water is absorbed more easily from the end grain)
- Provide gutters to avoid splash

In indoor applications, water leakages and interstitial condensation can cause water accumulation in building elements as well and must be prevented (Finch *et al.*, 2008; Janssens and Hens, 2003).

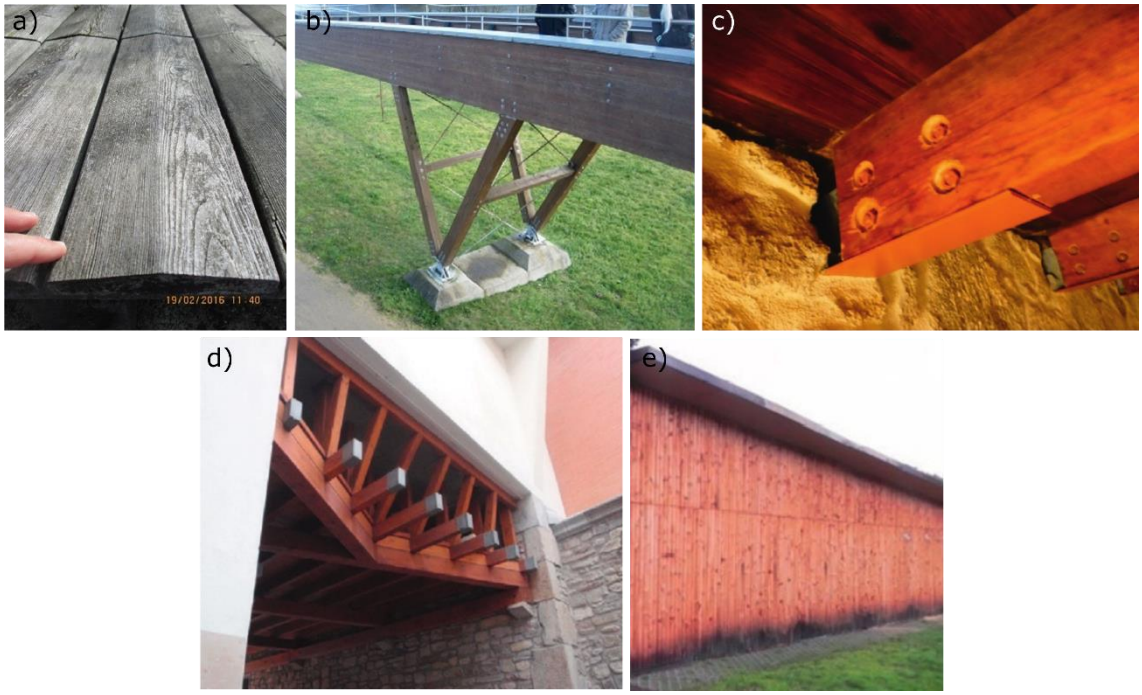

Figure 1-12 a) Decking with space between boards to avoid water accumulation, b) load-bearing pillars of wooden pedestrian bridge separated from the ground by concrete fundaments, c) separation between wood beam and wet wall, d) metal covering of end grain of exterior beams and e) wetting of cladding due to splash water in absence of a gutter. Adapted from Jones and Brischke (2017).

Fungicides

If a wood species is not durable, durability can be enhanced by applying fungicides. Originally, the most-used wood preservatives were Chromated Copper Arsenate (CCA), pentachlorophenol (PCP) and creosote (Coggins, 2008; Jones and Brischke, 2017). These are very effective but also toxic for the environment (Townsend *et al.*, 2006). In

1998, the Biocidal Products Directive (Directive 98/8/EC, 1998) was implemented to prevent application of environmentally harmful products and only 39 out of 81 previously included active ingredients remained on the European market of wood preservation (Jones and Brischke, 2017). Creosote is still used for wood protection in the EU, but is expected to be banned once valid alternatives are in place. Wood preservatives for the Do-It-Yourself (DIY) sector contain mainly organic active ingredients like Iodopropynyl Butyl Carbamate (IPBC), tebuconazole, propiconazole or pyrethroids. In heavy-duty applications such as highway fences and utility poles (UC 3.2 and UC4, Table 1-2), mainly copper-based preservatives are used (Jones and Brischke, 2017). Wood preservatives are often applied by brushing, spraying or short-term dipping. However, the main industrial treatments require an increased penetration depth and use vacuum pressure treatment.

Hydrophobic agents and coatings

Coatings can be applied to preserve wood, to improve its aesthetic appearance or both. When a coating has a low permeability, the moisture levels in the wood are low, positively impacting its service life (Miller, 2005). Typical coatings are pigmented paints and varnishes. Oil, waxes and paraffin are hydrophobic agents. When applied to wood or bio-based building materials, the overall material becomes more water repellent. This reduces the amount of capillary water uptake, reducing the risk of fungal decay. Oil treatment generally does not offer long lasting protection in UC3.2 and UC4 (Table 1-2). Treating solid wood with waxes or paraffin is technically challenging, because of their high melting points, but commercial products exist in Germany and Austria. Besides waxes and oil, other hydrophobic agents, such as silicone compounds and silane-based sol-gel coatings, can be applied for the same purpose as well (Sèbe and Brook, 2001; De Vetter *et al.*, 2009; Wang *et al.*, 2011). There are also several wood-fibre insulation boards on the market containing hydrophobic agents, such as paraffin and bitumen.

Wood modification

Wood modification is a complementary technology to the conventional wood preservation techniques, where the wood constituents of less-durable wood species are thermally and/or chemically altered to improve the durability (Jones *et al.*, 2018). The modified wood is non-toxic and should therefore not release any toxic substance during service into the environment (Hill, 2007). During thermal modification, the wood cell wall components are changed at high temperatures (above 150 °C) and under low oxygen conditions. Various chemical reactions take place, which can improve dimensional stability: removal of OH-groups, increased crosslinking within the cell wall polymers, changes in the mobility of the polymer network and bulking of thermally degraded components that have remained in the cell wall (Hill *et al.*, 2021). As thermal modification negatively influences strength properties, thermally modified wood is not used for structural purposes but mainly applied as cladding and decking. During chemical modification, the number of water sorption sites is reduced by letting

the OH-groups in the wood polymers (i.e. cellulose, hemicellulose and lignin) react with a stable, covalently bounded, less hydrophilic group (Rowell, 2012). Acetylation is a form of chemical modification, in which acetic anhydride is added to esterify OH-groups on the wood cell wall components, with acetic acid as a by-product. Acetylated wood absorbs less water than its non-modified equivalent due to this decrease in OH-group availability, not only due to the OH-substitution itself, but also due to the corresponding spatial confinement (Thybring *et al.*, 2020). Similar as in thermally modified wood, this improves wood properties like dimensional stability and durability. Another form of chemical modification is based on furfuryl alcohol (furfurylation).

1.5.4 Determining durability against Badiomycota by laboratory testing

The resistance of a bio-based building material against degradation by decay fungi, depends on its intrinsic or enhanced biological durability and its wetting and drying behaviour. The durability of a material is determined based on accelerated laboratory testing or field testing. Laboratory decay tests are performed in conditions that are optimal for fungi, so that a durability assessment can be made of a wood species or preservative treatment in a short period of time. The most widely used laboratory method for determining the natural durability of solid wood against wood-destroying fungi is the CEN TS 15083-1 test method (CEN TS 15083-1 standard, 2005). The efficacy of wood preservatives (fungicides) against basidiomycetes is assessed according to standard EN 113 (CEN EN 113 standard, 1996). Both tests subject wood specimens (50 x 25 x 15 mm^3) for 16 weeks to pure cultures of brown- and white-rot fungi selected for their strong ability to degrade wood (CEN TS 15083-1 standard, 2005). The specimens are weighed before and after exposure to the test fungus. Durability classes are assigned based on the median amount of mass loss due to degradation, as described in CEN EN 350 standard (2016) (Table 1-4).

Table 1-4 Durability class (DC) of wood to fungal attack by Basidiomycetes (CEN EN 350, 2016).

Durability class	Description	Mass loss (%)
DC 1	Very durable	≤ 5
DC 2	Durable	> 5 to ≤ 10
DC 3	Moderately durable	> 10 to ≤ 15
DC 4	Slightly durable	> 15 to ≤ 30
DC 5	Not durable	> 30

The standard laboratory method for determining the natural durability of solid wood against wood-destroying fungi (CEN TS 15083-1 standard, 2005), was found to be inadequate for the qualification of certain new wood products, such as chemically modified wood (acetylation, furfurylation, etc.), thermally treated wood, glue-laminated wood, wood-based panels and wood treated with water repellents (Kutnik *et al.*, 2014; Ringman *et al.*, 2014; Ormondroyd *et al.*, 2015; Candelier *et al.*, 2016; Jones and Brischke, 2017). The results of such a standard laboratory test might be biased due

to the lower equilibrium moisture content of thermally or chemically modified wood. Curling *et al.* (2015) also found the standard test to be suboptimal for bio-based insulation materials, as there were a number of issues related to the thickness of the material, transfer of water through specimens and the fragile nature of the insulation materials. For materials that have a certain macrostructural component, such as plywood and OSB, larger sample sizes would be preferable. Such a standard was developed for wood-based panels, which allows for larger specimens (50 mm x 50 mm x panel thickness) to be tested, allowing glue layers and panel structure to play a role (CEN ENV 12038 standard, 2002). Additionally, abovementioned standard tests were not designed to assess the impact of a material's moisture dynamics and time of wetness, which greatly affect fungal decay risk in service.

1.6 Problem statement and research aims

Many bio-based building materials are (to some extent) biodegradable, an excellent quality at the end of a material's service life as it solves waste issues, but a less desirable feature during use. When an organic material is exposed to favourable moisture and temperature conditions as well as to degrading organisms, its functional and aesthetic service life can decrease. The risk of fungal decay depends on the environment in which a material is applied and the material resistance.

A key aspect is how specific environmental conditions affect mycelial growth. Therefore, the following research aim is stated:

> **Aim 1. Assess the influence of temperature and relative humidity on fungal growth dynamics at mycelial level.**
> Most studies assessing the influence of environmental conditions on fungal growth rely on simple experimental set-ups where all but one environmental condition are fixed and the fungus grows on an optimal growth medium. Most of the studies assessing detailed fungal growth dynamics focus on small areas or the germination phase, tracking growth of a few hyphae not representative for the entire mycelium. In Chapter 2, our aim is to assess detailed fungal growth dynamics at mycelial level, including the mycelial area, number of tips and branching angle, at different environmental conditions. This chapter will build on the work of Guillermo Vidal-Diez de Ulzurrun on automated image-based analysis of spatio-temporal fungal dynamics (Vidal-Diez de Ulzurrun *et al.*, 2015)

A material's resistance to fungal decay depends on the material's natural durability and its hygroscopicity. Wood protection used to focus mainly on naturally durable wood species, often from tropical regions, or applying non-durable wood species that are treated with fungicidal wood preservatives. Due to the biocidal products directive (Directive 98/8/EC, 1998), many of the active ingredients of wood preservation products were banned in the EU. General awareness of the negative impact of biocidal

products on the environment initiated a new way of thinking about wood protection. Other material characteristics that could extend service life, such as a material's moisture dynamics and structure, are gaining importance. These are especially interesting when it comes to bio-based building materials, as there are many opportunities to alter material structure and moisture dynamics of engineered wood products and bio-based insulation materials. Unfortunately, in-depth knowledge on the intricate relationship between material characteristics and fungal behaviour is still lacking.

To contribute to the abovementioned potential, the following four research aims focus on unraveling the influence of material chemistry, moisture dynamics and structure on fungal susceptibility:

Aim 2. Develop a method suited to assess the influence of material chemistry on fungal susceptibility.

Usually, assessment of fungicidal components is done by extracting components of interests (fatty acids, organic acids, terpenes, tannins, and other benzenoid compounds) from a wood sample and assessing the effect of the extractive on the development of pure fungal cultures growing in or on a nutrient solution or agar. While effective, extraction procedures are quite complex, requiring several steps and various solvents, specific to the type of component targeted. It also does not allow an assessment of the fungicidal components in their entirety, as only specific components are targeted. Therefore, we aim to develop a method suited to assess the influence of fungicidal components, in their entirety, on the natural durability of a material in Chapter 3. The importance of material chemistry on the natural durability of 10 reference wood species, with durability classes ranging from I (Very durable) to V (Not durable), will be assessed. This method will also be used to assess the presence of fungicidal components in a selection of commonly used bio-based building materials.

Aim 3. Develop a method to assess the influence of RH and material moisture content on fungal decay in the presence of a moisture source.

The influence of moisture dynamics on the fungal susceptibility of wood, and the moisture dynamics of wood in general, has been a topic of great interest in wood research. Many efforts have been made to assess the minimum moisture threshold at which wood is at risk of fungal decay. Existing methods either assess the influence of RH on decay, without the presence of a liquid moisture source, or the level of decay in function of a moisture gradient, always at a RH of 100%, which is often insufficient and hence we aim to develop a method that is able to assess the influence of RH on decay in the presence of a moisture source, over time (Chapter 4). Whereas in Chapter 2 the influence of relative

humidity on mycelial growth is assessed, this chapter discusses a method to assess the influence of relative humidity and moisture content on actual wood degradation. Wood samples are to be exposed to brown rot at relative humidity conditions ranging from 11-100%, with the prerequisite that the fungus has access to a moisture source.

Aim 4. Apply state-of-the-art methods to better understand material moisture dynamics of commonly used wood-based panels and wood fibre insulation products.

Since a material's hygroscopicity affects the risk of fungal decay, substantial research has been done to assess and understand the moisture dynamics of solid wood, and especially thermally and chemically modified wood. However, research into the moisture dynamics of engineered wood products and bio-based insulation materials is limited. In Chapter 4, the materials will be exposed to liquid water in the so-called floating test, and water absorption and desorption will be measured over time to compare the materials' moisture dynamics. Then, three state-of-the-art techniques will be applied to better understand the differences in moisture dynamics. Since Low-Field Nuclear Magnetic Resonance (LNFMR) spectroscopy has been successfully applied to interpret changes in pore size distributions and hydrophilicity of wood due to chemical and thermal modification (Beck *et al.*, 2018; Cai *et al.*, 2020), a similar approach will be applied here to determine differences in water distribution between various bio-based building materials. X-ray CT, a method used to visualize internal material structure in a non-destructive way, will be used to gather complementary information on the pore size distribution of the materials in dry state. Additionally, Attenuated Total Reflectance Fourier Transform Infrared (ATR-FTIR) absorbance spectra will be obtained to assess the hydrophilicity of the bio-based building materials.

Aim 5. Develop a method to assess the influence of material structure on moisture dynamics and progress of fungal decay.

The current knowledge on the impact of material structure on fungal decay is mostly related to hyphae interacting with specific wood anatomical features, such as pits. Observations are usually made with light microscopy or SEM, for which samples are taken from a fungal decay experiment for examination at high resolution. A non-destructive method that has successfully been applied to assess fungal activity over time is isothermal calorimetry, in which heat production due to biochemical processes is related with fungal activity. Nevertheless, this technique does not offer any spatial information. To gain more insight into how a material's structure and moisture properties affect the degradation process, we propose the use of X-ray CT. X-ray CT is a promising technique for fungal decay research as it is fast, non-destructive and provides 3D images of the internal structure of a material. It has been applied to assess

decay before, yet by removal of samples from fungal cultures and drying before assessment with X-ray CT for easier analysis. Here, we aim to develop a method to non-destructively assess the degradation process with X-ray CT scanning. In that way, decay of individual wood specimens, which each have a unique anatomy, can be monitored over time.

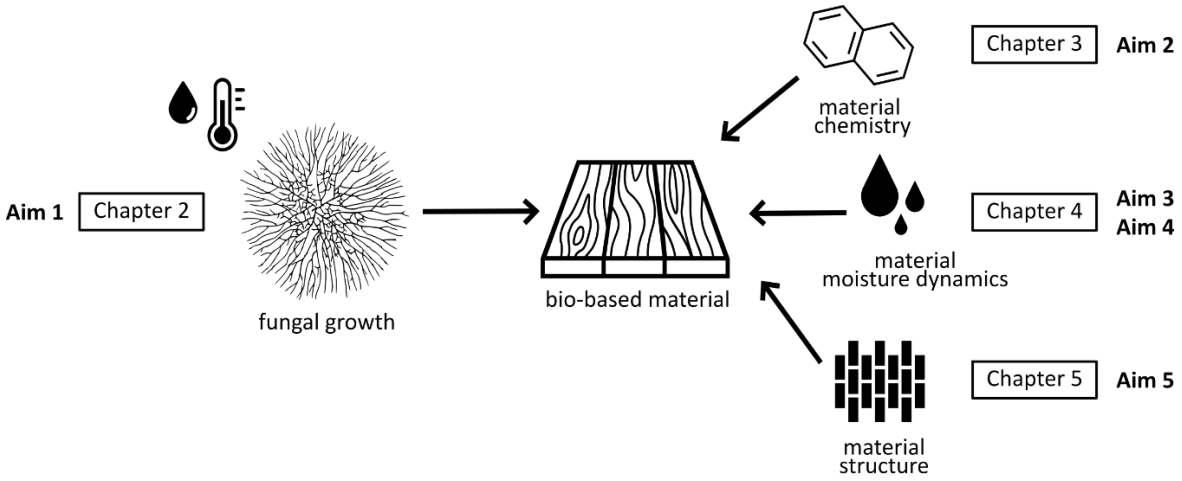

Figure 1-13 Thesis outline

Chapter 2

Influence of environmental conditions on mycelial development

This chapter is an adapted version from the paper published as:

De Ligne, L., Vidal-Diez de Ulzurrun, G., Baetens, J. M., Van den Bulcke, J., Van Acker, J., De Baets, B. (2019). Analysis of spatio-temporal fungal growth dynamics under different environmental conditions. *IMA fungus*, 10, 1-13. DOI: 10.1186/s43008-019-0009-3

Greenhuus
Grevelingenmeer, the Netherlands
Recreation homes built based on bio-based and circular building concepts
Architect: Kees van Wuyckhuyse

2.1 Introduction

Fungi are ubiquitous and grow even in the most extreme environments (Cooke, 1968). Each fungal species grows under a particular range of environmental conditions. Most species achieve maximal growth only under specific environmental circumstances (Mislivec and Tuite, 1970), referred to as the optimal growth conditions. Research on identifying these ranges is manifold and of use in various industries and research areas. Knowing the optimal growth conditions is, for instance, important when optimising industrial processes involving fungi, such as the production of cheese (Valík *et al.,* 1999), antibiotics (Berdy, 2005) and biofuel (Vicente *et al.,* 2009). Besides their applications, fungi also cause a remarkable amount of damage. Therefore, several studies have investigated the effects of environmental conditions on plant-pathogenic fungi, such as *Rhizoctonia solani* on potato and rice (Ritchie *et al.,* 2009; Feng *et al.,* 2017), *Puccinia purpurea* on sorghum (Dean *et al.,* 2012) and *Helminthosporium fulvum* on tomato, rice, wheat, etc. (Ibrahim *et al.,* 2011), and on fungi responsible for degradation of a wide range of building materials, such as gypsum drywall (Dedesko and Siegel, 2015), wood (Erikson *et al.,* 1990; Schmidt, 2006) and other bio-based materials (Rijckaert *et al.,* 1998; Jones and Brischke, 2017). The environmental conditions also play an important role in hyphal exploration of material surfaces (leaves, wood, inert materials) and in the initial mycelial colonization of materials (Carlile *et al.,* 2001; Li *et al.,* 2014).

Studies investigating the impact of environmental conditions on fungal growth are mostly limited to a few conditions and/or fungal species, as a consequence of the expensive and time-consuming laboratory experiments. Some studies focus on the resistance of a certain substrate to fungal attack, assessing, for example, the resistance of crops (Pardo *et al.,* 2005; Ibrahim *et al.,* 2011) or of building materials, to fungi (Brischke and Thelandersson, 2014). Fungal growth in these studies is usually measured as the mass loss of the studied substrate (Brischke and Rapp, 2008; Osono, 2015). Other studies examine the effects of the environmental conditions on fungal growth directly, by observing changes in the mycelium (Bonner and Fergus, 1960; Boddy, 1983; Pasanen *et al.,* 1991). Most of these studies rely on simple experimental set-ups where all but one environmental condition is fixed and the fungus grows on an optimal growth medium. The techniques used for assessing fungal growth often involve microscopes and/or imaging devices to capture images or videos of growing fungi (Etheridge, 1957; Ayerst, 1969; Magan and Lacey, 1984; Huang *et al.,* 2001; Gock *et al.,* 2003). Fungal growth characteristics, such as colony radius (Etheridge, 1957; Boddy, 1983; Pasanen *et al.,* 1991), the growth rate (Bonner and Fergus, 1960; Ayerst, 1969; Magan and Lacey, 1984; Gock *et al.,* 2003) or the number of germinated spores (Tommerup, 1983; Huang *et al.,* 2001) can be derived directly from such images. Unfortunately, up to this day, these analyses are often performed manually, although an image analysis method is for instance available for measuring the mycelial area (Ancin-Murguzur *et al.,* 2018). Such labour-intensive analyses hinder more detailed studies of fungal growth characteristics, such as the mean hyphal segment length and

the total length of the mycelium, or the number of tips across the entire mycelium, even though the latter characteristics provide crucial insights into fungal growth. The financial and human resources needed to conduct detailed fungal growth analyses prevent the replication of experiments, such that the natural variability of fungal growth is often neglected. In addition, most relevant studies on detailed fungal growth dynamics often focus on small areas (Ramakrishna *et al.,* 1993; Gougouli and Koutsoumanis, 2013; van Laarhoven *et al.,* 2015; Siripatrawan and Makino, 2015) or the germination phase (Brunk *et al.,* 2018), tracking growth of a few hyphae whose dynamics fail to represent the entire mycelium. Even though several studies compare the effect of environmental conditions on fungal growth over a certain period of time (Etheridge, 1957; Magan and Lacey, 1984; Pasanen *et al.,* 1991; Nielsen *et al.,* 2004), no elaborate time series analysis is performed to underpin the comparison.

Here we report on the influence of two of the most important environmental conditions, temperature and Relative Humidity (RH), on the growth dynamics of two fungal species using the (semi-) automated image analysis method of Vidal-Diez de Ulzurrun *et al.* (2015). *Coniophora puteana* and *Rhizoctonia solani*, were selected for assessment. Not only are these species economically important, they also have distinct growth dynamics (Vidal-Diez de Ulzurrun *et al.,* 2015). Time series analysis is performed, based on the Granger Causality Test, the Mann Whitney Test and Dynamic Time Warping, to quantitatively compare the effect of environmental conditions, both within and between species. The aim is to investigate how these environmental conditions influence the colony morphology of the two selected species and whether the fungal growth characteristics of the two fungal species respond differently to these different environmental conditions.

First, the two fungal species are presented and the image analysis method is explained, as well as the methods used for the time series analysis. Then, the overall behaviour of the measured fungal growth characteristics over time is presented, followed by a comparison between the growth dynamics of *C. puteana* and *R. solani* and an assessment of the effect of temperature and RH on the fungal growth dynamics of both species. This is followed by a discussion on the influence of different environmental conditions, the dynamics of several fungal growth characteristics and the added value of performing a time series analysis.

2.2 Material and methods

Selected species

Two filamentous fungi were selected for this study: *Coniophora puteana* (strain MUCL 11662, BAM 15) and *Rhizoctonia solani* AG4-HG-I (Laboratory of Phytopathology of Ghent University, isolate from lettuce (Van Beneden *et al.,* 2009): strain S010-1). *Coniophora puteana*, is a common brown rot fungus responsible for the degradation of wood and building materials in Germany, Scandinavia, Poland and Romania, and is found in 10% of damaged buildings in Belgium (Green III and Highley, 1997; Schmidt,

2006; Schmidt, 2007; Viitanen *et al.,* 2010a). It usually attacks wood which was moistened by water vapor or by contact with damp material in cellars or at the ground floor (Schmidt, 2006). *Coniophora puteana* has been used for nearly 80 years as a test fungus for wood preservatives in Europe and is part of the current standards for testing wood preservatives and natural durability of wood species (CEN EN 113 standard, 1996 ; CEN TS 15083-1 standard, 2005). *Rhizoctonia solani* is a plant pathogenic fungus with a large range of hosts (Dean *et al.,* 2012). It affects 5-10% of the total European sugar beet acreage (Büttner *et al.,* 2003), causes up to 30% yield loss on affected potato crops (Tsror, 2010), and up to 25% yield loss on affected cereals (MacNish and Neate, 1996). While chosen for its relevance to the mycology community at large, *R. solani* is also known to cause economic damage due to seedling blight in flax and hemp (Al-Beldawi *et al.*, 1982; McPartland and Cubeta, 1997; Hussein *et al.*, 2017), which are common renewable resources for bio-based building materials (Jones and Brischke, 2017).

Experimental set-up

Mother cultures were maintained on 8% malt agar substrate (2% agar Bacteriological No. 1; Oxoid, The Netherlands), 8% malt extract), as this concentration of malt proved successful in the previous work by Vidal-Diez de Ulzurrun (2015). They were kept for three days at (23±2) °C and an RH of (65±5) %RH in a climate cabinet (CTS Pharma climatic test chamber Series CP; CTS Hechingen, Germany). The mother cultures were retained in Petri dishes of 9 cm diameter. After three days of growth, a disc-shaped inoculum of about 10 mm diameter was cut from the periphery of the mother culture and placed at the centre of the bottom lid of a Petri dish (Figure 2-1). Finally, the top lid of the Petri dish was positioned on top of the bottom lid, as such restricting the height between top and bottom to 0.6 mm. In this way, vertical growth of the hyphae was limited and fungal growth was essentially restricted to two dimensions, which is a prerequisite for applying the image analysis procedure described below.

Images of the growing fungi were captured using a flatbed scanner (Epson perfection V750 Pro) on which two rows of three Petri dishes were mounted. The specimens were positioned on the scanner immediately after inoculation as such allowing the capture of early growth. Growth was monitored for 62 h, as preliminary experiments showed that further expansion of the mycelium was limited after this time. During this period, the Petri dishes were scanned automatically every hour using VueScan (version 9.5.19). The images had a resolution of 1200 dpi (resulting in pixels of approximately 21 µm) and were automatically cropped to the growing area of the mycelium. The final images had dimensions of 2125 x 2125 pixels per sample, corresponding to approximately 40 x 40 mm^2 and representing the central area of the Petri dish containing the initial inoculum.

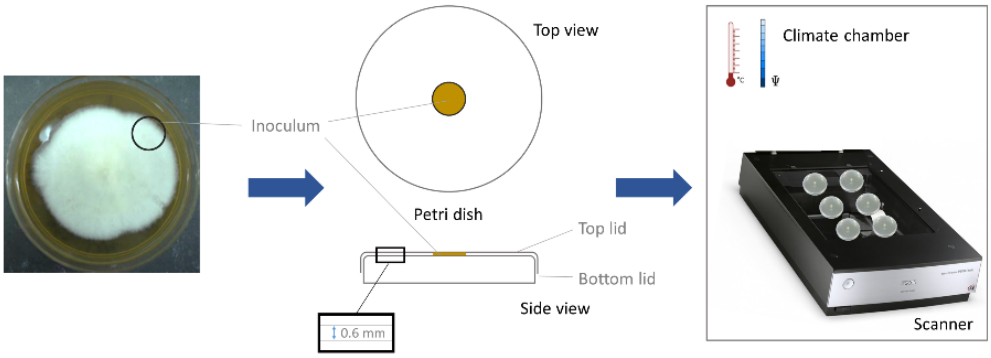

Figure 2-1 Schematic representation of the experimental set-up. A disc-shaped inoculum is taken from the periphery of the mother culture and positioned at the centre of the bottom lid of a Petri dish. The top lid of the Petri dish is positioned on top of the bottom lid, as such restricting the height between top and bottom lids to 0.6 mm. Then, the Petri dishes are transferred to the flatbed scanner in a climate chamber.

The flatbed scanner was placed in a climate cabinet with controlled temperature and RH. The specific values for our experiments were selected in order to cover those used in earlier similar experiments (e.g. Bonner, 1948; Bonner and Fergus, 1960; Trinci, 1969; Boddy, 1983; Tommerup, 1983; Magan and Lacey, 1984; Pasanen *et al.,* 1991; Ekesi *et al.,* 1999; Bjurman and Wadsö, 2000; Pardo *et al.,* 2005; Brischke and Rapp, 2008; Ritchie *et al.,* 2009; de Oliveira *et al.,* 2014), resulting in a full factorial experiment combining four temperatures (15, 20, 25 and 30 °C) and four relative humidity conditions (65, 70, 75 and 80 % RH). For reference values of typical environmental conditions occurring outdoors in Belgium (January and July) and indoors in spaces with specific end-uses (production and sales buildings, bathroom and swimming pool), see Table 2-1.

Table 2-1 Reference values for typical environmental conditions occurring outdoors in Belgium (January and July) and indoors in spaces with specific end-uses (production and sales buildings, bathroom and swimming pool).

Environmental conditions	**Mean T (°C)**	**Mean RH (%)**
Outdoor climate Belgium in January (KMI, 2021)	3.0	84
Outdoor climate Belgium in July (average T/RH) (KMI, 2021)	18.4	73
Indoor climate in production and sales buildings (Dietsch *et al.*, 2015)	18-27	25-41
Indoor climate in bathroom (Slávik and Cekon, 2014)	22-24	30-95
Indoor climate in swimming pool (Dietsch *et al.*, 2015)	28-31	45-89

In summary, a total of 16 environmental conditions were tested. Six specimens per environmental condition were initially prepared, as a maximum of six Petri dishes could be scanned simultaneously. Due to contamination in the form of dust and condensation, only four replicates per environmental condition could be included. For

each environmental condition, the mean of the four replicates was calculated, and this for all growth characteristics.

Quantification of fungal growth

The workflow for image analysis of fungal growth dynamics developed by Vidal-Diez de Ulzurrun *et al.* (2015) was adopted to assess the impact of environmental conditions on the growth dynamics of the selected species (Figure 8-1). First, the inoculum was digitally removed from all images since growth on the agar disc cannot be captured (Figure 2-2b). Subsequently, a line detection algorithm (Lopez-Molina *et al.* 2015), implemented in MATLAB (Version R2016b; The Mathworks, Massachusetts USA), was applied to obtain binary ridge maps of the growing fungus (Figure 2-2c). These ridge maps were converted into graphs (Figure 2-2d) using Mathematica (Version 10.0; Wolfram Research, Illinois USA). The nodes in the graphs (Figure 2-2e) represent growing tips and junctions of hyphae, and the edges represent the hyphal segments connecting them. Finally, several morphologic characteristics were derived from these graphs, an overview of which is presented in Figure 2-2e. For a full explanation on the computation of these characteristics, we refer to Vidal-Diez de Ulzurrun *et al.* (2015). The number of tips was calculated as the number of nodes that are connected to a single other node. The mycelial area was calculated as the area of the smallest convex polygon in which all nodes fit. The mean growth and branching angles at a given time are calculated by taking the mean of all growth and branching angles present in the mycelium at that time. Note that the mean growth angle, the mean branching angle and the mean hyphal segment length are analysed only after 10h of growth, because of their large standard deviation at the onset of growth, due to the presence of artificial nodes and edges along the inner boundary of the mycelium, which is intrinsic to the image analysis algorithm.

Mathematical and statistical data analysis

The dataset consists of time series of the extracted fungal growth characteristics. For every environmental condition and characteristic, the mean value of four replicates was calculated at every time step. By mutually comparing the time series observed under different environmental conditions, we assessed the impact of temperature, RH and their combined effect on fungal growth. In order to identify discrepancies between time series, we used the Granger Causality Test (Granger, 1969), the Mann Whitney Test (Mann and Whitney, 1947), and we computed the Dynamic Time Warping distance (Berndt and Clifford, 1994)

The Granger Causality Test (GCT, Granger, 1969) is based on the idea that if the prediction of one time series is improved by incorporating the information of a second time series, the latter is said to have a causal influence on the former (Guo *et al.,* 2010). When this is not the case, one can assume that the time series show a significantly different behaviour. The Mann Whitney test (MWT) assesses whether the medians of two distributions differ significantly (Mann and Whitney, 1947). In this paper, the MWT

was used to verify whether the difference of the medians of two time series is equal to zero. Dynamic Time Warping (DTW) is a well-known method for finding an optimal alignment between two given time series. In this paper, DTW was used to indicate how distinct the growth curves corresponding to different conditions are, compared to the average DTW distance found between replicates of those conditions. Additionally, autocorrelation tests were performed on the four replicates for every characteristic to see whether two time series indeed behave differently, or whether the abovementioned tests only pinpointed them as being different due to random fluctuations in the data. All analyses were performed in Mathematica (Version 10.0, Wolfram Research, Illinois USA).

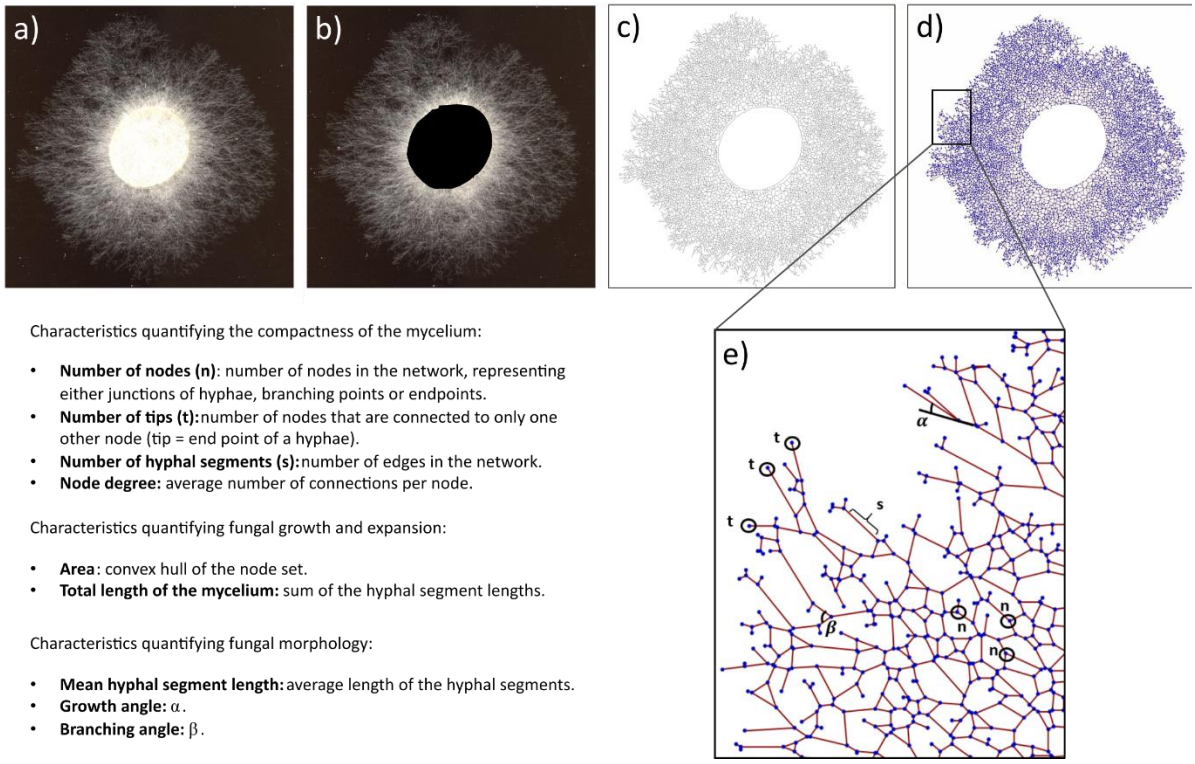

Figure 2-2 Summary of the entire process of mycelium characteristic extraction of an image of *C. puteana* after 60h mycelial growth at 20°C and 75% RH. a) Initial image, b) pre-processed image, c) binary ridge map, d) graph and e) representation of characteristics quantifying fungal morphology.

2.3 Results

General fungal growth dynamics

Several fungal growth characteristics were assessed over time for each species (Figure 2-2e). An example of the main fungal growth characteristics in function of time is given in Figure 2-3, showing the results obtained at 25°C and 80% RH. Under this condition, the number of tips increased over the first 20h for *Coniophora puteana* and *Rhizoctonia solani*, after which growth ceased. The mycelial area, on the other hand, continued to increase gradually even beyond those first 20 hours. Across all conditions, a few general trends could be inferred: the mycelial area and the number of tips increased

over time in a sigmoidal manner, whereas the mean hyphal segment length remained fairly constant. The growth and mean branching angles fluctuated irregularly over time.

Since the mean hyphal segment length remains almost constant, the mean value was calculated for each condition (Table 2-2), and averaged over all obtained conditions 176.5 ± 7.8 µm (*R. solani*). There are no differences in mean hyphal segment length across the 16 conditions, within the accuracy determined by the scanner resolution (approx. 21 µm). The overall mean hyphal segment length for *R. solani* is thus 176.5 ± 21 µm. A similar approach was followed for the mean hyphal segment length for *C. puteana*, calculated as 183.2 ± 21 µm.

Table 2-2 Mean hyphal segment length (µm) of *R. solani* averaged over four replicates and over time.

RH/temp	65% RH	70% RH	75% RH	80% RH
15°C	181.1 ± 4.4	174.6 ± 3.9	181.7 ± 2.9	180.0 ± 4.7
20°C	181.5 ± 7.4	181.9 ± 9.8	168.1 ± 5.5	178.1 ± 3.5
25°C	178.7 ± 10.7	180.0 ± 11.3	178.0 ± 3.3	172.0 ± 4.5
30°C	170.6 ± 3.2	172.2 ± 9.2	168.6 ± 2.5	176.3 ± 2.6

The mean growth angle and mean branching angle seem to vary randomly in function of time, yet within rather narrow boundaries (Figure 2-4). Mean branching angles varied between 1.22-1.56 rad (*C. puteana*) and 1.28-1.58 rad (*R. solani*), whereas mean growth angles varied between 0.69-0.82 rad (*C. puteana*) and 0.70-0.86 rad (*R. solani*).

Comparison of growth dynamics

Table 2-3 compares the fungal growth characteristics of the two species, for the 16 environmental conditions. Based on the MWT, the growth characteristics of both fungi were found to differ for nearly every characteristic and condition. For example, at 25°C and 80% RH (Figure 2-3), one can clearly see a difference in absolute value between the species for several characteristics: the mycelial area and the number of tips formed by *R. solani* were more than twice as large than those of *C. puteana*. Based on the results of the GCT, the differences between *C. puteana* and *R. solani* were more pronounced for some characteristics than for others. The mycelial area, the number of tips, the mean edge length, and the mean growth and branching angles differed between the two species in at least 10 of the 16 tested conditions (Table 2-3). The autocorrelation for these characteristics indicated clear trends, with the exception of the mean growth and branching angles whose autocorrelation was only 0.2. This demonstrates that these two characteristics fluctuated randomly (Figure 2-3), making the results of the GCT for the growth and mean branching angles irrelevant. Nonetheless, a difference in mean growth angle between the two species can be assessed visually in Figure 2-4.

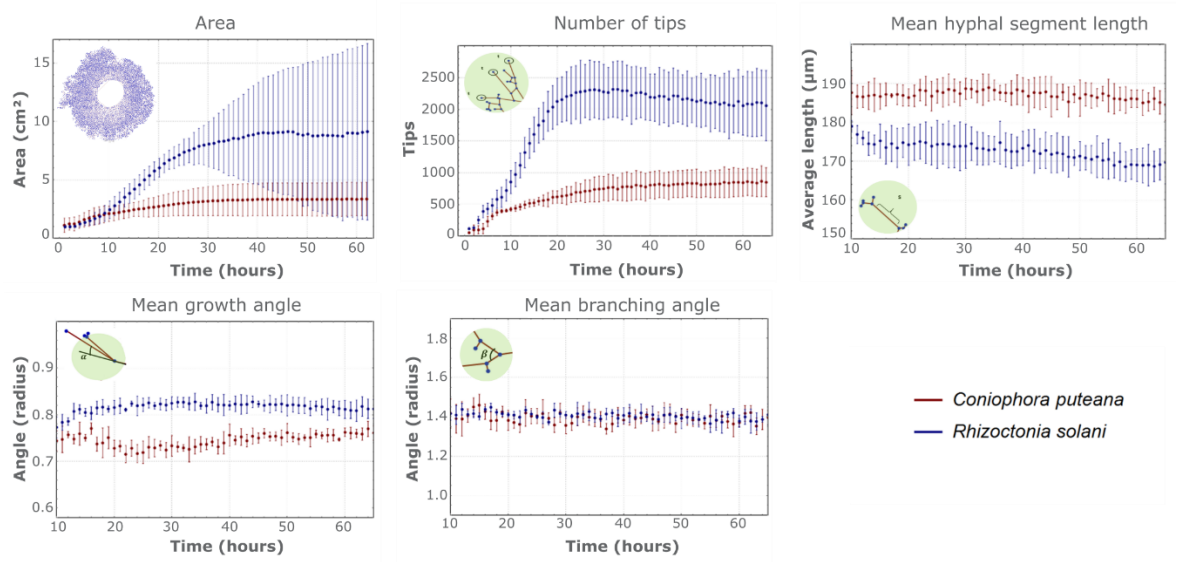

Figure 2-3 Fungal growth characteristics in function of time at 25°C and 80% RH for *C. puteana* (red) and *R. solani* (blue). The dots represent the average value of four replicates, with the bars indicating the standard deviation.

Table 2-3 Comparison of growth characteristics of *C. puteana* and *R. solani* for 16 combinations of temperature and RH.

Environmental condition	**Area**		**Number of tips**		**Mean hyphal segment length (after 10h)**		**Mean growth angle (after 10 h)**		**Mean branching angle (after 10 h)**	
	GCT	MWT	GCT	MWT	GWT	MWT	GWT	MWT	GWT	MWT
15°C, 65% RH	x	x	x	x	x	x	x	x	x	x
15°C, 70% RH			x	x	x	x		x	x	x
15°C, 75% RH	x	x		x	x	x	x	x	x	x
15°C, 80% RH	x	x	x	x	x	x		x	x	x
20°C, 65% RH	x	x	x	x	x	x		x	x	x
20°C, 70% RH	x	x	x	x	x	x	x	x	x	x
20°C, 75% RH	x	x	x	x	x	x		x	x	x
20°C, 80% RH		x		x	x	x	x	x	x	x
25°C, 65% RH	x	x	x	x	x	x	x	x	x	x
25°C, 70% RH	x	x	x	x	x	x	x	x	x	x
25°C, 75% RH	x	x	x	x		x	x	x	x	x
25°C, 80% RH	x	x	x	x	x	x	x	x	x	x
30°C, 65% RH		x	x	x	x	x	x	x	x	x
30°C, 70% RH		x		x	x	x	x	x	x	x
30°C, 75% RH		x		x	x	x	x	x	x	x
30°C, 80% RH		x	x	x	x	x		x	x	x

x: p-value of the GCT is >0.05, meaning that the time series for *C. puteana* cannot be used to predict the corresponding series for *R. solani* and/or vice versa (= time series are different). x: p-value <0.05 for the MWT, meaning that the median difference between two corresponding time series is not equal to zero (= time series are different).

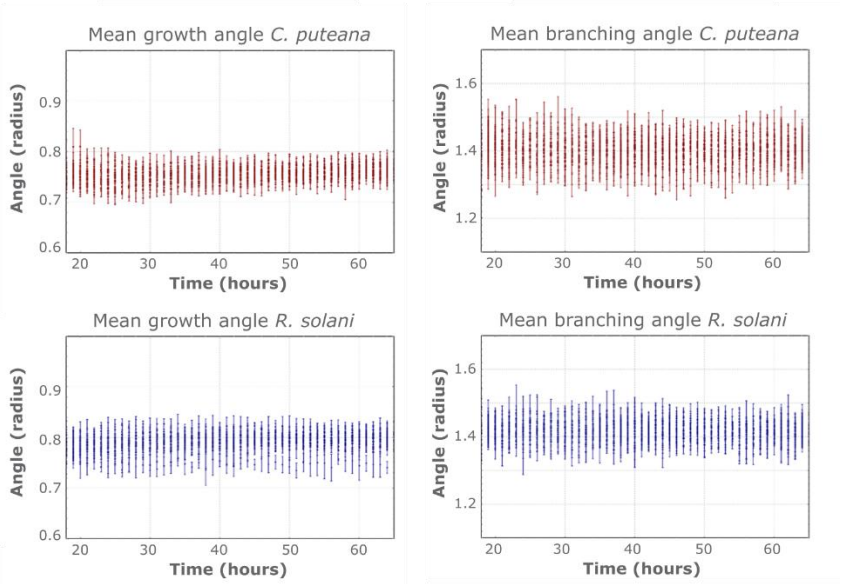

Figure 2-4 Mean growth and branching angles of *C. puteana* (red) and *R. solani* (blue), for four replicates of 16 conditions. The mean growth and branching angles at a given time were calculated by taking the mean of all growth and branching angles present in the mycelium at that time.

Effect of temperature and relative humidity on fungal growth

Temperature and RH often had a combined influence on fungal growth dynamics. At 20°C and at 25°C (*C. puteana*) and at 15°C and 25°C (*R. solani*), the growth curves representing the evolution of the mycelial area over time clearly differed across the four RHs. For instance, for *C. puteana* at 20°C and 75% RH, the mycelial area was more than twice as large than at an RH of 70%, while only limited growth occurred at 65% and 80% RH (Figure 2-5a). Similarly, at a RH of 75%, growth curves differed across the four temperatures, which was confirmed by DTW and most of the GCT and MWT (Figure 2-5b).

In contrast, an RH of 65% (independent of temperature) for *C. puteana* and a temperature of 30°C (independent of RH) for both *C. puteana* and *R. solani* always resulted in limited fungal growth, as confirmed by DTW and the GCT (Figure 2-6).

The influence of temperature and RH on the evolution of the number of tips was similar as for the mycelial area (Figure 2-7). Some environmental conditions caused substantially more variation, as was the case for the mycelial area and the number of tips at 20°C and 70% RH and 25°C and 75% RH for both fungi (Figure 2-7c,d), and for the mycelial area at 25°C and 80% RH. The optimal growth conditions for mycelium development over an inert surface, defined as the conditions where the largest area and highest number of tips were reached after 62 hours, occurred at 20°C and 75% RH and at 25°C and 80% RH for *R. solani* AG4-HG-I and at 20°C and 75% RH for *C. puteana* MUCL 11662 (Suppl. Figure 8-2 to 8-5).

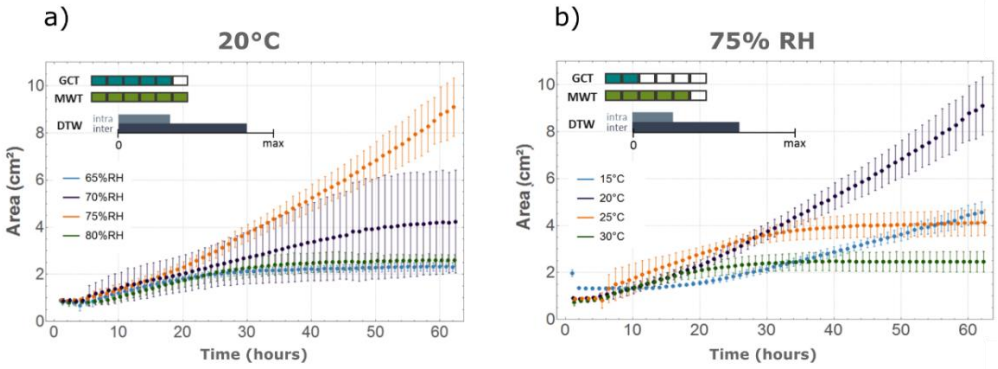

Figure 2-5 Evolution of mycelial area (cm^2) over time for *C. puteana* at a) 20°C, for four relative humidity conditions (65, 70, 75 and 80 % RH) and b) 75% RH, for four temperatures (15, 20, 25 and 30°C), showing a clear combined effect of temperature and RH. The dots represent the mean values over four replicates, with the bars indicating the standard deviation. For each graph, six pairwise GCT and MWT were performed on the means of each of the four conditions represented in that graph. The two colour scales indicate for how many of those pairwise comparisons a difference was found according to GCT (blue) and MWT (green). The third scale represents the difference between the average DTW distance between the four conditions represented in the graph (inter) and a reference ground value, being the average DTW distance among the replicates of each curve in that graph (intra).

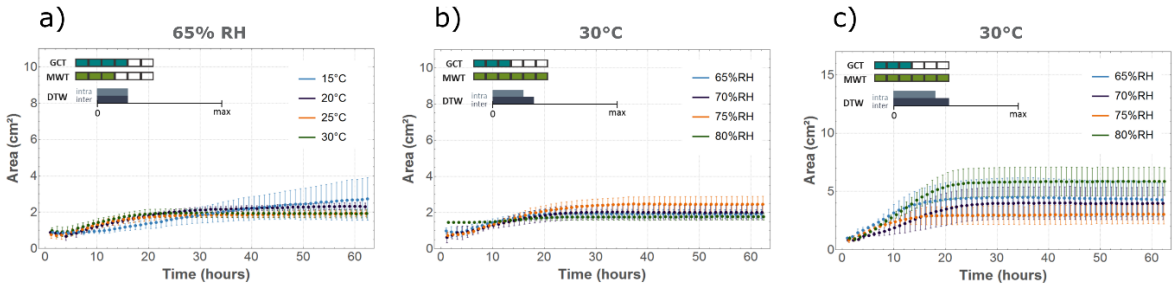

Figure 2-6 Evolution of mycelial area (cm^2) over time for *C. puteana* at a) 65% RH, for four temperatures (15, 20, 25 and 30°C), 30°C, for four relative humidity conditions (65, 70, 75 and 80 % RH) and c) for *R. solani* at 30°C, for four relative humidity conditions (65, 70, 75 and 80 % RH). For all these conditions, limited growth occurred. The dots represent the mean values over four replicates, with the bars indicating the standard deviation. For each graph, six pairwise GCT and MWT were performed on the means of each of the four conditions represented in that graph. The two colour scales indicate for how many of those pairwise comparisons a difference was found according to GCT (blue) and MWT (green). The third scale represents the difference between the average DTW distance between the four conditions represented in the graph (inter) and a reference ground value, being the average DTW distance among the replicates of each curve in that graph (intra).

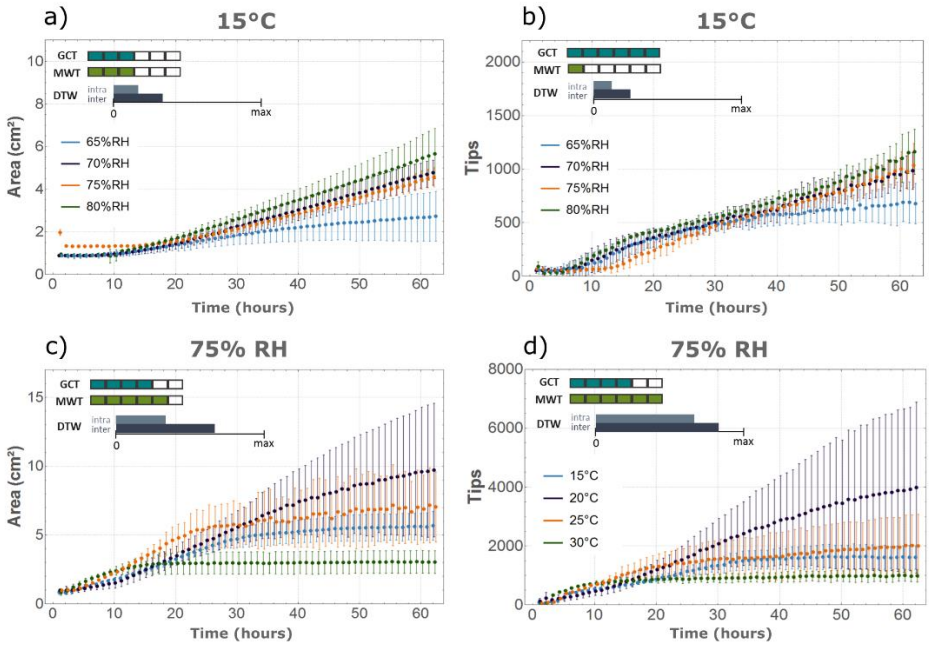

Figure 2-7 Evolution of mycelial area (cm^2) and the number of tips over time for *C. puteana* (a, b) and *R. solani* (c, d). The influence of temperature and RH on the evolution of the number of tips was similar as for the mycelial area. The dots represent the mean values over four replicates, with the bars indicating the standard deviation. For each graph, six pairwise GCT and MWT were performed on the means of each of the four conditions represented in that graph. The two colour scales indicate for how many of those pairwise comparisons a difference was found according to GCT (blue) and MWT (green). The third scale represents the difference between the average DTW distance between the four conditions represented in the graph (inter) and a reference ground value, being the average DTW distance among the replicates of each curve in that graph (intra).

2.4 Discussion

Temperature and RH are known to significantly affect fungal growth dynamics (Bonner, 1948; Bonner and Fergus, 1960; Mislivec and Tuite, 1970; Pasanen *et al.,* 1991). This has been observed both in laboratory conditions (Boddy, 1983; Gougouli and Koutsoumanis, 2013; Tommerup, 1983; van Laarhoven *et al.,* 2015; Huang *et al.,* 2001; Gock *et al.,* 2003) and in natural environments (Kauserud *et al.,* 2010; Gange *et al.,* 2011). However, such studies rarely assess the combined effect of temperature and RH.

A study by Ciliberti *et al.* (2015), considering the influence of temperature and RH simultaneously on grape rot (*Botrytis cinerea*), points at an interaction effect between both factors. A combined effect of temperature and RH on radial growth (Bonner and Fergus, 1960; Pasanen *et al.,* 1991) and germination time (Bonner, 1948; Mislivec and Tuite, 1970) can be noted from an examination of the results presented in these studies, although the authors do not mention this as such. Our study confirms that there is indeed a combined effect of temperature and RH on several fungal growth

characteristics, for both *C. puteana* and *R. solani*. Furthermore, the optimal temperature ranges for a given species often differ between different studies. For instance, for *C. puteana* 22-25°C (Schmidt *et al.* 2002), 20°C (Etheridge 1957), 20-25°C (Seehann and Riesebell, 1988), 28°C (Wälchli, 1977) and 20-32°C (Jones and Brischke, 2017) were reported as optimal temperature ranges. This wide variety can partly be explained by neglecting the effect of RH, as Etheridge (1957) and Seehann and Riesebell (1988) do not mention the RH used, while Schmidt *et al.* (2002) maintain a non-specified high RH. However, it is more likely that the genetic variation between the strains is the main reason for these differences in the optimal temperature range. Schmidt *et al.* (2002) reported an optimal temperature of 22.5°C for 7 of the 15 isolates of *C. puteana*, while a temperature of 25°C was optimal for 8 isolates. *Rhizoctonia solani* covers a species complex of several anastomosis groups (AG, grouped based on the ability of hyphal fusion between isolates) that differ widely in host range and biological characteristics (Gondal *et al.*, 2019). A wide range of optimal temperatures is, therefore, reported as well, including 20 and 25°C (Anguiz and Martin, 1989), 20-25°C (Ritchie *et al.,* 2009), 22-25°C (Chand and Logan, 1983), 25°C (Grosch and Kofoet, 2003), 24-27°C (de Oliveira *et al.,* 2014), 25-30°C (Harikrishnan and Yang, 2004) and 30-35°C (Baird *et al.,* 1996). We found that the optimal conditions for mycelial development over an inert surface for *C. puteana* (strain MUCL 11662, BAM 15) were reached at 20°C and 75% RH and for *R. solani* AG4-HG-I at 20°C and 75% RH, and 25°C and 80% RH.

Fungi can grow at very low levels of RH if water is available on the surface (Pasanen *et al.,* 1991). When only a limited amount of water is available, *in casu* in our set-up, RH plays a significant role in mycelial development. In this paper, an RH of 65% was limiting for mycelium development over the inert Petri dish surface, irrespective of the temperature, for *C. puteana*. None of the tested RH conditions was limiting for *R. solani*. This does not preclude that RH is never the main limiting factor for *R. solani*, but only that the ranges for which we tested might not have included an RH low enough to limit the mycelium development of *R. solani*. A temperature of 30°C was limiting for fungal growth, irrespective of the RH, both for *C. puteana* and *R. solani*. This can possibly be explained by dehydration of the exploring hyphae at this temperature. When water availability is not an issue, optimal temperatures up to 32°C for *C. puteana* and 35°C for *R. solani* have been reported (Baird *et al.* 1996, Jones and Brischke, 2017).

Growth of filamentous fungi over time is typically sigmoidal, with a lag phase at lower growth rates, followed by an exponential growth phase, and a brief stationary phase, after which the fungus dies (Trinci, 1969; Trinci, 1974; Montini *et al.,* 2006; Meletiadis *et al.,* 2001). The growth curves presented in this chapter (Suppl. Figure 8-2 to Figure 8-5) are sigmoidally shaped when temperature and/or RH do not limit growth, and correspond to those in Montini *et al.* (2006) and Meletiadis *et al.* (2001). The set-up we used does not allow distinguishing between living and dead hyphae. When the mycelial area or the number of tips do no longer increase, growth has ceased. Fungal

growth ceased either early on in the experiment, indicating that the environmental conditions had a limiting effect on fungal growth (for instance for *R. solani* at 30°C, as shown in Figure 2-6), or only after a large mycelial area had formed, indicating that the substrate was the limiting factor (for instance for *R. solani* at 25°C and 80% RH, as shown in Figure 2-3).

Very few studies on fungal growth dynamics examine the mean hyphal segment length of a fungal network, as most determine the hyphal growth unit, which is the total length of the mycelium divided by the total number of tips (Carlile *et al.,* 2001). The values for mean hyphal segment length determined in this paper, being 183.2 ± 21.0 µm (*C. puteana*) and 176.5 ± 21.0 µm (*R. solani*), do agree with those presented by Vidal-Diez de Ulzurrun *et al.* (2015). *Coniophora puteana* and *R. solani* have similar mean hyphal segment lengths, which are comparable to those of *Phanerochaete velutina* (186.3 ± 7.4 µm) and *Penicillium lilacinum* (168.9 ± 23.7 µm) (Vidal-Diez de Ulzurrun *et al.,* 2015). In contrast, the mean hyphal segment lengths of *Trichoderma viride* (209.1 ± 12.2 µm) and *Mucor hiemalis* (117.0 ± 84.0 µm) are significantly longer and shorter, respectively (Hutchinson *et al.,* 1980; Vidal-Diez de Ulzurrun *et al.,* 2015). It seems that the mean hyphal segment length (i.e. the mean length of the hyphal segments) can be a distinguishing morphological characteristic between fungal species. Nevertheless, one should be cautious, as nutrient concentration has been shown to affect internodal length as well (Camenzind *et al.*, 2020).

Generally, filamentous fungi form branches at approximately right angles to the parent hyphae (Carlile *et al.,* 2001). For *R. solani* specifically, right-angled branching angles were noted in young mycelium by Kamel *et al.* (2009). Here, mean branching angles were found between 1.22-1.56 rad (*C. puteana*) and 1.28-1.58 rad (*R. solani*), which are overall notably smaller than right angles (1.57 rad). This can also be observed in Figure 2-8, where some branching angles of *R. solani* are highlighted and calculated with ImageJ (Version 2, Fiji, Schindelin *et al.* 2015).

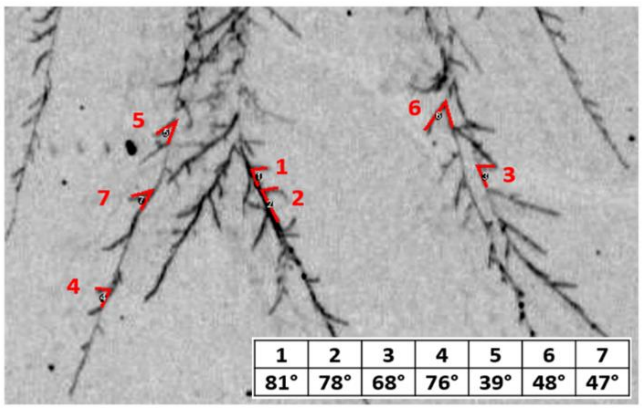

Figure 2-8 Manual indication of branching angles on *R. solani* hyphae at 20°C and 75% RH. Branching angles are highlighted and calculated with ImageJ (Schindelin *et al.* 2015).

Hyphae have the tendency to maintain a certain direction of growth (Riquelme *et al.*, 1998). The growth angle is defined as the difference between the angle of a segment and the angle of its preceding segment (Figure 2-2e), and as such gives an indication of the growth direction of the hyphae. In general, hyphae will maintain their direction while elongating and small growth angles will be found. A low value for the mean growth angle therefore indicates that there are almost no changes in the growth direction, while larger values possibly imply a complex network full of branches. The mean growth angles in this chapter were similar for *C. puteana* (0.70-0.86 rad) and *R. solani* (0.69-0.82 rad), and indicate that branching happens frequently (Figure 2-4). Vidal-Diez de Ulzurrun *et al.* (2015) report similar values for the mean branching angle and the mean growth angle for *C. puteana* and *R. solani*. When investigating the periphery of the mycelium, clear hyphal elongation can be noted. For example, for *R. solani* at 25°C and 80% RH, the number of edges, tips and nodes did no longer increase after 20 hours, while the area continued to increase (Figure 2-3). Given that the mycelial area was measured as the convex hull of the mycelium and no new tips were formed, this indicates that only the length of the hyphal segments increased. Indeed, at the end of the growing period, hyphal elongation occurred at the periphery of the mycelium while branching subsided (Figure 2-9). This elongation of the so-called "leading hyphae" (hyphae extending at the mycelium edge (Vinck *et al.*, 2005; Lew, 2011) is typical for nutrient-poor conditions, where branching is suppressed to maximise the extension of these leading hyphae (Esser and Lemke, 1995).

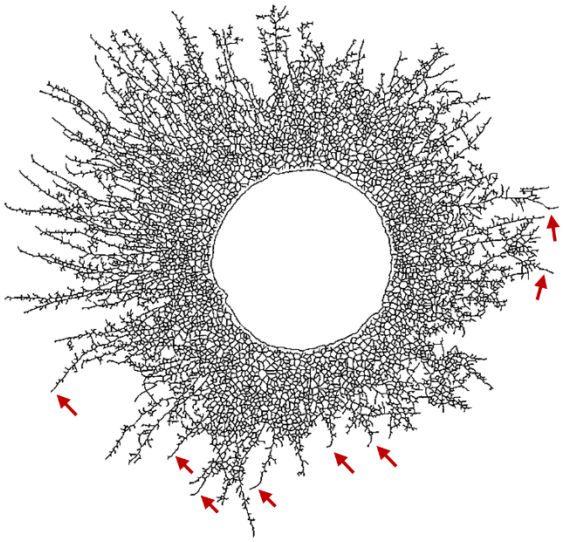

Figure 2-9 Elongation of hyphal segments at the periphery of the mycelium. Binary image, representing the mycelium of *R. solani* after 30 hours of growth, at 25°C and 80% RH.

Under optimal growth conditions, growth characteristics differed significantly between replicates, see, for example, the large standard deviation for the mycelial area at 20°C and 70% RH, 25°C and 80% RH (both fungi) and at 25°C and 75% RH (*R. solani*) (Suppl. Figure 8-3), and for the number of tips at 20°C and 70% RH (both fungi), 25°C and 80% RH (*C. puteana*) and 25°C and 75% RH (*R. solani*) (Figure 2-5). Even though the set-up guaranteed as little variation between the specimens as possible, small differences might have occurred in, for example, the amount of substrate, the initial humidity of the agar disc and the number of hyphae on the agar disc, while natural variability obviously always has to be considered.

Temporal changes

Various studies assessing the effect of environmental conditions on fungal growth characteristics neglect time. They either assess fungal growth characteristics after a fixed number of days (Bonner and Fergus, 1960; Ibrahim *et al.,* 2011; Ciliberti *et al.,* 2015; Pardo *et al.,* 2005) or use average growth rate (Ayerst, 1969; Boddy, 1983; Tommerup, 1983; van Laarhoven *et al.,* 2015), yet taking temporal changes into account is important. For instance, for an RH of 65% the mycelial area of *R. solani* after 62 hours was the same at 15°C and 20°C, but at 20°C it reached this value earlier (Figure 2-6). Therefore, computing this characteristic after 60 hours only would not allow for the detection of the different behaviour. In most studies the growth curves are usually visually compared (Pasanen *et al.,* 1991; Ramakrishna *et al.,* 1993; Nielsen *et al.,* 2004). Clearly, a time series analysis, as applied in this study allows for an objective comparison of fungal growth behaviour as a function of time. This enables a more thorough and objective comparison of the influence of environmental conditions, and allows for verifying whether or not there is a combined effect of temperature and RH on fungal growth dynamics.

2.5 Conclusions

The method presented here enables an objective and in-depth analysis of the effect of environmental conditions on various fungal growth characteristics, to be carried out in a rather short period of time (62 h). It offers an updated and broader alternative to the classical studies on fungal growth dynamics with narrow observation areas and/or a limited number of characteristics. Moreover, it can be performed with low-cost imaging devices, such as scanners. Comparing fungal growth based on time series analysis is an innovative approach which enabled a more thorough and objective comparison of the influence of environmental conditions, and allowed to verify the combined effect of temperature and RH on fungal growth dynamics. RH plays an important role in mycelial development when a limited amount of water is available. An RH of 65% (*C. puteana*) and a temperature of 30°C (*C. puteana* and *R. solani*) resulted in limited fungal growth. Optimal conditions for mycelial development over an inert surface occurred at 20°C and 70% RH (*C. puteana*) and at 20°C and 75% RH, and 25°C and 80% RH (*R. solani*). Several fungal growth characteristics showed sigmoidal growth over time, which is typical for filamentous fungi, while the mean

hyphal segment length remained constant over time. By measuring several fungal growth characteristics, elongation of the “leading hyphae” could also be observed.

The method presented here allows for a quantitative and thus objective mutual comparison of different growth characteristics as a function of time and could be deployed for a number of research topics where detailed assessment of fungal growth dynamics is of interest, for example when investigating differences in phenotype between genetic variants of the same species, testing the influence of different growth substrates on the amount of branching and the hyphal segment lengths, to study local behaviour within a fungal colony, more specifically a differing morphology between the central region and the peripheral region and as parameters for realistic modelling.

Chapter 3

Influence of material chemistry on natural durability

3.1 Introduction

3.2 Revealing the impact of decay-influencing characteristics other than fungicidal components in wood

3.3 Assessing fungicidal components in bio-based building materials

Cork house
Palafrugell, Spain
House with cork as exterior cladding
Architects: Emiliano López Mónica Rivera Arquitectos
© José Hevia | lopez-rivera.com/project/two-cork-houses/

3.1 Introduction

The natural durability of wood has been mainly studied focusing on wood cell wall polymers and the extraction and evaluation of fungicidal compounds. Wood cell wall polymers (cellulose, hemicellulose and lignin) are the main components of wood and it is well known that cellulose and hemicellulose (Figure 3-1) are essential nutrients for fungal growth (Zabel and Morrell, 2012; Cragg *et al.*, 2015).

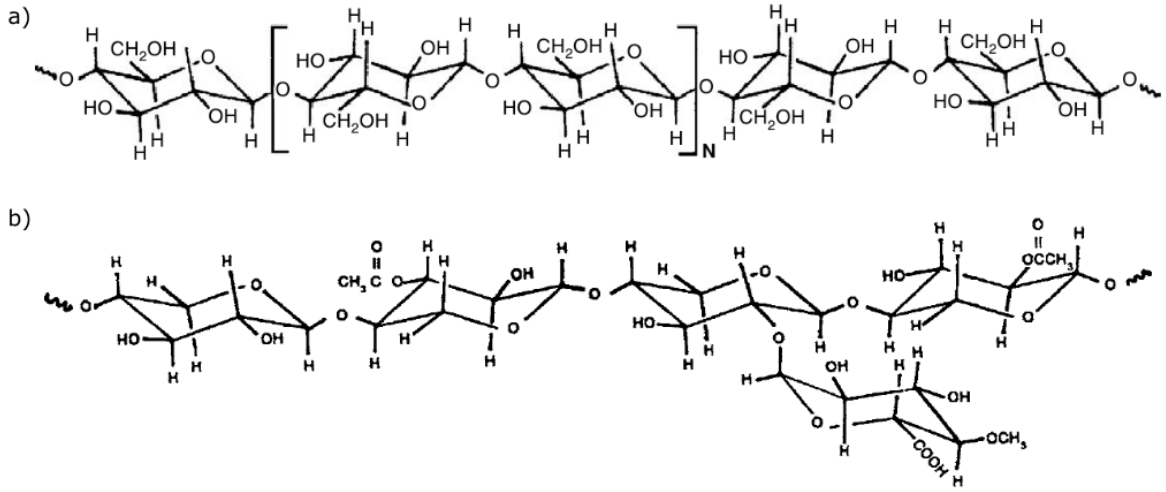

Figure 3-1 Partial structure of a) cellulose b) O-acetyl-4-O-methyl-glucuronoxylan, a hemicellulose. Adapted from Rowell (2012).

Lignin (Figure 3-2a), however, acts as a barrier against decay. Brown- and white-rot fungi have developed different mechanisms to circumvent this barrier. While brown-rot fungi can tap into cellulose and hemicellulose as a nutrient source by slightly modifying the lignin, white-rot fungi can degrade lignin (Figure 3-2b) (Schmidt, 2006; Floudas *et al.*, 2012). For the latter fungi, the type of lignin directly affects the decay rate. In softwoods for instance, guaiacyl is the main lignin type, typically resulting in a slower decay rate of white-rot fungi on softwoods compared to hardwoods (Highley, 1982; Schmidt, 2006; Schwarze, 2007; Li *et al.*, 2015).

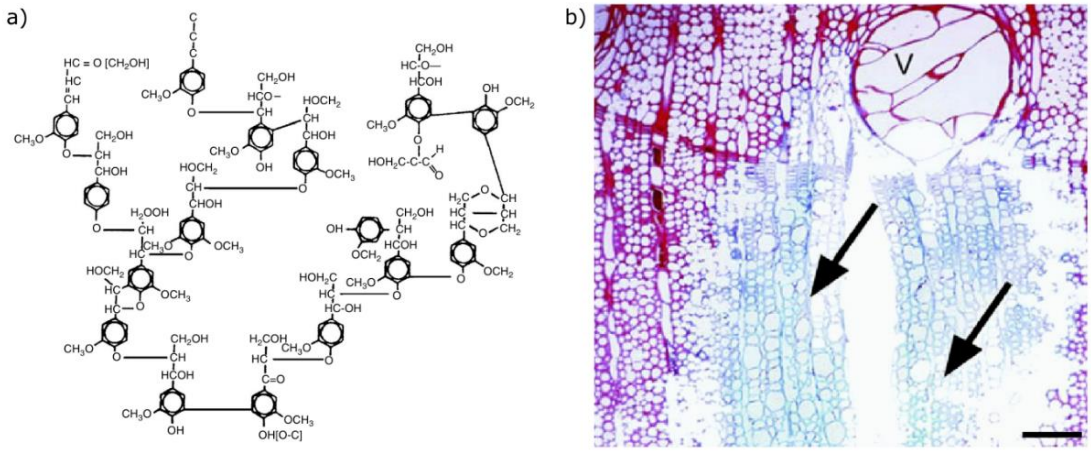

Figure 3-2 a) Partial structure of lignin, adapted from Rowell (2012). b) Transverse section of oak wood degraded by the white-rot fungus *Grifola frondosa,* stained with safranin and astra-blue. Delignified regions (light blue, arrows), surrounded by intact cell regions (red). Bar, 50 mm. V=vessel. Adapted from Schwarze (2007).

Similarly, the extraction and evaluation of potential fungicidal wood components (fatty acids, organic acids, terpenes, tannins, and other benzenoid compounds) have been studied extensively (Figure 3-3). The most common method for evaluating the toxicity of such extracted components is by assessing the effect of an extractive on the development of pure fungal cultures growing in or on a nutrient solution or agar (Hart, 1989; Tchinda, 2018). The effect of a specific fungicidal component can also be assessed by impregnating a wood specimen with such a component and evaluating its decay resistance. However, artificially impregnating wood with an extractive is different from the natural interaction between extractive and (heart)wood. Furthermore, a uniform concentration is hard to achieve. The effect of extractives on the overall durability of wood can also be tested by comparing decay between extracted and non-extracted specimens. It is important to note, however, that often only a weak correlation can be found between a wood's durability and the concentration of extractives (Scalbert, 1992), except in the case of certain highly fungicidal extractives such as tropolones in Cupressaceae (Hart, 1989). This confirms that, for most wood species, other components or material characteristics besides fungicidal extractives contribute to the overall natural durability. Chemical components that have been overlooked, for instance, are moisture-regulating components, even though these are considered important in the natural durability of certain heartwood species (Harju *et al*., 2002; Song *et al*., 2014; De Angelis *et al*., 2018).

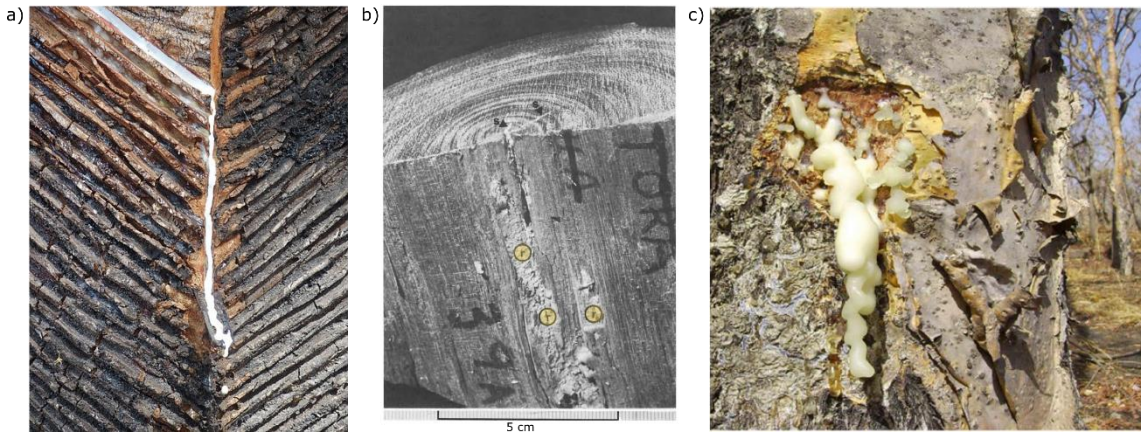

Figure 3-3 a) Latex streaming from rubber tree *Hevea brasiliensis* (Willd. ex A. Juss.) Müll. Arg. © Krishna Naudin b) Portion of a log of *Intsia bijuga* (Colebr.) Kuntze showing crystals of pure robinetin (r), adapted from Hillis (2012), c) Frankincense resin in *Boswellia papyrifera*, adapted from Bongers *et al*., (2019).

In section 3.2, the 'paste test' is introduced, which was developed during this PhD to determine the presence of fungicidal components in wood and bio-based building materials and to assess their effect on fungal growth. In combination with the 'mini-block' test (Bravery, 1978), the paste test was applied to assess the presence of fungicidal components in 10 wood species and reveal the role of material characteristics besides fungicidal components. In section 3.3, 18 commonly used bio-based building materials were subjected to the paste test, to assess whether their components had a growth-inhibiting effect on mycelial development of decay fungi.

3.2 Revealing the impact of decay-influencing characteristics other than fungicidal components in wood

This section is an adapted version of:
De Ligne, L., Van den Bulcke, J., Baetens, J.M., De Baets, B., Wang, G., De Windt, I., Beeckman, H., Van Acker, J. (2020) Unraveling the natural durability of wood: revealing the impact of decay-influencing characteristics other than fungicidal components. Holzforschung. DOI: 10.1515/hf-2020-0109.

With the advent of new renewable materials and modification technologies, there is an increasing need for more insight into how different material characteristics, such as the material's chemistry, structure and moisture dynamics, influence durability. The current standards for testing (treated) wood give an adequate indication of durability, but were not designed to provide fundamental insight into the aforementioned characteristics. Therefore, we developed the 'paste test' to determine the presence of fungicidal components in wood and their influence on fungal growth. In combination with the 'mini-block' test (Bravery, 1978) the importance of fungicidal components on the natural durability of 10 wood species was assessed. In the 'paste test', wood is pulverized to a fine powder, limiting the influence of wood anatomy on fungal growth,

and mixed with water and agar, to minimize the role of moisture-regulating components. The 'mini-block' test (Bravery, 1978) was used to test the durability of solid wood blocks, for which other material characteristics besides fungicidal components are expected to play a role as well. Both sapwood and heartwood specimens of 10 wood species were subjected to the 'paste' and 'mini-block' tests. Since sapwood generally does not contain fungicidal components (Hart, 1989; Hillis, 2012), sapwood specimens were included to confirm the validity of the 'paste test' and to reveal the role of material characteristics besides fungicidal components. In this section, we propose the combination of the paste and mini-block test as a way to assess whether besides fungicidal components, other material characteristics play a crucial role in the durability of a wood species.

3.2.1 Material and Methods

Wood specimens: Mini-blocks of 30 × 10 x 5 (axial) mm^3 were prepared from 10 wood species, covering the full range of natural durability. Table 3-1 gives an overview of the 10 wood species, their durability class (CEN EN 350 standard, 2016), absorption and desorption class (Van Acker *et al*., 2014), and a selection of wood-anatomical features described in literature: vessel/fibre ratio, tracheid proportion and parenchyma content (Wagenführ and Scheiber, 1974). The absorption and desorption classes described in Van Acker *et al*. (2014) are determined on the basis of the floating test, in which wood specimens (50 x 50 x 25 mm^3) are laid afloat a water surface for 144 hours of absorption and left to dry for 144 hours of desorption in a climate chamber (20°C and 65% RH) (CEN TS 16818 standard, 2018). Beech (*Fagus sylvatica* L.) and European cherry (*Prunus avium* L.) are not commonly applied in construction, but are often used for furniture and wooden floors, and as veneer or multiplex for interior design (Houtinfobois, 2021). African padauk (*Pterocarpus soyauxii* Taub), Movingui (*Distemonanthus benthamianus* Baill.), Sapele (*Entandrophragma cylindricum* Sprague) and Sweet chestnut (*Castanea sativa* Mill.) are applied for the same indoor purposes, as well as for exterior woodwork, such as window frames, doors, cladding and decking. Black locust (*Robinia pseudoacacia* L.) is used for interior purposes, cladding and decking and for various outdoor applications, such as fences and poles (Houtinfobois, 2021). Norway spruce (*Picea abies* (L.) Karst) and Scots pine (*Pinus sylvestris* L.) are commonly used as construction materials in the Northern hemisphere (Schmidt, 2006), both as solid wood beams or as processed wood products, such as wood-based panels or wood-fibre insulation materials.

To confirm whether the paste test adequately eliminates the influence of structure and moisture-regulating components on fungal growth, wood specimens with clear differences in structure and hygroscopic components, but with similar nutritional values and fungicidal components, need to be selected. The heartwood of the selected wood species (Table 3-1) contains various fungicidal and moisture-regulating components. Removing these from heartwood is an arduous process requiring a sequence of severe leaching methods. Still, a complete removal of all fungicidal

components from the heartwood cannot be guaranteed (Pettersen, 1984). Therefore, sapwood, generally containing no fungicidal components (Hart, 1989; Hillis, 2012), was used. Leaching is, however, still necessary in order to better mimic the heartwood, as leaching removes nutrients such as starch. Thus, from each species, 40 heartwood and 40 sapwood specimens were collected for the mini-block tests and 20 heartwood and 20 sapwood specimens for the paste test, with the exception of *Robinia pseudoacacia* for which no adequate sapwood specimens could be obtained, due to the small amount of sapwood present on the available *Robinia pseudoacacia* wood sources. The sapwood specimens were leached according to EN 84. First, the sapwood specimens were water saturated under a vacuum corresponding to 4kPa in a desiccator for two hours, after which they remained submerged for 14 days in water. The water was refreshed at the end of the first and second day of immersion and then seven more times during the remaining 12 days (CEN EN 84 standard, 1997). The heartwood specimens can contain both fungicidal substances as well as moisture-regulating components, while sapwood specimens were leached and assumed free of fungicidal components, yet moisture-regulating components might still have been present.

Fungal species: White-rot fungus *Trametes versicolor* (strain MUCL 11665) and brown-rot fungus *Coniophora puteana* (strain MUCL 11662) were used, since both fungi have evolved differently and have developed different mechanisms of degradation (Goodell and Jellison, 1990; Mester *et al*., 2004; Schmidt, 2006; Floudas *et al*., 2012). It is also obligatory to test both fungi for standard testing of (natural) durability against Basidiomycetes (CEN EN 350 standard, 2016; EN 113 standard, 1996; CEN TS 15083-1 standard, 2005).

Mini-block test: All specimens were conditioned in a climate chamber with (20±2) °C and (65±5) % relative humidity. The mini-block test specimens were weighed (m_1 [g]) to the nearest 10^{-4}g and sterilised using 25-50 kGy Gamma irradiation (Synergy Health, Etten-Leur, The Netherlands). Ten additional heartwood and sapwood specimens per species were weighed ($m_{1,ref}$ [g]), then oven-dried at 103 °C ± 2 °C for 24h and weighed ($m_{0,ref}$ [g]) once more to the nearest 10^{-4}g to determine an average reference moisture content (MC [-]) per species:

$$MC = \frac{m_{1,ref} - m_{0,ref}}{m_{0,ref}} \quad (3\text{-}1)$$

This average moisture content was then used to determine the dry weight of the mini-block specimens (m_0 [g]):

$$m_0 = \frac{m_1}{MC+1} \quad (3\text{-}2)$$

Table 3-1 Durability (EN350 standard, 2015), absorption and desorption class (Van Acker *et al.*, 2014), vessel/fibre ratio, tracheid proportion and parenchyma content (Wagenführ and Scheiber, 1974) of selected wood species. The durability class of a wood species in EN350 is assigned according to the Basidiomycete test that resulted in the highest median mass loss, which could be a white- or brown-rot fungus (CEN EN 350 standard, 2016). The absorption class ranges from 1-8, with 1 indicating the wood specimen has absorbed less than 750 g water per m^2 of specimen surface and 8 indicating the specimen has absorbed more than 5000 g water per m^2 of specimen surface after 144h of absorption. The desorption class ranges from 1-8, with 1 indicating that less than 250 g water per m^2 of specimen surface remained after 144h of desorption and 8 indicating that more than 2000 g water per m^2 of specimen surface remained after 144h of desorption.

Wood species	Durability of heartwood against Basidiomycetes in lab conditions	Absorption / Desorption class heartwood	Average vessel/fibre ratio (%)	Parenchyma content (%)
Hardwoods				
Pterocarpus soyauxii Taub	DC 1	4/2	16.3	23.0
Robinia pseudoacacia L.	DC 1-2	2/4	25.9	6.0
Castanea sativa Mill.	DC 1	5/4	46.5	Insignificant
Distemonanthus benthamianus Baill.	x	2/3	37.8	14.0-23.0
Entandrophragma cylindricum Sprague	DC 3-4	4/5	39.3	10.5-30.5
Prunus avium L.	x	5/4	76.6	Insignificant
Aucoumea klaineana Pierre	DC 4-5	3/3	28.8	0.0-3.0
Fagus sylvatica L.	DC 4-5	6/7	99.8	3.5-7.0
Softwoods			Tracheïd proportion (%)	
Picea abies (L.) Karst	DC 4-5	5/5	93.1	-
Pinus sylvestris L.	DC 2-5	5/5	95.3	0.0-5.8

Wood specimens were exposed to actively growing, pure cultures of *Coniophora puteana* and *Trametes versicolor* (20 heartwood and 20 sapwood specimens each). Both fungi were cultivated on Petri dishes (90 mm diameter, 16 mm deep) containing 20 ml of 3% malt / 2% agar medium (Thermo Fisher Diagnostics B.V., Landsmeer, The Netherlands). The mini-blocks were placed on sterilised metal meshes, with three mini-blocks in each Petri dish (Figure 3-4). The Petri dishes were incubated for 10 weeks at 22°C and 70% relative humidity. Subsequently, the mini-blocks were cleaned, weighed, oven-dried and weighed again (m_2 [g]) to determine the loss in dry mass (ML [-]) due to fungal decay:

$$ML = \frac{m_0 - m_2}{m_0} \quad (3\text{-}3)$$

The durability of the specimens was rated between 1 (Very durable) and 5 (Not durable) based on the percentage of mass loss due to fungal decay, as described in standard CEN TS 15083-1 (2005). This rating scale is intended for larger block sizes (50 x 25 x 15 mm^3) exposed for 16 weeks, but Deklerck *et al.* (2019) reported that there is adequate variation in mass loss for mini-blocks of various wood species, exposed for 8 and 12 weeks, to compare durability of the wood species. Additionally, mini-block durability ratings were similar as those described in standard EN350 (Table 3-2) (CEN EN 350 standard, 2016).

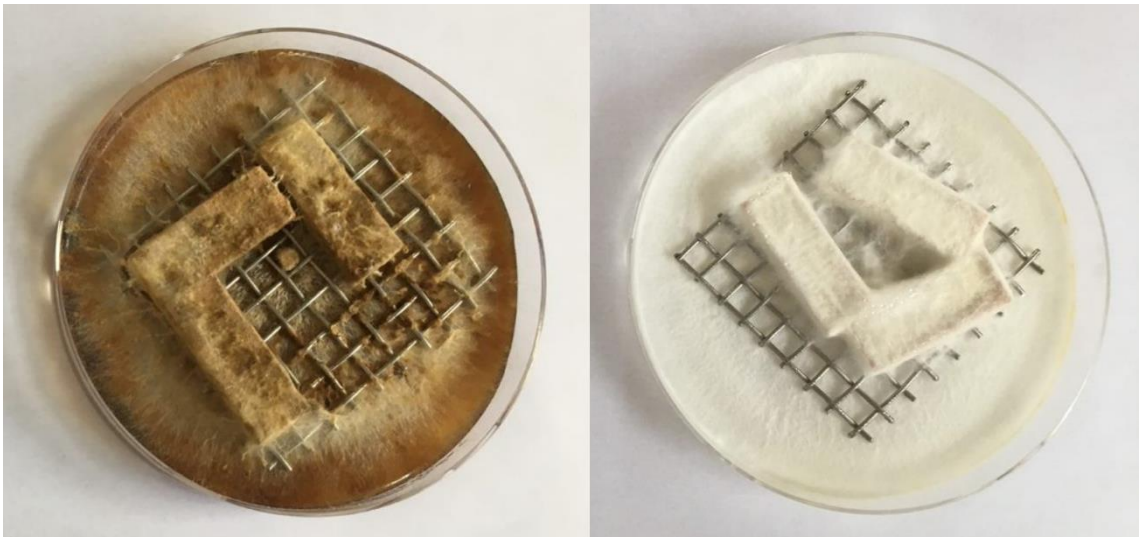

Figure 3-4 Mini-blocks of *Entandrophragma cylindricum* Sprague sapwood after 10 weeks of fungal decay by *C. puteana* (left) and *T. versicolor* (right).

Paste test: The heartwood and leached sapwood specimens were grinded to a coarse powder with a cutting mill with mesh size 0.25 mm (SM 200, Retsch GmbH, Haan, Germany), and then milled to a fine powder (particle size <0.1 mm) with a centrifugal mill (ZM 200, Retsch GmbH, Haan, Germany). The powders were sterilised using 25-50 kGy Gamma irradiation (Synergy Health, Etten-Leur, The Netherlands). For each combination of wood species and fungal type, 6 heartwood and 6 sapwood pastes were prepared. The pastes consisted of 20 ml agar medium (2% malt, 2% agar) and 1.2 g wood powder per Petri dish. The pastes were inoculated with a fungal inoculum disc of 0.7 cm^2. Again, *C. puteana* and *T. versicolor* were used. Additionally, 6 Petri dishes containing only agar medium were inoculated as controls.

The Petri dishes were incubated for 10 days at 22°C and 70% relative humidity. Images of the growing fungi were captured twice a day using a flatbed scanner (Epson perfection V750 Pro) on which two rows of three Petri dishes were mounted, inspired by Vidal-Diez de Ulzurrun *et al.* (2015). The mycelial area was calculated by means of an automated image analysis method developed in-house. First, the region of each Petri dish was extracted from the background by the circular Hough transform method (Hough, 1962). Subsequently, the mycelial area in each Petri dish was segmented by combining a region growing algorithm, adaptive thresholding and mathematical morphological processing, all implemented in MATLAB (Mathworks Inc., 2018). Adequate processing was manually verified for each image, and unsuccessfully analysed images (19% for *C. puteana* and 53% for *T. versicolor*) were reprocessed with the Wand Tool in Fiji (Schindelin *et al.*, 2012). The logistic was fitted per Petri dish (see Figure 3-5 for an example on *Pinus sylvestris* sapwood), so that the logistic growth rate (k [cm^2/day]) could be inferred per replicate:

$$f(x) = \frac{L}{1+e^{-k(x-x_0)}} \quad (3\text{-}4)$$

with L the maximum of f and *k* the logistic growth rate or steepness of the curve.

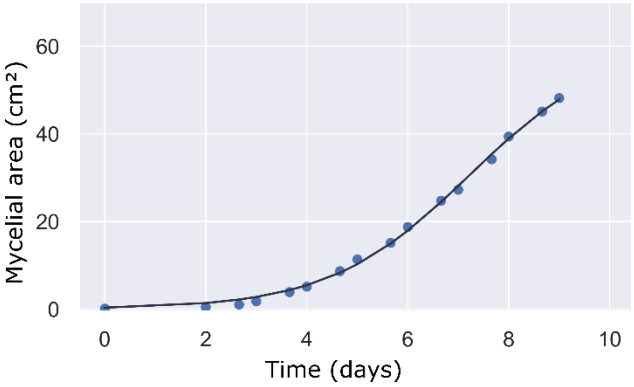

Figure 3-5 Logistic growth curve (Eq. 4) fitted to mycelial development of *C. puteana* growing on a paste of *Pinus sylvestris* sapwood.

3.2.2 Results and discussion

Assessing fungicidal components with the paste test

In the paste test, the wood was ground to a fine powder with a particle size smaller than 0.1 mm. Therefore, the influence of the material structure on fungal growth should be limited. By mixing the wood powder with agar and water, water saturation of the wood powder was ensured, thereby also limiting the influence of water-regulating components. The paste test should thus give an indication of how the overall wood chemistry, consisting of the nutritional value and fungicidal components, influences the fungal susceptibility of a wood species.

First, an assessment was made to test whether the paste teste adequately eliminates the influence of structure and moisture-regulating components. Fungal growth on the leached sapwood pastes is presented relative to the median growth rate of *C. puteana* and *T. versicolor* growing on a paste of pure malt agar without wood powder (5.2 ± 0.7 and 11.9 ± 1.9 cm^2 day-1, respectively). *Trametes versicolor* grew at a similar rate on the different sapwood pastes compared to the pure malt agar pastes (Figure 3-6). Since the growth rate was similar on all leached sapwood pastes, this confirms that leaching sapwood removes any fungicidal component that has a growth inhibitory effect on *T. versicolor*. Furthermore, it also confirms that the paste test adequately eliminates the influence of structure and hydrophobic components on mycelial development of *T. versicolor* and thus allows to assess the influence of wood-fungicidal components. *Coniophora puteana* grew faster on wood pastes than on the control pastes, with the exception of *Prunus avium* (Figure 3-6). The wood powder thus had a growth-promoting effect on *C. puteana*, indicating that *C. puteana* is cellulose-specific. While the growth rate of *C. puteana* was relatively low on *Prunus avium* and comparable to the growth rate on pure malt agar paste, it grew much denser (Figure

3-7b) on the sapwood of *Prunus avium* than on all other sapwood pastes, which had a mycelial density similar to the one displayed on the paste of *Pterocarpus soyauxii* sapwood (Figure 3-7a). The lower growth rate on *Prunus avium* sapwood was therefore most likely not the result of any fungicidal effect. Typical display of a growth inhibiting effect on the mycelial development of *C. puteana* can be seen for *Pterocarpus soyauxii* heartwood (Figure 3-7c) and *Prunus avium* heartwood (Figure 3-7d). However, if this accumulation of mycelium were to occur abundantly in future experiments, it might be interesting to quantify this mycelium density in addition to mycelial area. In general, the paste test on leached sapwood specimens resulted in similar fungal growth behaviour for the 10 wood species, indicating that grinding and moisture saturation adequately removes the influence of structure and moisture-regulating components on fungal growth.

Secondly, an assessment was made whether the paste test can be used to determine the presence of fungicidal components in wood. The results of the heartwood pastes (Figure 3-6) confirmed that the heartwood of *Pterocarpus soyauxii*, *Castanea sativa*, *Distemonanthus benthamianus*, *Prunus avium* and *Pinus sylvestris* clearly contain fungicidal components that are growth inhibiting for *C. puteana*. While the growth rate of *C. puteana* approached zero, the one of *T. versicolor* was merely reduced.

The overall heartwood natural durability according to the mini-block test of the 10 wood species is shown in Figure 3-8. The results from the paste tests (Figure 3-6) and mini-block tests (Figure 3-8) were compared to determine if in addition to fungicidal components other wood characteristics, such as the wood-anatomical structure or hydrophobicity, have an impact on the overall natural durability of a wood species. Due to their size, the anatomical structure and water-regulating components were not expected to have a similar effect for mini-blocks as for wood in practice. Nevertheless, both factors seemed to have a considerable impact on durability, even in a mini-block test set-up as shown in Table 3-2. This table gives an overview of the heartwood durability of the 10 wood species and specific factors that have an impact on their resistance against *C. puteana* and *T. versicolor*. Note that the heartwood durability classes according to the mini-block test (DC_m HW) correspond to the heartwood durability classes described in standard CEN EN 350 (Table 3-2).

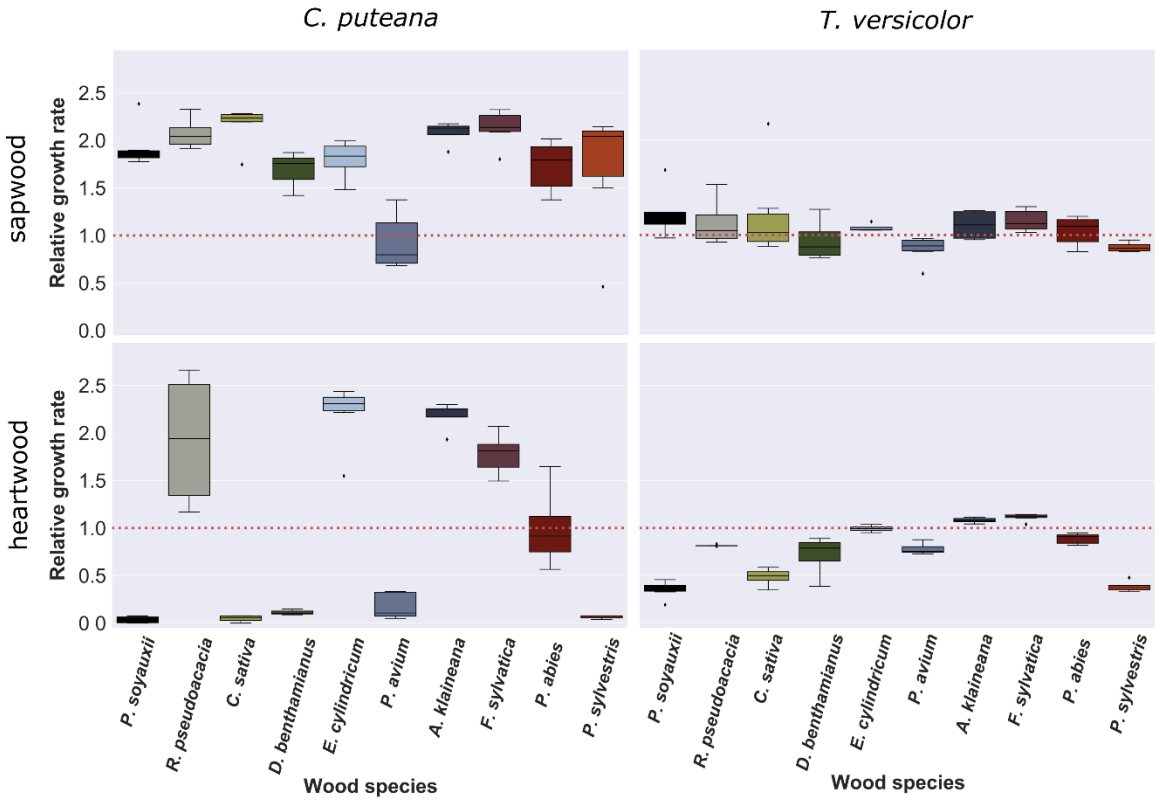

Figure 3-6 Paste test: Relative growth rate of *C. puteana* and *T. versicolor*, growing on sapwood and heartwood pastes of ten wood species. The red dotted line corresponds to the median growth rate on malt agar medium without wood powder (5.25 cm^2 day^{-1} for *C. puteana* and 11.7 cm^2 day^{-1} for *T. versicolor*).

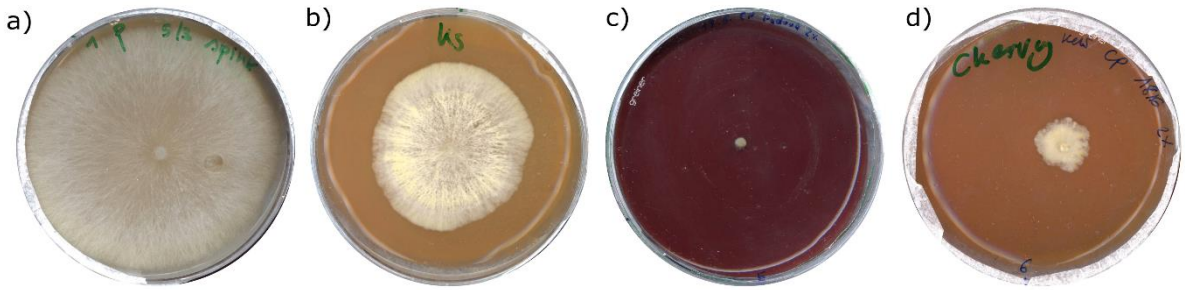

Figure 3-7 Mycelium of *C. puteana* 9 days after inoculation on pastes of a) leached *Pterocarpus soyauxii* sapwood, b) leached *Prunus avium* sapwood, c) *Pterocarpus soyauxii* heartwood and d) *Prunus avium* heartwood.

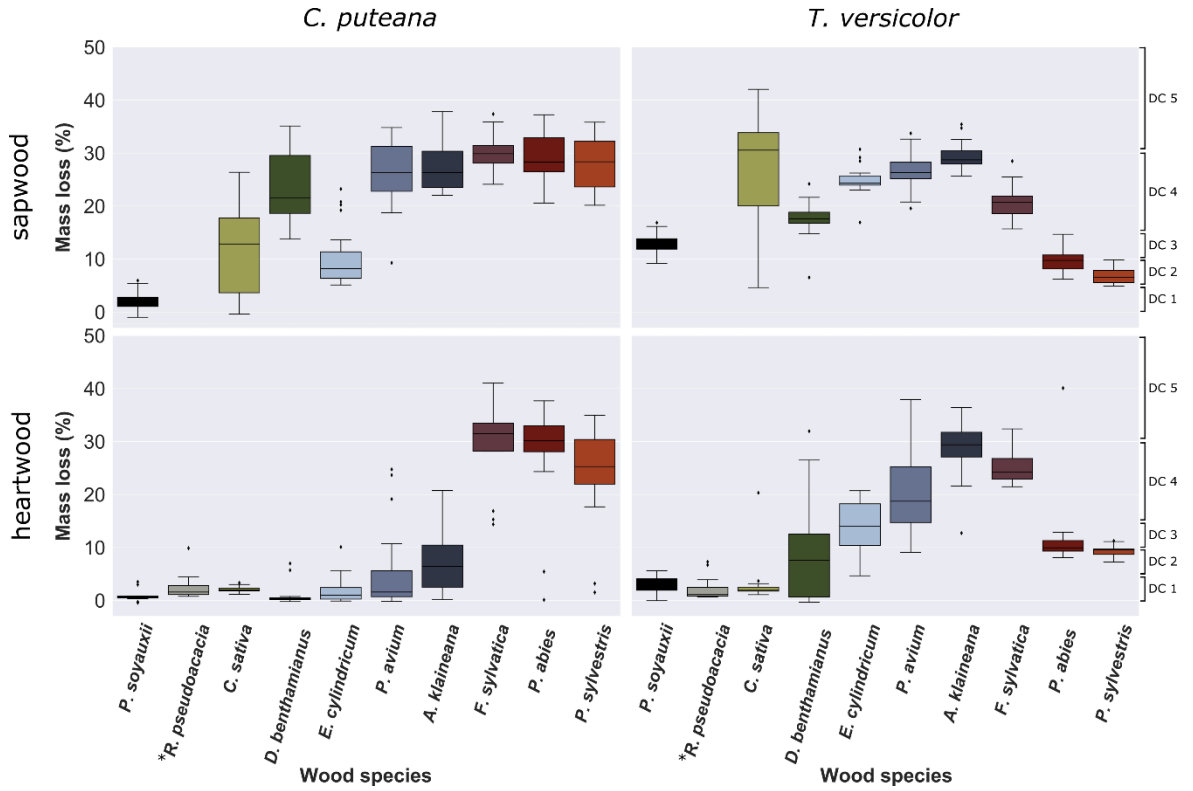

Figure 3-8 Mini-block test: Mass loss after 10 weeks of fungal decay by *C. puteana* and *T. versicolor*, growing on sapwood and heartwood mini-blocks of ten wood species. The axis on the right displays the durability classes as described by CEN TS 15083-1 standard (2005). **Robinia pseudoacacia* was excluded from the sapwood mini-block test due to limited sapwood availability.

Impact of moisture-regulating components on natural durability

When analysing each wood species, it became apparent that different wood species owe their durability to different factors. For instance, *Pterocarpus soyauxii* clearly contained fungicidal components, as shown in the results from the heartwood paste test (Figure 3-6) and supported by previous studies on its extractives (Mounguengui *et al.*, 2016). Growth of *C. puteana* on the *Pterocarpus soyauxii* heartwood paste was limited, and the growth rate of *T. versicolor* was two times lower than on pure malt agar medium (2% MEA). However, the fungicidal components were not the only responsible factors for the high durability of *Pterocarpus soyauxii*: sapwood mini-blocks, without any fungicidal components, showed resistance against degradation as well. *Pterocarpus soyauxii* thus contains moisture-regulating components and/or has an anatomical structure that acted as a barrier to fungal growth. This additional protection was more effective against *C. puteana* (sapwood mini-block DCm 1) than against *T. versicolor* (sapwood mini-block DCm 3). Jankowska *et al.* (2018) indeed found a high percentage of moisture-regulating components in *Pterocarpus soyauxii* heartwood, in the form of extractives soluble in ethanol-chloroform, which correspond to waxes, fats, resins and oils (ASTM D1107-96 standard, 2013), and extractives soluble in cyclohexane, which probably correspond to oleoresins (Hillis, 2012). *Castanea sativa* gave similar results as *Pterocarpus soyauxii*, though less pronounced. In literature, the

high durability of *Castanea sativa* heartwood is attributed to its high concentration of tannins (Scalbert, 1991; Eichhorn *et al*., 2017).

Table 3-2 Overview of factors contributing to the overall natural durability of the heartwood of ten wood species against degradation by *C. puteana* and *T. versicolor*, based on the paste and mini-block tests. DC_m gives the durability class based on the median amount of mass loss (ML) after 10 weeks of degradation in a mini-block set-up, based on CEN TS 15083-1 standard (2005) (DC_m1: ML <5%, DC_m2: 5%<ML≤10%, DC_m3: 10%<ML≤15%, DC_m4: 15%<ML≤30%, DC_m5: 30%<ML) for heartwood (HW) and sapwood (SW). A potential effect of fungicidal components (F) and water regulating components and/or structure (WR/S) is indicated with an 'x'. In the WR/S columns the 'u' (unknown) is used when the influence of moisture-regulating components and/or structure can neither be proven nor rejected. DC HW EN350 indicates the heartwood durability class of the wood species according to standard CEN EN 350, Annex B. The durability class of a wood species in EN350 is assigned according to the Basidiomycete test that resulted in the highest median mass loss, which could be a white or brown rot fungus (CEN EN 350 standard, 2016).

Wood species	Commercial name	Coniophora puteana				Trametes versicolor				DC HW EN350
		DC_m HW	DC_m SW	F	WR/S	DC_m HW	DC_m SW	F	WR/S	
Hardwoods										
Pterocarpus soyauxii Taub	African padauk	DC_m 1	DC_m 1	x	x	DC_m 1	DC_m 3	x	x	DC 1
Robinia pseudoacacia L.	Black locust	DC_m 1	/	x	u	DC_m 1	/	x	x	DC 1-2
Castanea sativa Mill.	Sweet chestnut	DC_m 1	DC_m 3	x	x	DC_m 1	DC_m 5	x	u	DC 1
Distemonanthus benthamianus Baill.	Movingui	DC_m 1	DC_m 4	x	u	DC_m 2	DC_m 4	x	u	/
Entandrophragma cylindricum Sprague	Sapele	DC_m 1	DC_m 2		x	DC_m 3	DC_m 4		x	DC 3-4
Prunus avium L.	European cherry	DC_m 1	DC_m 4	x	u	DC_m 4	DC_m 4	x	x	/
Aucoumea klaineana Pierre	Okoumé	DC_m 2	DC_m 4		x	DC_m 4	DC_m 4			DC 4-5
Fagus sylvatica L.	Beech	DC_m 5	DC_m 4			DC_m 4	DC_m 4			DC 4-5
Softwoods										
Picea abies (L.) Karst	Norway spruce	DC_m 5	DC_m 4			DC_m 2	DC_m 2			DC 4-5
Pinus sylvestris L.	Scots pine	DC_m 4	DC_m 4	x		DC_m 2	DC_m 2	x		DC 2-5

The natural durability of *Robinia pseudoacacia* is attributed to phenolic compounds and the flavonoid robinetin (Hart, 1989; Dünisch *et al*., 2010), while flavonoids in general have only a very low toxic effect on decay fungi (Hart, 1989). The growth rate of *T. versicolor* on *Robinia pseudoacacia* heartwood paste was indeed only 0.8 times the growth rate on pure malt agar medium, indicating the presence of fungicidal components effective against *T. versicolor*. However, it did not contain components fungicidal for *C. puteana* (Figure 3-6). It is therefore plausible that moisture-regulating components and/or anatomical structure also have impact on the high durability of the heartwood of this wood species against both fungi. Indeed, *Robinia pseudoacacia* has excellent moisture properties, as it is classified in absorption class 2, indicating a low amount of water absorption during a floating test (Van Acker *et al*., 2014), although it performs less on desorption (class 4).

The high durability of *Distemonanthus benthamianus* heartwood against *C. puteana* (DC_m 1) and *T. versicolor* (DC_m 2) seemed to be due to the presence of fungicidal components only (Figure 3-6), since sapwood mini-blocks of these species were not resistant (Figure 3-8). However, moisture-regulating components could be present in the heartwood and not in the sapwood, which have an additional effect on the overall durability. This was demonstrated by the heartwood resistance of *Aucoumea klaineana* (DC_m 2) against *C. puteana*. The *Aucoumea klaineana* heartwood paste had no fungicidal effect (Figure 3-6) and the sapwood mini-block test neither indicated an influence of moisture-regulating components nor of wood structure (Figure 3-8). This could point to the presence of moisture-regulating components in the heartwood, not present in leached sapwood mini-blocks, which is plausible since both *Distemonanthus benthamianus* and *Aucoumea klaineana* belong to absorption and desorption classes 2/3 and 3/3 (Table 3-1) and contain high concentrations of sterols and terpenes (Mounguengui *et al*., 2016). These molecules were important in heartwood durability of *Aucoumea klaineana* against *C. puteana* (DC_m 2), but did not seem to affect the resistance against *T. versicolor* (DC_m 4). *Entandrophragma cylindricum*, like *Aucoumea klaineana*, is a distinct example of a wood species where moisture-regulating components and/or structure were of importance for the heartwood durability, given the absence of any fungicidal effect in the heartwood paste test, and the higher durability of the (leached) sapwood (Table 3-2). *Entandrophragma cylindricum* indeed contains a relatively high concentration of extractives soluble in cyclohexane (Jankowska *et al*., 2018), which probably corresponds to oleoresins (Hillis, 2012). Note that *Entandrophragma cylindricum* neither belongs to a good absorption class, nor desorption class (Table 3-1). However, the floating test might give a distorted result in the case of *Entandrophragma cylindricum*, as this species has interlocking grain patterns leading to increased absorption through the longitudinal face.

The high durability of *Prunus avium* heartwood (DC_m 1) against *C. puteana* seemed to be primarily due to the presence of fungicidal components (Figure 3-6), since sapwood mini-blocks of this wood species were degraded substantially by *C. puteana* (Figure 3-8). Nevertheless, moisture-regulating components in the heartwood, not present in the (leached) sapwood, could be of importance (see above). It should be noted, however, that in a previous study on *Prunus avium* extractives, Kebbi-Benkeder *et al*. (2015) found high concentrations of flavonoids, but did not mention fatty acids or resin acids. Also, *Prunus avium* belongs to absorption class 5 and desorption class 4 (Table 3-1). The growth rate of *T. versicolor* on *Prunus avium* heartwood paste was 0.8 times the growth rate on a pure malt extract paste. Then again, fungicidal components only had a minor effect on the heartwood resistance against *T. versicolor* (DC_m 4), which could be attributed to a stronger effect or higher accessibility of the fungicidal components in a paste set-up than in an actual mini-block test.

Fagus sylvatica did not seem to have much protection against fungal attack under laboratory conditions (Table 3-2), which is already well known (CEN EN 350 standard,

2016). There was no indication of structure/moisture-regulating components having a major impact, and the heartwood paste test indicated no fungicidal effects. In fact, the heartwood mini-blocks (DC_m 5) seemed to be slightly more degraded by *C. puteana* than the leached sapwood (DC_m 4), although the mass losses were not found to be significantly different based on Welch's t-test for testing unequal variances (p-value= 0.824; Welch, 1938).

Picea abies and *Pinus sylvestris* were not durable against brown-rot fungus *C. puteana*, while they showed a high resistance against *T. versicolor*. This confirms common knowledge, since white-rot fungi are known to degrade softwoods slower than hardwoods, due to the difference in the main lignin type (Highley, 1982). It should be noted, however, that both species indicated fungicidal activity against *C. puteana* and *T. versicolor*, while the heartwood was not or only slightly more durable than the sapwood (Figure 3-8). This fungicidal activity was most prominent for *Pinus sylvestris*, with heartwood paste results similar to those of *Pterocarpus soyauxii*, maybe due to stilbenes in *Pinus sylvestris* (Chiron *et al.*, 2000). In practice, wood containing stilbenes often decomposes slowly. When tested on a nutrient agar substrate, stilbenes have been shown to be highly fungicidal (Hart, 1989). On a woody substrate, however, the toxicity of stilbenes is reduced with 90 up to 99% (Hart, 1989). Furthermore, even though conifers contain resins (Schmidt, 2006; Rissanen, 2019), both wood species belong to absorption and desorption class 5 (Table 3-1). Obviously, the type of moisture-regulating component as well as the location in the wood structure can be of major importance. Furthermore, since *C. puteana* is a true softwood-degrading specialist, the fungus might have developed another way to circumvent this particular arrangement of moisture-regulating components.

Impact of wood anatomy on natural durability

Although the test set-up can be used to assess the importance of fungicidal effects versus other decay-influencing factors, it did not allow to distinguish between the impact of moisture-regulating components and structure separately. Also, anatomical structure and moisture dynamics are often related, especially in the over-hygroscopic range (Fredriksson, 2019; Brischke and Alfredsen, 2020). For instance, wood with a low density can take up more water, as it has a larger volume of voids. Also, the size of the pit openings in the wood cells affects the desorption rate of wood (Fredriksson, 2019). The wood-anatomical structure also affects degradation and degradation patterns, as the ratio of different cell types influences the penetration and colonization ability of fungal hyphae, and determines whether the fungus can tap into the nutrient sources in the wood structure (Bravery, 1975; Daniel, 2003; Schwarze, 2007; Antwi-Boasiako and Atta-Obeng, 2009). When the paste and mini-block test indicated an influence of structure and/or moisture-regulating components, the latter concurred with literature on such components in the respective wood species and literature on moisture dynamics, such as the absorption and desorption classes described in Van Acker *et al.* (2014). Similarly, a connection between wood-anatomical features (Table 3-2) and

durability might be found. The wood species of interest are those for which also the sapwood mini-blocks are durable against degradation, as was the case for *Pterocarpus soyauxii*, *Castanea sativa* and *Entandrophragma cylindricum* against *C. puteana* (Figure 3-8). One of the wood-anatomical features that has been correlated to durability is the number of vessels versus the amount of fibres in the wood, or the vessel-fibre ratio (Table 3-1). Antwi-Boasiako and Atta-Obeng (2009) attribute the high durability of the Ghanaian hardwood species *Milicia excelsa* (Welw.) C.C. Berg to its low vessel-fibre ratio (5-20%), indicating that the wood species contained relatively less vessels as compared to the other assessed wood species, which had a vessel-fibre ratio of about 20-50%. This factor is therefore also a likely contributor to the high durability of *Pterocarpus soyauxii*, which has an average vessel-fibre ratio of 16.3%. Another feature that possibly increases decay resistance is a high parenchyma content (Table 3-1), although only against brown-rot fungi. Schwarze (2007) postulates that this resistance is related to the cell wall morphology of parenchyma cells, possibly reflecting a low co-evolutionary adaptation of brown rot fungi to the xylem of hardwood species. *Entandrophragma cylindricum* and *Pterocarpus soyauxii* both have high parenchyma contents, supporting this theory. However, similar parenchyma contents did not seem to lead to a similar resistance against *C. puteana* in the case of *Distemonanthus benthamianus*.

Importance of testing both brown-rot and white-rot fungi

In general, unravelling the durability of heartwood mini-blocks against *T. versicolor* was less straightforward than for *C. puteana*, since the former was less affected by the fungicidal components in the paste set-up. Both fungi have evolved differently and have developed different mechanisms of degradation (Goodell and Jellison, 1990; Mester *et al.*, 2004; Schmidt, 2006; Floudas *et al.*, 2012). The results from this study emphasized the importance of testing with both fungi, since some wood-protection mechanisms resulted in a high resistance against one fungus, but not against the other. The lignin barrier, for instance, resulted in DC_m 2 for softwoods against *T. versicolor* and DC_m 4 and 5 against *C. puteana*. Furthermore, hydrophobicity and/or anatomy also affected the growth of both fungi differently. While *Pterocarpus soyauxii* sapwood was classified as DC_m 1 against *C. puteana*, these wood characteristics had a lesser effect on *T. versicolor* (DC_m 3). A similar behaviour was found for *Entandrophragma cylindricum*, for which the sapwood was classified as DC_m 4 and the heartwood as DC_m 3 for *T. versicolor*, indicating an effect of moisture-regulating components and/or anatomical structure, but less important than in the case of *C. puteana*. Finally, the mode of action of fungicidal components affecting fungal growth was of importance as well. Since the extracellular enzymes of brown-rot and white-rot fungi differ in their mode of action and molecular size, many wood-fungicidal components are not able to affect growth of a broad spectrum of fungal species, but act fungus specific (Hart, 1989), which was confirmed by our results. Not only had fungicidal components less impact on the mycelial development of *T. versicolor* than of *C. puteana*, there were also

wood species for which the fungicidal components appeared to be more effective against *C. puteana*.

3.2.3 Conclusions

The approach presented in this section is useful to assess the importance of fungicidal effects on the durability of wood and wood-based products, and to reveal the impact of other decay-influencing factors such as wood-anatomical features, moisture-regulating components and lignin type. It does not allow to distinguish between the impact of moisture-regulating components and wood anatomy. When the paste and mini-block tests hinted at an effect of moisture-regulating components on the durability, literature on such components and moisture dynamics in the respective wood species agreed with these findings. When it comes to wood-anatomical features, vessel-fibre ratio and parenchyma content were selected as factors possibly influencing decay, although many other wood-anatomical features could be of importance. The low vessel-fibre ratio of *Pterocarpus soyauxii* likely contributed to its high durability. A high parenchyma content could possibly play a role in the durability of *Pterocarpus soyauxii* and *Entandrophragma cylindricum* sapwood and heartwood, although this was, for instance, not the case for *Distemonanthus benthamianus* sapwood resistance against brown-rot fungus *C. puteana*. Overall, it is clear that different wood species owe their durability to a combination of properties. While some species combined fungicidal components with proper moisture control (*Pterocarpus soyauxii*), other species were (moderately) durable due to their fungicidal components (*Prunus avium*), or relied partly (*Robinia pseudoacacia*, *Distemonanthus benthamianus*, *Castanea sativa*) or mainly (*Aucoumea klaineana*, *Entandrophragma cylindricum*) on moisture-regulating components. In the case of white rot, the presence of guaiacyl lignin also seemed to play a role (*Picea abies*, *Pinus sylvestris*).

Fungicidal components were not always of major importance for the durability of a wood species. We hereby emphasize the importance of moisture-regulating components and wood anatomy on the durability of wood.

3.3 Assessing fungicidal components in bio-based building materials

This section is an adapted version of:
De Ligne, L., Caes, J., Omar, S., Van den Bulcke, J. Baetens, J.M., De Baets, B., Van Acker, J. (2020) Performance of bio-based building materials – durability and moisture dynamics. Proceedings IRG Annual Meeting 2020 (online conference), 16 pp.

Paste test

Bio-based building materials are usually made from natural fibres in combination with additives, such as glue, fire retardants and biocides. Both the fibres as well as the added components can have fungicidal properties. It has, for instance, been shown that the amount and type of glue applied in oriented strand board (OSB) affects its durability against decay fungi (Okino *et al*., 2007). However, it is not always clear whether this increased durability is an effect of fungicidal properties, or if the amount of glue affects other material properties that can affect durability, such as the material structure or moisture performance. In section 3.2, the 'paste test' was shown to be an adequate method for assessing the influence of fungicidal components in wood. In this section, the same method was applied on 18 commonly used bio-based building materials.

Adapted mini-block test

The mini-block test is presumably not suited for testing the overall durability of a bio-based building material. It has the same issues as described earlier in section 1.5.4 for the standard laboratory method for determining the natural durability of solid wood against wood-destroying fungi (CEN TS 15083-1 standard, 2005), on which the mini-block test was based. The impact of sample size is even more pronounced, as the mini-block volumes (30 × 10 x 5 mm^3) are 12.5 times smaller than the standard wood samples (50 x 25 x 15 mm^3).

Moisture related issues might occur as well and influence the results. Laboratory tests are performed under optimal conditions for the test fungus. The fungal growth medium does not only contain nutrients for the fungus, but also ensures a moisture content sufficient for fungal activity. If a wood specimen did not reach the required moisture content, the test may be declared invalid according to the strict interpretation of the standard test (CEN TS 15083-1 standard, 2005). However, the moisture dynamics of engineered wood products and modified wood may have changed in such a way that abovementioned criteria are not met. For instance, thermal and chemical modifications change the wood-water interactions in such a way that the resulting Equilibrium Moisture Content (EMC) of modified wood is lower than the one for the equivalent non-modified wood (Verma *et al*., 2009; Ringman *et al*., 2014; Ormondroyd *et al*., 2015; Candelier *et al*., 2016). The modified wood specimens might not reach a sufficient high moisture content (MC) during the test period for the fungus to reach significant degradation. This does not mean, however, that these materials cannot eventually become wet enough for degradation. Kamdem *et al*. (2002) confirmed that

after a period of six weeks exposure, the modified wood specimens did become wet and noted moisture contents varying between 72% and 156%. We therefore need to contemplate whether the set-up of the standard needs to be adapted, for instance by increasing the initial moisture content of the modified wood and bio-based materials, or whether fungal decay needs to be observed under the same humidity conditions as for non-modified solid wood (Ormondroyd *et al*., 2015). Defoirdt *et al*. (2010), for instance, propose to include a pre-treatment to bring wood-plastic composites to a high moisture level before the fungal test.

As a preliminary experiment, we decided to condition a selection of bio-based materials to a MC of 20-30%, before exposure to brown-rot fungus *Coniophora puteana*, to see whether they would be degraded in optimal moisture conditions. For a more insightful understanding of how material structure and moisture dynamics relate to decay of bio-based building materials, see Chapters 4 and 5.

3.3.1 Material and methods

Bio-based materials: 18 commonly used bio-based building materials were selected (Table 3-3). To have a broad view on the fungicidal properties of bio-based building materials in general, we opted for materials that differ in basic components (wood, cork, cotton, flax, cellulose fibre), additives (such as glue, paraffin, bitumen, fire retardants and boric acid) and production process. Four commonly used wood-based panels (radiata pine plywood, thermally modified and unmodified three-layer spruce panel and oriented strand board), thermally modified spruce wood and seven wood fibre insulation materials were used. The wood fibre insulation materials contain different additives, differ in density and were made with different production processes. In the wet production process, wood chips and shavings are ground down into wood fibre pulp and mixed with water and possibly additives, such as paraffin. This mix forms a continuous fibre mat, from which half of the water is removed with a mechanical press (Figure 3-9). The lignin in the wood fibres serves as a natural binding agent when heated with water, so no binding agent needs to be added. In the dry production process, the wood fibre pulp is glued together with isocyanate (Figure 3-10). The adhesives are cured and hardened through exposure to a mixture of water vapour and air. In addition, six non-wood-fibre insulation materials based on flax, cork, cotton or cellulose fibre were tested as well.

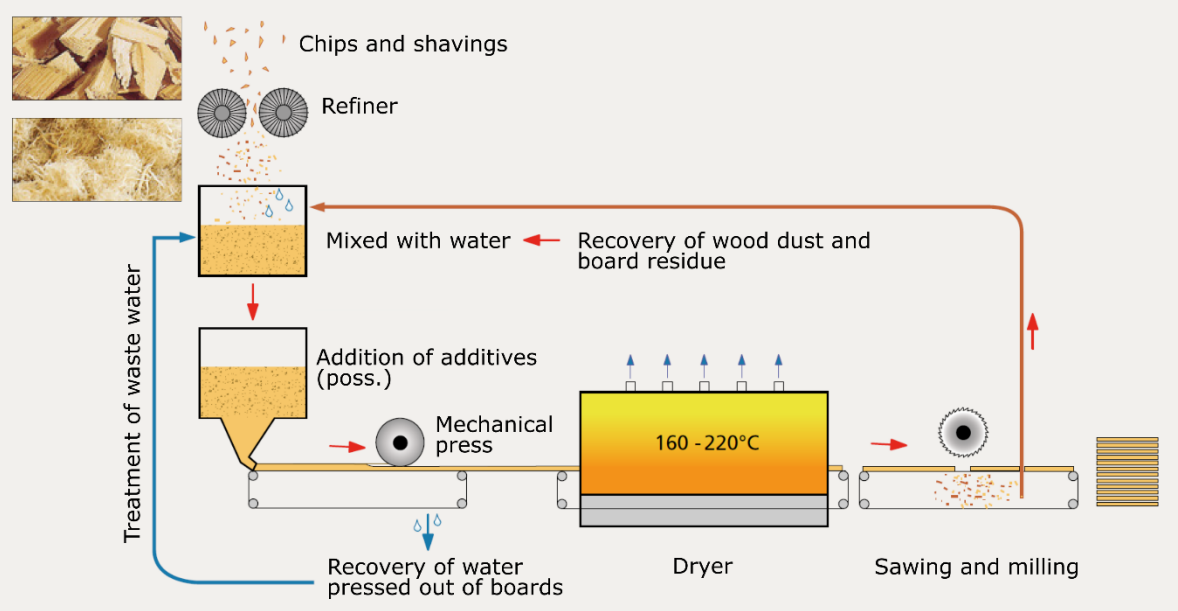

Figure 3-9 Illustration of wet production process. Adapted from Dederich *et al.* (2019).

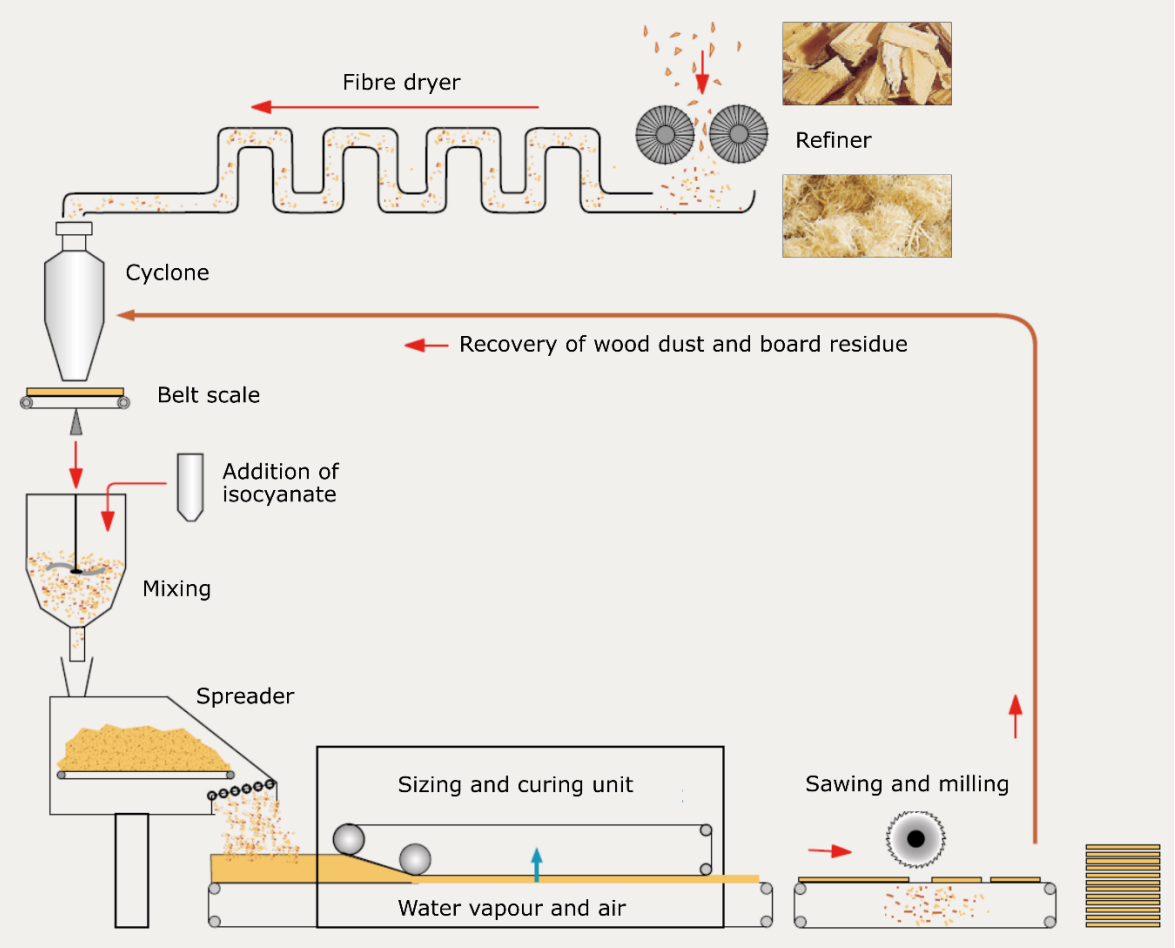

Figure 3-10 Illustration of dry production process. Adapted from Dederich *et al.* (2019).

Table 3-3 Overview of selected bio-based materials and their main components and/or treatments.

Label	Material	Components and/or treatment
Wood-based panels		
PLY	Plywood Radiata pine	Radiata pine veneers, glue (non-specified)
TMT	Thermally modified spruce	Process: 1) Hydrothermolysis up to 170°C 2) drying 3) heated again to up to 180^{0}C in dry conditions without oxygen
SWP	Three-layer spruce binder	Spruce, isocyanate adhesive
TMSWP	Thermally modified three-layer spruce binder	Thermal modification of spruce wood (approx. 200°C) before binder production. Adhesive non-specified.
OSB	Oriented strand board	Scots pine fibres, isocyanate adhesive
Wood-fibre insulation		
WFIB1	Wood fibre insulation mat 1	Norway spruce/Scots pine fibres, ammonium phosphate, polyolefin fibres
WFIB2	Wood fibre insulation board 2	Norway spruce/Scots pine fibres, wet production
WFIB3	Wood fibre insulation board 3	Norway spruce/Scots pine fibres, isocyanate adhesive (4%), paraffin (4%), dry production
WFIB4	Wood fibre insulation board 4	Norway spruce/Scots pine fibres, aluminium sulphate, paraffin (4%), dye, wet production
WFIB5	Wood fibre insulation board 5	Norway spruce/Scots pine fibres, isocyanate adhesive (4%), paraffin (4%), aluminium sulphate, silicates, hydrophobic products, dry production
AIWF	Air-injected wood fibre insulation	Norway spruce/Scots pine fibres
BWFIB	Porous wood fibre board with bitumen	Norway spruce/Scots pine fibres, bitumen emulsion
Non-wood-fibre insulation		
Cell	Cellulose fibre insulation	Cellulose fibres (recycled paper), boric acid, magnesium sulphate
C	Cotton insulation	77% recycled textile fibres, 15% polyester fibres and 8% other (fire retardant and biocide (non-specified))
FI	Flax insulation	Flax fibres, binder (unspecified), fire retardant (unspecified)
ECB	Expanded cork board	Cork granules expanded at high temperature. No additives.
ECG	Expanded cork granules	Cork granules expanded at high temperature. No additives.
NECG	Non-expanded cork granules	No additives.

Fungal species: The brown-rot fungus *Coniophora puteana* (strain MUCL 11662) was used for the paste test, since this fungus is highly sensitive to the presence of fungicidal components, as shown in section 3.2. Additionally, the selected wood-based materials were primarily made from softwood species, and brown-rot fungi preferentially decay softwood (Highley, 1982). For the adapted mini-block test, both *C. puteana* and *Trametes versicolor* (strain MUCL 11665) were used, since both fungi have evolved differently and have developed different degradation mechanisms (Goodell and Jellison, 1990; Mester *et al.*, 2004; Schmidt, 2006; Floudas *et al.*, 2012). Both fungi are also mandatory test fungi in standard testing of (natural) durability against Basidiomycetes (CEN EN 350 standard, 2016; CEN EN 113 standard, 1996; CEN TS 15083-1 standard, 2005).

Paste test: In the paste test (see section 3.2.1), the bio-based materials were ground to a fine powder with a particle size smaller than 0.1 mm, thus limiting the influence of the material's structure on fungal growth. By mixing the powder with agar and water, the powder was water saturated, thereby also limiting the influence of hydrophobic components. The resulting paste was poured in a Petri dish (6 replicates per material) and inoculated with *C. puteana*. Mycelial growth was assessed over time with a flatbed scanner, from which the logistic growth rate for each paste was derived. The growth rate on bio-based material pastes was represented relative to the growth rate of *C.*

puteana on a pure malt agar paste (8.7 cm^2 day^{-1}). The paste test thus gives an indication of how the nutritional value and fungicidal components influence the fungal susceptibility of a bio-based material.

Adapted mini-block test: *Coniophora puteana* and *Trametes versicolor* were grown in Petri dishes (diameter 9 cm), filled with 20 ml malt agar medium (3% malt, 2% agar). Mini-blocks (30 × 10 x 5 mm^3) of Scots pine sapwood, OSB, BWFIB, PLY, TMT, WFIB3 and WFIB5 were oven dried, weighed and sterilized under steam at 121°C. For Scots pine sapwood and TMT, the longitudinal direction of the mini-block corresponded to the direction of the wood grain. For OSB and the wood fibre insulation boards, the top side of the mini-block corresponded to the top side of the original board, while for PLY the plies were positioned at the top side (Figure 3-11). After sterilisation, the mini-blocks were placed in a vacuum desiccator and water saturated under vacuum. Then, the mini-blocks were conditioned in a laminar flow and regularly weighed until a MC in the range of 20-30% was reached. When the desired MC was reached, they were wrapped in aluminium foil and stored in the fridge. At the start of the experiment, the MC of all blocks was determined, before placing the mini-blocks on the fungal cultures. After 8 weeks of exposure to *C. puteana* and *T. versicolor*, the mini-blocks were cleaned, weighed, oven dried and weighed again, to determine the MC at the end of the test and the mass loss due to fungal decay (see section 3.2.1).

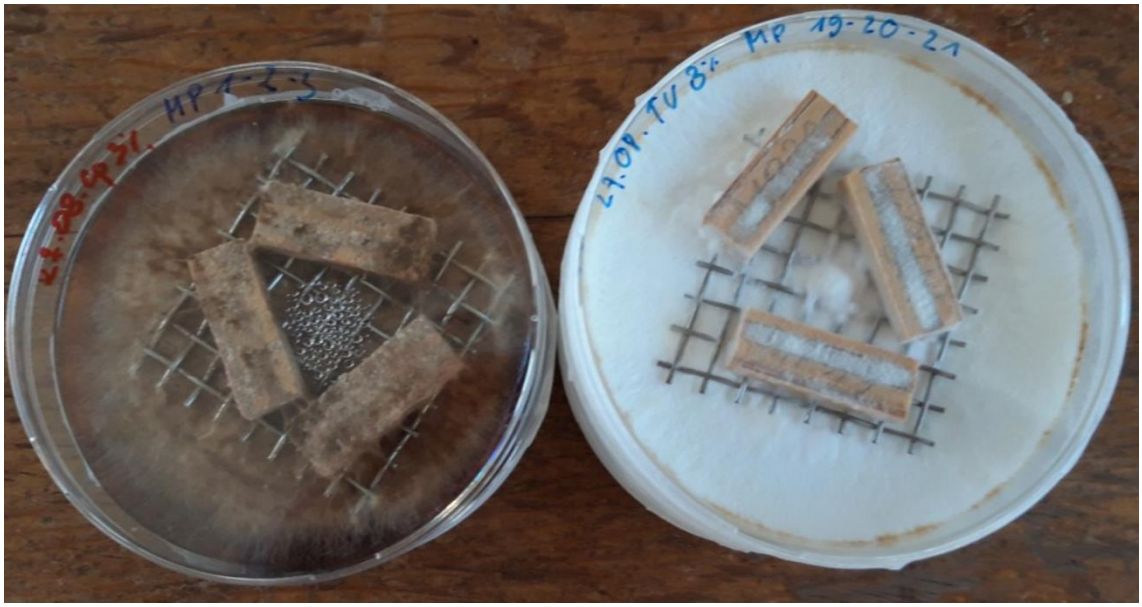

Figure 3-11 Mini-blocks of radiata pine plywood after 10 weeks of fungal decay by *C. puteana* (left) and *T. versicolor* (right).

3.3.2 Results and discussion

Presence of fungicidal components in bio-based materials

In section 3.2, it was shown that it is important to test both brown- and white rot fungi when unraveling durability. However, when only assessing fungicidal components, *C. puteana* has shown to be much more sensitive to fungicidal components than *T. versicolor*. Since the selected wood-based materials are primarily made from softwood species, it was decided to perform the paste test with *C. puteana*. In section 3.2, five out of 10 heartwood pastes had a growth inhibiting effect on *C. puteana*, with the growth rate close to zero. None of the bio-based material pastes had such an effect on *C. puteana*, with the exception of cellulose fibre insulation (Cell), which contains boric acid (Figure 3-12 and Figure 3-13). Note that although the product information of cotton insulation (C) mentioned a biocide (non-specified), this additive was not fungicidal or the additive was not homogenously present in the product.

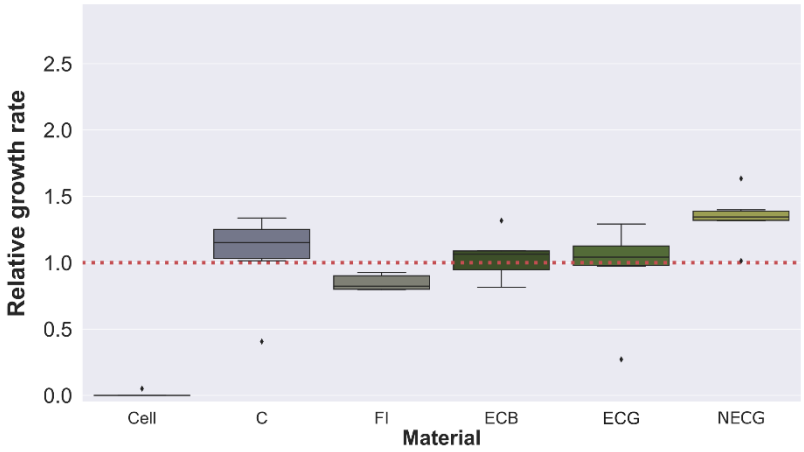

Figure 3-12 Relative growth rate of *C. puteana* growing on pastes of non-fibre insulation materials. The red dotted line corresponds to the median growth rate on malt agar medium without wood powder (8.7 cm^2 day^{-1} for *C. puteana*). Cell = Cellulose fibre insulation, C = Cotton insulation, FI = Flax insulation, ECB = Expanded cork board, ECG = Expanded cork granules and NECG = Non-expanded cork granules

When the relative growth rate is 1, mycelial growth on the bio-based material paste was as fast as on a malt agar paste. In general, the bio-based material pastes promoted mycelial development of *C. puteana* (Figure 3-12 and Figure 3-13). Differences in growth rate were not straightforward to explain. For instance, wood fibre insulation boards (WFIB2-WFIB5) are composed of Norway spruce (*Picea abies*) and/or Scots pine (*Pinus sylvestris*) fibres, and originated from the same producer. They are made from a mixture of sapwood and heartwood. The mycelial growth rate on the pastes of wood fibre boards was lower than on sapwood pastes of solid Norway spruce and Scots pine (see section 3.2.2, Figure 3-6). While the Scots pine heartwood was highly fungicidal in the heartwood paste test, likely due to the presence of stilbenes, no such extreme effect was visible for the wood-fibre insulation materials. This indicates that either no

Scots pine heartwood was present in the samples, or that the production process altered the stability of stilbenes (pinosylvins). Differences in growth rate between wood fibre boards were likely related to the additives in these products or due to the production process. WFIB2 and WFIB4 were made according to a 'wet' production process, meaning that the wood fibres were mixed with abundant water after which they were dried and pressed into a board. During pressing, water soluble nutrients could have leached. Another possibility is that the lower growth rate on WFIB4 was caused by the presence of aluminium sulphate and/or dye. The higher growth rate on WFIB3 and WFIB5 could be caused by the hydrophobic components such as the polyolefin fibres and the paraffin, making the paste surface smoother, in contrast to WFIB2 which only contains pine fibres. From experience, we know that the mycelium of *C. puteana* covers blocks coated with an inert sealant much faster than regular wood blocks. It could be that pastes from bio-based materials containing significant amounts of hydrophobic components cause a similar behaviour in *C. puteana*. This seemed indeed to be the case for WFIB1 (15% polyolefin fibres), BWFIB (bitumen) and Non-Expanded Cork Granules (NECG), but not for the Expanded Cork Board (ECB) and granules (ECG).

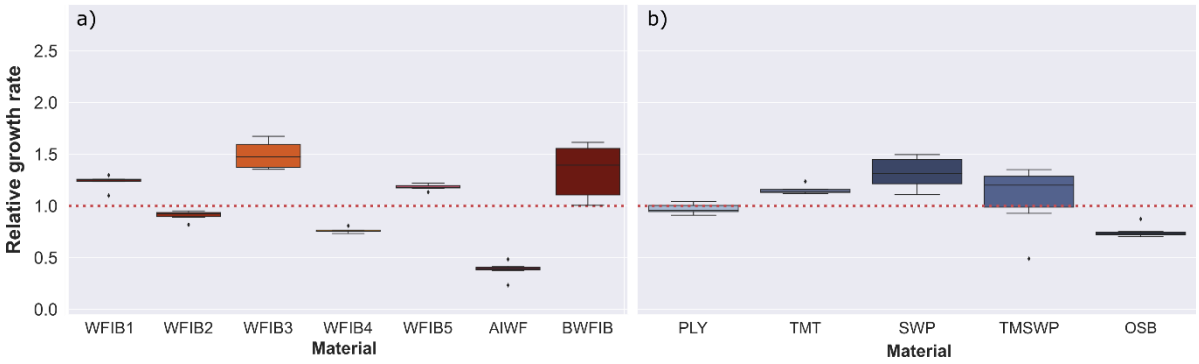

Figure 3-13 Relative growth rate of *C. puteana* growing on pastes of a) wood-fibre insulation materials b) wood-based panels. The red dotted line corresponds to the median growth rate on malt agar medium without wood powder (8.7 cm^2 day^{-1} for *C. puteana*). WFIB 1-4 = Wood fibre insulation board type 1-4, AIWF = Air-injected wood fibre insulation, BWFIB = Bituminised wood fibre board, PLY = Plywood Radiata pine, TMT = Thermally modified spruce, SWP = Three-layer spruce binder, TMSWP = Thermally modified three-layer spruce binder and OSB = Oriented strand board.

Coniophora puteana was also able to grow well on pastes of wood-based panels, although there seemed to be a slight growth inhibiting effect on OSB (Figure 3-13b). Note that thermally modified wood products did not cause any fungicidal effect for *C. puteana*.

Mycelium density

The growth rate on pastes of Air-Injected Wood Fibre insulation (AIWF) was significantly lower than on the other wood-fibre insulation products. However, a closer look at the mycelium showed that the hyphal growth was much denser on this material (Figure 3-15, AIWF) than on any of the other wood-fibre insulation materials (Figure

3-15, WFIB1-5). Likely, more easily available nutrients were present in this paste as compared to the others. To confirm whether the mycelium of *C. puteana* grows denser when more nutrients are available, mycelial development was compared for a malt agar paste with 2% malt and a malt agar paste with 5% malt. The average growth rate did not differ significantly, but clear differences in mycelial density could indeed be observed (Figure 3-14). Similarly, the mycelium on WFIB1 was denser than on the others, but not as extreme as AIWF. Additionally, the mycelium was arranged in concentric circles. Colonies from the same fungal strain have been shown to vary in macroscopic growth patterns when growing on different media in previous studies, typically displaying banded, irregular or radially aligned variations in biomass density (Davidson, 1996). Cotton and flax insulation pastes showed denser mycelium as well. Even though both were grinded as fine (0.1 mm) as the other bio-based materials, the powder had formed aggregates when mixed into a paste and clumps of powder could be discerned, possibly inducing the fluffy growth pattern of the fungus.

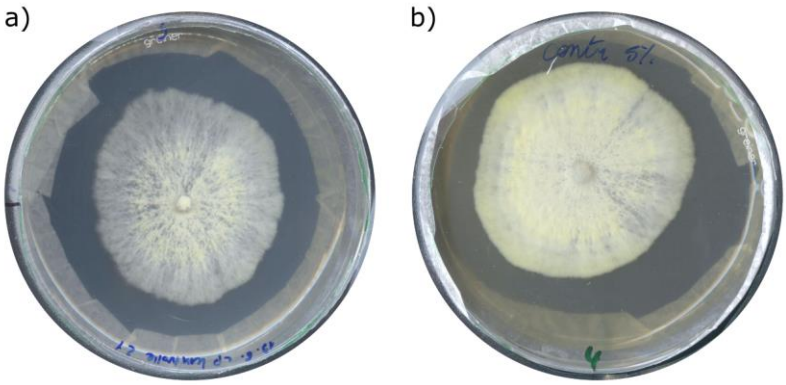

Figure 3-14 Mycelium of *C. puteana* 6 days after inoculation on a) 2% malt agar b) 5% malt agar.

Figure 3-15 Mycelium of *C. puteana* 2, 4, 6 and 8 days after inoculation on pastes of 18 bio-based building materials (next three pages).

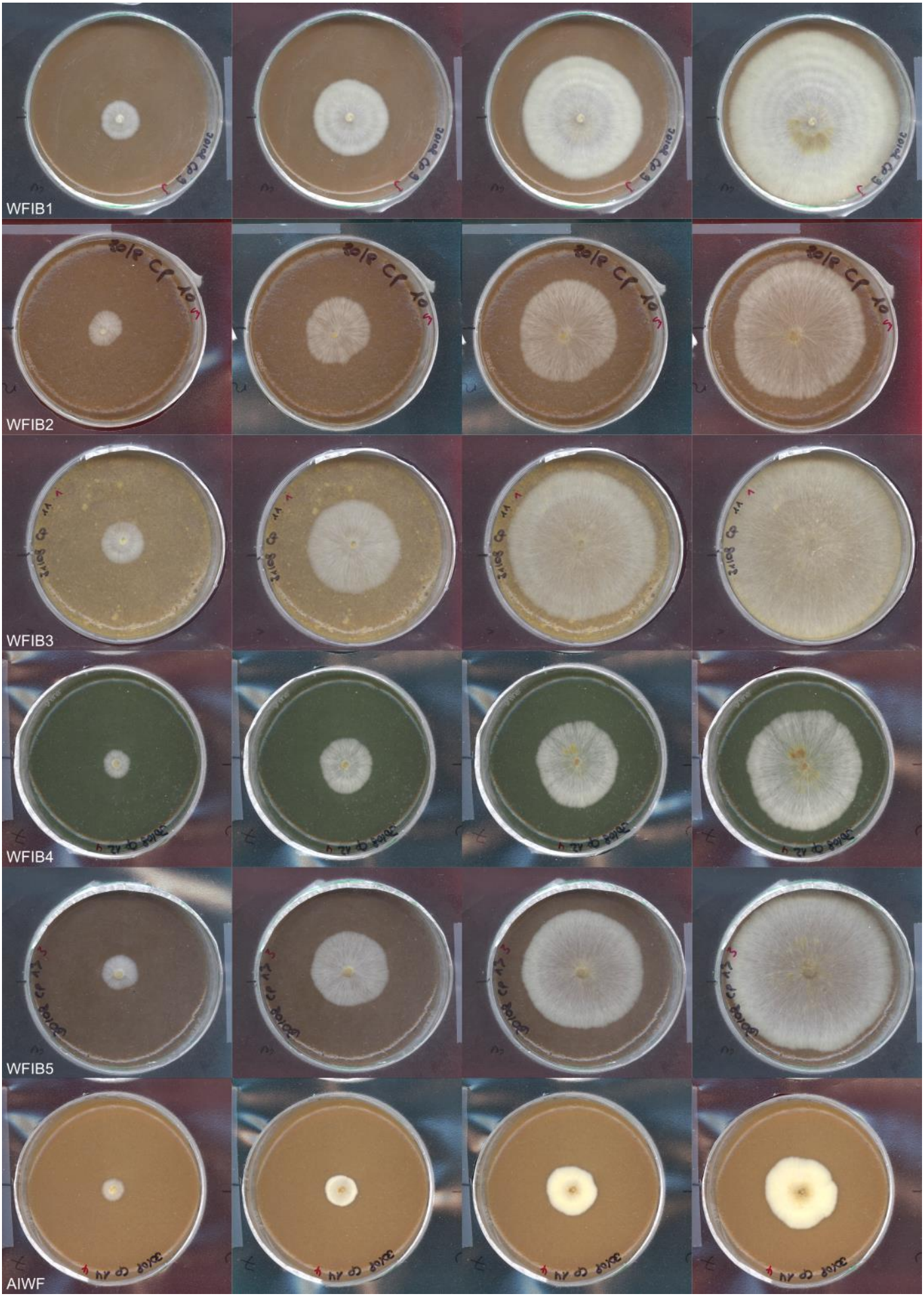
WFIB1
WFIB2
WFIB3
WFIB4
WFIB5
AIWF

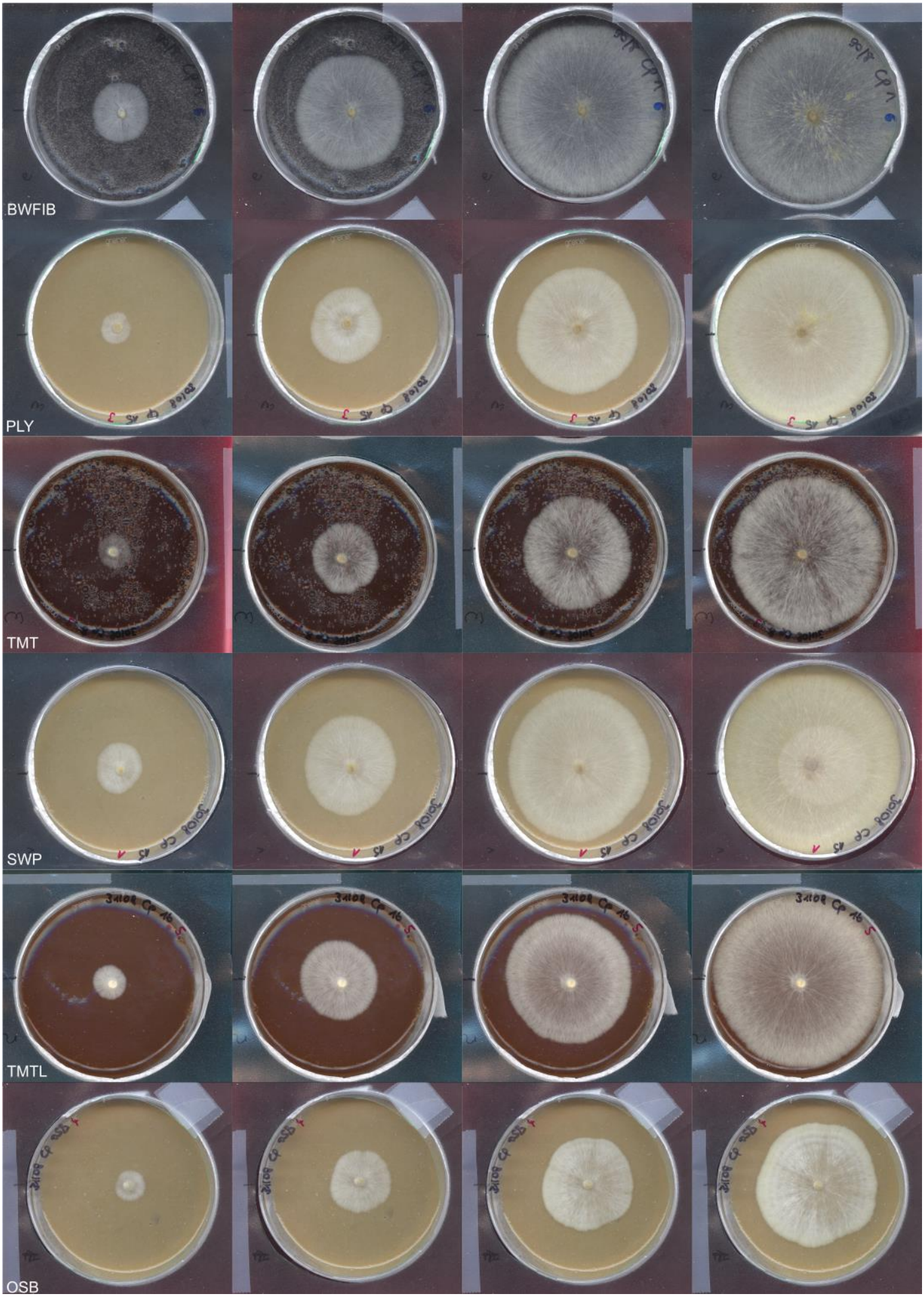
BWFIB
PLY
TMT
SWP
TMTL
OSB

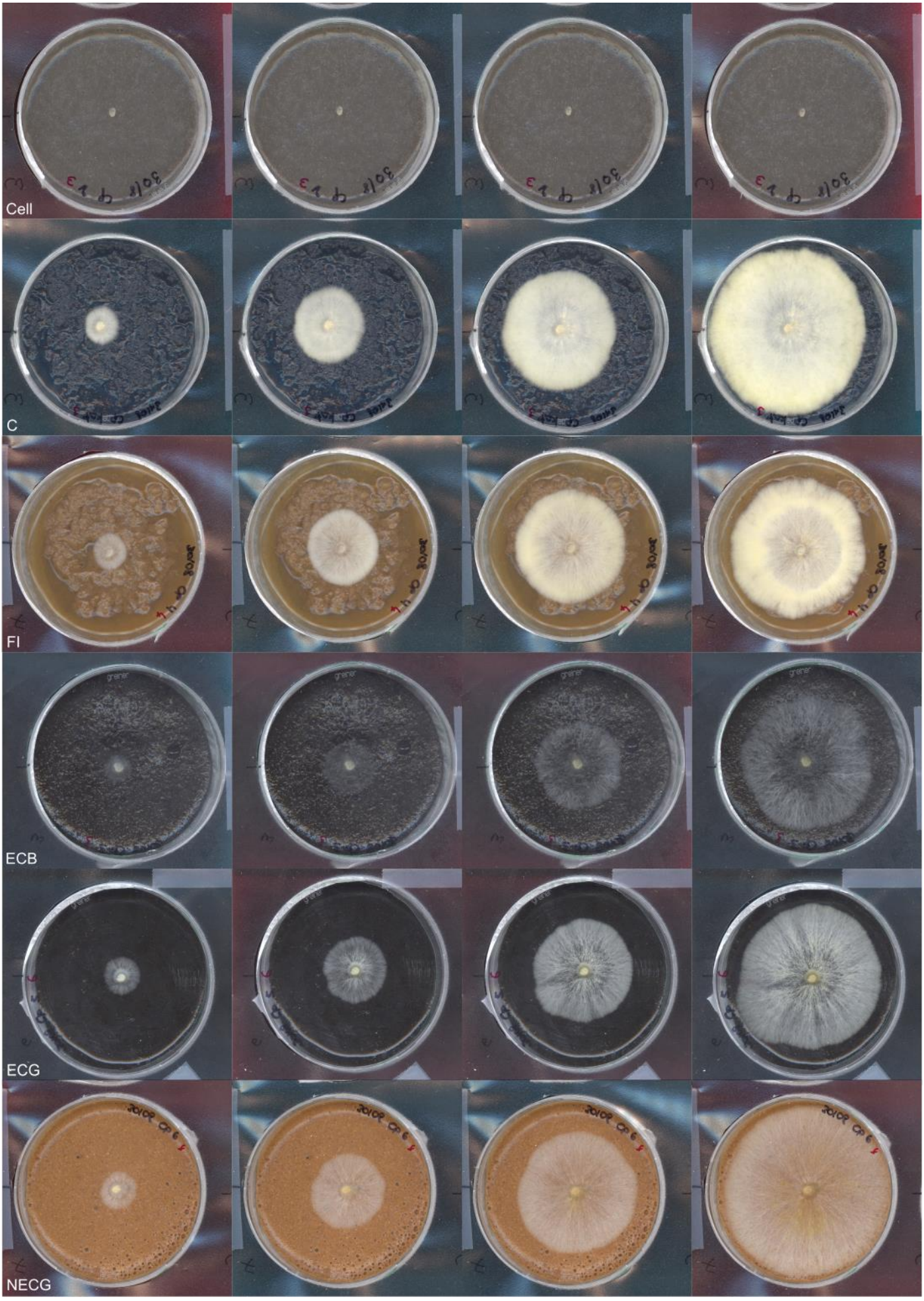
Cell
C
FI
ECB
ECG
NECG

Adapted mini-block test

After 8 weeks of degradation by *C. puteana,* all specimens were degraded up to 30% mass loss and more, except for thermally modified spruce (Figure 3-16). The results for OSB correspond with the findings of Amusant (2009) and Fojutowksi (2009), reporting mass losses of 20-45% for different OSB-panels after degradation by *C. puteana* in an ENV12083 test set-up. We showed that the bitumen emulsion in BWFIB was not fungicidal for *C. puteana*. In the mini-block set-up, the fungus did not seem to be affected by the bitumen emulsion either, although the amount of mass loss was lower than for the Wood Fibre Insulation Board 3 (WFIB3). Possibly, this was related to a lower amount of wood fibres (presence of a bitumen fraction), but could be impacted by accessibility as well. The Radiata Pine Plywood (PLY) was severely degraded as well. Do note that in this mini-block set-up, the edges of the plywood were not sealed and the specimen size did not allow for the glue layers to have much impact on the degradation process. When plywood edges are sealed, glue layers have been shown to significantly restrict decay progress (Van den Bulcke *et al.*, 2011). The MC of the Thermally Modified spruce specimens (TMT) ranged from 25 to 30 % at the start of the experiment and had increased up to 60-90% after 8 weeks. Although similar MCs led to 30% mass loss for Scots pine, the TMT showed mass losses of only 3%. From the paste test, we know that there is no influence of fungicidal components. It seems that, although the MC is sufficiently high, the fungus was not able to degrade the thermally modified wood.

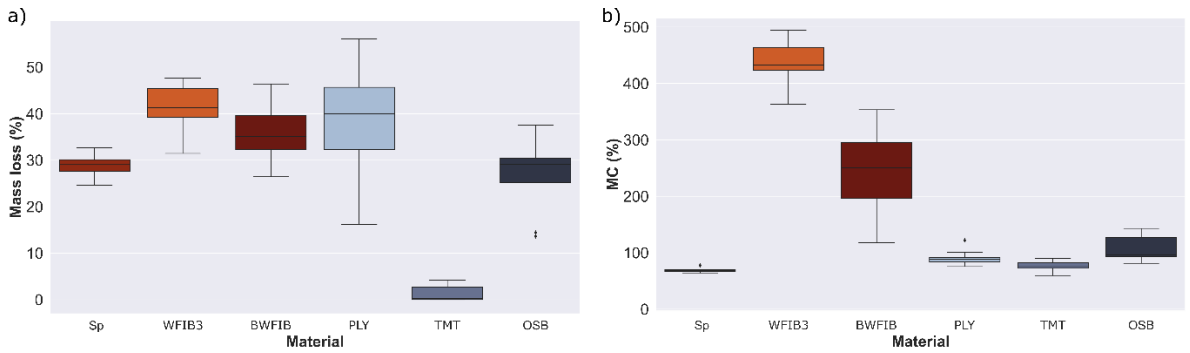

Figure 3-16 Mass loss (a) and moisture content (b) of Scots pine heartwood (Sp), oriented strand board (OSB), porous bituminized wood fibre board (BWFIB), radiata pine plywood (PLY), thermally modified spruce (TMT) and wood fibre insulation board 3 (WFIB3) after 8 weeks of degradation by *C. puteana*.

The selected bio-based materials showed a higher resistance against degradation by *T. versicolor* (Figure 3-17). The wood fibre insulation materials and wood-based panels were made from softwood species. In softwoods, guaiacyl is the main lignin type, which is known to affect the decay rate of white-rot fungi, resulting in a slower decay rate on softwoods compared to hardwoods (Highley, 1982; Schmidt, 2006; Schwarze, 2007; Li *et al.*, 2015). The mass loss on the wood fibre insulation boards and wood-based panels was indeed similar as the mass loss on Scots pine.

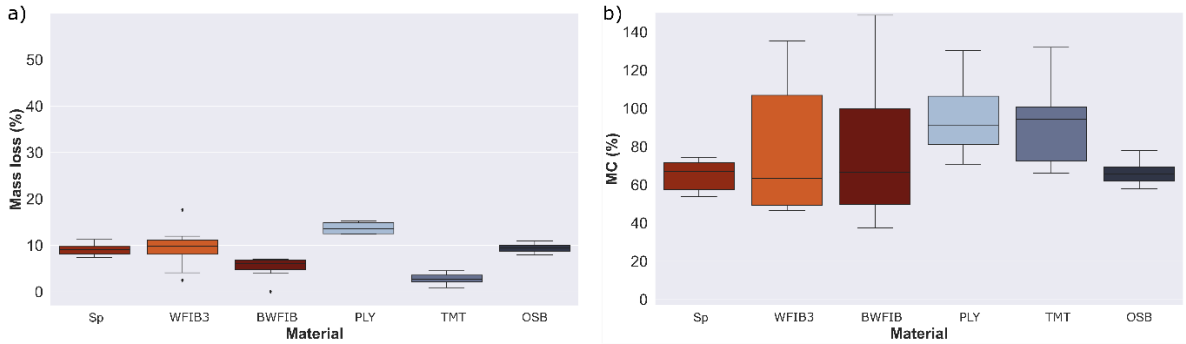

Figure 3-17 Mass loss (a) and moisture content (b) of Scots pine heartwood (Sp), oriented strand board (OSB), porous bituminized wood fibre board (BWFIB), radiata pine plywood (PLY), thermally modified spruce (TMT) and wood fibre insulation board 3 (WFIB3) after 8 weeks of degradation by *T. versicolor*.

As argued in the introduction of this section, a mini-block test set-up is not suited for assessing the overall durability of bio-based building materials against Basidiomycetes, as the specimen size is too small to allow for the glue-layers and structure to have an influence on the degradation process and issues can occur due to the fibrous nature of some of the materials. It did show, however, that the assessed bio-based materials were not durable when they became and remained water saturated and when the hyphae could enter from the sides. In the case of modified wood, bringing the specimens to a MC of 20-30% did not make the specimens susceptible to decay by *C. puteana*.

3.3.3 Conclusions

In general, the selected bio-based building materials did not have any fungicidal properties, with the exception of cellulose fibre insulation for which the fungal growth rate was almost zero. The added components did influence the nutrient value of the pastes, with the mycelium growing less dense on pastes of wood-fibre insulation materials containing paraffin and bitumen. The pastes of thermally modified spruce and spruce binder were not fungicidal. The resistance of thermally modified spruce against fungal decay by *C. puteana* in the adapted mini-block test, was therefore not related to any fungicidal components. The mini-block test set-up was not suited for assessing the overall durability of bio-based building materials against Basidiomycetes, as the specimen size is too limited to allow for the glue-layers and structure to have an influence on the degradation process and issues can occur due to the friable nature of some of the materials. It did show, however, that the assessed bio-based materials were not durable when water saturated and when the hyphae could enter from the sides.

Chapter 4

Influence of material moisture dynamics on natural durability

Farmhouse, Toten, Norway
The wooden terrace and cladding are more than 100 years old and were recycled from the original barn that stood there before.
Architects: Jarmud/Vigsnæs AS Architects MNAL

4.1 Introduction

Moisture is a key parameter determining onset of fungal growth and progress of fungal decay of wood and bio-based building materials. Its impact starts at the early beginning, when spore colonization of a material surface and spore germination takes place. Field tests are used to determine fungal infestation and decay occurring naturally in outdoor exposure conditions, either in ground (CEN EN 252 standard, 2014) or above ground. There are, however, limited studies examining the onset of decay fungi in UC2-3. Vanpachtenbeke *et al*. (2019) designed an experimental set-up to assess onset of decay in timber frame walls at high relative humidity conditions. Onset of fungal growth was not observed for tests without a liquid water source. Even when a liquid water source was available, fungal spores were clearly present (mould, unidentified species) but wood decay could not be confirmed after 9 months of exposure (Figure 4-1).

Figure 4-1 The evolution of mould growth on specimens exposed to 25°C and 97% RH. From left to right: Scots pine planed, Scots pine sawn, OSB, Norway spruce planed, Norway spruce sawn. Adapted from Vanpachtenbeke *et al*. (2019).

Several studies have tried to assess the influence of Relative Humidity (RH) on fungal growth and to determine the minimum moisture threshold that allows fungal growth and decay on wood. These laboratory test methods correspond to situations where decay is already established and further expands in (part of) the construction. In laboratory test assessing the influence of RH on degradation, wood specimens are often pre-inoculated with a fungus and kept at a certain RH condition, established with salt solutions (Saito *et al*., 2012, Figure 4-2). To avoid an increased moisture content (MC) of the test specimens due to the pre-inoculation step, the test specimens can also be conditioned at the respective RH, after which an inoculated specimen, or a piece of mycelium, when using 100% RH, is introduced in the set-up and placed underneath the conditioned test specimen (Brischke *et al*. 2017, Figure 4-2b). Whether or not decay occurs at a certain RH depends on the fungus, wood species and the set-up used. Degradation can to occur below 97% RH in experiments where wood samples were inoculated with hyphae, in contrast to the experiment of Vanpachtenbeke *et al*.

(2019), where fungal spores or hyphae are not artificially introduced. Brischke *et al*. (2017), for instance, found significant decay for Norway spruce (*Picea abies* (L.) Karst) wood at 96% RH by *Coniophora puteana,* whereas *Trametes versicolor* did not cause significant Mass Loss (ML) below 100% RH on this wood species, but did degrade beech wood at 96% RH. No decay occurred below 100% RH in the set-up of Saito *et al*. (2012) for the brown rot fungus *Fomitopsis palustris* on Japanese red pine wood (*Pinus densiflora*). However, Brischke and Alfredsen (2020) refer to a German study by Ammer (1963), who found 2% mass loss at 85% RH for *C. puteana* on Norway spruce in a similar set-up as the one of Saito *et al*. (2012). Likely, the preconditioning of the specimens on malt agar medium, and the corresponding higher MC, made the specimens more susceptible to decay at 85% RH than in the set-up of Brischke *et al*. (2017). It is generally accepted that when no liquid moisture source is present, decay does not occur below 85% RH.

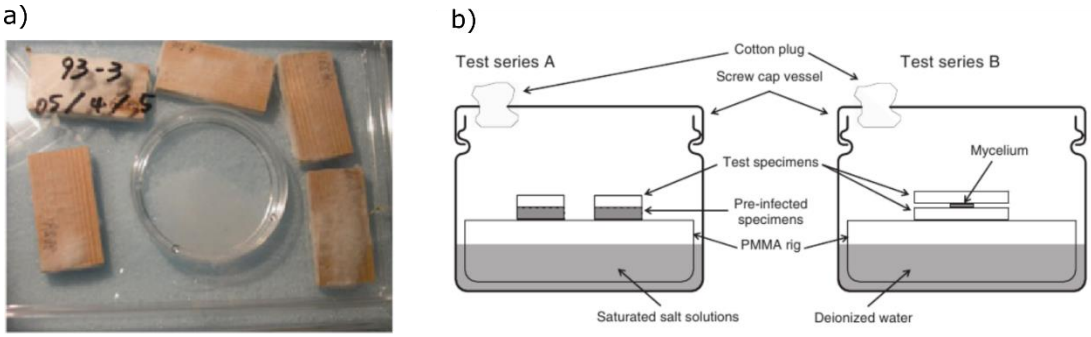

Figure 4-2 a) Pre-inoculated test specimens in the presence of a saturated salt solution (Saito *et al*. 2012) b) Inoculation of conditioned test specimens via pre-inoculated wood specimens in the presence of a saturated salt solution (series A) and via mycelium in the presence of deionized water (series B) (Brischke *et al*. 2017).

To determine the minimal MC threshold for fungal decay, various studies performing a so-called 'pile-test' have been reported on. In a pile-test, wood specimens are stacked and placed in Erlenmeyer flasks, closed off with a cotton plug (Figure 4-3a). Usually, the bottom of the pile is exposed to malt agar inoculated with a decay fungus (Stienen *et al*., 2014; Meyer *et al*., 2015; Meyer *et al*., 2016). Due to the malt agar medium and the cotton plug, the RH in the Erlenmeyer flasks is 100% and condensation on the inside of the Erlenmeyer flask occurs (Figure 4-3b). In several studies, a metal ring was placed between the 7th and 8th specimen, to avoid direct moisture transport from the agar throughout the pile (Stienen *et al*., 2014; Meyer *et al*., 2015). However, Stienen *et al*. (2014) showed that the moisture gradient over the pile was similar with or without the ring after 12 weeks, and that moisture was transported by the fungal mycelium from the bottom to the upper parts of the piles. After 16 weeks, the MC and mass loss (ML) of every specimen was measured. While there is a consensus that the availability of free water in cell walls is critical for decay (fibre saturation), the aforementioned studies show that mass loss can occur for specimens with a moisture content far below fibre saturation point (FSP). For instance,

Scots pine (*Pinus sylvestris* L.) sapwood specimens with a MC of 15.2% had 2.2% ML[2] when degraded by *Trametes versicolor* (Meyer, 2015). Probably the MC was not homogeneous across the specimens and degradation also was similarly heterogeneously, at for instance the bottom part which might have been at a higher MC. The specimens were 5 mm thick, and from X-ray CT images, we know that the MC can vary greatly over 5 mm (see Chapter 5, Figure 5-4). Nevertheless, we know for sure that at 100% RH and in the presence of a nutrient and moisture source, decay fungi are able to overgrow wood and transport water to moisten and degrade it. Such conditions occur for wood in ground contact (Brischke and Alfredsen, 2020). This is, however, not usually the case for wood exposed above ground, although it can occur, for instance for wood in contact with a wet wall.

Brischke *et al*. (2017) proposed an alternative set-up, where the malt agar is replaced by deionized water and the pile is inoculated by inserting pre-inoculated specimens into the pile after a stable moisture gradient is reached (Figure 4-3c). In that case, no metal ring was placed so that the moisture gradient is established through water transport in the pile, prior to inserting inoculated specimens. This resulted in MC gradients starting from 20-25% MC at the bottom of the piles to 10% MC at the top. *Coniophora puteana* was able to significantly degrade (>20% ML) part of the beech and Norway spruce wood in this pile-test set-up and the lowest MC at which decay occurred for Norway spruce was at 25.6%, which is 4.8% below its FSP. The lowest MC at which more than 2% ML occurred for *Trametes versicolor* on Norway spruce was 16.3%. Nevertheless, only limited decay (<5% ML) occurred over the entire pile for *Trametes versicolor*. White-rot fungi are after all known not to grow well without a moisture source. While the agar medium was removed as nutrient and moisture

[2] Note that when performing standard tests of natural durability of wood against Basidiomycetes, the lowest durability class has a boundery of 5% mass loss and that any differences between 0 and 3% mass loss are considered insignificant, as the error margin due to the procedure is 3%.

source, one can argue whether this set-up truly reflects decay without the presence of a moisture source. The authors confirmed that the hyphae of *C. puteana* had reached the deionized water in the set-up, most probably using it as a moisture source for water transportation. In practice, when no moisture source would be present, decay by *C. puteana* in this set-up might be more limited and hence similar to what occurred in the experiments of Ammer (1963) and Saito *et al*. (2012).

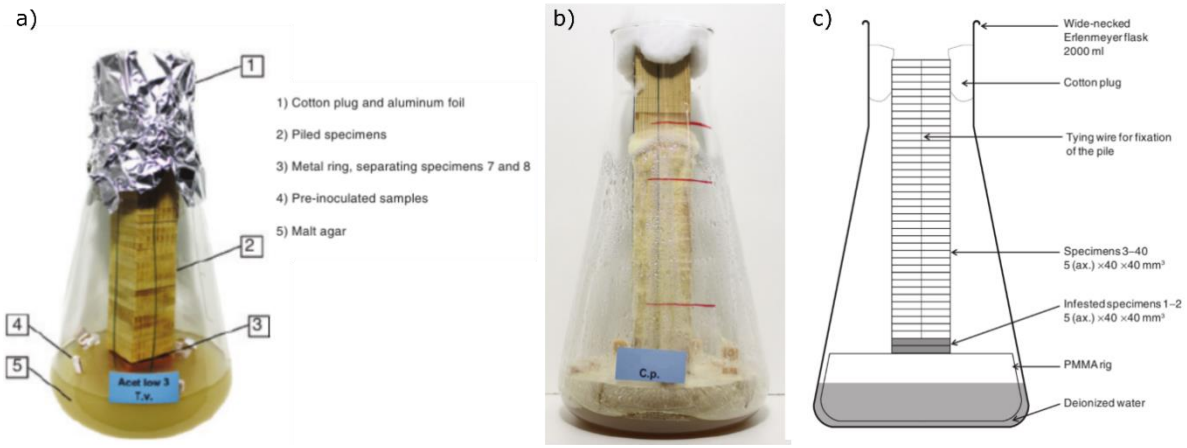

Figure 4-3 a) Typical pile-test set-up, with malt agar medium (Meyer *et al*., 2016) b) pile of Norway spruce sapwood after 3 weeks of incubation with *Coniophora puteana* (Meyer *et al*., 2015) c) pile-test set-up without malt agar medium, inoculation via pre-infected test specimens (Brischke *et al*., 2017).

4.2 Influence of relative humidity and material moisture content on fungal decay

The experiments in section 4.2 were performed in collaboration with dr. ir. Michiel Van Pachtenbeke and part of the data was incorporated in his PhD thesis (Van Pachtenbeke, 2019). In this PhD thesis (De Ligne, 2021), the data are supplemented with data from additional experiments, resulting in a more complete overview of the impact of relative humidity (RH) on fungal decay.

Each of the aforementioned experiments assessed either the influence of RH on fungal decay, without a moisture source, or the level of decay in terms of a moisture gradient, always at a RH of 100%. In this section, we propose a method to assess the influence of RH on fungal decay, in the presence of a moisture and nutrient source, over time. An adapted version of the mini-block test is presented for Norway spruce and Scots pine in 12 different set-ups, with varying relative humidity (11-100% RH), including three experiments where the mini-blocks were preconditioned. Mass loss and MC of the mini-blocks were followed over time (0-57 days).

4.2.1 Material and methods

Wood specimens: 504 mini-block specimens with dimensions of 30 x 10 x 5 mm^3 were prepared from Scots pine (*Pinus sylvestris* L.) sapwood and Norway spruce (*Picea abies* (L.) Karst.) sapwood. All specimens were numbered, oven dried at 103 °C for 24 hours and weighed to the nearest 10^{-4}g to determine their oven dry weight again ($m_{0,dry}$ [g]).

Fungal species: Brown rot fungus *Coniophora puteana* (strain MUCL 11662) was used as a test fungus.

Adapted mini-block test

Instead of Petri dishes, open glasses with a volume of 330ml were sterilized and filled to the brim with malt agar medium containing 2% agar and 3% malt (Thermo Fisher Diagnostics B.V., Landsmeer, The Netherlands). The larger volume was necessary to ensure the presence of a moisture source for 8 weeks, since agar medium dries out at low RH. After the agar medium had solidified, the agar medium was inoculated with *C. puteana*. The glasses were covered with lids of Petri dishes and placed in a climate chamber at (20±2) °C and (70±5) %RH (CTS Pharma climatic test chamber Series CP; CTS Hechingen, Germany). When the fungal mycelium (nearly) covered the entire malt agar medium surface, sterilized metal grids (50 x 50 mm^2) were placed on the agar surface, preventing direct contact between the agar surface and the wood specimens. Five mini-blocks were placed in each recipient.

Additionally, 126 mini-blocks were preconditioned at 40, 60 and 80% MC to assess the influence of the initial MC. After sterilisation, these mini-blocks were placed in a vacuum desiccator and water saturated under vacuum. Then, the mini-blocks were conditioned in a laminar flow and regularly weighed until the desired MC ±5% was reached. When the desired MC was reached, they were wrapped in aluminium foil and stored in the fridge. At the start of the experiment, the MC of all blocks was determined, before placing the mini-blocks on the fungal cultures.

Relative humidity set-ups

Twelve different set-ups were prepared (Table 4-1). Relative humidity conditions between 11 and 100% were created, using various saturated salt solutions and water. For every test set-up and wood species, two plastic containers (dimensions 400 x 300 x 110 mm^3) were sterilized and filled with five malt agar glasses, each containing five mini-block specimens. For the set-ups with saturated salt solutions, five petri dishes (diameter 90 mm) containing the saturated salt solution were added (Figure 4-4a). The salt solutions were renewed regularly during the experiment, to maintain the required RH and a ventilator ensured homogeneous mixing of the humid air. For the set-ups with 100% RH, sterile deionized water was added on the bottom of the box (Figure 4-4b). All boxes were stored in a climate chamber at (20±2) °C.

Every three days, three specimens per wood species were taken randomly from each set-up, cleaned and weighed ($m_{1,wet}$ [g]) to 10^{-4} g to determine their MC [-]:

$$MC = \frac{m_{1,wet} - m_{1,dry}}{m_{1,dry}} \quad (4\text{-}1)$$

Afterwards, the specimens were oven dried and weighed again ($m_{1,dry}$ [g]) to determine their mass loss (ML [-]):

$$ML = \frac{m_{0,dry} - m_{1,dry}}{m_{0,dry}} \quad (4\text{-}2)$$

Table 4-1 Selected saturated salt solutions / preconditioning step, with corresponding target relative humidity (RH) and the expected equilibrium moisture content of Scots pine and Norway spruce sapwood when no agar or fungus would be present (Omega, 2021; Vanpachtenbeke, 2019).

Salt solution / preconditioning	Target RH (%)	Expected initial MC (%) at equilibrium
LiCl	11	3-4
CH_3CO_2K	22	5-6.5
MgCl	33	6-8
K_2CO_3	43	8-10
$Mg(NO_3)_2$	54	10-12
$NaNO_2$	66	12-15
NaCl	75	14-18
KCl	85	15-21
H_2O	100	±30
H_2O / preconditioned at 40% MC	100	±40
H_2O / preconditioned at 60% MC	100	±60
H_2O / preconditioned at 80% MC	100	±80

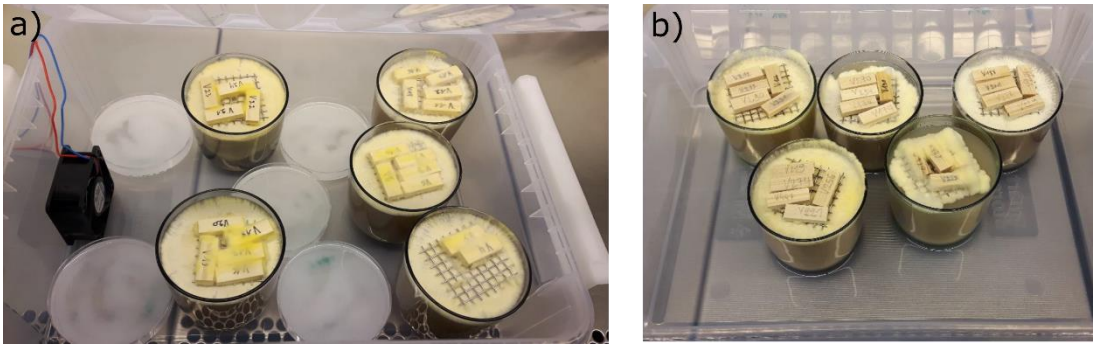

Figure 4-4 Example of *C. puteana* cultures in glass recipients (330 ml) with spruce sapwood specimens. a) Set-up with saturated NaCl solutions and a ventilator, after 6 days of exposure. b) Set-up with fungal cultures positioned in deionized water.

Statistical data analysis

The Kruskal-Wallis H-test was applied to determine whether the median MC of the mini-blocks differed significantly for different levels of preconditioning, as well as the median ML. The Kruskal-Wallis H-test is a non-parametric statistical test indicating whether the medians of two or more groups are different. When the difference

between the medians is significantly different, a post-hoc test needs to be applied to pinpoint for which groups the medians are different. Therefore, the multiple comparison test by Dunn (1961) was applied for this purpose and Benjamini-Hochberg correction (Benjamini and Hochberg, 1995) was performed to control the false discovery rate (Type I error).

4.2.2 Results and discussion

The MC of the wood blocks increased at the start of the experiment to MCs much higher than the expected wood equilibrium moisture content at a certain RH (Table 4-1). In a preliminary experiment without a fungus, the presence of the malt agar medium was found to increase the MC with 5-10% after 3 days, while in the presence of both malt agar and *Trametes versicolor*, the MC had increased with 13-20%. Consequently, we may conclude that the presence of the malt agar and fungus increased the MC of the mini-blocks substantially, even in an early stage. It could indeed be discerned that *C. puteana* mycelium had already started to cover the bottom part of the mini-blocks after 3 days. Nevertheless, clear differences in MC and decay were observed for different relative humidity conditions.

Mycelial growth and decay

At 11% and 22% RH, *Coniophora puteana* had difficulties to completely cover the mini-blocks and maintain hyphal growth further away from the agar medium. Likely, the hyphae dehydrate due to the low RH. Nevertheless, the MC of the Scots pine and Norway spruce blocks ranged mainly between 20-35% and decay was present, though mostly limited (Figure 4-5 and Figure 4-6). At 43% to 85% RH, the fungus degraded the mini-blocks up to 20-30% ML. Considerable amounts of ML (>10%) started to occur after 21-36 days. Even though the RH differed between the different set-ups, the MC of the mini-blocks after 21 days in the 43 to 85% RH set-ups varied between 40 and 60%. This wide range in MC was likely a result of the variety in mycelial growth and mycelial encapsulation, due to impact of the ventilator. While the ventilator was used to distribute the air evenly, it dehydrated the hyphae overgrowing the nearest mini-blocks. At 43, 54 and 66% RH, part of the mini-blocks was completely covered with hyphae, while others were not or only partly covered (Figure 4-7a). At 75 and 85% RH, all mini-blocks were covered with mycelium. The impact of the ventilator was still noticeable, with the specimens the farthest away having a denser mycelium than the specimens closer to the ventilator. In the set-ups with 100% RH, no ventilator was added and all blocks were covered with a dense mycelium after 27 days (Figure 4-7b). The MC of those mini-blocks was much higher, with average MCs ranging from 80 to 250% (Figure 4-9 and Figure 4-10).

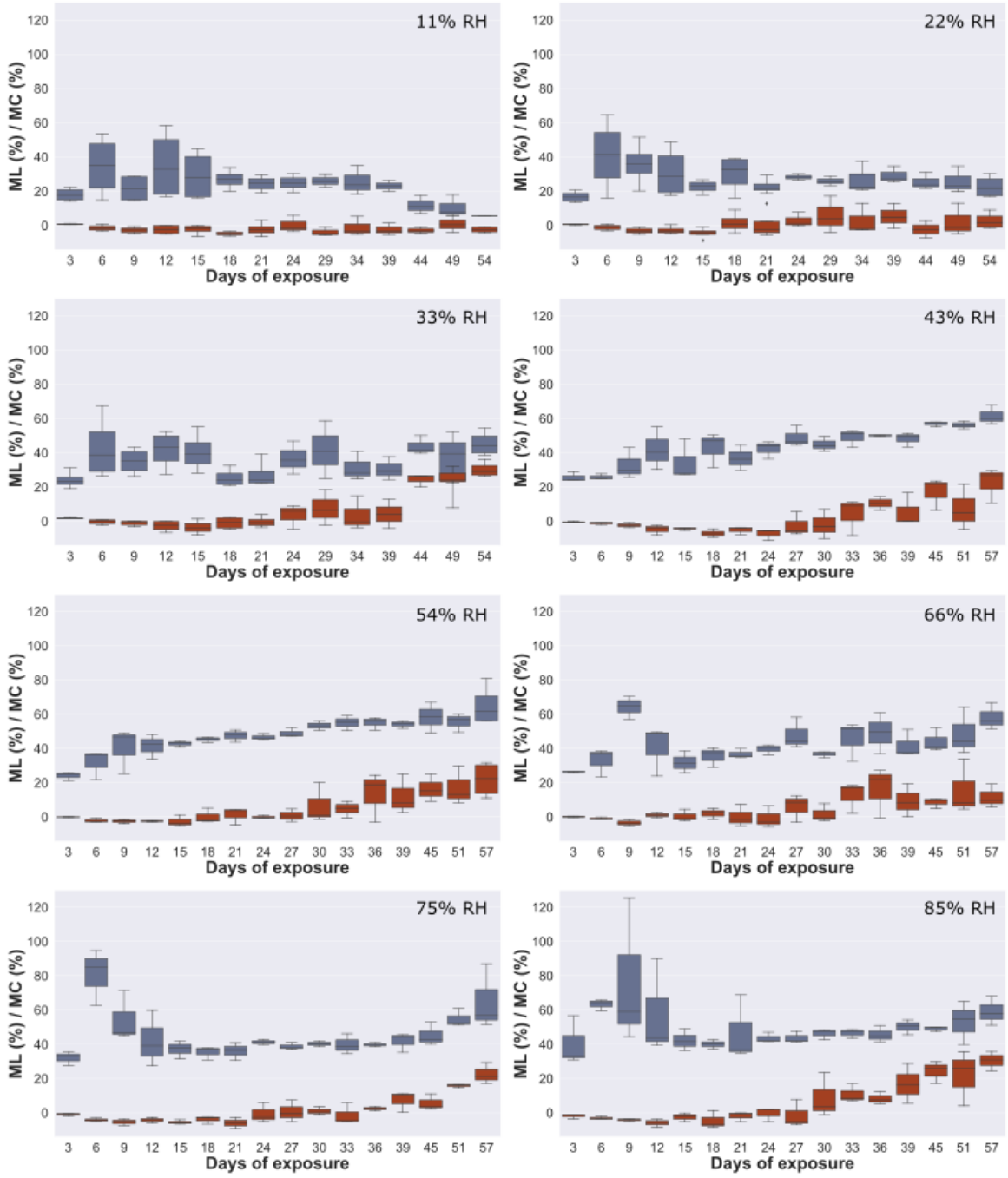

Figure 4-5 Mass loss (ML (%), red) and moisture content (MC (%), blue) of Scots pine sapwood mini-blocks over time at 11%, 22%, 33%, 43%, 54%, 66%, 75% and 85% RH. The boxplots represent three specimens harvested at each measurement time (days of exposure).

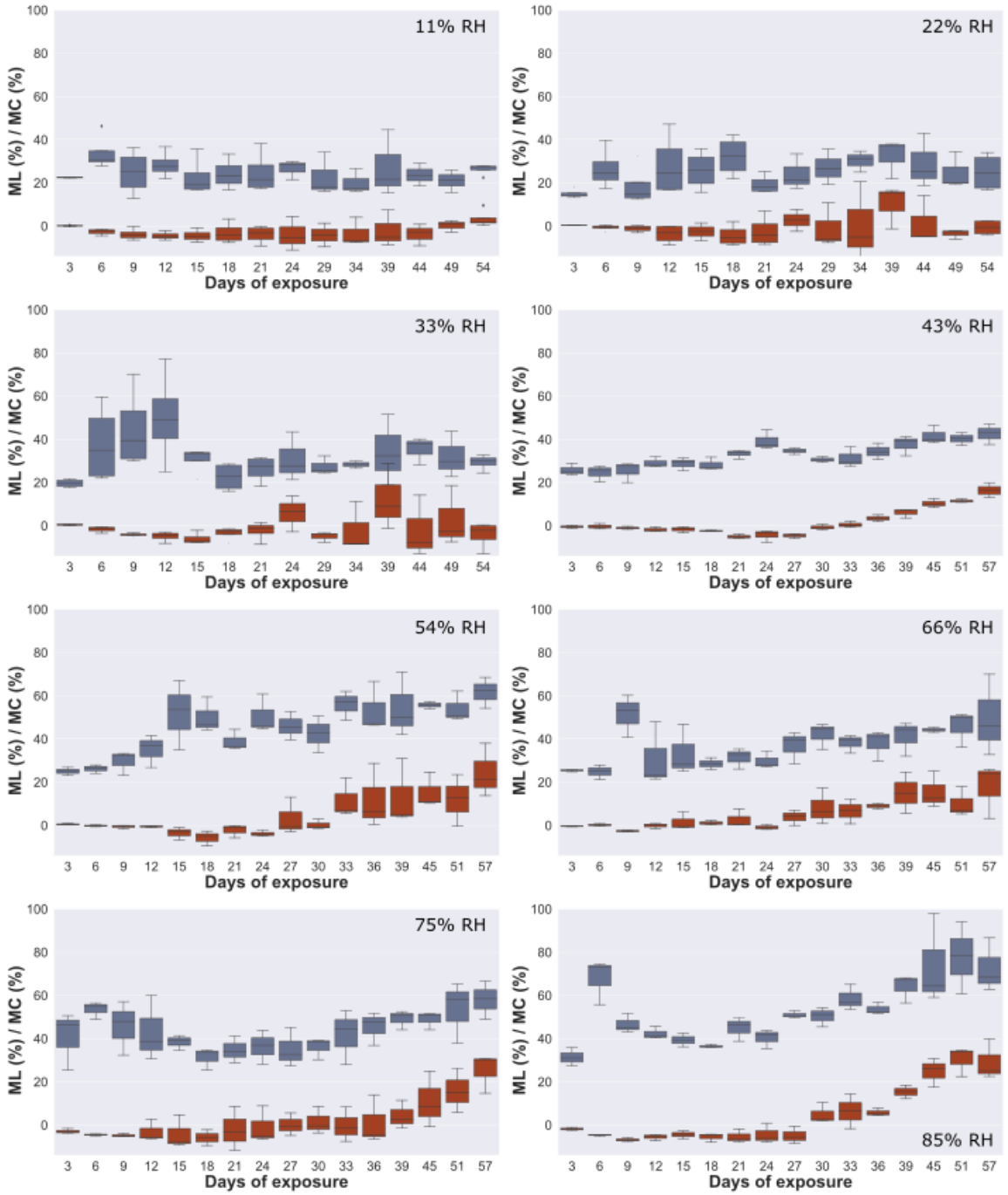

Figure 4-6 Mass loss (ML (%), red) and moisture content (MC (%); blue) of Norway spruce sapwood mini-blocks over time at 11%, 22%, 33%, 43%, 54%, 66%, 75% and 85% RH. The boxplots represent three specimens harvested at each measurement time (days of exposure).

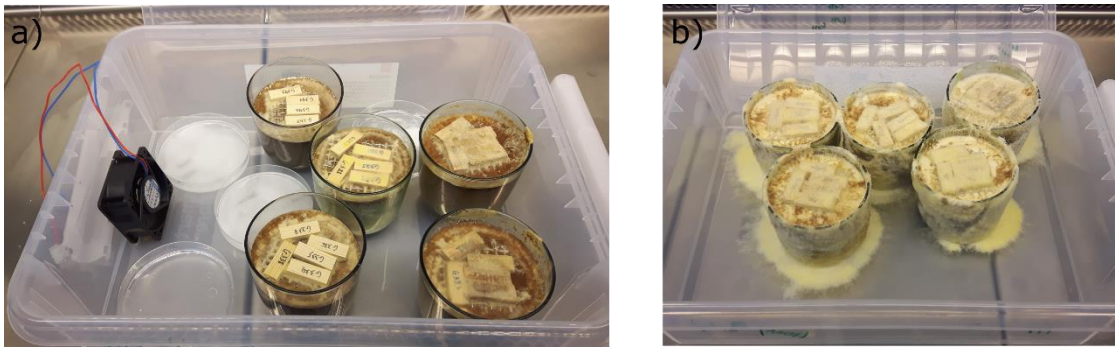

Figure 4-7 Scots pine mini-blocks 27 days after exposure to *C. puteana* in a 43% RH set-up with ventilator (a) and a 100% RH set-up (b).

Effect of preconditioning

For the 100% RH set-up, the influence of preconditioning the wood blocks to 40, 60 and 80% initial MC was assessed as well. The effect was most visible at the beginning of the experiment, with higher MCs in relation to the preconditioning. This effect lasted throughout the experiment, with the average MC of Scots pine sapwood after 21-57 days differing significantly for the blocks that had been preconditioned at 40, 60 and 80% MC (Figure 4-8a, Kruskal-Wallis H-test p-value<0.05). However, these differences in MC did not correspond to a significant difference in mass loss (Kruskal-Wallis H-test p-value=0.08). For Norway spruce, the MC of the blocks conditioned at 60 and 80% RH was similar. Both differed significantly from the non-conditioned blocks and the blocks conditioned at 40% MC (Figure 4-8b). The mass loss of the blocks conditioned at 80% MC was significantly lower than in absence of preconditioning. In Figure 4-8b, it can also be seen that the mass loss at 100% RH with no preconditioning was higher than at other RH. Too wet circumstances negatively affected the amount of fungal decay, a phenomenon that is commonly known as 'waterlogging'.

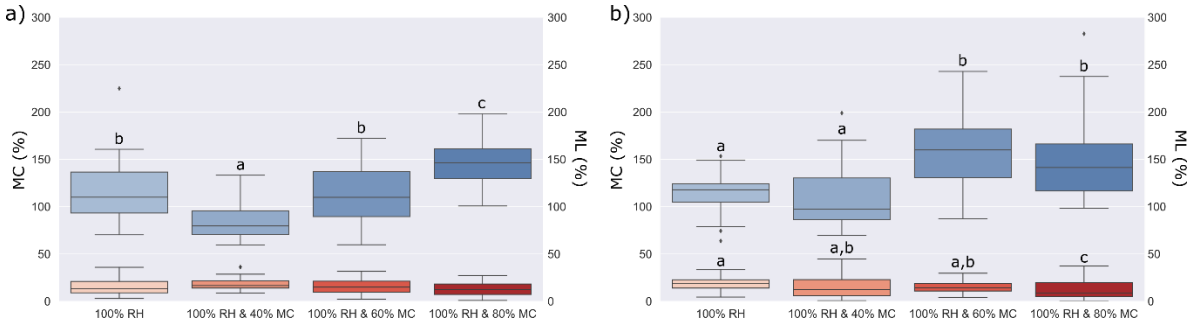

Figure 4-8 Moisture content (MC, blue) and mass loss (ML, red) of Scots pine sapwood (a) and Norway spruce (b) mini-blocks after 21 to 57 days of exposure. The Kruskal-Wallis H-test was applied for testing differences in median MC and ML, with Dunn's multiple comparison test as post-hoc with Benjamini-Hochberg correction. Based on Dunn's test, the conditions were grouped (a, b, c).

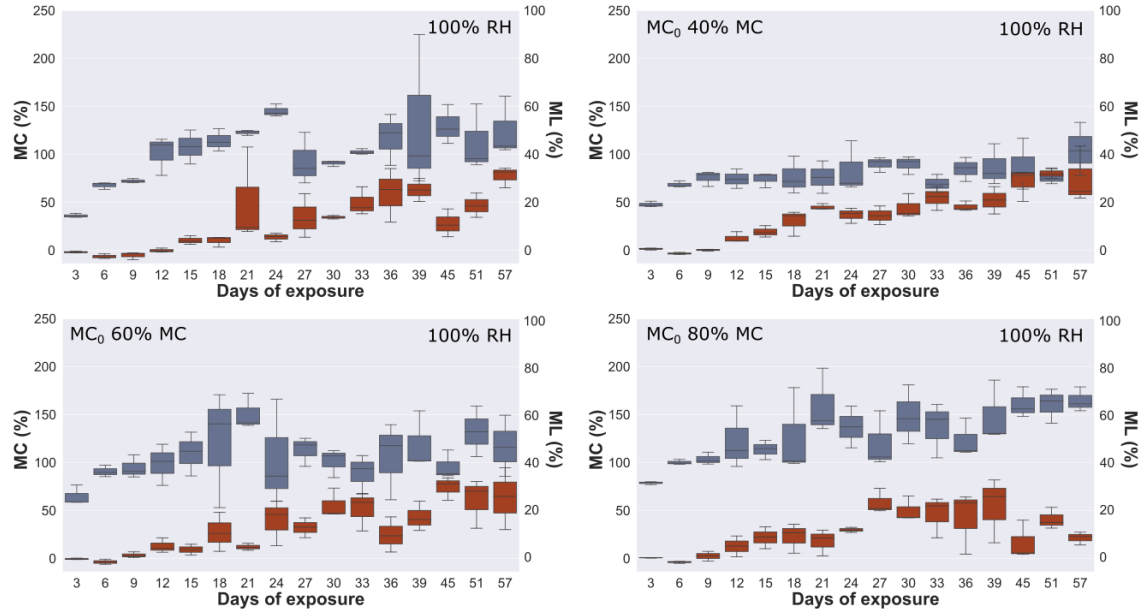

Figure 4-9 Mass loss (ML (%), red) and moisture content (MC (%); blue) of Scots pine sapwood mini-blocks over time at 100% RH, for different conditions of initial moisture content (no conditioning, 40%, 60% and 80% MC). The boxplots represent 3 specimens per measurement time, per condition. Note that ML is represented by the right axis.

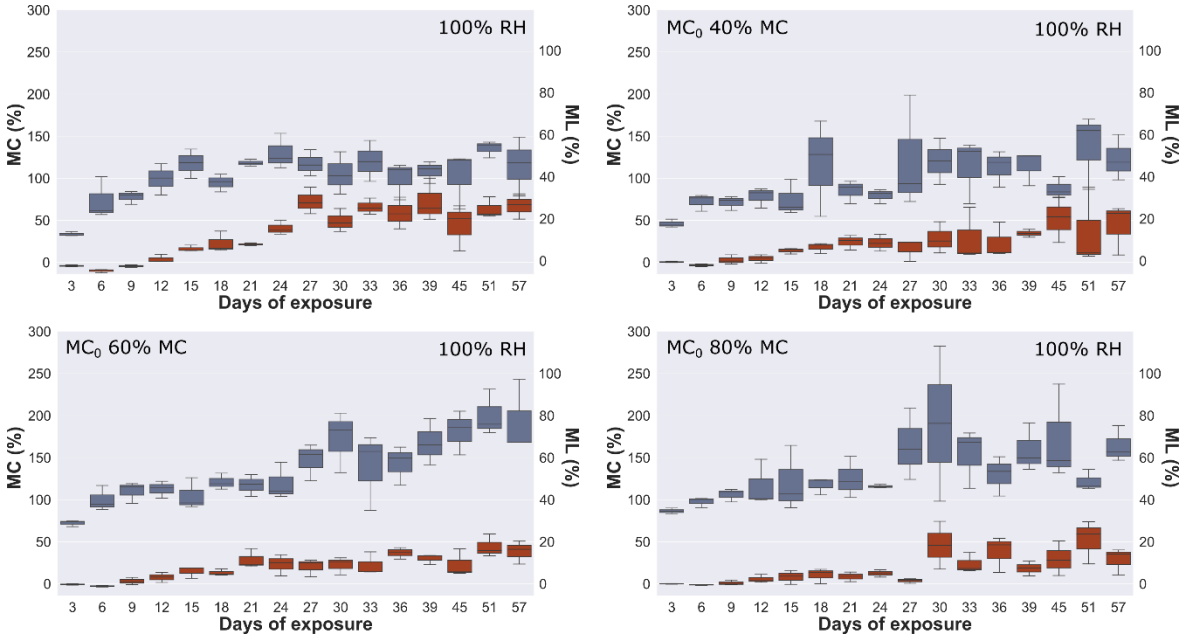

Figure 4-10 Mass loss (ML (%), red) and moisture content (MC (%); blue) of Norway spruce mini-blocks over time at 100% RH, for different conditions of initial moisture content (no conditioning, 40%, 60% and 80% MC). The boxplots represent 3 specimens per measurement time, per condition. Note that ML is represented by the right axis.

Minimal moisture content for decay

In the presence of a moisture and nutrient source, decay has been shown to occur below fibre saturation point, which corresponds to 30.3 and 34.6% MC for Norway spruce and Scots pine, respectively (Meyer *et al*., 2015; Brischke *et al*., 2017). In our 11% and 22% set-ups, the MC of Scots pine sapwood generally remained below 34.6% (FSP). No decay (<1% mass loss) occurred below 20% MC and limited decay (<5% mass loss) occurred below 25% ML for this species (Figure 4-11). Between 25-30% MC, some specimens had lost more than 10% of their mass, confirming that decay can occur below FSP. None of the Norway spruce specimens in the 11% RH set-up had more than 10% mass loss (Figure 4-12). Decay also occurred below FSP.

At 43 – 100% RH, the MC of the mini-blocks after 21 days was nearly always higher than FSP for Norway spruce and Scots pine sapwood. When severe degradation occurred (>30% mass loss), the corresponding specimens had a MC between 50-85% MC (Scots pine, Figure 4-11) and 50-130% (Norway spruce, Figure 4-12). Most of the specimens that had a MC between 70-110% had more than 10% mass loss and none of them had less than 5% mass loss. However, similar to the pile-tests, the fungus induced the moisture conditions, as wood in equilibrium in a climate chamber at 43 to 85% RH would not reach an MC above 21%. Besides producing water by metabolising sugars from the agar medium and wood cell wall polymers to carbon dioxide and water, brown-rot fungi are also known to transport water into wood in experiments with significant amounts of free water, explaining these higher MC (Schmidt, 2006; Stienen, 2014; Thybring, 2017). Since brown-rot fungi degrade cellulose and hemicellulose, while leaving the lignin mostly intact, very high MCs (>110%) could be an indication that little degradation occurred, as the water sorption capacity of the degraded wood is reduced as compared to undegraded wood (Rawat, 1998; Thybring, 2017). Above 110% MC, many of the specimens indeed only had 0-10% mass loss, indicating that the specimens were too wet for degradation (waterlogging).

A peculiar phenomenon occurred during most of the experiments, as negative mass loss, or 'mass gain' of up to 11% was observed. The lower the RH condition, the longer these mass gains persisted, presumably because at higher RHs mass loss increased, thus masking the negative mass loss. Three hypotheses were explored to explain these mass gains: 1) mass increase due to malt agar uptake, 2) precipitation from the salt solution and 3) fungal presence. To assess whether the mass increase could be explained by malt agar uptake, a reference experiment was performed without a fungus. However, the latter caused a dry mass increase of at most 1%. To confirm that salt had not precipitated from the salt solutions in the air, another reference experiment was performed on Scots pine specimens without a fungus, in the presence of a salt solution. There, no mass gains (<0.2%) were observed. The mass gains were therefore related to the presence of the fungus, either directly, due to the fungal mass of hyphae growing into the wood, or indirectly, due to increased malt agar uptake. An estimation of the fungal mass was made as follows. Since there was no information

available on MC and density of *C. puteana* mycelium, data on vegetative mycelium of 'unidentified Basidiomycetes' growing on twigs from a study by Lodge (1987) was used. In that study, the vegetative mycelium had a MC of 62.7%, and the wet and dry density of the mycelium were 0.88 and 0.35 g/cm³, respectively. A mass gain of 11%, corresponding to approximately 0.06 g would therefore indicate a dry mycelial volume of 0.17 cm³. The corresponding wet mycelial volume would supposedly fill 0.43 cm³, which would be 28% of the entire wood block volume (1.5 cm³). Theoretically, this would be possible, as the porosity of Norway spruce is about 70% (Plötze and Niemz, 2011). However, no such dense growth could be observed and part of the mini-blocks were even free of mycelium. Increased agar uptake in the presence of the fungus is more likely, as in the low RH set-ups, the mini-blocks were often not even completely covered by hyphae and the recipients held abundant malt agar. Also, the mass gains disappear quickly, which would be logical, as the fungus uses malt agar as a nutrient.

Issues and suggestions for improvement

Designing a laboratory set-up to assess the effect of material MC on decay is challenging (Brischke and Alfredsen, 2020). In the experiment presented here, several issues were identified. Some of them were related to the particular set-up and can be solved in view of future experiments. It would be advisable, for instance, to optimise the ventilator settings, by reducing direct air flow over the specimens and providing ventilation in pulses instead of continuously. It would be interesting as well to measure the RH over time, to see whether the conditions remain stable. Also, the number of specimens should be increased to at least five replicates, but preferably ten or more. To make this feasible, the frequency of measuring could be reduced to, for instance, once every five days. Instead of using saturated salt solutions, a similar set-up could be made by using climate cabinets, although sterility would then be a challenge. One issue that would remain, is that the fungus influences the MC of the mini-blocks when it grows in or on the blocks and when it starts to degrade. This makes it difficult to define critical MCs at which materials are at risk.

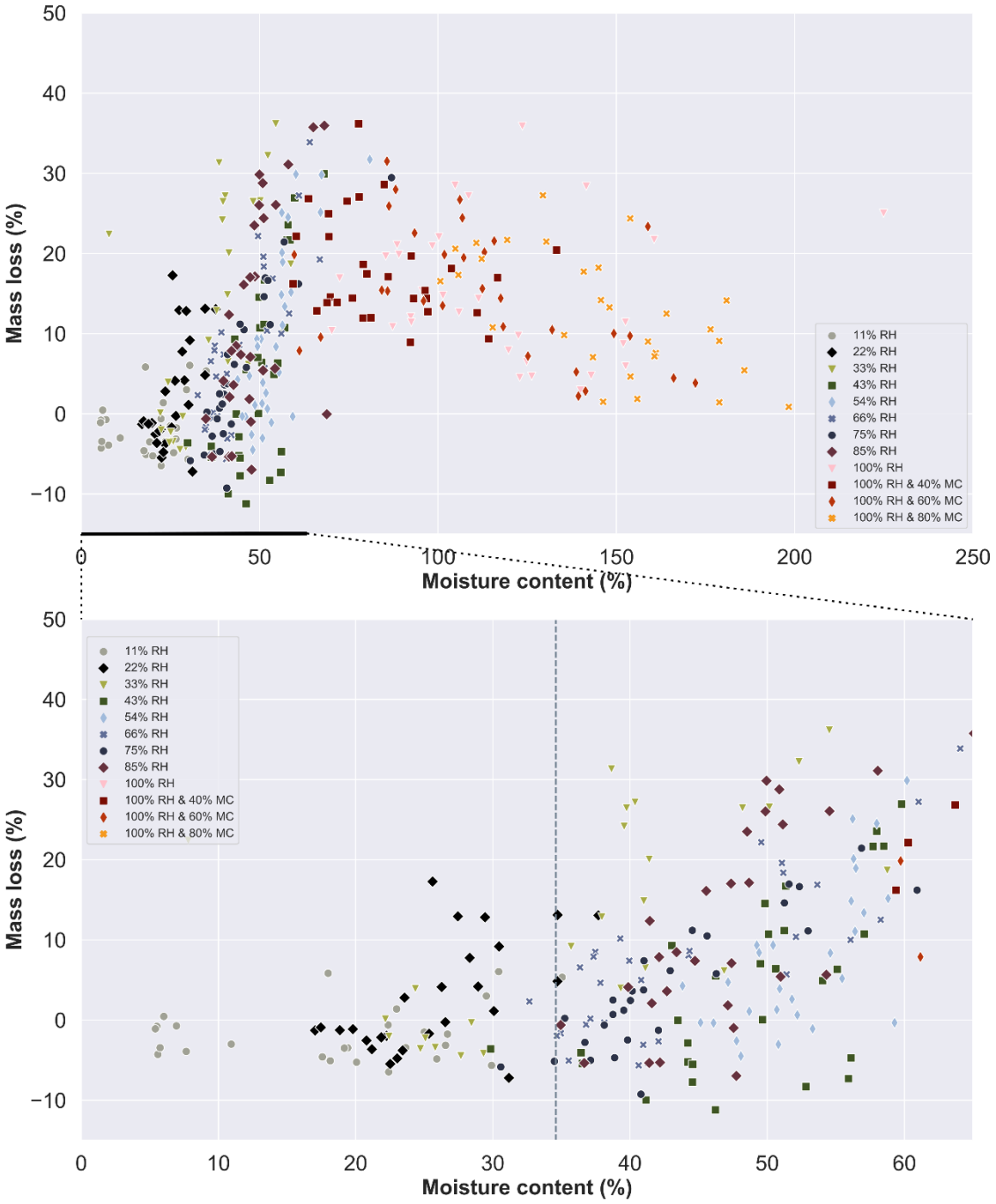

Figure 4-11 Moisture content and mass loss for Scots pine mini-blocks with 21 days or more exposure to *C. puteana* in different relative humidity (RH) set-ups. FSP=34.6% MC

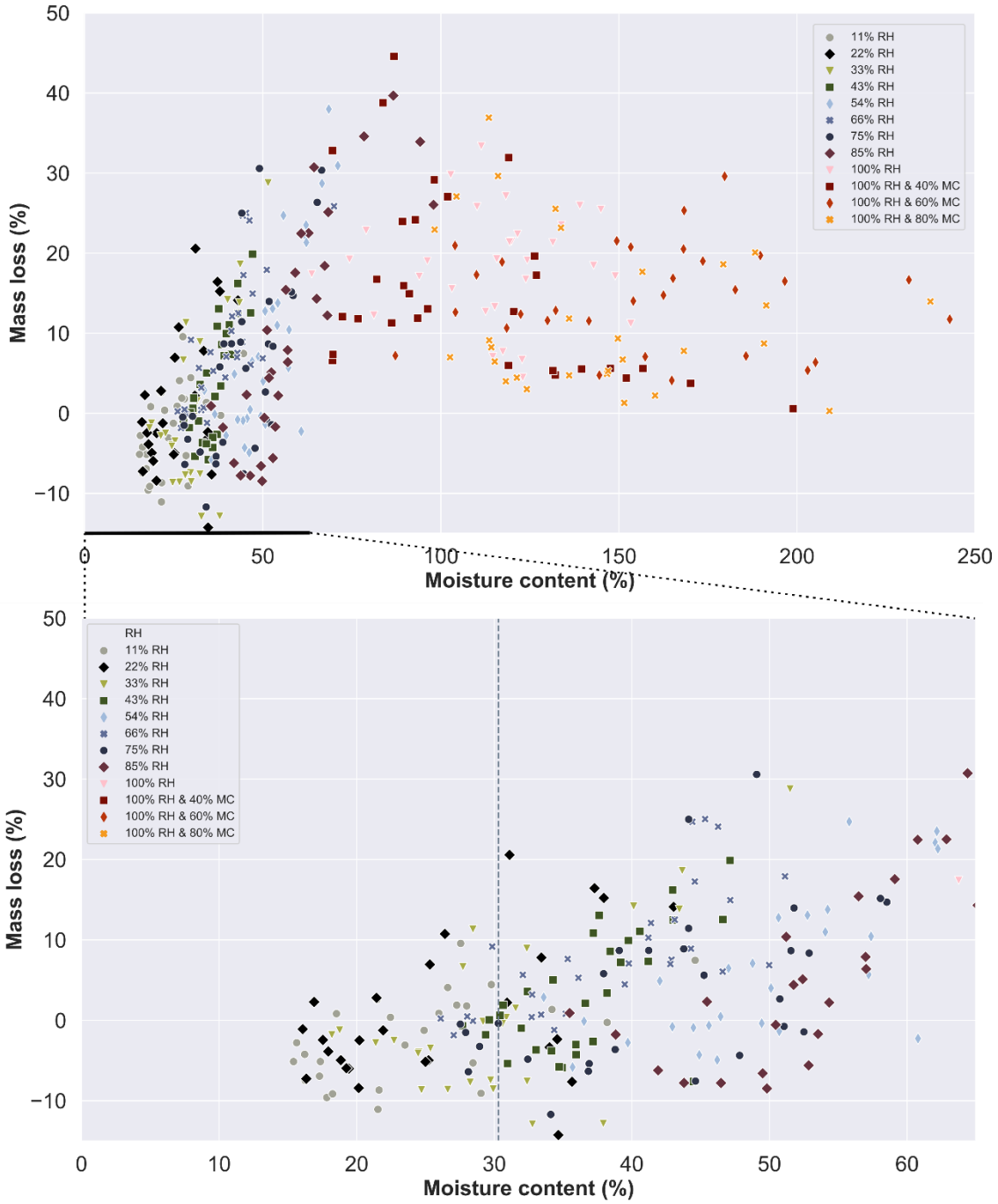

Figure 4-12 Moisture content and mass loss for Norway spruce mini-blocks with 21 days or more exposure to *C. puteana* in different relative humidity (RH) set-ups. FSP=30.3% MC

4.2.3 Conclusions

When wood specimens are in contact with viable mycelium, wood with a low MC can be at risk. From the pile tests, we know that *Coniophora puteana* is able to overgrow and moisten dry wood specimens in the presence of a moisture source and at high relative humidity. In our experiments, the fungus was able to degrade well at 100% RH, though too high MCs limited fungal decay due to waterlogging. However, when the RH was below 100%, mycelial development and decay slowed down. For instance, at 75% and 85% RH, the fungus was able to overgrow the specimens, but the mycelium was less dense. At low relative humidity conditions (11-22% RH), *C. puteana* had difficulties overgrowing the mini-block specimens. Even with the moisture source, the MC of the specimens largely remained below FSP and decay was limited. When no moisture source is present, hyphae are known to dehydrate when the RH is not high (Chapter 2). These results are not so easy to translate to the actual risk in practice. In case of a limited moisture source, mycelial development over a material surface might, for instance, be restricted to the surroundings of the moisture source. There is also a time lag before a wet material is colonized by spores of decay fungi and before they start to develop into viable mycelium, as well as competition from other micro-organisms.

4.3 Moisture dynamics of bio-based building materials

This section will be published as:
De Ligne, L., Thybring, E.E., Thygesen, L.G., Omar, S., Baetens, J.M., De Baets, B., Van den Bulcke, J., Van Acker, J. (in preparation)

Wood and wood fibre products are hygroscopic materials, meaning that they can attract, hold and release water molecules (Skaar, 1988). This interaction with moisture has an important impact on the properties (strength and stiffness) and performance of bio-based building materials (Ross, 2010; Jones and Brischke, 2017). Due to their hygroscopic nature, wood and other bio-based building materials can act as moisture-buffering materials (Li *et al.,* 2012; Rode *et al.,* 2006). This is an excellent characteristic, as a more constant air humidity reduces the energy needed for heating and cooling of an interior space and improves the air quality (Osanyintola and Simonson, 2006; Lozhechnikova *et al.,* 2015). In the hygroscopic moisture range, generally from 0 to about 95-98% relative humidity (RH), the hygroscopic nature of wood and bio-based building materials can thus be an advantage, as the moisture is absorbed by the wood cell walls and bound to the wood cell wall polymers through hydrogen bounding (Fredriksson, 2019). However, when liquid water is present, for instance due to condensation or leakage indoors or in outdoor exposure applications, hygroscopic materials take up water in cell lumen, pits and macro voids (such as the space between strands in oriented strand board) and the risk of fungal decay increases (CEN EN 335 standard, 2013; Brischke and Alfredsen, 2020). The service life of a material depends on its durability and its moisture dynamics. Materials that have a low wetting ability or dry out easily, for instance, are less susceptible to fungal degradation, as the Time of Wetness (ToW) is short (Van Acker *et al.*, 2014). Understanding how material porosity and chemistry affect moisture dynamics is therefore essential for their efficient use, as well as for product optimisation. In this section we assess the moisture dynamics of three commonly used wood-based panels, thermally modified wood and five wood fibre insulation materials. Liquid water absorption and water vapour desorption is assessed with the floating test CEN TS 16818 standard (2018). Three complementary techniques are applied to elucidate the influence of material characteristics on the liquid water absorption and desorption behaviour of these materials: X-ray CT to assess the porosity of the materials, Attenuated Total Reflectance Fourier Transform Infrared (ATR-FTIR) spectroscopy, to provide a chemical characterisation of the materials and Low-Field Nuclear Magnetic Resonance (LNFMR) spectroscopy, to determine the 'water populations' when the material is water saturated, which gives an indication of material porosity from macro voids to cell wall water.

4.3.1 Material and Methods

Bio-based materials

To have a broad view on the moisture dynamics of bio-based building materials in general, we opted for materials with different structures (solid wood, veneer-based, strand-based and fibre-based) and that differ in density and additives (glue, paraffin, bitumen). Three commonly used wood-based panels (radiata pine plywood, three-layer spruce panel and oriented strand board), thermally modified spruce wood and six wood fibre insulation materials were used. The wood fibre insulation materials contain different additives, differ in density and were made with different production processes. In the wet production process, wood chips and shavings are ground down into wood fibre pulp and mixed with water and possibly additives, such as paraffin. This mix forms a continuous fibre mat, from which half of the water is removed with a mechanical press (see section 3.3.1, Figure 3-9). The lignin in the wood fibres serves as a natural binding agent when heated with water, so no binding agent needs to be added. In the dry production process, the wood fibre pulp is glued together with isocyanate (see section 3.3.1, Figure 3-10). The adhesives are cured and hardened through exposure to a mixture of water vapour and air.

Table 4-2 gives an overview of the selected materials, their main components and/or production process, the panel thickness (mm) and density (kg/m³) at 12% MC. Additionally, pore volume estimations (%) based on the material density and based on the X-ray CT images (section X-ray CT) are included and the average moisture content (MC) after water saturation (section LFNMR). The pore volume estimations based on density were calculated as follows:

$$pv = 1 - \frac{D_{mat}}{D_{cell}} \qquad (4\text{-}3)$$

with pv the pore volume (%), D_{mat} the material density (kg/m³) and D_{cell} the density of cellulose (1500 kg/m³). Since the wood species of the insulation materials was not specified, we opted to use cellulose density instead of the cell wall density, as the latter is wood species specific.

Table 4-2 Overview of material properties: components and/or treatment, panel thickness (mm), density (kg/m³), pore volume (%) estimation based on the material density relative to a solid reference density of 1500 kg/m³ (density of cellulose as reference value), pore volume estimation of reference specimens (5 x 5 x 10 mm) assessed with X-ray micro CT (resolution of 6 µm) and average MC (%) of LFNMR specimens (5 x 5 x 10 mm³) after water saturation under vacuum pressure. *Latewood pores with a diameter smaller than 7 µm were not visible with X-ray micro CT. x: not included in X-ray CT and LFNMR analysis.

Label	**Material**	Components and/or treatment	Plate thickness in dry state (mm)	Density (kg/m³)	Pore volume (%) estimation based on material density	Pore volume (%) estimation based on X-ray CT*	Average MC (%) LFNMR specimens after saturation
PLY	Plywood radiata pine	Radiata pine veneers, glue (non-specified)	18	550	63	36	184 ± 9
TMT	Thermally modified spruce	Process: 1) Hydrothermolysis up to 170°C 2) drying 3) heated again to up to 180^{0}C in dry conditions without oxygen	18	380-450	70-75	29	247 ± 18
SWP	Three-layer spruce panel	Spruce, isocyanate adhesive	19	470	69	26	251 ± 93
OSB	Oriented strand board	Scots pine fibres, isocyanate adhesive	18	600-680	55-60	45	136 ± 15
BWFIB	Porous wood fibre board with bitumen	Norway spruce/Scots pine fibres, bitumen emulsion	22	270	82	76	517 ± 38
WFIB1	Wood fibre insulation board 1	Norway spruce/Scots pine fibres, ammonium phosphate, polyolefin fibres	25	50	97	92	762 ± 171
WFIB2	Wood fibre insulation board 2	Norway spruce/Scots pine fibres, wet production	60	160	89	53	777 ± 57
WFIB3	Wood fibre insulation board 3	Norway spruce/Scots pine fibres, isocyanate adhesive (4%), paraffin (4%), dry production	40	140	91	80	579 ± 19
WFIB4	Wood fibre insulation board 4	Norway spruce/Scots pine fibres, aluminium sulphate, paraffin (4%), dye, wet production	5	250	83	69	548 ± 81
WFIB5	Wood fibre insulation board 5	Norway spruce/Scots pine fibres, paraffin (4%), wet production	40	160	89	x	x

Floating test

To assess the moisture behaviour of the selected bio-based materials, a floating test was performed according to CEN TS 16818 standard (2018). In the floating test, specimens are laid afloat a water surface to determine liquid water absorption over 144h. Subsequently, they are left to dry for 144h to determine the rate of water vapour desorption. The edges of the specimens (50 x 50 mm^2 x panel thickness) were sealed with a solvent-borne polyurethane paint containing a polyisocyanate curing agent, mixed with a hardener, to prohibit water from entering through the sides (SigmaDur 520, PPG Industries). The specimens (five replicates per material) were conditioned (65% RH, 20°C) for two weeks and weighed (m_i). Then, specimens were put on the water surface of containers filled with deionized water inside the conditioning room. The specimens were blotted on a wet cloth and weighed (m_x) at several time intervals (5s, 30s, 1min, 10min, 5min, 10min, 30min 1h, 4h, 8h, 24h, 48h, 72h, 144h). Since some of the selected materials were expected to absorb water very fast, a high temporal resolution was chosen at the beginning of the experiment. After 144 hours of absorption, the materials were put on drying racks in a conditioning room (65% RH, 20°C) and were weighed again after 1h, 4h, 8h, 24h, 48h, 96h and 168h to assess the desorption rate. After 168 hours of desorption, the specimens were oven dried at (103 ± 2) °C and weighed again (m_0).

The water uptake (g/cm^2) was calculated over time, using Eq. 4, with *A* being the test surface area of the specimen in cm^2, m_x the mass of the specimen and m_i the initial mass of the specimen in g.

$$W = \frac{m_x - m_i}{A} \quad (4\text{-}4)$$

Table 4-3 Classification of absorption based on water uptake and release (g/cm^2) after 144 h, adapted from Van Acker *et al.* (2014).

Class	Maximal water uptake (g/cm^2) after 114h of absorption
1	0.75
2	0.95
3	1.15
4	1.35
5	1.75
6	2.75
7	5.00
8	∞

Absorption and desorption curves were fitted to the water uptake (g/cm^2) datapoints based on Eq. 5 and Eq. 6 respectively, similar to Van Acker *et al.* (2014):

$$f(t) = a t^b \quad (4\text{-}5)$$

$$f(t) = a + be^{-\frac{t}{c}} \quad (4\text{-}6)$$

The residual moisture content after *t* hours of desorption was calculated as follows:

$$rm_t = MC_i - MC_t \quad (4\text{-}7)$$

with MC_i the initial moisture content and MC_t the moisture content after t hours of desorption.

A side-effect of the wet production process is that the bottom layer of the wood fibre panels is denser and harder than the rest of the panel. In an additional floating experiment, five specimens of WFIB2 and WFIBF5 were therefore laid afloat with the hard bottom side and five with the soft top side in water contact. Additionally, the influence of having a defect in the hard bottom side was assessed by drilling a bore hole of 5 mm diameter and 5 mm deep for five additional specimens of WFIB2 and WFIBF5.

Low-Field Nuclear Magnetic Resonance measurements

Low-Field Nuclear Magnetic Resonance (LNFMR) spectroscopy is a technique used to assess the relaxation time of the hydrogen nuclei in water molecules after excitation by a radio frequency pulse. The relaxation time depends on how tight the water is bound, which depends on the chemical and physical environment of the water molecule. The spin-spin relaxation time or T_2 value of water molecules in smaller pores is shorter than in larger pores, when the pore wall surfaces are similar (Fredriksson and Thygesen, 2017). Therefore, LFNMR can be applied to gain knowledge on the water populations in a material.

Five replicates (5 x 5 x 10 mm^3) for each material were water saturated under vacuum pressure with a vacuum pump. Excess surface water was removed by applying a wet cloth without drying the specimens. The specimens were put in a pre-weighed glass LFNMR tube, after which the wet weight of the specimen was measured with an accuracy of 10^{-4}g. The average moisture content (MC) of the LFNMR specimens after water saturation is listed in Table 4-2. A solid Teflon rod was inserted into the glass LFNMR tube to fill the remaining space (Figure 4-13), thereby limiting water evaporation from the specimen during the experiment. The glass LFNMR tube containing the specimen was placed in a Bruker mq20 minispec with a 0.47T permanent magnet (Bruker, Billerica, MA, USA) to perform LFNMR measurements. The temperature in the LFNMR around the specimen was kept constant at 22 °C by circulation of water in the probe using a Julabo Refrigiated and Heating Circulator (Julabo GmbH, Seelbach, Germany). The specimen was allowed to thermally equilibrate in the instrument for two minutes before starting each measurement. The Carr-Purcell-Meiboom-Gill (CPMG) pulse sequence was used to measure the spin-spin relaxation

time (T_2) of the specimens with a pulse separation (τ) of 0.1 ms, 8000 echoes, 32 scans and a recycle delay of 30s. Exponential decay analysis (Instratov and Vyvenko, 1999) was applied to the recorded LFNMR decay curves to give smooth, continuous distributions of T_2 relaxation times. The range for the distribution was set to 0.2–2500 ms for wood-based panels and 0.2–4200 ms for wood fibre insulation materials. This larger range was necessary for fibre based insulation materials, since the water-saturated specimens contained much more water, presumably located in larger pores than solid wood based specimens. Relative peak area and T_2 values corresponding to maximum peak intensity were determined for each peak. The Kruskal-Wallis H-test, a non-parametric statistical test, was applied for testing whether the median T_2 values and median relative peak areas of the assessed bio-based materials were different. When the difference between medians was significant, Dunn's multiple comparison test (1961) was applied to pinpoint for which materials the medians were different. Benjamini-Hochberg correction (Benjamini and Hochberg, 1995) was performed to control the false discovery rate (Type I error).

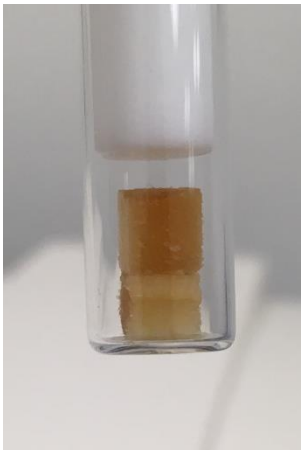

Figure 4-13 SWP specimen in LFNMR tube with Teflon rod. Due to the specimen size, only two out of three layers are included. SWP = Three-layer spruce panel.

Attenuated total reflectance Fourier transform infrared spectroscopy

To assess whether the bio-based building materials differed in chemical composition, Attenuated Total Reflectance Fourier Transform Infrared (ATR-FTIR) spectroscopy was applied. In ATR-FTIR, a beam of infrared light passes through a crystal on which a sample is positioned (Djajadi *et al.*, 2017). Depending on the interaction with the sample and the wavenumber, an FTIR absorbance spectrum is obtained, providing information on the presence of certain functional groups, such as CH_2, OH, and C=O. Each material was grinded to a powder with a particle size smaller than 0.1 mm using a centrifugal mill (ZM 200, Retsch GmbH, Haan, Germany). The powder was dried in a BINDER VD23 vacuum oven (BINDER GmbH, Tuttlingen, Germany) for 24 hours. For each material, three ATR-FTIR measurements were performed on the oven-dried powders using a Nicolet 6700 FT-IR, Pike Technologies GladiATR diamond

spectrometer (Thermo Scientific, Waltham, MA, USA), with a working temperature of 25 °C. The spectral range included was 3700–500 cm^{-1} and spectra were obtained using 64 scans (128 for the background) and a resolution of 2.0 cm^{-1}. After applying individual linear baselines, the area underneath the peaks in wavenumber regions 2815-2985 cm^{-1} (associated with CH- and CH_2-stretching) and wavenumber regions 3050-3550 cm^{-1} (associated with OH-stretching) were calculated, and the peak area ratio relative to the holocellulose peak (870-920 cm^{-1}) was determined for each material (Djajadi *et al.*, 2017; Lupoi, 2015).

X-ray CT

X-ray CT was used to obtain a 3-D visualisation of the internal material structure and to determine the pseudo pore distributions of the assessed bio-based materials.

Image acquisition

For PLY, TMT, SWP and OSB, one of the specimens (5 x 5 x 10 mm^3) previously exposed to LFNMR was selected. To prevent cracks, the water-saturated specimens were allowed to dry at room temperature before oven drying, which was necessary to determine the moisture content at water saturation. For BWFIB, WFIB1, WFIB3 and WFIB4, water saturation under vacuum pressure and subsequent drying after the LFNMR measurement had altered the internal structure of the specimens considerably. Therefore, new specimens were selected for X-ray CT scanning of these materials. One specimen per material (5 x 5 x 10 mm^3) was placed on a sample holder and scanned with the Nanowood scanner at the Centre for X-ray Tomography at Ghent University (UGCT; http://www.ugct.ugent.be). All specimens were scanned at an average voltage of 50 kV, a target current of 100 µA, and an exposure time of 1000 ms per image, resulting in an approximate scan time of 38 min per specimen obtaining 2001 projections. Reconstruction was performed using Octopus (Vlassenbroeck *et al.,* 2007), a tomography reconstruction package for parallel and cone-beam geometry. The resulting high-resolution scans had an approximate voxel pitch of 5-7 µm. Reconstructed images of the specimens were visualized using Octopus Analysis (Brabant *et al.,* 2011). Due to the scan resolution and the specimen size, this set-up allowed for assessment of pores with a minimum radius of 7 µm and a maximum radius of 11.2 mm. A bilateral filter was applied on the reconstructed images, followed by thresholding in Octopus Analysis (Brabant *et al.,* 2011), resulting in a binary image volume, with white voxels representing the wood mass and black voxels representing the pores. The minimum pore size analysed was 1 voxel. From this binary image volume, the pore volume (%) was assessed (Table 4-2). Due to the scan resolution, part of the latewood pores was obscured after thresholding, resulting in significant differences between the pore volume estimation based on density and the one estimated based on the CT-images. This discrepancy was highest for materials that did not have macro voids, such as plywood, modified spruce and spruce binder, as a large part of their pore volume is covered by small latewood pores. The total pore volume based on CT is thus an approximation of all pores that are at least larger than 7 µm.

By consecutive expanding and shrinking of the thresholded volume in Octopus Analysis, a pseudo pore size distribution was acquired (Figure 4-14). The relative pore volume was calculated as follows:

$$rpv_n = \frac{pv_n}{pv_{tot}} \quad (4\text{-}8)$$

with rpv_n the relative pore volume of the pores that were filled by *n* consecutive expand, pv_n the pore volume after *n* expanding steps followed by *n* shrinking steps and pv_{tot} the total pore volume when no expansion or shrinking had been applied.

Expand and shrink approach
First, all white voxels that were located next to a black voxel were extended *n* times with 1 voxel. Next, all white voxels that were located next to a black voxel were shrunk *n* times with 1 voxel in Octopus analysis. Simply put, if expanded one time (*n*=1, see Figure 4-14 in 2-D), small pores (black voxels) were filled up by the surrounding white voxels, while larger pores became smaller. After the subsequent shrink step, the white voxels that were located next to black voxels, shrunk by 1 voxel, thus opening the pores back up again. Since small pores were filled up, those were not opened up again during the shrink step and therefore remained filled. For each *n* consecutive expand and *n* consecutive shrink steps, the total pore volume was assessed. The number of consecutive expand and shrinks steps (*n*) was increased until no more pores remained (pore volume of 0.02%).

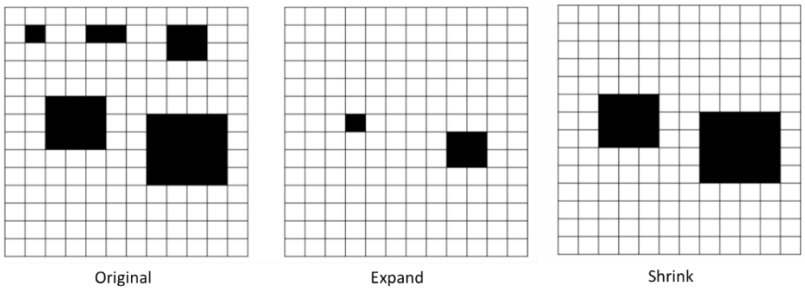

Figure 4-14 Illustration expand and shrink approach with *n*=1.

The Euclidean distance from pore centre to pore wall was assessed based on the thresholded binary image volume in Python (Python Software Foundation, https://www.python.org/). Based on the Euclidean distance transform function (EDT) in the multidimensional image transform package (package: scipy.ndimage, function: distance_transform_edt), the Euclidean distance from every pore voxel to the nearest pore wall was calculated in 3D (Figure 4-15). Additionally, skeletonization was applied on the binary image volume in 3D, to assess the location of the centre voxel(s) of each

pore (package: skimage.morphology, function: skeletonize_3d). Note that for a perfect sphere, the centre of the pore is represented by one voxel, while for a cylindrical pore the centre is represented by a line. To determine the Euclidean distance from pore centre to pore wall, the EDT matrix was multiplied with the skeletonization matrix, so that only the Euclidean distance from the pore centres to the pore walls was listed. A pseudo-pore distribution based on the Euclidean distance from pore centre to pore wall was determined by dividing the occurrence of each Euclidean distance by the total amount of assessed Euclidean distances from pore centre to pore wall.

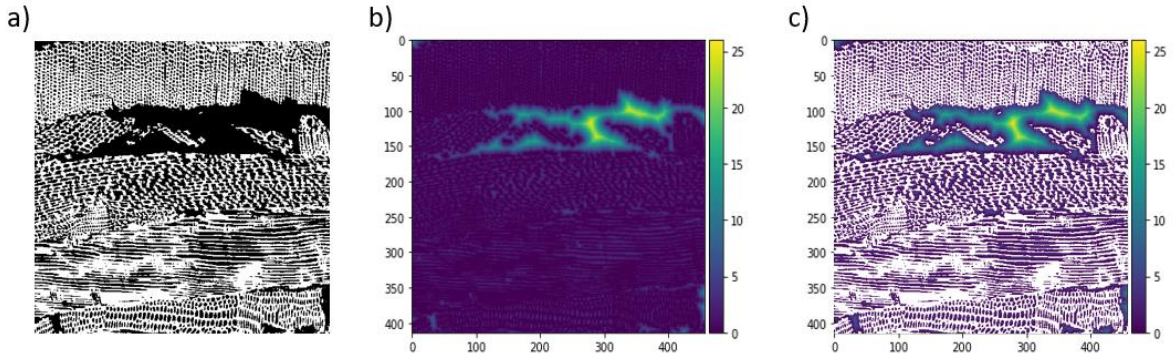

Figure 4-15 Example of Euclidean distance transform (EDT) on an X-ray CT image of OSB. a) Binary image b) result EDT c) result EDT visualised on top of binary image. The colour bar on the right-hand side indicates the Euclidean distance in voxels.

4.3.2 Results and discussion

Water absorption and desorption properties were assessed with the floating test, during which bio-based materials were laid afloat a water surface and the amount of absorbed water was registered at predetermined time intervals. The total amount of liquid water absorbed after 144h differed substantially between bio-based materials, with some of the wood fibre insulation boards (WFIB) with water uptakes up to 100 times higher (Figure 4-16b) than those of the wood-based panels (Figure 4-16a). Wood with a lower density, and therefore a higher porosity, typically absorbs more water (Fredriksson, 2019). This principle can easily be extended to bio-based materials in general and was clearly the case for wood fibre board type 1, which had an estimated porosity of 97% (Table 4-2). WFIB2 and WFIB3 had similar overall porosities, but their water absorption and desorption properties were different. Clearly, other phenomena besides overall porosity affect the water absorption capacity of insulation materials and wood-based panels as well.

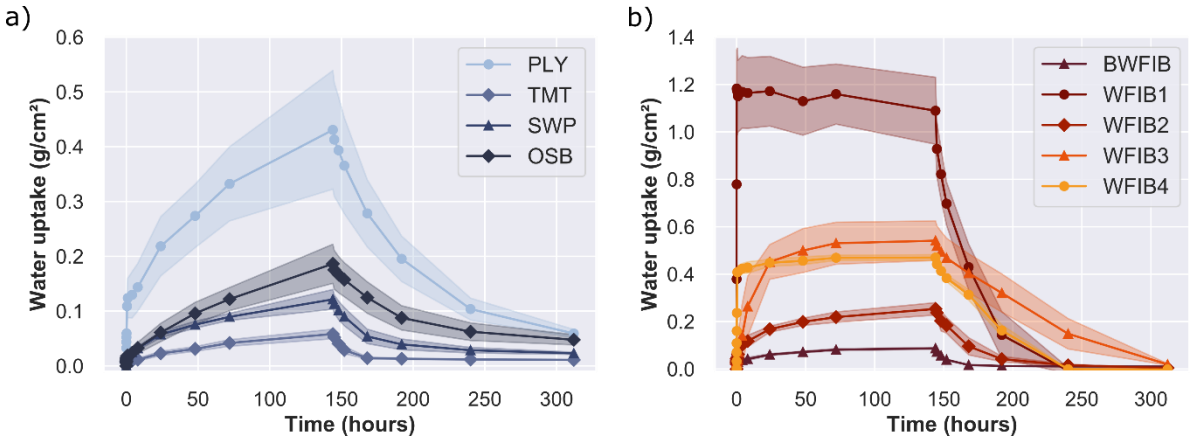

Figure 4-16 Mean liquid water uptake (g/cm^2) with standard deviation over 144 hours of absorption and 168 hours of desorption in a floating test. a) Wood-based panels: radiata pine plywood (PLY), thermally modified spruce (TMT), three-layer spruce binder (SWP) and oriented strand board (OSB). b) Insulation materials: porous bituminised wood fibre board (BWFIB) and wood fibre insulation type 1-4 (WFIB1-4).

Characterization of water populations with LFNMR

Wood-based panels and thermally modified wood

The water populations of each material were assessed with LFNMR. The spin-spin relaxation time (T_2) indicates how closely the water is interacting with the solid material. For untreated softwood, usually three peaks are observed: the 1st peak related to cell wall water at T_2 < 4 ms (Fredriksson and Thygesen, 2017; Beck *et al.*, 2018), the 2nd peak related to free water located in pits and the 3rd peak related to water in tracheid lumen (T_2 > 40 ms). The thermally modified wood and wood-based panels (Figure 4-17) did show the typical distribution pattern, apart from OSB which had an additional peak at 262.8 ms (Table 4-4). Peak 1, peak 2 and peak 3 T_2 values of radiata pine plywood corresponded very well to those assessed for untreated radiata pine in a previous study by Beck *et al.* (2018) (Table 4-4). The relative area under each peak was of the same order of magnitude as well (Table 4-5). The plywood production process did not seem to have an apparent influence on pore distribution and pore surface hydrophobicity. In the X-ray CT images (Figure 4-18), only a very small glue layer could indeed be observed in between intact radiata pine layers, with no excess of glue filling up pores in the proximity of the glue layer. Similarly, the T_2 times of peak 2 and 3 of the three-layer spruce panel specimens are in the same order of magnitude as those found by Fredriksson and Thygesen (2017) for solid Norway spruce, as well as the relative areas. Thus, when the wood anatomy of a species remains intact, the water populations of the wood-based panel were not affected in water-saturated state.

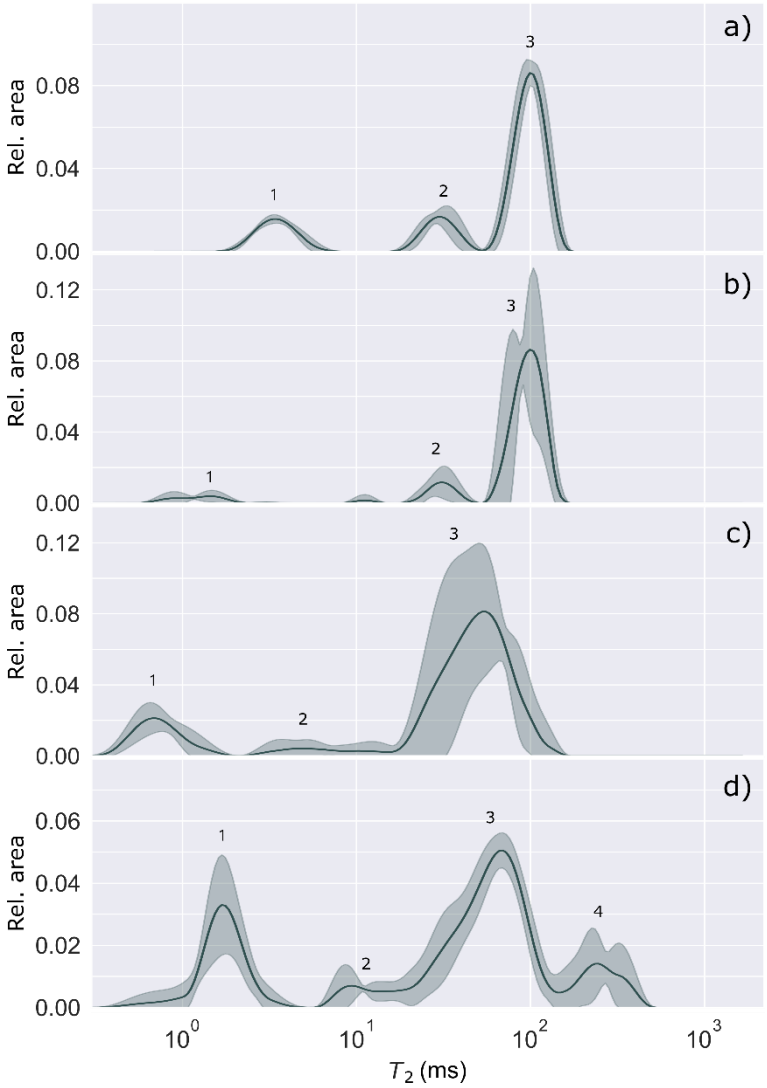

Figure 4-17 Continuous T2 distributions (with peak numbers 1, 2, 3 and 4) of four wood-based panels, showing the mean values (line) and standard deviation (filled zone). a) Radiata pine plywood (PLY), b) thermally modified spruce (TMT), c) three-layer spruce binder (SWP) and d) oriented strand board (OSB).

The LFNMR relaxation time distributions of Oriented Strand Board (OSB) specimens, however, contained a fourth peak. In previous LFNMR studies, peaks in this region were attributed to surface water on the wood specimens (Fredriksson and Thygesen, 2017; Beck *et al.,* 2018). However, properly removing excess water from all sides of the specimen with a wet cloth should avoid peaks related to surface water. As the fourth peak was absent in the other wood-based panel specimens, its consistent presence in the OSB specimens was therefore a clear indication of water in pores larger than tracheid lumens. With X-ray CT, pores with Euclidean distances from centre to pore wall of 12-150 µm could indeed be observed between the wood strands. From the X-ray CT images, it could be observed as well that the wood anatomy of the separate strands had remained relatively intact, with the tracheids being clearly discernible (Figure 4-18).

Table 4-4 Mean values of the T_2 (ms) determined by continuous curve fitting and reference values for solid Radiata pine and Norway spruce wood. The Kruskal-Wallis H-test was applied for testing differences in median T_2 values, with Dunn's multiple comparison test as post-hoc test with Benjamini-Hochberg correction. Based on Dunn's multiple comparison test, the materials were grouped (a-h). For each material, the assigned group letter is put in bold, while the other letters indicate the groups which had similar (=not significantly different) T_2 values.

	Peak 1		Peak 2		Peak 3		Peak 4		Peak 5		Peak 6	
	mean	**std**	**mean**	**std**	**mean**	**std**	**mean**	**std**	**mean**	**std**	**mean**	**std**
PLY	3.4 a,b,c	0.1	30 a,b	3.6	101 a,b,c	7.8						
TMT	1.3 b,c,d,e	0.3	26 a,b	8.9	97 a,b,c	12.8						
SWP	0.8 c,d,e	0.1	7 b,c	3.4	57 a,b,c,d,e	20.0						
OSB	1.8 a,b,c,d	0.2	11 a,b,c	2.0	69 a,b,c,d	7.1	263 a,b	59.0				
BWFIB	1.1 b,c,d,e	0.5	85 b,c	4.0	38 b,c,d,e	12.4	123 b,c	41.1	482 a,b,c	45.4		
WFIB1	1.8 a,b,c,d,e	0.6	10 a,b,c	5.1	46 b,c,d,e	10.5	200 a,b,c	81.5	728 a,b	141.3		
WFIB2	1.1 b,c,d,e	0.6	5 b,c	3.1	32 c,d,e	11.0	119 a,b,c	16.9	398 b,c,d	61.1		
WFIB3	1.4 a,b,c,d,e	0.3	7 b,c	2.5	35 c,d,e	10.0	93 b,c	16.1	282 c,d	41.2	937	46.9
WFIB4	1.8 a,b,c,d,e	0.9	13 a,b,c	8.4	70 a,b,c,d	11.6	287 a,b	59.3				
Reference												
Radiata pine[1]	3		20-30		100-110							
Norway spruce[2]	1.3-2.2		4.8-18.2		LW: 45.4-77.4 EW: 57.6-103.8							

[1]Beck et al (2018); [2]Fredriksson and Thygesen (2017)

Table 4-5 Mean relative area (-) under each peak determined by continuous curve fitting. The Kruskal-Wallis H-test was applied for testing differences in median relative area, with Dunn's test as post-hoc with Benjamini-Hochberg correction. Based on Dunn's multiple comparison test, the materials were grouped (a-h). For each material, the assigned group letter is put in bold, while the other letters indicate the groups which had similar (=not significantly different) areas.

	Peak 1		Peak 2		Peak 3		Peak 4		Peak 5		Peak 6	
	mean	**std**	**mean**	**std**	**mean**	**std**	**mean**	**std**	**mean**	**std**	**mean**	**std**
PLY	0.16 a,**b**,c,d	0.02	0.15 **a**,b,c	0.02	0.69 a,**b**,c,d,e	0.04						
TMT	0.06 b,c,**d**,e	0.01	0.11 a,**b**,c,d	0.04	0.84 **a**,b,c,d	0.04						
SWP	0.16 a,**b**,c,d	0.03	0.05 a,b,**c**,d,e	0.02	0.77 a,b,**c**,d,e,f	0.07						
OSB	0.24 **a**,b,c	0.05	0.05 a,b,**c**,d,e	0.02	0.54 a,b,c,**d**,e,f,g	0.10	0.12 b,**c**,d	0.02				
BWFIB	0.06 b,c,**d**,e	0.02	0.03 b,c,**d**,e	0.01	0.12 d,e,f,**g**,h	0.06	0.23 a,**b**,c	0.06	0.58 **a**,b	0.06		
WFIB1	0.05 c,d,**e**	0.01	0.03 b,c,**d**,e	0.01	0.20 b,c,d,**e**,f,g,h	0.07	0.13 b,**c**,d	0.02	0.61 **a**,b	0.02		
WFIB2	0.04 c,d,**e**	0.02	0.04 b,c,**d**,e	0.02	0.15 c,d,e,**f**,g,h	0.04	0.27 a,**b**,c	0.03	0.55 a,**b**,c	0.10		
WFIB3	0.06 b,c,**d**,e	0.01	0.01 c,d,**e**	0.01	0.04 e,f,g,**h**	0.01	0.06 c,**d**	0.02	0.10 b,**c**	0.01	0.75	0.01
WFIB4	0.07 a,b,**c**,d,e	0.02	0.10 a,**b**,c,d	0.07	0.45 a,b,c,**d**,e,f,g	0.06	0.38 **a**,b	0.04				
Reference												
Radiata pine[1]	0.10-0.27		0.01-0.04		0.63-0.85							
Norway spruce[2]	0.16 a,**b**,c,d	0.02	0.15 **a**,b,c	0.02	0.69 a,**b**,c,d,e							

[1]Beck et al (2018); [2]Fredriksson and Thygesen (2017)

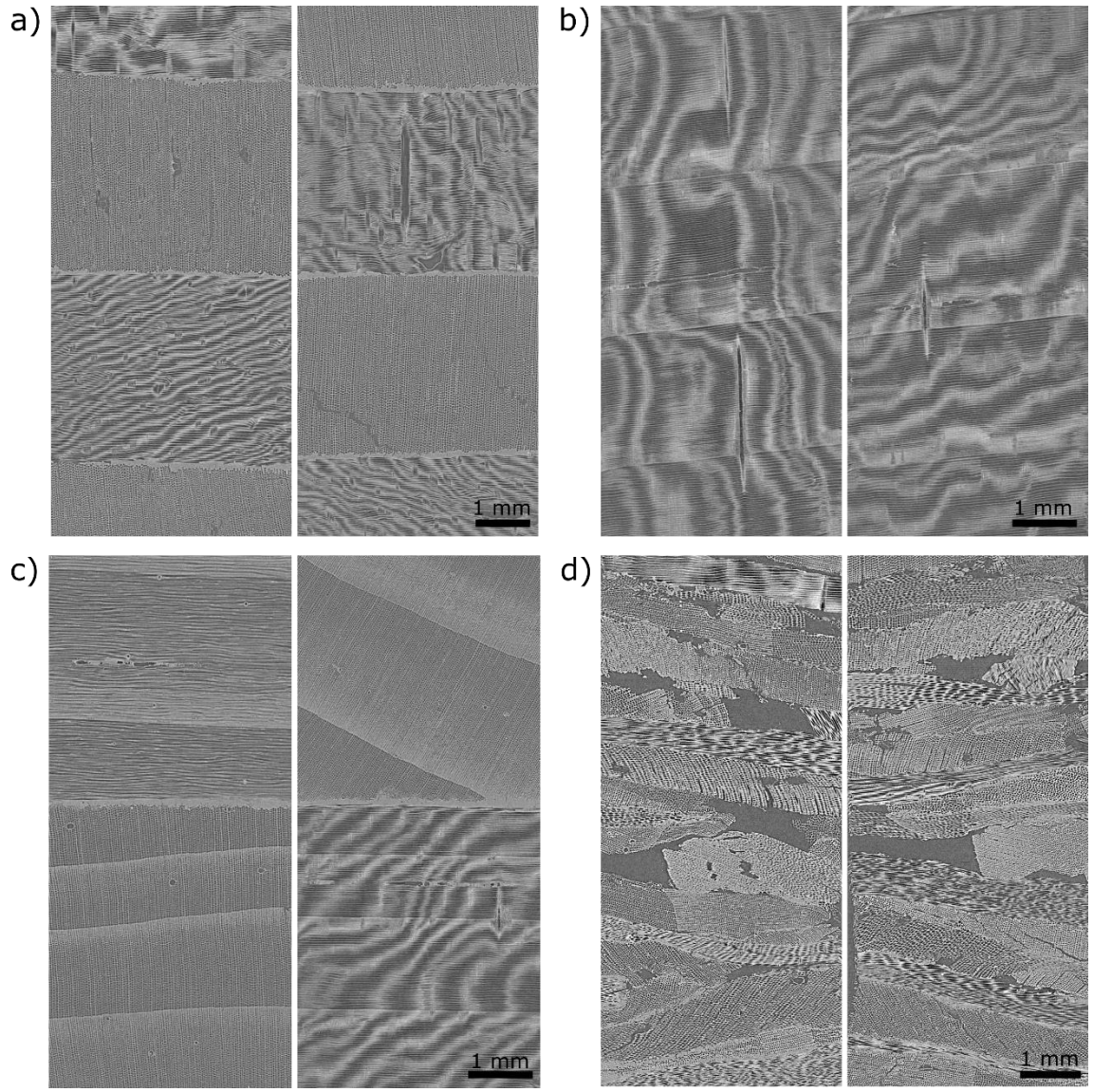

Figure 4-18 X-ray CT visualisation of the wood-based panels, with a slice displaying the front view (left) and the side view (right) for each specimen (5 x 5 x 10 mm^3). a) Radiata pine plywood (PLY), b) thermally modified spruce (TMT), c) three-layer spruce binder (SWP) and d) oriented strand board (OSB).

For wood-based panels, there was a good correlation between the LFNMR data and the pseudo pore distributions assessed with X-ray CT (Figure 4-19). OSB clearly differed from plywood (PLY), three-layer spruce panel (SWP) and thermally modified spruce (TMT). For the latter three wood products, 99% of the pores were filled after 2 consecutive shrink and expand steps (Figure 4-19b). Since pits (peak 2) cannot be observed at a scan resolution of 6 µm, the pore distributions of PLY, SWP and TMT corresponded to the LFNMR tracheid peak (peak 3). It can therefore be assumed that the pores filled after 2 consecutive shrink and expand steps in OSB likewise corresponded to peak 3. Indeed, 82% of the combined relative area of peak 3 and 4 was represented by peak 3, corresponding well to the amount of pore volume (78%)

covered by pores that were filled after 2 consecutive shrink and expand steps (Figure 4-19).

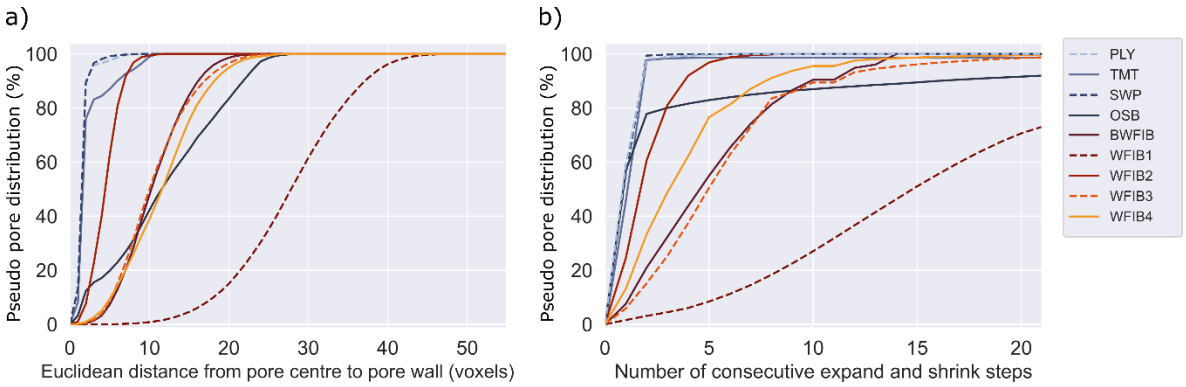

Figure 4-19 Cumulative representation of pseudo-pore distributions (X-ray micro CT at 6 µm resolution) of one reference specimen per material based on Euclidean distance – skeletonization approach (a) and on shrink and expand approach (b). PLY = Plywood Radiata pine, TMT = Thermally modified spruce, SWP = Three-layer spruce binder, OSB = Oriented strand board, BWFIB = Bituminised wood fibre board and WFIB1-4 = Wood fibre insulation board type 1-4.

Thermally modified wood

Wood modification changes the hydrophobicity of the pore surface and has been shown to significantly affect LFNMR relaxation time distributions by causing shifts in T_2 times. Acetylation has been shown to cause an increase in T_2 up to about 25 ms for peak 2 and up to about 100 ms for peak 3 for pine wood, depending on the degree of acetylation (Beck *et al.,* 2018). Here, thermally modified Norway spruce showed three peaks, with an increased T_2 time for peaks 2 and 3 as compared to the LFNMR relaxation time distributions assessed by Fredriksson and Thygesen (2017). The mean T_2 value of peak 2 was significantly higher than that of untreated Norway spruce. Peak 3 had a mean T_2 value of 97.5 ms, which, although high, remained in the range of T_2 values previously reported for earlywood of Norway spruce (57.6-103.8 ms). However, since the CT-images showed a clear presence of both earlywood and latewood (45.4-77.4 ms), the increased T_2 value of peak 3 was most likely due to thermal modification. These results correspond with the study of Cai *et al.* (2020), in which the T_2 values of peaks 2 and 3 had increased for thermally modified spruce. Likewise, thermal modification has been shown to increase T_2 value of peak 2 and 3 in Radiata pine, Chinese fir, loblolly pine, Scots pine and European ash (Guo *et al.*, 2018; Gao *et al.*, 2019; Wang *et al.*, 2019; Cai *et al.*, 2020). The following hypotheses are put forward to explain the increase in T_2 values: increase in lumen diameter due to removal of extractives and resin and deformation and merging of lumen tracheids, a rougher lumen surface due to microcracking and partial elimination of hydroxyl groups due to degradation of hemicelluloses (Guo *et al.*, 2018; Cai *et al.*, 2020).

Wood fibre insulation materials

The LFNMR relaxation time distributions of the wood fibre insulation materials generally contained five peaks, with the exception of WFIB4 which had four and WFIB3

which had six (Figure 4-20). The peaks were less distinctive than those of the wood-based panels, with overlapping peaks in the region of 10 ms and higher. Since these materials consist of wood fibres, the first two peaks were expected to correspond to peak 1 at a T_2 <4 ms (cell wall water) and peak 2 (water in pits). The mean T_2 values for peaks 1 and 2 were indeed in the range expected for Norway spruce. On the CT-images, loosely connected wood fibres were clearly distinguishable in the porous wood fibre insulation materials (Figure 4-21), especially when scrolling through the virtual 3D volume. Since intact tracheid structures occurred across the volume, we would expect a peak in the range of the T_2 values occurring for tracheid lumen in Norway spruce (45-104 ms) as well. For WFIB1 and WFIB4, this appeared to be the case. For WFIB2, WFIB3 and BWFIB, peak 3 was located at a T_2 value lower than the range for solid Norway spruce wood (Table 4-4, Fredriksson and Thygesen, 2017). Either the tracheid size of the wood fibres had decreased, for instance due to densification during the production process, or the shifts in T_2 values were caused by the presence of additives. Although WFIB3 and BWFIB contain hydrophobic additives in the form of paraffin and bitumen, respectively, it is unlikely that the tracheid lumen size is decreased by the tracheid lumens being filled with aforementioned additives, as the peak 3 location for WFIB3 and BWFIB was similar as for WFIB2. In a study on solid pine wood, T_2 values were little affected by wax treatment as well (Wang *et al.*, 2019).

Peaks 4, 5 and 6 do not occur in LFNMR relaxation time distributions of solid Norway spruce and Scots pine (Fredriksson and Thygesen, 2017; Beck *et al.*, 2018). Since they were located on the right-hand side of the tracheid peaks, their clear and consistent presence in the LFNMR relaxation time distributions of wood fibre insulation materials was related to water located in the space between wood fibres (tracheid bundles). The wood fibre insulation materials were indeed highly porous, with porosities ranging from 82-97% (based on density) and 53-92% (based on X-ray CT-images), see Table 4-2. Pseudo pore distributions were assessed based on X-ray CT images of each material (Figure 4-19), of which cross sections are displayed in Figure 4-21. Unlike for OSB, the relative pore volumes taken in by pores in the same order of magnitude as tracheids as assessed by X-ray CT did not correspond well with the ones estimated with LFNRM. In contrast to wood-based panels, which have a more rigid matrix and lower macro porosity, the pore structure of wood fibre insulation materials changed significantly during water absorption. The pore size distributions based on X-ray CT images of dry wood fibre insulation specimens were therefore unfit for comparison with the LFNRM spectra of water-saturated specimens. A distinct example is WFIB1, which is composed of loosely connected wood fibres with an overall porosity of 97% and a density of 50 kg/m^3. During water absorption, the fluffy nature of the material is completely lost and the wood fibres were in closer contact, eliminating part of the pores that were present in dry state. Instead of WFIB1, which had the largest pores in dry state (Figure 4-19), WFIB3 had a peak with the largest T_2 value (Figure 4-20). It can also be noted that, although the pseudo-pore distributions of BWFIB, WFIB3 and WFIB4 were very similar in dry state, their LFNMR relaxation time distributions differed

significantly (Table 4-4, Figure 4-20). Although the X-ray CT images could not be used to provide a correct estimation of the pseudo-pore volume in water-saturated state, the images were useful for detecting intactness of the original wood fibres.

The LFNMR relaxation time distributions of WFIB1, WFIB2 and BWFIB were similar. They all contained five peaks and the T_2 values and relative areas under each peak did not differ significantly based on the Kruskal-Wallis H-test with Dunn's multiple comparison test as post-hoc test. Note that the MC is not the mass fraction of water, but the ratio of water mass (total mass of water in the wood) to wood mass (the dry mass of the wood alone). The MCs of the water saturated WFIB specimens are all more than 100%, as the water mass is greater than the wood fibre mass.

Even though the water-saturated BWFIB specimens had an average MC of 517%, being more than 200% lower than that of WFIB1 and WFIB2 (Table 4-2), the water populations experienced similar constraints in all three wood fibre products. This difference in moisture content at water saturation can be contributed to the bitumen fraction in BWFIB, clearly inducing hydrophobicity, thereby reducing the water-holding capacity. In the LFNMR spectrum of WFIB3, peaks 3-6 did not overlap, in contrast to the other wood fibre insulation materials. Also, the width of peak 6, representing the bulk of the water volume, was 40% smaller than the main peak (peak 5) of WFIB1, WFIB2 and BWFIB, indicating less variation in pores of similar sizes. This additional peak (peak 6) at the highest T_2 value could be an indication of a more rigid matrix, as the pore structure of WFIB3 had apparently withheld better against shrinking/collapse during water saturation than the other wood fibre insulation materials, which had similar pore distributions in the dry state (Figure 4-19). Presumably, this rigidity was caused by the dry production process with isocyanate glue. Although WFIB3 contained the largest pores, its moisture content at water saturation was, similar to BWFIB, about 200% lower than that of WFIB1 and WFIB2 due to its hydrophobic components (Table 4-2).

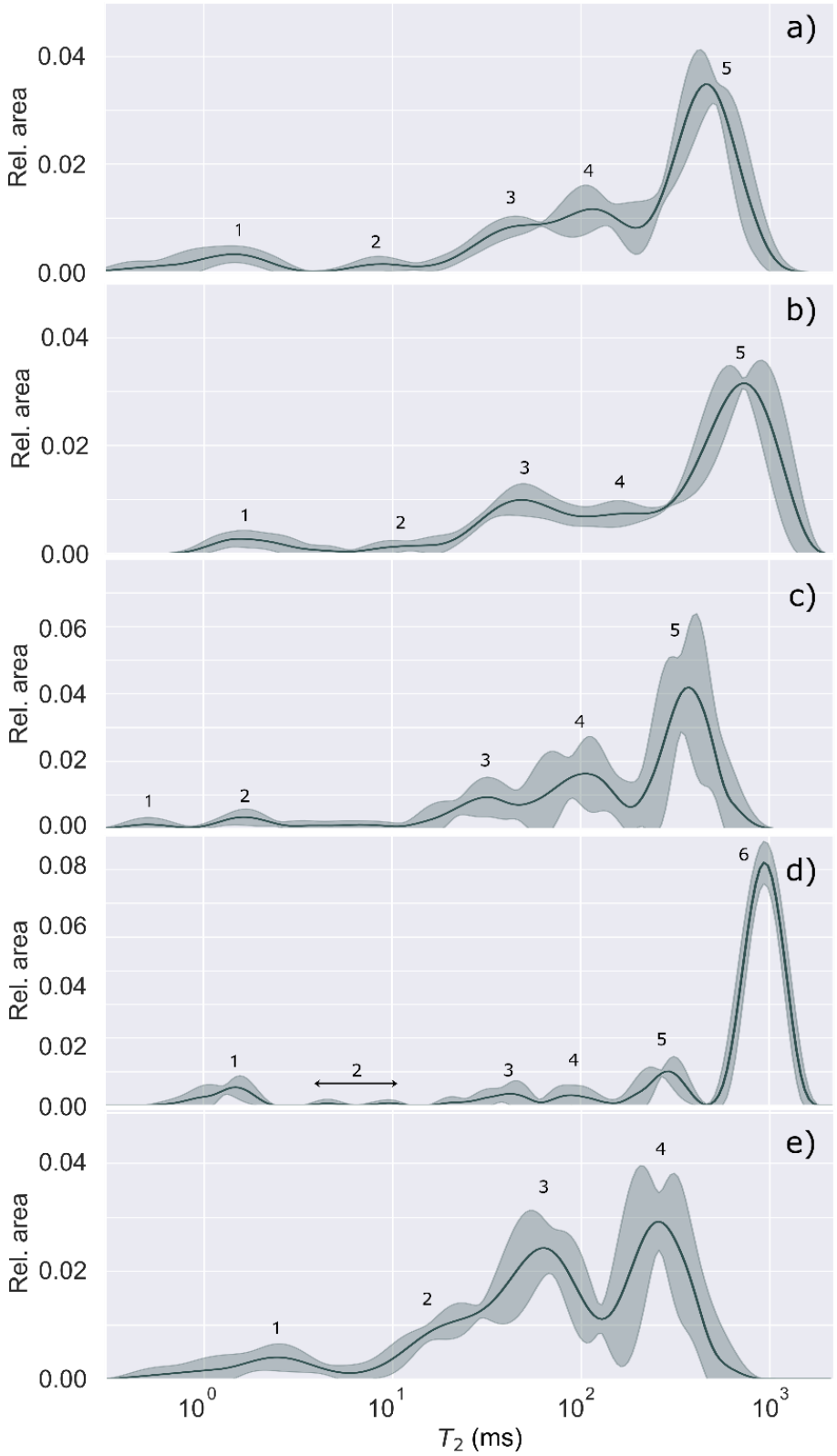

Figure 4-20 Continuous T_2 distributions (with peak numbers 1-6) of five wood fibre insulation materials, showing the mean values (line) and standard deviation (filled zone). a) Porous bituminised wood fibre board (BWFIB) and b-e) wood fibre insulation type 1-4: b) WFIB1, c) WFIB2, d) WFIB3, e) WFIB4

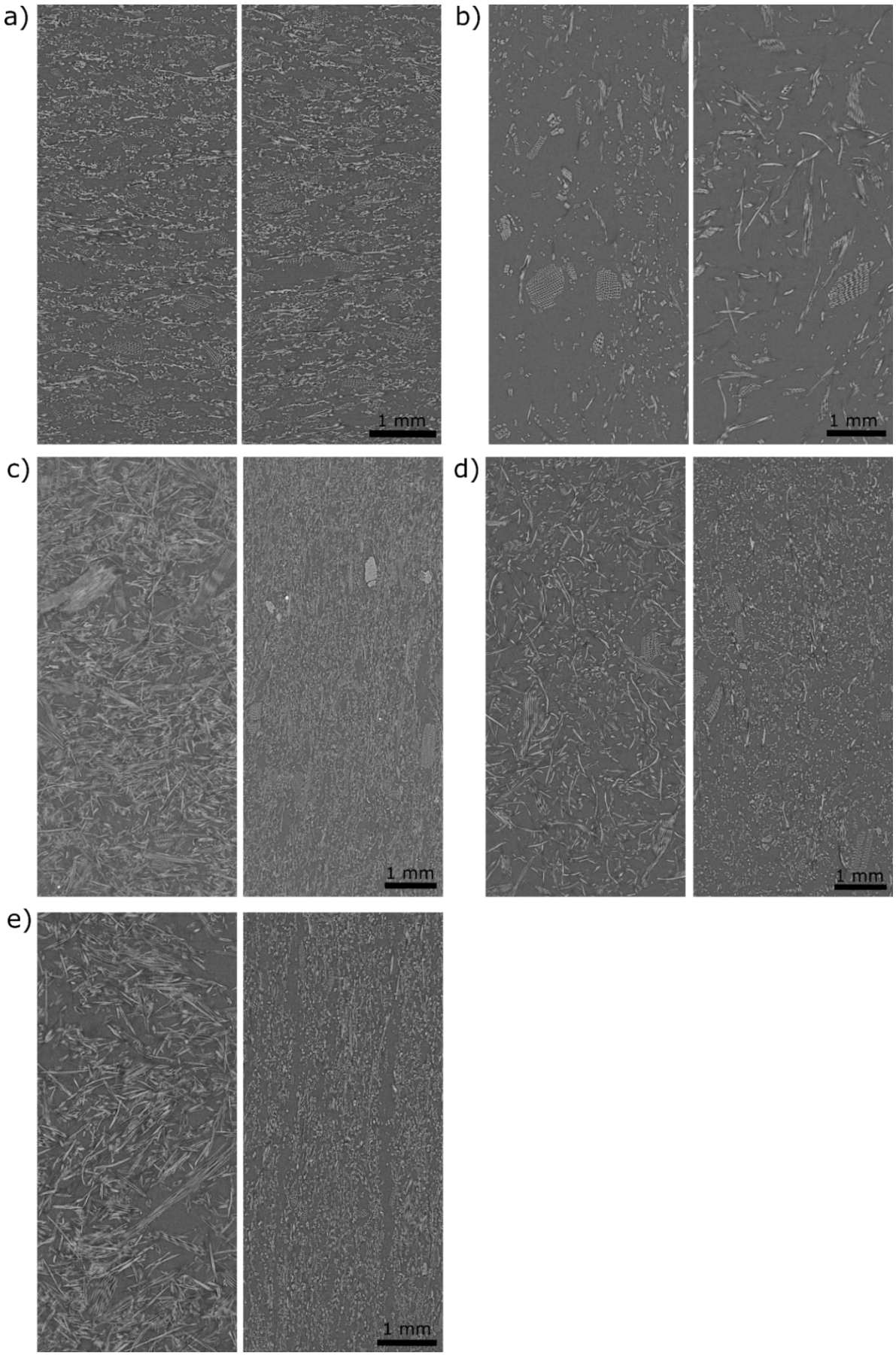

Figure 4-21 X-ray CT visualisation of the wood-fibre insulation materials, with a slice displaying the front view (left) and the side view (right) for each specimen (5 x 5 x 10 mm^3). a) Bituminised wood fibre board (BWFIB) and b-e) wood fibre insulation type 1-4: b) WFIB1, c) WFIB2, d) WFIB3, e) WFIB4

Hydrophobicity assessment with ATR-FTIR

In order to quantify the hydrophobicity of the selected bio-based materials, ATR-FTIR peak ratios for the area underneath the peaks between 2815-2985 cm^{-1} (associated with CH- and CH_2-stretching) and 3050-3550 cm^{-1} (associated with OH-stretching) were calculated relative to that of holocellulose (Djajadi *et al.*, 2017; Lupoi, 2015). The peak ratios associated with CH- and CH_2-stretching of WFIB2 and WFIB4 (Figure 4-22a, right) were similar than those of the wood-based panels (Figure 4-22a, left). The CH- and CH_2-stretching peak ratios of wood fibre insulation boards containing polyolefin fibres (WFIB1), isocyanate adhesive and paraffin (WFIB3) and bitumen (BWFIB) were two, four and five times higher than the other wood-based products, respectively. This increase in absorbance at the regions around wavenumber 2935 cm^{-1} and 2862 cm^{-1} indicated an increased presence of alkanes (Khanifah *et al.,* 2018). Since the wood fibres used in the four wood fibre board types originated from the same source, the absorbance increase is most probably the result of the hydrophobing agents (Table 4-2), being bitumen for porous bituminized fibre board, polyolefin fibres for WFIB1 and paraffin for WFIB3. Indeed, paraffin consists of alkanes and FTIR spectra of pure paraffin have their main peak in this region as well (Khanifah *et al.,* 2018). Polyolefin fibres are made up for at least 85% by ethene, propene or other olefin units, which consist of CH_2 and CH bounds (Mather, 2009). Similarly, bitumen contains a considerable number of alkanes. Since alkanes and polyolefins are hydrophobic compounds, a high abundance of these compounds is expected to increase the overall hydrophobicity of these materials. However, while a higher FTIR peak ratio for CH- and CH_2-stretching corresponded to a lower MC in saturated state for BWFIB and WFIB3 (Table 4-2), this was not the case for WFIB1. Likely, the nature and distribution of the hydrophobic components is important. Bitumen and paraffin cover part of the wood fibres, reducing the total amount of available cell wall polymer surface and thereby also part of the water-binding sites (Lozhechnikova *et al.*, 2015). The polyolefin fibres, being loose hydrophobic fibres, are unlikely to cover the wood fibres in such a way that water-binding sites cannot be reached. Note that the relative peak area ratio of WFIB4 is as low as in the wood-based panels. Likely, the amount of paraffin in that specific product is much lower than in WFIB3 or the presence of isocyanate caused the higher peak ratio for WFIB3.

The relative peak ratio associated with OH-groups was slightly higher for thermally modified wood than for wood-based panels (Figure 4-22b). This is counter-intuitive, as the hydroxyl groups are reduced due to depolymerisation of hemicellulose during thermal modification (Boonstra, 2008). However, the relative lignin percentage, and corresponding OH-groups from phenolic groups, increase due to carbohydrate degradation. The higher relative OH-peak ratio of porous bituminized fibre board was expected, as bitumen contains phenols and carboxylic acids (Michon *et al.*, 1996).

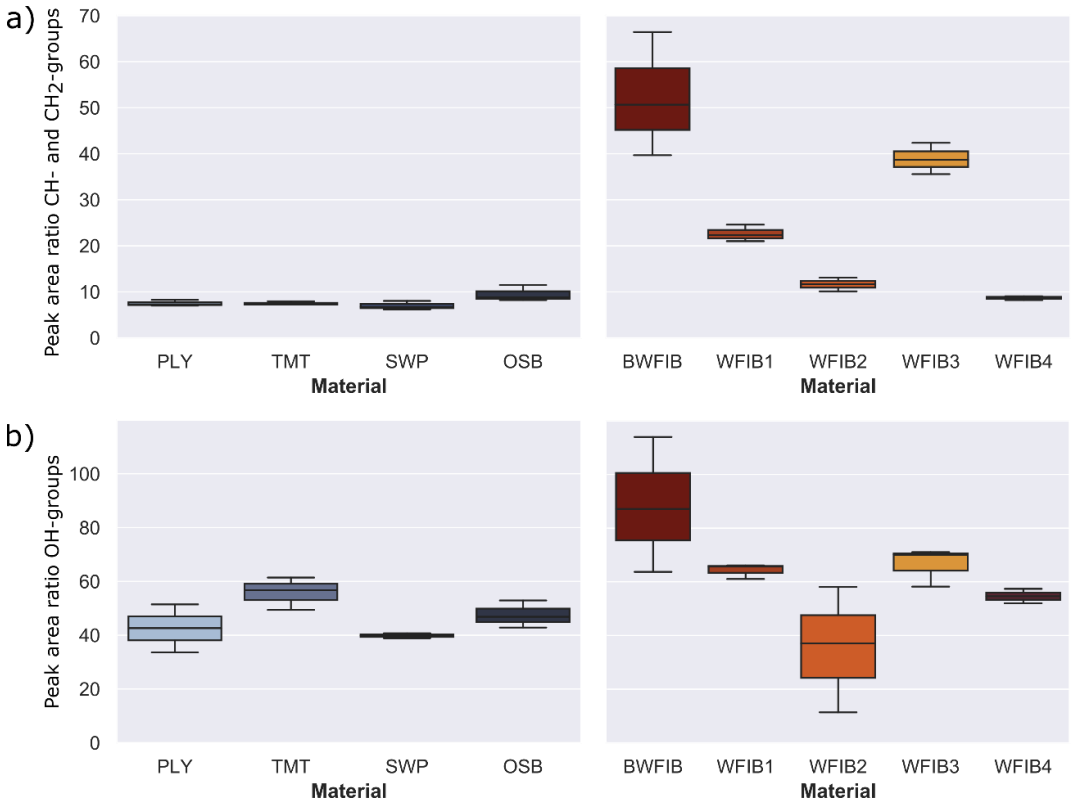

Figure 4-22 ATR-FTIR peak area ratios of wavenumber regions associated with a) CH and CH_2 stretching (2818-2985 cm^{-1}) and b) OH-stretching (3050-3550 cm^{-1}) relative to the wavenumber region of holocellulose (870-920 cm^{-1}) assessed on oven-dry wood powder of wood-based panels (left) and wood-fibre insulation materials (right). PLY = Plywood Radiata pine, TMT = Thermally modified spruce, SWP = Three-layer spruce binder, OSB = Oriented strand board, BWFIB = Bituminised wood fibre board and WFIB1-4 = Wood fibre insulation board type 1-4.

Water absorption and desorption properties

Solid wood-based panels and thermally modified wood

Radiata pine plywood (PLY) absorbed significantly more water during the floating test than the other wood-based panels and had a water uptake of 0.44 g/cm^2 after 144 hours of water absorption (Figure 4-16a). Parameter a_1, affecting the steepness of the absorption curve, was much times higher (Table 4-6). A previous study by De Windt *et al.* (2018) showed that the moisture dynamics of plywood is highly dependent on the wood species of the (top) veneers (De Windt *et al.*, 2018). The water uptake of radiata pine plywood indeed differed from the water uptake of birch plywood (0.24 g/cm^2) and okoumé plywood (0.19 g/cm^2) after 144 hours of absorption, and was lower than for solid radiata pine (0.67 g/cm^2), as described by Van Acker *et al.* (2014). The water uptake of the three-layer spruce panel (SWP) was slightly lower (0.12 g/cm^2) than the values for solid Norway spruce (0.14 and 0.15 g/cm^2) reported by Van Acker *et al.* (2014). SWP is composed of three solid wood plates glued together, while OSB is made up out of wood strands. These differences in material structure did not affect the initial water absorption phase, as the absorption curves of OSB and three-layer spruce panel were similar during the first 24 hours of absorption. After 24 hours, however, the OSB specimens did absorb water at a higher absorption rate. Its material structure (Figure

4-18) and the presence of pores substantially larger than tracheids (Figure 4-19) clearly affected its water absorption rate (Figure 4-16a). Thermally modified spruce (TMT) had the lowest water uptake after 144h of absorption of all tested materials. Clearly, its increased pore surface hydrophobicity due to the thermal treatment decreased the water absorption, at least for the duration of the absorption phase of the floating test. During the desorption phase, most of the absorbed water in TMT had desorbed in the first 24 hours of desorption, after which the desorption rate reduced. The water had desorbed faster in PLY than OSB, as indicated by the higher b_2 value (Table 4-6). PLY and OSB had a higher residual moisture content (rm) after 96h and 144h of desorption (Table 4-7). Clearly, water has more difficulty desorbing from OSB and plywood due to the material structure, which enhances the risk of water entrapment in practice (De Windt el al., 2018).

Table 4-6 Absorption class, values at 144 hours of absorption and parameters of fitted curves for absorption and desorption phases. PLY = Plywood Radiata pine, TMT = Thermally modified spruce, SWP = Three-layer spruce binder, OSB = Oriented strand board, BWFIB = Bituminised wood fibre board and WFIB1-5 = Wood fibre insulation board type 1-5.

Label	Absorption (Eq. (4-5))				Desorption (Eq. (4-6))		
	Absorption class	144h g/cm²	a_1 (10^{-5} g/cm²)	b_1 (-)	a_2 (10^{-5} g/cm²)	b_2 (10^{-5} g/cm²)	c_2 (-)
PLY	7	0.43	9	0.30	5	38	51
TMT	1	0.06	1	0.46	1	5	8
SWP	4	0.12	2	0.41	3	9	21
OSB	6	0.19	1	0.57	5	14	42
BWFIB	2	0.09	3	0.20	1	7	8
WFIB1	8	1.09	97	0.06	-2	103	26
WFIB2	1	0.03	7	0.26	1	24	24
WFIB3	8	0.54	12	0.34	-28	80	162
WFIB4	7	0.47	30	0.12	-5	51	54

Table 4-7 Residual moisture content (rm) (%) after 48, 96 and 144 hours of desorption. * Negative values indicate a possible mass loss due to leaching and fibre loss. PLY = Plywood Radiata pine, TMT = Thermally modified spruce, SWP = Three-layer spruce binder, OSB = Oriented strand board, BWFIB = Bituminised wood fibre board and WFIB1-5 = Wood fibre insulation board type 1-5.

Label	rm48		rm96		rm144	
	mean	**std**	**mean**	**std**	**mean**	**std**
PLY	20.98	4.37	11.12	2.05	6.34	0.67
TMT	2.25	0.20	2.03	0.14	1.89	0.12
SWP	4.68	1.34	3.40	0.71	2.73	0.35
OSB	8.05	2.23	5.73	1.62	4.37	0.96
BWFIB	2.07	0.13	1.81	0.11	1.70	0.06
WFIB1	203.93	137.23	-11.65*	19.31	-13.06*	19.64
WFIB2	2.20	0.62	0.83	0.23	0.23	0.08
WFIB3	20.64	4.91	9.52	3.93	1.25	0.20
WFIB4	109.99	11.37	-0.51*	0.66	-1.26*	0.36
WFIB5	125.16	64.19	91.51	52.41	43.17	23.89

Wood fibre insulation materials

Due to its high porosity (Table 4-2) and its large pores (Figure 4-19 and Figure 4-21), WFIB1 absorbed water fast and reached its full absorption potential after 5 min (Figure 4-16b). Since WFIB1 is made from loosely connected wood fibres and has a very low density (Table 4-2), the material collapsed during water absorption. The other wood fibre insulation materials were denser (Table 4-2) and had a more rigid structure, though clear signs of shrinking and swelling was observed during the experiment. For instance, more than 100% of the pore volume of WFIB4 was filled with water during the first hour of absorption, indicating that the material had swollen and could therefore contain more water than the calculated pore volume in dry state. Unlike the water uptake of WFIB1, which reached a plateau after 5 min, the water uptake of WFIB4 continued to increase up to 72h of absorption after which it remained stable (Figure 4-16b). The LFNMR relaxation time distributions indicated that water occupied smaller pores in WFIB4 as compared to WFIB1 in water-saturated state, possibly explaining the presence of this secondary capillary absorption phase after the primary absorption phase. Also, WFIB4 was 14% less porous than WFIB1 in dry state (Table 4-2). The lower water uptake is likely due to the smaller board thickness of WFIB4 as compared to WFIB1. Indeed, when normalized over sample thickness, the moisture concentration of WFIB4 is two times higher than WFIB1 (Suppl. Figure 8-6). The water uptake of WFIB2 and BWFIB was more than 4 times lower than that of WFIB1, even though WFIB2 and BWFIB had similar LFNMR relaxation time distributions as WFIB1. WFIB1 is a loose wood-fibre mat with a density of 50 kg/m^3. Water can enter easily and the fibres stick together. Likewise, the water uptake of WFIB3 was twice as low as WFIB1, even though it contained the largest pores in water-saturated state. This large difference in water absorption rate is likely related to the hydrophobic properties and production process of each product. Indeed, WFIB3 and BWFIB contain paraffin and bitumen, respectively. The bitumen treatment appeared to be more effective as a water repellent than the paraffin treatment for these specific products. However, as WFIB2 does not contain any additives, the production process itself also played an important role. WFIB2 is a dense material, with the fibres organised in layers, as can be seen in Figure 4-21c. Presumably, these layers or the fibre bounds in general prevent the water from penetrating deeply into the material. It seems that the wet production process prevented water taken up better than the dry production process with isocyanate in combination with paraffin as additive (WFIB3), possibly due to a better fibre bounding. As the wet production process causes a densification of the bottom fibres, we assessed whether the lower water uptake was caused by this better fibre bounding or whether it was related to the densified bottom layer. Figure 4-23 illustrates the liquid water uptake (g/cm^2) of three WFIBs produced with a wet production process. Clearly, the wet production process does not necessarily result in a stronger fibre bounding, as there was a high variability in the moisture dynamics of WFIB5, with values going from 0.5 to 2.4 g/cm^2 (Figure 4-23 and Figure 4-24). When the softer top of the WFIB2 specimens was placed in water contact instead of the densified bottom, the mean water absorption after 144h increased from 0.25 to 0.4 g/cm^2. However, when the

softer top of the WFIB5 specimens was placed in water contact, water absorption of 2.4 g/cm^2 occurred. Interestingly, when exposed to the softer side, the variability was limited. The variability of WFIB5 in water contact with the hard bottom side, was therefore likely due to inconsistencies in the harder bottom layer. Note that presence of bore holes did not affect the water absorption significantly, as the water absorptions were within the error margin of the specimens without a bore hole, both for WFIB2 and WFIB5. As the water absorption of the WFIB2 specimens with the top side in water contact was still below 0.5 g/cm^2, the main influence of the wet production process was not related to the thicker bottom layer, but to a more general better bounding over the whole specimen. Presumably, the addition of paraffin in WFIB5 had a negative impact on the bounding strength between fibres in the wet production process, making it easier for water to enter, although it could also be that the wet production process in general provides inconsistent water uptake results. Note that the low water uptake of WFIB4 is misleading, as the specimens were water saturated and could not take up more water due to the limited thickness (5 mm).

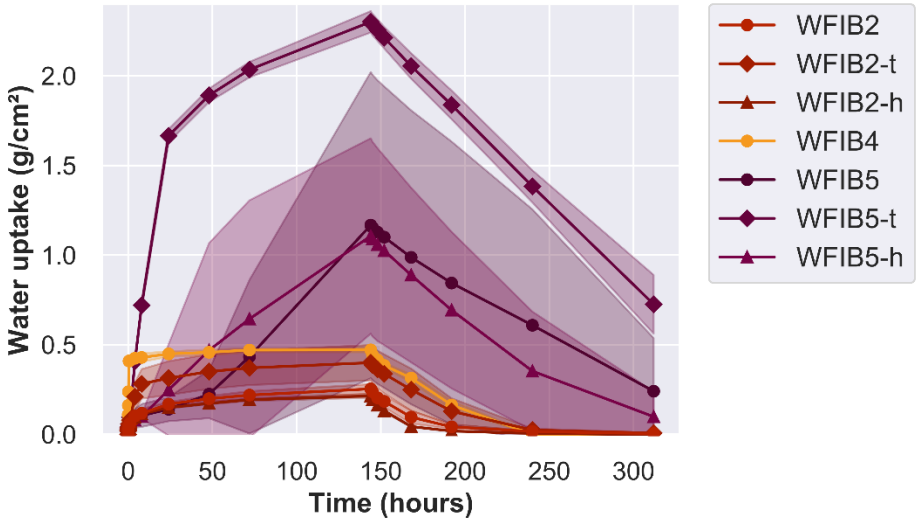

Figure 4-23 Mean liquid water uptake (g/cm^2) with standard deviation over 144 hours of absorption and 168 hours of desorption in a floating test. Comparison of wood fibre insulation boards (WFIB) made with wet production process (WFIB2, WFIB4 and WFIB5). Specimens were laid atop the water surface with the densified bottom side, without (-) or with a hole (h) or with the undensified top (t) in contact with the water surface.

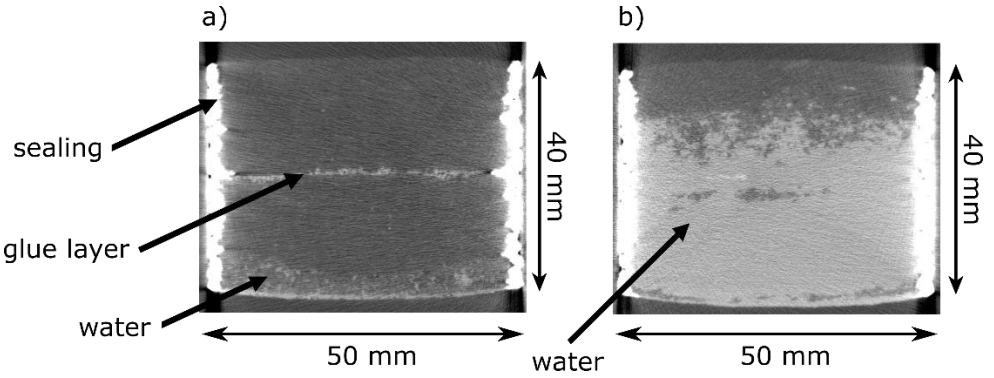

Figure 4-24 Difference in water absorption between a wood fibre insulation board type 5 (WFIB5) specimen which had absorbed 0.3 g/cm³ (a) and a specimen which had absorbed 2.0 g/cm³ (b) after 144 hours of absorption. X-ray CT scan taken after 144 hours of absorption and 1 hour of desorption.

Implications for service life

Materials that absorb little water or dry out fast have less risk of fungal decay. In an extensive study on the moisture dynamics of plywood, a good correlation was found between the results from the floating test and the actual moisture dynamics of plywood in outdoor exposure (De Windt *et al.*, 2018). Based on the residual moisture content, use class recommendations were given. For instance, plywood with a residual moisture content lower than 3.5% was suggested to be suited for extended service life in UC3.1 and UC3.2, while in UC3.1 a rm below 5.5% would be suited for a short to average service life. Besides residual moisture content, other parameters could additionally be used to predict service life. The absorption class, derived from the water uptake after 144h of absorption, gives an indication of the water absorption capacity of a material (Table 4-6). Furthermore, several absorption and desorption parameters were derived to better describe the moisture dynamics of the assessed materials.

TMT, BWFIB and WFIB2 performed very well on the moisture dynamics indicators. TMT and WFIB2 were classified in absorption class 1, BWFIB in absorption class 2, indicating a low amount of water uptake during the absorption phase (Table 4-6). These values corresponded to those found by Van Acker *et al.* (2014) for ipé, teak, walaba and thermally modified spruce, poplar and pine wood. Additionally, TMT and BWFIB had low c-values for desorption, indicating that they are fast-drying materials. The residual moisture content after 48 hours (rm48) for the three materials was below 2.5%. De Windt *et al.* (2018) classified plywood with a rm below 2.5% after 72 hours of desorption, as a product that is expected to have a long service life in UC1 to UC3, and even UC4. Since the durability of BWFIB and WFIB2 against Basidiomycetes is low (see section 3.3), it should not be recommended in water or ground contact (UC4). Assuming that the same criteria are applicable to TMT, BWFIB and WFIB2, our results indicate that these particular products can be used up to UC3.2 (above ground, exposed to prolonged wetting conditions). Indeed, TMT is often applied as cladding in outdoor exposure conditions (Jones *et al.*, 2018).

WFIB1, WFIB3 and WFIB4 absorbed much water and were classified in absorption classes 7 and 8 (Table 4-6). Although the water uptake by WFIB1 was twice as high than by WFIB3, both were classified in absorption class 8. It could be recommended to expand the absorption classes to better differentiate water absorption in bio-based insulation materials. Nonetheless, all wood fibre insulation materials were able to dry down to a rm below 2.5% after 144h of desorption, with the exception of WFIB5 (Table 4-7). WFIB1 and WFIB4 already reached a rm below 2.5% after 96h of desorption. UC2 and possibly UC3.1 are therefore recommendable.

The absorption class of PLY, OSB and SWP was 7, 6 and 4, respectively. While SWP reached a rm below 3.5% after 96h and below 2.5% after 144h, the rm in PLY remained higher than 5.5% after 144h. Water accumulation might be an issue for these specific OSB and PLY products.

4.3.3 Conclusions

Water absorption and desorption characteristics of bio-based materials were not only dependent on overall porosity but were influenced by the material's hydrophobic properties, production process and pore size distribution. Thermal modification and hydrophobic additives had a major impact on the water absorption and desorption characteristics (TMT, WFIB3 and BWFIB), although the production process and pore distributions of those materials might still have had an influence on the absorption and desorption rates as well. Thermal modification caused higher peak 2 and peak 3 T_2 values in the LFNMR relaxation time distributions of TMT. The hydrophobic additives such as bitumen and paraffin did, however, not induce a shift to higher T_2 values in the LFNMR relaxation time distributions of BWFIB and WFIB3, respectively. We were able to prove that when the wood anatomy of a wood species was not altered substantially when producing the bio-based product, the water populations of the wood-based panel were similar to those of solid wood, as was the case for plywood and the three-layer spruce panel. However, the material structure of OSB and plywood contributed to water entrapment in the floating test as water desorbed slowly in the desorption phase and the residual moisture content was higher than 5%. In contrast, all but one wood-fibre insulation material had excellent desorption properties due to their high porosity, a valuable quality in regard to water-buffering capacity. Assuming that the residual moisture content criteria described in De Windt *et al.* (2018) are applicable to bio-based building materials in general, TMT, BWFIB and WFIB2 would be expected to have an extended service life up to UC3.2. For WFIB1 and WFIB4 UC2 and possibly UC3.1 would be recommendable. However, to guarantee an extended service life, the moisture dynamics as assessed by the floating test should be compared to actual moisture performance in outdoor exposure conditions for these materials, or at least for a selection of reference materials.


CHECKT
APERITIEVEN
BIER ½ MAAND

Chapter 5

Influence of material structure on natural durability

This chapter will be published as:

De Ligne, L., Van den Bulcke, J., De Muynck, A., Caes, J., Baetens, J.M., De Baets, B., Van Hoorebeke, L., Van Acker, J. (in preparation)

Café de Walrus
Ghent, Belgium
Acoustic cork insulation as exterior cladding
© Eurabo | www.eurabo.be/nl/referenties/isokurk-kurk-toepassingen

5.1 Introduction

Wood anatomy (the variability and ratio of different cell types) has an influence on degradation (Daniel, 2003). In a laboratory test set-up, Bravery (1975) showed that initial hyphal penetration of a wood block happens via the major longitudinal pathways, being vessels for birch and beech (hardwoods) and earlywood tracheids and resin canals for Scots pine (softwood). Depending on the wood species, the ray cells are rapidly invaded as well. Then the hyphae make use of naturally occurring openings in the wood, such as pits, while some fungi are able to create their own holes (bore-holes). In section 3.2, it was postulated that the low vessel-fibre ratio of *Pterocarpus soyauxii* contributed to its high durability. Also, a high parenchyma content was hypothesized to play a role in durability.

Standard fungal tests mainly measure the mass loss caused by decay fungi after a certain degradation period (CEN EN 350 standard, 2016). While very relevant for assessing durability of wood, these standard methods do not offer much information on the ongoing processes in the material during degradation. In-depth knowledge on the intricate material-fungus relationship and especially knowledge on how wood and material structure affect the degradation process is lacking. To gain more insight into how a material's structure and moisture properties affect the degradation process, X-ray CT is considered. X-ray CT is a promising technique for fungal decay research as it is fast, non-destructive and provides 3-D images of the internal structure of a material (Van den Bulcke *et al*., 2009). Already back in 1997, it was applied by Bucur *et al*. to assess the wood density profiles of degraded beech and pine specimens after 1-5 months of degradation. Macchioni *et al*. (2007) performed X-ray CT on smaller sized specimens of beech and Scots pine, which were degraded for 1-6 weeks. While informative, the method described in both studies requires the specimens to be removed from the fungal cultures (at monthly and weekly intervals, respectively) and dried. It therefore does not allow to monitor decay of individual wood specimens, which each have a unique anatomy. For the purpose of this study, we developed a method to non-destructively assess the degradation process over time with X-ray CT scanning. Furthermore, we used semi-automated scanning and analysis to allow for many specimens to be processed simultaneously. This chapter presents the degradation progress of *Coniophora puteana* on mini-blocks of beech (*Fagus sylvatica* L.), okoumé (*Aucoumea klaineana* Pierre), Scots pine (*Pinus sylvestris* L.) and Norway spruce (*Picea abies* (L.) Karst).

5.2 Material and methods

Fungal species

The brown rot fungus *Coniophora puteana* (strain MUCL 11662) was used since it is an obligatory test fungus for standard testing of (natural) durability of wood against Basidiomycetes (CEN EN 350 standard, 2016; CEN EN 113 standard, 1996; CEN TS 15083-1 standard, 2006).

Decay test

Durability tests were performed according to the mini-block method (Bravery, 1978; Deklerck *et al*., 2019), since a smaller specimen size and shorter test period are beneficial for experiments with X-ray CT (De Ligne *et al*., 2019). Fifteen mini-blocks of beech (*Fagus sylvatica* L.), okoumé (*Aucoumea klaineana* Pierre), Scots pine (*Pinus sylvestris* L.) and Norway spruce (*Picea abies* (L.) Karst) (30 x 10 x 5 mm^3) were oven dried (24h at 103°C) and weighed ($m_{0,dry}$ [g]). The wood specimens were positioned in a specimen holder of dry floral foam and scanned with X-ray CT, to obtain the dry 3D volume of the mini-blocks before degradation. The mini-blocks were sterilised using gamma irradiation and placed on malt agar (3% malt, 2% agar) inoculated with *C. puteana*. The wood specimens were exposed to the fungus when the mycelial area had reached a radius of about 1.5 cm. They were placed on a plastic mesh to avoid direct contact with the agar and a reference material was placed on top of each mini-block (Figure 5-1). The reference material had a twofold purpose: fixing the position of the mini-block inside the Petri dish and for conversion of attenuation coefficients to approximate density values (see subsection X-ray CT, Eq. 3).

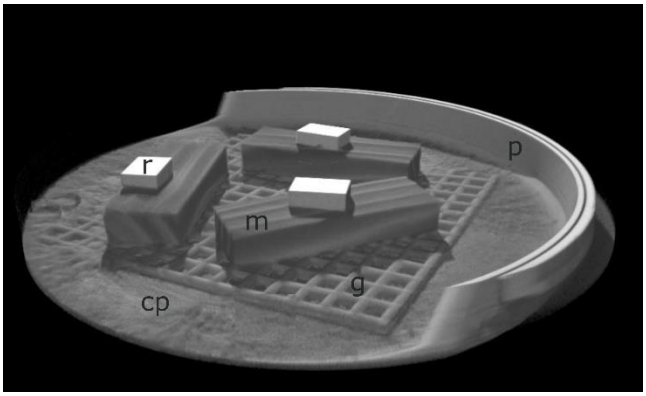

Figure 5-1 3D rendering of a Petri dish set-up at the start of the experiment VGStudio Max (Volume Graphics GmbH). Cp = *C. puteana*, g = plastic grid, m = mini-block, p = Petri dish, r = reference material. Note that part of the Petri dish has been removed virtually for the purpose of visualization.

The Petri dishes were kept at 20°C and 75% relative humidity (RH) for 10 weeks and scanned with X-ray CT at weekly intervals. After 10 weeks of degradation, the mini-blocks were removed from the Petri dishes and weighed ($m_{1,wet}$ [g]), to calculate the moisture content (MC [-]) at the end of the experiment (Eq. (5-1)). Subsequently, they were oven dried and weighed ($m_{1,dry}$ [g]) to assess the mass loss (ML [-]) due to degradation (Eq. (5-2)), and scanned one last time.

$$MC = \frac{m_{1,wet} - m_{1,dry}}{m_{1,dry}} \quad (5\text{-}1)$$

$$ML = \frac{m_{0,dry} - m_{1,dry}}{m_{0,dry}} \quad (5\text{-}2)$$

Additionally, for 6 specimens per species, the same procedure was used yet without fungal inoculation, to investigate moisture uptake from the agar and moisture decrease through water evaporation without fungal presence, with X-ray CT. This will be referred to as the 'reference experiment'.

X-ray CT

Fungal resistance to X-rays

X-rays are a form of ionizing radiation and can as such damage living organisms and impede growth. Even though the energies of X-rays required for material sciences are rather low and most probably the applied doses are far below lethal doses for fungi (Uber and Goddard, 1934; Van den Bulcke *et al.*, 2009), we evaluated whether the growth behavior of *C. puteana* was influenced by repeated exposure. Extreme dose tests were performed, where each time five replicates of *C. puteana* were exposed to 3, 12 and 24 hours of X-ray radiation generated by a directional closed-type Hamamatsu X-ray tube operated at 80 kV, 12 W. Petri dishes containing a standard malt agar medium (40% malt, 2% agar) were inoculated with a circular piece of fungal inoculum (0.7 cm^2). Exposure started one hour after transferal of the inoculi to the Petri dish. A control experiment was carried out in parallel, where the control cultures were kept in a similar environment as that of the scanner, but without exposure to X-rays.

To assess whether X-ray radiation had a negative impact on degradation over the 10 week period of the experiment, a parallel decay test with 15 blocks per species was performed in which the specimens were not exposed to X-ray CT. This will be referred to as the 'parallel experiment'.

Image acquisition

During 10 weeks of decay, the Petri dishes were scanned weekly with the Nanowood scanner at the UGent Centre for X-ray Tomography (UGCT, www.ugct.ugent.be). The Petri dishes were stacked and secured with surgical tape in stacks of ten (Figure 5-2, 3). The entire stack of Petri dishes could not be scanned at once, given the limited field of view of the detector. Therefore, using the z-stage of the scanner the scan height was automatically changed after each scan cycle (Figure 5-2, 6). As such, the Petri dishes were automatically scanned two by two. To avoid unnecessary exposure of the fungal cultures that were not in the field of view, a wooden board with lead cladding was positioned in front of the stack of Petri dishes, thus blocking the X-rays, apart from a central slit that allowed X-rays to pass through two Petri dishes that were scanned (Figure 5-2, 7). All specimens were scanned at an average voltage of 70 kV, a power of 7 W and an exposure time of 500 ms, resulting in an approximate scan time of 17 min

per pair of Petri dishes and a resolution of 100 µm. For scanning of the dry mini-blocks before and after the decay test, the same scan settings were used.

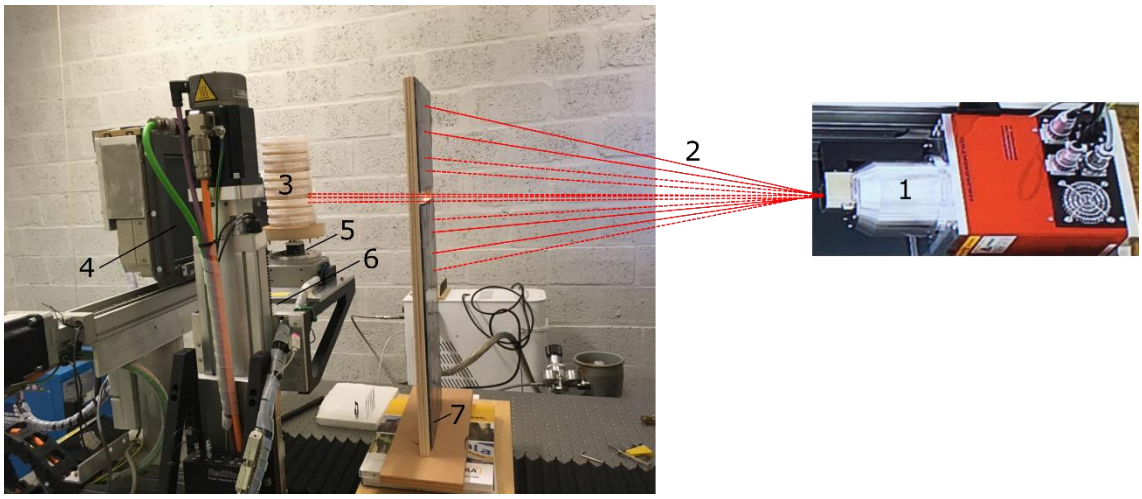

Figure 5-2 Schematic of X-ray CT set-up. 1) X-ray source, 2) X-rays (not visible for the human eye), 3) stack of 10 Petri dishes, 4) detector, 5) rotation stage, 6) z-stage and 7) wooden board with lead cladding.

Image reconstruction and analysis

X-ray CT images were batch reconstructed (De Muynck *et al.*, 2015) with beam hardening correction. To facilitate the segmentation of the mini-blocks from the reconstructed greyscale volumes, a custom-written macro in Fiji (Schindelin *et al.*, 2012) was used. The grey values in the mini-block volumes were then converted to density values, using the reference material, which has a similar elemental composition to wood and a known density, and air (1.2 kg/m^3) (Eq. 3). As such, the average weekly determined density of each mini-block could be calculated based on the grey values.

$$D_i = D_{ref} \frac{GV_i - GV_{air}}{GV_{ref} - GV_{air}} \quad (5\text{-}3)$$

with D_i the density value of voxel i (g cm^{-3}), D_{ref} the density value of the reference material (1.4 g cm^{-3}), GV_i the grey level of voxel i, GV_{air} the grey level of air and GV_{ref} the grey level of the reference material. These calculations were done in Python (Python Software Foundation, https://www.python.org/).

Note that for the scans of the oven-dry blocks before and after the decay test, this density corresponds to the actual wood density, and the density decrease due to fungal decay can easily be assessed. However, for the scans during the decay test, this density indicates the wet wood density, which is increased by malt agar uptake, hyphal mass and water transport by the fungus and, once decay has started, might decrease due to fungal decay of cell wall components into carbon dioxide (gas) and water. Since mass degradation by the fungus is masked by these other factors, 12 variables were identified to characterize degradation patterns (Figure 5-3): maximal density (D_{max}),

minimal density (D_{min}), density where the density curve is flattening (D_{knee}) and the corresponding number of weeks at which those densities occurred (T_{max}, T_{min} and T_{knee}, respectively), as well as the density after 10 weeks of degradation (D_{end}), the slope between D_{max} and D_{knee} (m_{knee}), D_{max} and D_{min} (m_{min}), D_{max} and D_{end} (m_{end}) and the difference between D_{max} and D_{min} (ΔD_{min}), D_{max} and D_{end} (ΔD_{end}). The point of D_{knee} and T_{knee} was assessed with the KneeLocator function (package: kneed, function: KneeLocator, software: Python Software Foundation, https://www.python.org/). To determine which of the aforementioned degradation variables are related to mass loss after 10 weeks, the following procedure was applied in RStudio (RStudio Team, 2019). First, Pearson correlation was performed to check for correlation among the degradation variables. One variable was retained when two or more variables were correlated (Pearson correlation > 0.5, Suppl. Figure 8-7), resulting in the following remaining variables: D_{max}, T_{max}, m_{min} and ΔD_{min}. Since three mini-blocks were put together in a Petri dish, the other mini-blocks in the Petri dish could influence the density variation of their neighbors. Therefore, after scaling the variables, Linear Mixed Effect models were applied with Petri dish as a random effect. Since the number of samples was limited to 15 per wood species, the number of explanatory variables needed to be reduced even further. Therefore, six models containing the wood species and a combination of two of the remaining variables (D_{max}, T_{max}, m_{min} and ΔD_{min}) and an additional model exclusively containing the wood species were tested and compared based on the Akaike Information Criterion (AIC).

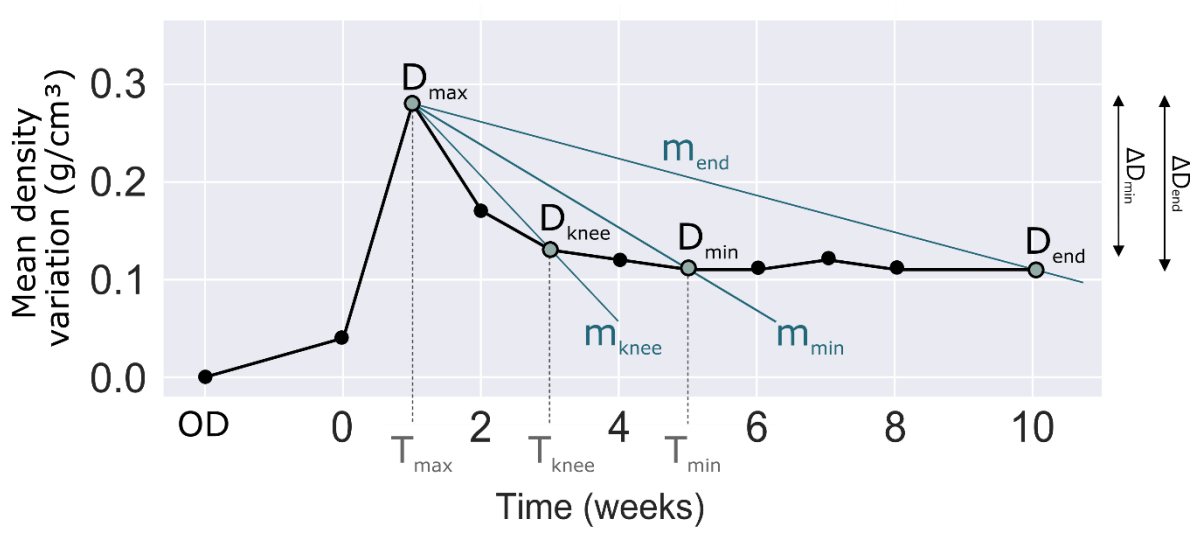

Figure 5-3 Example curve representing mean density variation over time with indication of variables of interest: maximal density (D_{max}), minimal density (D_{min}), density where the density curve is flattening (D_{knee}) and the corresponding number of weeks that those densities occurred (T_{max}, T_{min} and T_{knee}, respectively), as well as the density after 10 weeks of degradation (D_{end}), the slope between D_{max} and D_{knee} (m_{knee}), D_{max} and D_{min} (m_{min}), D_{max} and D_{end} (m_{end}) and the difference between D_{max} and D_{min} (ΔD_{min}), D_{max} and D_{end} (ΔD_{end}).

Additionally, a greyscale profile was taken along the longitudinal direction of each mini-block (length of 30 mm), representing the average grey value per slice, for 300 slices of 100 µm thick. Based on this greyscale profile, the density per slice was determined (Eq. 3) and presented relative to the corresponding oven-dry density along the longitudinal direction (Eq. 4, Figure 5-4a). To determine whether the density change differed significantly along the longitudinal direction, the average density increase over five sub volumes (10 x 5 x 5.2 mm^3) was determined: outer left zone (L), left to middle zone (LM), middle zone (M), middle to right zone (MR) and outer right zone (R) (Figure 5-4b).

$$\text{Density variation } \left(\frac{g}{cm^3}\right) = D_j - D_{OD,j} \tag{5-4}$$

where D_j is the average density value of slice j (g cm^{-3}) and $D_{OD,j}$ is the average oven dry density value of slice j (g cm^{-3}).

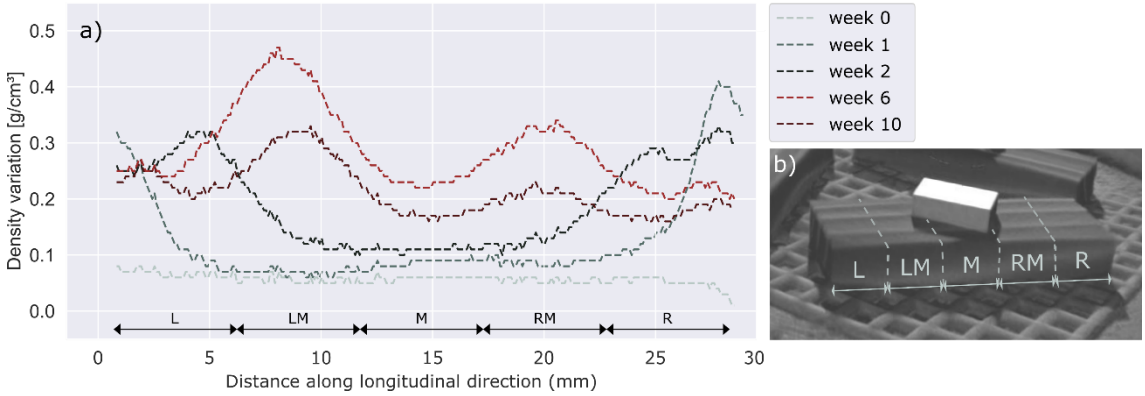

Figure 5-4 a) Density variation along the longitudinal direction of a Scots pine mini-block, after 0, 1, 2, 6 and 10 weeks of degradation. Density increases from the sides to the middle due to water uptake and water production by the fungus. Density decreases from week 6 to week 10 due to fungal degradation of the wood mass. b) Indication of sub volumes: outer left zone (L), left to middle zone (LM), middle zone (M), middle to right zone (MR) and outer right zone (R).

Statistical data analysis

The Kruskal-Wallis H-test was applied to determine whether the median ML, as well as the MC, of the wood specimens of the X-ray CT experiment differed significantly from the median ML and MC in the parallel experiment. The Kruskal-Wallis H-test is a non-parametric statistical test indicating whether the medians of two or more groups are different. When the difference between the medians is significantly different, a post-hoc test needs to be applied to pinpoint for which groups the medians are different. Therefore, the multiple comparison test by Dunn (1961) was applied for this purpose and Benjamini-Hochberg correction (Benjamini and Hochberg, 1995) was performed to control the false discovery rate (Type I error). The same procedure was applied for comparing density variations between three zones along the longitudinal direction of the wood blocks.

5.3 Results and discussion

Fungal resistance to X-rays

Exposure to X-ray radiation (tube setting 80kV, 12 W), had a delaying effect on mycelial development, with the duration of exposure directly related to the delay in growth (Figure 5-5). The Petri dishes containing non-exposed fungal inoculi and fungal inoculi exposed for three hours, were completely overgrown after six days (mycelial area = 63.6 cm^2). For 12 hours and 24 hours exposure, hyphal expansion seemed to have halted during exposure to X-ray radiation. Nevertheless, *C. puteana* recovered well after an extreme dose of 24 hours X-ray radiation, as the Petri dishes were fully overgrown after eight days, and 3 hours of exposure had only a minor influence on the growth rate. Therefore, a weekly exposure of 17 minutes to X-ray radiation (70 kV, 7 W) was not expected to significantly inhibit degradation.

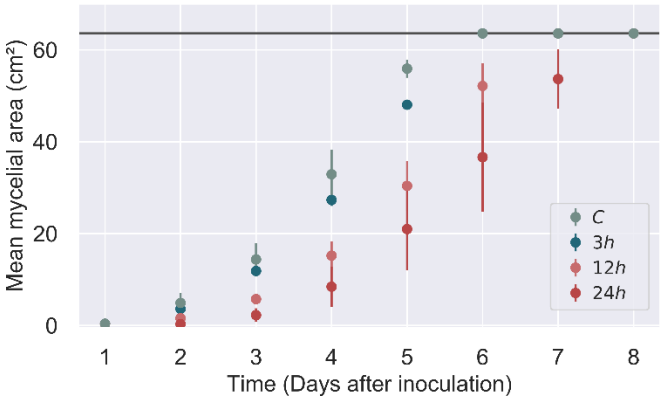

Figure 5-5 Mycelial growth of *C. puteana* exposed to 0, 3, 12 and 24 hours of X-ray radiation (80 kV, 12 W). X-ray exposure started one hour after inoculation.

Indeed, the percentage of mass loss after 10 weeks of degradation by *C. puteana* did not differ significantly between the specimens that had been exposed to X-rays and the specimens from the parallel experiment (Figure 5-6a), except for okoumé. Although the average mass loss of the exposed specimens was mostly lower than those of the parallel experiment, the differences were in the same order of magnitude as the variation that is expected with fungal testing. Also, spruce, Scots pine and beech could all be classified as DC4 based on the median mass loss, both for the X-ray CT exposed specimens as the non-exposed specimens (Suppl. Figure 8-11). We therefore concluded that *C. puteana* remained virulent during the experiment.

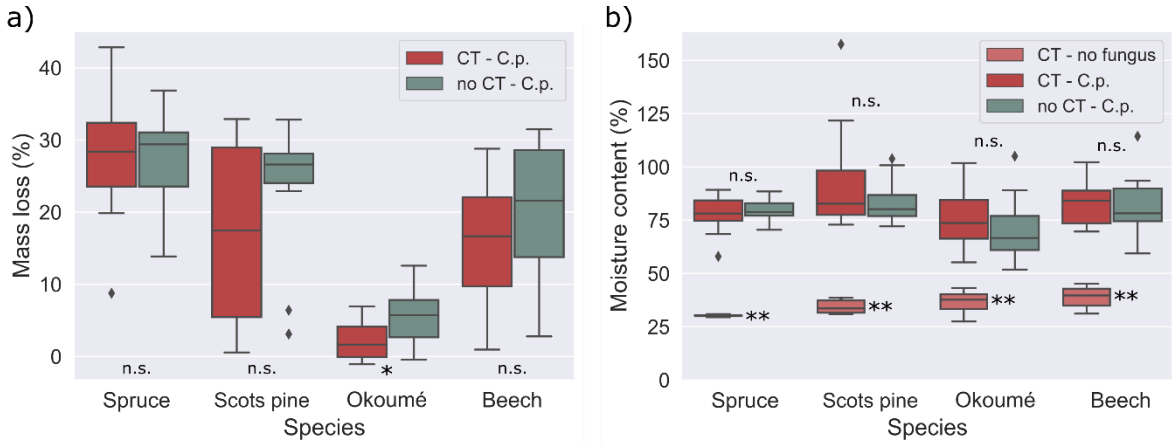

Figure 5-6 Mass loss (a) and moisture content (b) after 10 weeks, for specimens that had been weekly exposed to X-rays and *C. puteana* (CT – C.p.), to *C. puteana* but not to X-rays (no CT – C.p.) and specimens that were in a set-up with only agar and no fungus (CT – no fungus). Significant statistical difference based on the Kruskal-Wallis H-test is indicated: significance codes 0 '***' 0.001 '**' 0.01 '*' 0.05 '.' 0.1 'n.s.' 1

Assessing density with X-ray CT

De Ridder *et al.* (2010) showed that X-ray CT in combination with the use of a reference material is an excellent technique for assessing wood density. In previous studies, X-ray CT has also successfully been applied for assessing wood moisture content (Lindgren, 1992; Watanabe, 2012). In this study, a good correlation (R^2=0.94) was found between the oven-dry density based on X-ray CT (Eq. 3) and those gravimetrically determined (Figure 5-7a), before and after the degradation experiment. During the degradation test, several factors could affect the density of the mini-blocks: moisture uptake from the agar and moisture production by the fungus were expected to increase the average density of the mini-block, while water evaporation and mass loss due to degradation were expected to decrease it. At the end of the experiment (week 10), the blocks were scanned and the wet weight was determined before oven drying. Likewise, this wet density at week 10 based on X-ray CT correlated well (R^2=0.93) to those gravimetrically determined (Figure 5-7b). In the remainder of the chapter, the 'wet density' is referred to as 'density', while the density after oven drying is referred to as 'oven-dry density'.

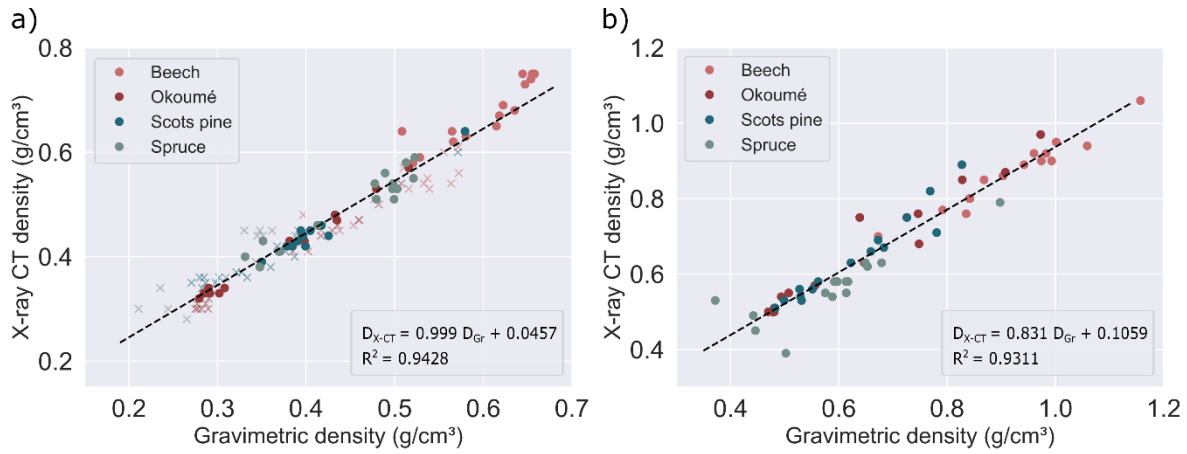

Figure 5-7 a) Comparison of oven-dry density determined gravimetrically (x-axis) and with X-ray CT (y-axis), for mini-blocks before (o) and after (x) the degradation experiment, b) comparison of (wet) density at week 10 determined gravimetrically (x-axis) and with X-ray CT (y-axis).

By performing a reference experiment without a fungus, density changes due to water uptake from the agar and water evaporation could be quantified (Figure 5-8). Since the mini-blocks varied in density at the start of the experiment, relative changes in density were calculated. For all wood species, the density increased during the first two weeks due to malt agar uptake by the wood specimens, hyphal penetration and possibly water transport by the fungus (see section 'Water transport by the fungus'). Beech and okoumé absorbed slightly more malt agar than spruce and Scots pine. Afterwards, density remained stable, except the one of okoumé which decreased again after 8 weeks, likely due to water evaporation. Presumably its larger vessel size (Table 5-1) caused the okoumé specimens to dry out faster than those of the other wood species.

Table 5-1 Average vessel/fibre ratio, tracheid proportion, vessel diameter, fibre lumen, tracheid lumen, fibre length, tracheid length, porosity and parenchyma content (Wagenführ and Scheiber, 1974) of selected wood species, with EW=earlywood, LW=latewood.

Wood species	Average vessel/fibre ratio (%)	Vessel diameter	Fibre lumen	Fibre length	Porosity
Hardwoods					
Aucoumea klaineana Pierre	28.8	55-245 µm	5.5-26.5 µm	635-1810 µm	72%
Fagus sylvatica L.	99.8	8-85 µm	3.5-11.2 µm	600-1300 µm	55%
Softwoods	Tracheid proportion (%)		Tracheid lumen	Tracheid length	
Picea abies (L.) Karst	93.1		EW: 16-45 µm LW: 6.4-22 µm	1300-4800 µm	71%
Pinus sylvestris L.	95.3		EW: 18.5-54.3 µm LW: 11.7-24.6 µm	1800-4500 µm	67%

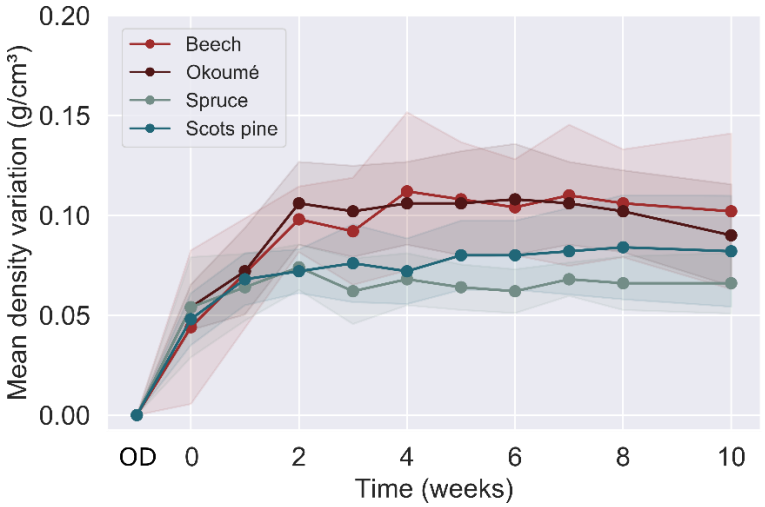

Figure 5-8 Mean density variation of wood blocks in a set-up without fungus, representing moisture uptake from the agar medium over a period of 10 weeks, as assessed by X-ray CT: mean (points) and standard deviation (shaded area).

Relating degradation patterns to mass loss after 10 weeks

Seven linear mixed effect models were fitted to the mass loss of the mini-blocks after 10 weeks of degradation. Table 5-2 gives an overview of the tested models with corresponding AIC value. As model 5 had the lowest AIC value, the mass loss after 10 weeks was most significantly correlated with the difference between D_{max} and D_{min} (ΔD_{min}), the week at which the maximal density occurred (T_{max}) and the wood species from which the mini-block originated. Note that the AIC values are close to each other, but that the value of model 5 (-132.06) is much lower than that of the reference model containing only species and Petri dish as explanatory variables (-118.18).

Table 5-2 AIC values for seven linear mixed effect models, fitted to the mass loss of the mini-blocks after 10 weeks of degradation. PD = Petri dish, ML = mass loss, D_{max} = maximal density, T_{max} = the week at which the max density occurred, m_{min} = the slope between D_{max} and D_{min} and ΔD_{min} = the difference between D_{max} and D_{min}. The best model is the one with the lowest AIC value.

Nr	Linear mixed effect model	AIC
1	ML ~ D_{max} + Tmax + species + (1|PD)	-129.83
2	ML ~ D_{max} + m_{min} + species + (1|PD)	-122.37
3	ML ~ D_{max} + ΔD_{min} + species + (1|PD)	-128.47
4	ML ~ Tmax + m_{min} + species + (1|PD)	-125.50
5	ML ~ Tmax + ΔD_{min} + species + (1|PD)	-132.06
6	ML ~ m_{min} + ΔD_{min} + species + (1|PD)	-120.02
ref	ML ~ species + (1|PD)	-118.18

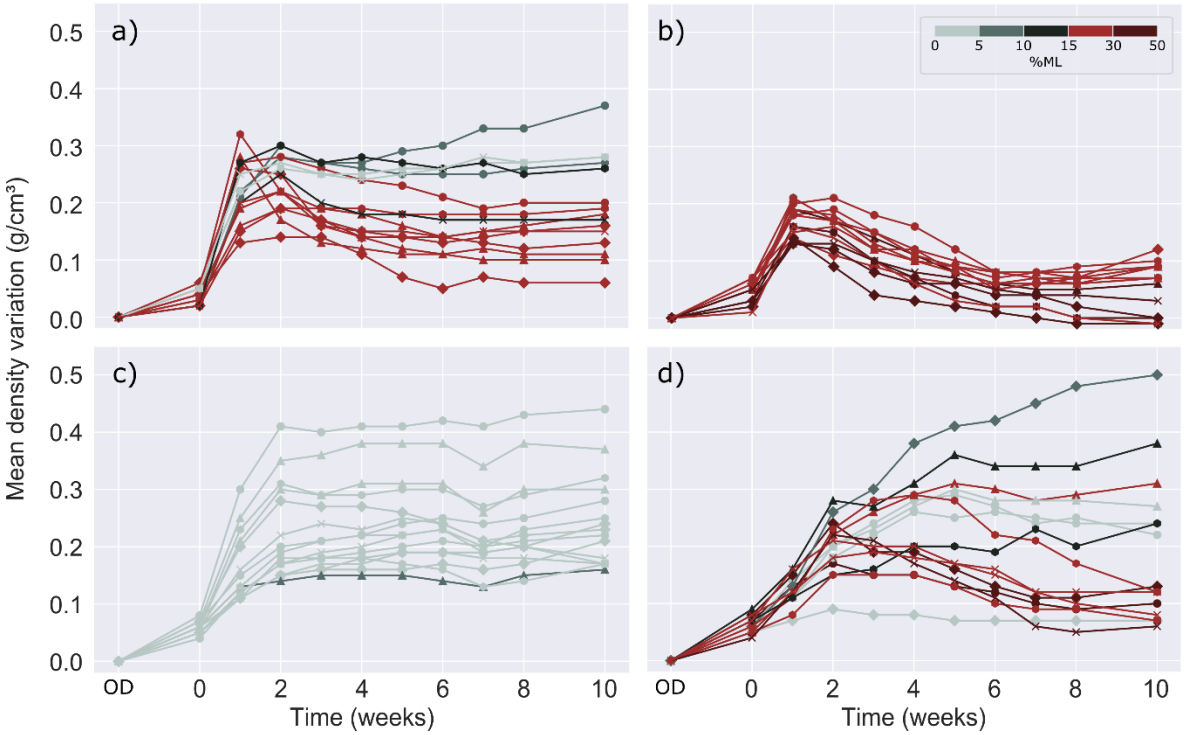

Figure 5-9 Mean density variation over time (g/cm³) relative to the oven-dry density (OD) for 15 specimens of a) beech b) spruce c) okoumé and d) Scots pine during 10 weeks of degradation by *C. puteana*, as assessed with X-ray CT. The colour of the curve gives an indication of the amount of mass loss (ML) after 10 weeks of degradation. Curves with the same marker shape represent specimens that were placed together in the same Petri dish.

The maximal density (D_{max}) reached during the degradation experiment (Figure 5-9) was for all species much higher than in the reference specimens (Figure 5-8). During the first 1-2 weeks of the degradation experiment, the mycelium of *C. puteana* covered the entire Petri dish surface, with its mycelial area increasing from 7.0 to 63.3 cm², and (partly) covered and presumably invaded the wood. Since fungi metabolise sugars, which are easily available in agar medium, into carbon dioxide and water (Schmidt, 2006), the increase in density could therefore be related to the moisture production by the fungus. After this initial increase in density, the density of the mini-blocks either remained stable (ΔD_{min} low), decreased significantly (ΔD_{min} high) or increased. The mass loss after 10 weeks and ΔD_{min} were highly correlated, with a Pearson correlation of 0.72 (Suppl. Figure 8-7), indicating that the larger the difference in ΔD_{min}, the higher the mass loss. Indeed, for all specimens with less than 5% ML, the density remained stable after the initial water uptake (Figure 5-9), similar as in the reference experiment without a fungus (Figure 5-8). The spruce specimens, which were most severely decayed (Figure 5-9b), showed the highest ΔD_{min}. Since brown-rot fungi degrade cellulose and hemicellulose, while leaving the lignin mostly unhampered, the water sorption capacity of the degraded wood is reduced (Rawat, 1998; Thybring, 2017). Besides a density decrease due to wood mass being metabolized into carbon dioxide (gas), part of the moisture that was produced during degradation of the wood will

therefore not have remained in the mini-block, resulting in an additional decrease in density over time for mini-blocks that were highly degraded.

Species and intra species variation in degradation patterns

Obviously, wood species was highly correlated to the amount of mass loss (Table 5-2). Specimens of beech and spruce mostly had a ML between 15-30% and more than 30% (Figure 5-9 a and b). This is as expected, since both species are known to be susceptible to the brown-rot fungus *C. puteana* (CEN EN 350 standard, 2016; De Ligne *et al*., 2020). Okoumé clearly has a mechanism limiting fungal decay by *C. puteana*, as all but one specimen had less than 5% mass loss after 10 weeks of incubation (Figure 5-9 c). The density of all okoumé specimens increased up to two weeks, after which it stabilized. The variation in maximal density could be attributed to the angle of the vessels (Pearson correlation of 0.95, Suppl. Figure 8-8). Okoumé specimens with vessels parallel to the longitudinal direction took up the least amount of water. Though this caused the maximal density to vary, this variation was not correlated to mass loss level (Pearson correlation of -0.25, Suppl. Figure 8-8). In Chapter 3.2, we postulated that the durability of okoumé against degradation by *C. puteana* is related to the presence of hydrophobic components in the heartwood. Scots pine showed a high variation in degradation patterns, and mass loss ranged from 0.5 - 32.9% (Figure 5-9 d). A closer look at the wood structure of the specimens revealed that the number of growth rings is strongly related to this variation. Scots pine specimens with less than 10% mass loss had more than eight growth rings per cm in the specimen, while the specimens with more than 10% mass loss had only two to four growth rings per cm. This inverse linear relationship between mass loss and number of growth rings was confirmed with Pearson correlation (Pearson correlation of -0.84, Suppl. Figure 8-9). The presence of fungicidal components in Scots pine heartwood, called pinosylvins (classified as a stilbene), is known to be variable. Belt *et al*. (2017) found that there are a lot of similarities in the distributions of pinosylvins and lignin on a cellular level, pointing towards an interaction between the two components. Wood with many growth rings per cm, has grown slowly, and contains more lignin (Novaes *et al*., 2010). It is, therefore, likely that heartwood with many growth rings per cm has a higher concentration of pinosylvins, which could explain the higher resistance of the mini-blocks with more growth rings per cm. Wood anatomy might differ as well between wood specimens that had grown fast and slow and affect hyphal progress and water uptake. In their study on the influence of anatomical differences on fluid passage in Scots pine sapwood, Zimmer *et al*. (2014) found that specimens from trees growing in better growing conditions and sufficient water supply had larger pit dimensions and more pits, which increased the interconnectedness and was presumed to be the cause of enhanced transverse fluid passage. Presumably, hyphal penetration and water uptake in wood specimens with few growth rings per cm (grown fast) could similarly be enhanced by such wood anatomical differences.

In Figure 5-10, oven-dry density profiles of two Scots pine and two spruce mini-blocks are shown. For the Scots pine mini-block with eight growth rings per cm (Pine 2), which had an overall mass loss of 1%, the absolute oven-dry density decrease was lower than 0.05 g/cm³, both for the assessed latewood zones as well as the earlywood zones. For the Scots pine mini-block with three to four growth rings (Pine 1), which had an overall mass loss of 28%, the absolute oven-dry density decrease was higher in the latewood zones than in the earlywood zones (Figure 5-10 b). Latewood zones have a higher oven-dry wood density, and therefore more wood mass for the fungus to degrade. However, when we look at the oven-dry density decrease of the earlywood and latewood zones relative to the initial oven-dry density of that zone, the fungus had degraded up to 30% of the assessed earlywood zones and up to 21% of the latewood zones (Figure 5-10 c). This shows that the fungus was able to degrade both zones, but had easier access to the earlywood. Do note that the conclusions made here are tentative, due to the limited amount of data. The same was observed for both spruce specimens. Contrary to Scots pine, the mass loss of spruce specimens was not correlated to the number of growth rings (Pearson correlation of -0.12, Suppl. Figure 8-10). Indeed, in the spruce specimen with six growth rings, both latewood and earlywood had been degraded well.

Water transport by the fungus

All but one specimen of the Scots pine mini-blocks with more than eight growth rings per cm had less than 5% ML. The specimen with a ML between 5-10%, had a density that was not stable after the initial increase due to water uptake but continued to increase up to the end of the experiment (Figure 5-9d). The small amount of mass loss did not cause a decrease in the overall density. On the contrary, the presence of the fungus caused a density increase much higher than the density of the non-decayed specimens (<5% ML). Since the density increase was higher than could be expected from fungal respiration in the case of 8% mass loss, the increasing density is likely an indication of the fungus transporting water into the mini-block. Such an occurrence of high moisture contents in wood specimens that have only slightly been degraded, has been shown before for brown-rot fungi, particularly in experiments with significant amounts of free water (Thybring, 2017). A similar phenomenon could also be observed for one of the beech specimens with a ML between 5-10% (Figure 5-9 a).

Degradation along the longitudinal direction of the mini-blocks

A greyscale profile was taken along the longitudinal direction of each mini-block, and the average density was calculated relative to the oven-dry density before the experiment, to detect degradation progress along the longitudinal axis of the mini-block (Figure 5-4a). Since degradation patterns were expected to differ over the longitudinal direction, 5 zones were identified: outer Left and Right zone (L&R), the Middle zone (M) and the zone between the Left and Middle zone and the Middle and Right zone (LM&MR) (Figure 5-4b). Figure 5-11 displays the average density variation in each zone after 0, 1, 2, 6 and 10 weeks of degradation for all wood species.

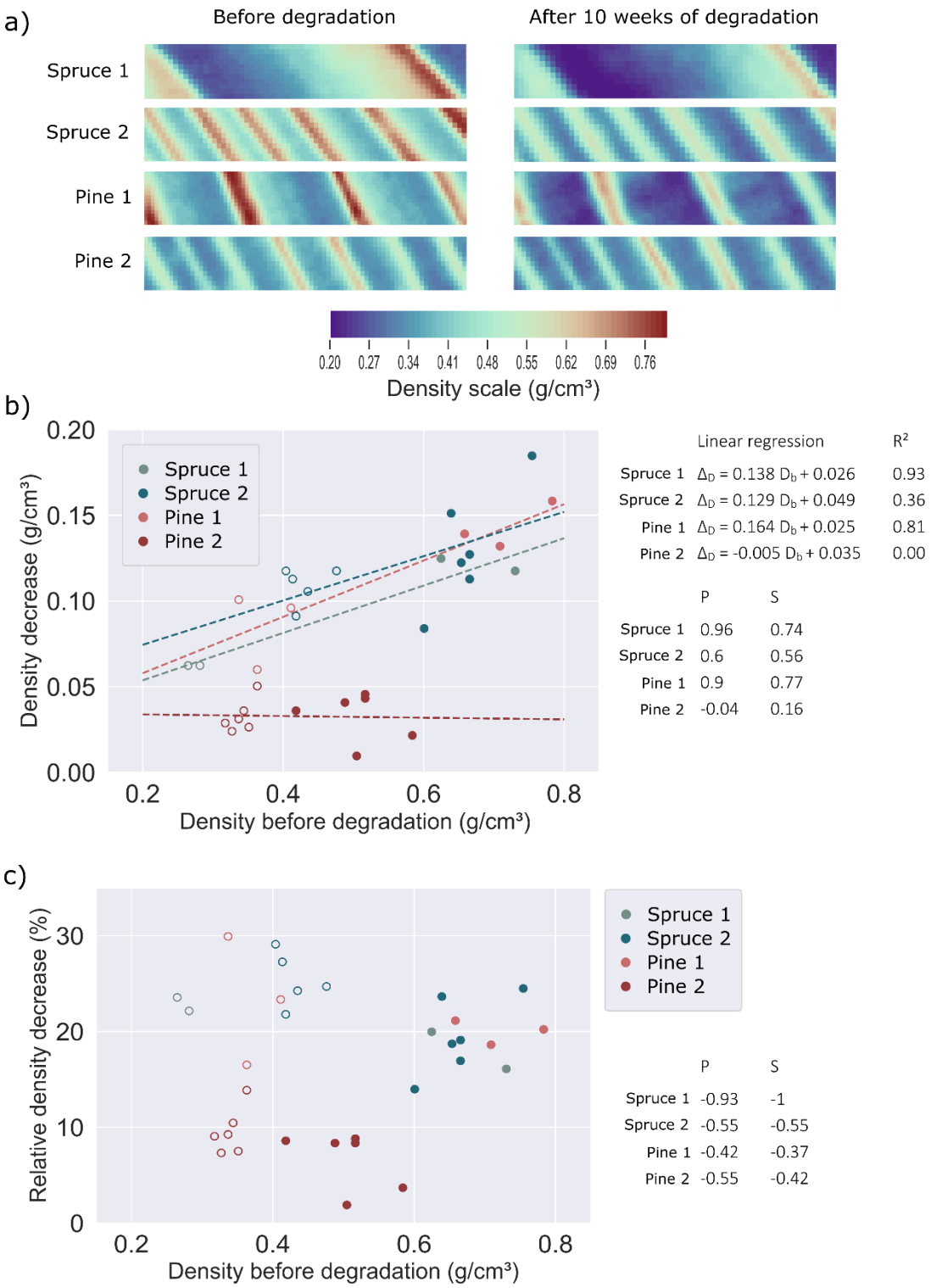

Figure 5-10 a) Visualization of oven-dry density of two spruce (Spruce1 and Spruce2) and two Scots pine (Scots pine1 and Scots pine2) specimens with different numbers of growth rings per cm, before and after degradation. The density visualizations represent a region of approximately 0.75 x 6.00 mm and the density in each pixel was averaged over 85 X-ray CT slices (c.a. 5.80 mm) b) Absolute oven-dry density decrease (g/cm³) of latewood (•) and earlywood (o) zones compared to the oven-dry density (g/cm³) in those zones before degradation. Pearson (P) and Spearman (S) correlations are indicated as well as the result of a linear regression for each specimen. c) Oven-dry density decrease divided by the initial oven-dry density (%). Note: the overall mass loss of the specimens after 10 weeks was as follows: Spruce1: 25% ML, Spruce2: 24% ML, Scots pine1: 28% ML, Scots pine2: 1% ML.

For beech, spruce and okoumé, the density variation appeared to increase and decrease homogeneously over the mini-blocks (Figure 5-11a-d). For the beech mini-blocks with less than 10% ML (Figure 5-11a) the density increased up to 2 weeks and then remained stable, with the difference in density after 2 weeks and the density after 10 weeks around 0 (Figure 5-12a). The density increase of the beech mini-blocks with more than 10% ML in the first week was not significantly different from the blocks with less than 10% ML (Figure 5-11a and b). After week 2, however, the density decreased homogeneously over the specimen (Figure 5-11b) and the density was significantly lower than those of the mini-blocks with less than 10% ML (Figure 5-11a). Clearly, the fungus did not experience any issues in the longitudinal direction (=vessel direction) and was able to degrade all zones simultaneously (Figure 5-12b). Although beech wood has wide vessels (Table 5-1), it is also known to form tyloses, saclike intrusions which block xylem vessels, after felling of the tree and while the tree is alive (Ebes, 1937; Murmanis, 1975). In beech wood where intense heartwood formation has occurred, the presence of tyloses hinders impregnation with preservative treatments (Murmanis, 1975). A similar effect was expected for water uptake and hyphal penetration in this experiment, but this was not the case. However, heartwood formation in beech is not uniform and 'false heartwood' formation is known to occur (Ravcko and Cunderlik, 2010). The latter is a phenomenon where wood has the appearance of heartwood but not its qualities. Similar to the beech specimens with more than 10% ML, the spruce specimens were degraded homogenously along the specimen (Figure 5-11c and Figure 5-12b). The okoumé specimens showed a high variation in density, as mentioned above. Nevertheless, the density difference between week 2 and week 10 was significantly higher in the outer left and right zone than in the middle zones of the mini-blocks (Figure 5-12a), as water had been taken up rather fast in the outer zones. For Scots pine, the density increase due to water uptake and moisture production by the fungus was significantly higher in the outer zones than in the middle zone, both for blocks that had less than 10% ML (Figure 5-11 e) as well as those with more than 10% ML (Figure 5-11 f). Degradation of Scots pine occurred gradually along the mini-block, with the outer zones more severely degraded than the middle zone (Figure 5-12b). Clearly, the fungus was not able to degrade the middle of the mini-block immediately. Previous studies have shown that initial hyphal penetration of a wood block occurs via the major longitudinal pathways, being vessels for hardwoods and tracheids and resin canals for softwoods, respectively (Bravery, 1975), and concurs with our findings for Scots pine. It could be that components inherent to the Scots pine heartwood, such as resin acids and fatty acids (Ekeberg *et al*., 2006) were responsible for this delay in fungal progress along the longitudinal axis. Stilbenes could be involved as well by inhibiting fungal growth, but as this delay also occurred for specimens that were degraded up to 30% mass loss, the latter is unlikely to be the cause.

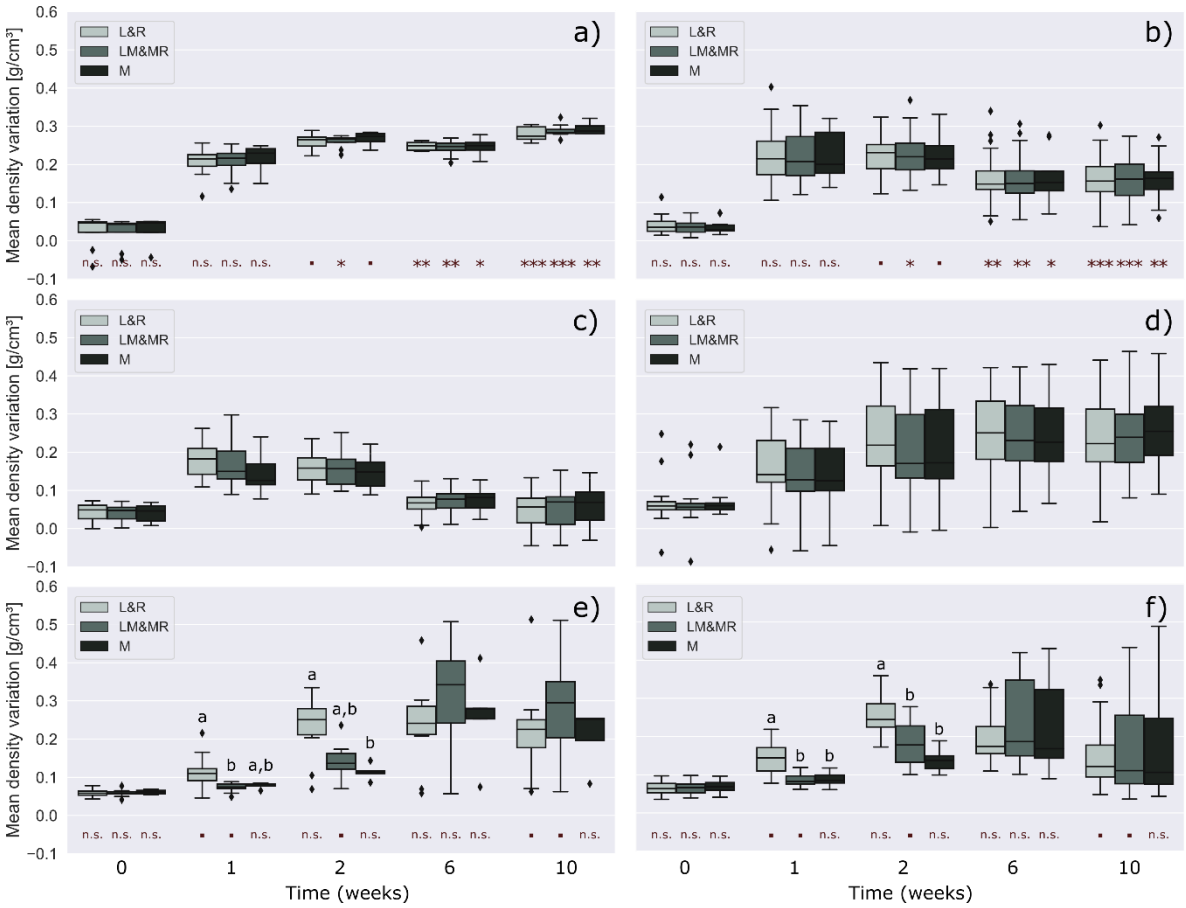

Figure 5-11 Density variation over time averaged over three zones (10 x 5 x 5.2 mm^3) along the longitudinal direction of the wood blocks: outer left and right zone (L&R), middle zone (M) and the zone between the left and middle zone and the middle and right zone (LM&MR), see Figure 5-4b. a) beech <10% ML, b) beech >10% ML, c) spruce, d) okoumé, e) Scots pine <10% ML, and f) Scots pine >10% ML. For those regions where the density was significantly different (Kruskal-Wallis H-test p-value <0.05) between regions, a letter (a,b) was assigned based on Dunn's multiple comparison test with Benjamini-Hochberg correction. Different letters indicate significant statistical difference. For beech (a and b) and Scots pine (e and f), the Kruskal-Wallis H-test was applied to test for significant differences in median density variation of each region between <10% ML (a and e) and >10% ML (b and f): significance codes 0 '***' 0.001 '**' 0.01 '*' 0.05 '.' 0.1 'n.s.' 1.

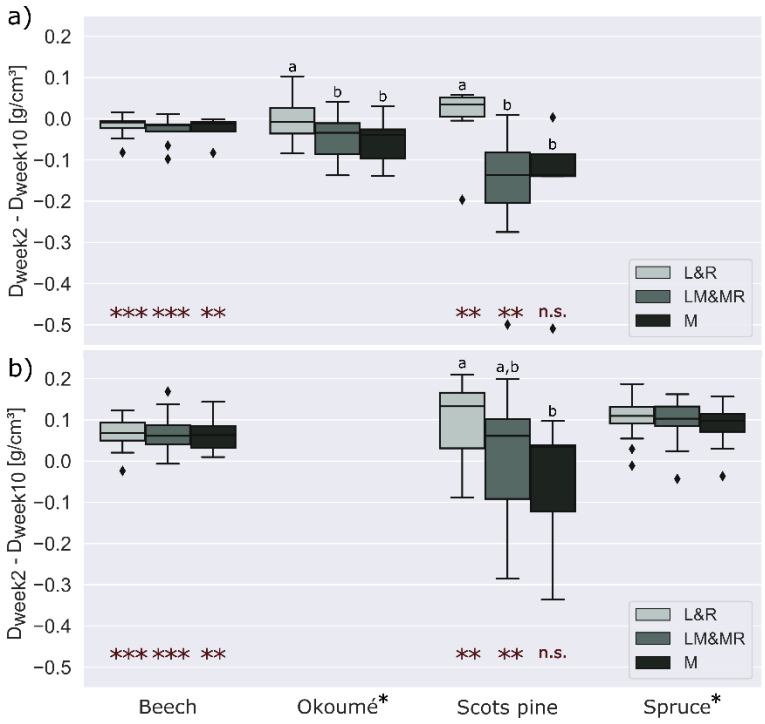

Figure 5-12 Density difference between density at week 2 and density at week 10, averaged over three zones (10 x 5 x 5.2 mm³) along the longitudinal direction of the wood blocks: outer left and right zone (L&R), middle zone (M) and the zone between the left and middle zone and the middle and right zone (LM&MR). a) Specimens with <10% ML and b) specimens with >10%. *All okoumé specimens had <10% mass loss and all spruce specimen had more than 10% ML.

Limitations of the method

Although the effect of certain wood anatomical characteristics, such as the number of growth rings and the vessel orientation, could be evaluated, the resolution of the set-up did not allow to analyse decay progress on cell wall level. Increasing the resolution would be possible by drastically reducing the specimen size and set-up. As this would increase scan time, it would be recommended to reduce the number of specimens as well. Note that non-invasively visualizing fungal penetration of certain wood cell types might still be a challenge, as the fungus produces water during fungal decay, which might obscure the 'visibility' of the wood cells. In that case, conventional destructive methods for visualising decay of wood cells, such as high-resolution light microscopy and scanning electron microscopy, can be used. Nonetheless, the method clearly shows that localized decay can be visualized, quantified and related to wood structure at a submillimetre scale. For future experiments on wood-based panels, such as plywood and OSB, a larger sample size is recommendable, to investigate the influence of glue layers and fibre orientation. Besides existing materials, it would be interesting as well to fabricate barrier systems to test theories and design new materials and structural modification strategies.

5.4 Conclusions

X-ray micro CT is a useful, non-destructive tool for assessing the progress of decay and determining the influence of wood structure. For instance, latewood zones and earlywood zones in softwoods were easily discernible, allowing to determine whether the fungus preferred degradation of one over the other. Another advantage is that progress of decay could be monitored on the same wood specimens, along the longitudinal axis of the wood block. Non-durable wood species, such as beech and spruce, were easily accessible in longitudinal direction (=vessels/tracheid direction) and decay occurred homogenously along the wood specimens. For Scots pine, decay progress was evidently hampered. High moisture contents in wood specimens that were only slightly degraded, were a clear indication of *C. puteana* transporting water into the wood block. The resolution of the set-up did not allow to analyse decay progress on a cellular level. For instance, although the vessel direction of okoumé specimens influenced the water uptake of the specimens, this factor was not related to the amount of mass loss and the protection mechanism of okoumé against degradation by *C. puteana* could not be observed with X-ray CT. This could be remedied by increasing the scan resolution, which would require a reduction of the specimen size. As the current method is most suited on a submillimetre scale, it would be most useful to gain insight in decay of wood species which have a distinct macro structure and for wood-based products and bio-based materials, where the effect of glue layers, porosity, strand size and orientation on decay progress has not been unraveled. It would also be interesting to take a similar approach for assessing decay progress of other brown-rot fungi, as well as various white-rot and soft-rot fungi, as different fungal species vary in physiology and have different modes of action.

Chapter 6

Conclusions

Urbach tower, Germany
The curved timber components that give the tower its unique structure were designed and produced as flat panels that deform autonomously into predicted curved shapes when dried.
Designed by the Institute for Computational Design and Construction and the Institute of Building Structures and Structural Design at the University of Stuttgart.

6.1 Research findings

Most bio-based building materials are (to some extent) biodegradable. When an organic material is exposed to favourable moisture and temperature conditions as well as to degrading organisms, its functional and aesthetic service life can decrease. The risk of fungal decay depends on the environment in which a material is applied and the material resistance.

When it comes to the influence of environment, a key aspect of importance is how specific environmental conditions affect mycelial growth. Hyphae of *Coniophora puteana* (strain MUCL 11662, BAM 15) showed clear signs of distress at a RH of 65% and dehydration also occurred at a temperature of 30°C. This shows that mycelial expansion in case of a limited moisture source is restricted at RH conditions of 65% and below. Mycelium of *C. puteana* was able to expand and grow at an RH of 70-85%, even with a limited moisture source. Nonetheless, this does not mean that the fungus is able to actively decay in such conditions. On the contrary, there is a scientific consensus that wood decay does not occur below 85% RH when no liquid moisture source is present (Brischke and Alfredsen, 2020).

In the case of a moisture source, *C. puteana* experienced difficulties to overgrow and moisten wood specimens at low RH conditions (11-22% RH). An RH of 43% and higher seemed no longer to inhibit fungal growth thus enabling the fungus to moisten and decay non-durable wood specimens. As the RH is often higher than 43% outdoors and in certain indoor spaces (such as bathrooms and swimming pools), water accumulation should be prevented as much as possible, which has been reported before.

We also found that fungicidal components are not always of major importance for the durability of a wood species. Wood species such as *Aucoumea klaineana* and *Entandrophragma cylindricum* mainly relied on moisture-regulating components and the wood anatomy of *Pterocarpus soyauxii* likely increased its durability. It is important to recognise that material moisture dynamics and structure can have a (major) influence on durability, especially as there are many opportunities to optimize the structural design and to alter the material's moisture dynamics of bio-based building materials.

Indeed, hydrophobic additives, wood modification and the production process have a major impact on the material moisture dynamics of bio-based building materials. The assessed thermally modified wood, wood fibre board with bitumen and wood fibre insulation board type 2 are expected to have an extended service life in outdoor exposure conditions, assuming that the residual moisture content criteria described for plywood in De Windt *et al.* (2018) are applicable to bio-based building materials in general.

This work also presented the first LFNMR relaxation time distributions of wood fibre insulation materials and engineered wood products. We showed that when the wood anatomy is not altered substantially when producing a wood-based panel, the water populations are similar to those of solid wood, as was the case for plywood and the three-layer spruce panel. An additional peak was consistently present in OSB, and the wood-fibre insulation materials contained four to six peaks. This proves that water in macro voids remains susceptible to interactions with the pore walls, which allows to distinguish water populations for different kinds of macroporous materials.

X-ray micro CT proved to be a useful, non-destructive tool for assessing the progress of decay and determining the influence of wood structure over time. Non-durable species, such as beech and spruce, were easily accessible in the longitudinal direction (=vessels/tracheid direction) and decay occurred homogeneously along the wood specimens. For Scots pine, decay progressed more slowly.

6.2 Research achievements

Aim 1. Assess the influence of temperature and relative humidity on fungal growth dynamics at mycelial level.

A semi-automated image analysis method developed by Vidal-Diez de Ulzurrun *et al.* (2015) was adopted to assess the impact of temperature and relative humidity on mycelial growth dynamics of *C. puteana* and *R. solani*. The method effectively provided an objective and in-depth analysis of the effect of environmental conditions on various fungal growth characteristics (including the mycelial area, number of tips and branching angle), in a rather short period of time (62 h) and by making use of low-cost imaging devices.

While suited for assessing the effect of temperature and RH on mycelial development in case of a limited moisture source, the added value of the method is the detailed quantification of fungal growth characteristics, which allowed to observe elongation of the 'leading hyphae". The method is, therefore, most suited for research questions where detailed assessment of fungal growth dynamics is of interest, such as tracking differences in phenotype between genetic variants of the same species, testing the influence of different growth substrates on the amount of branching and the hyphal segment lengths, to study local behaviour within a fungal colony, such as differences in growth behaviour and morphology between the central region and the peripheral region and to acquire parameters for realistic modelling.

Aim 2. Develop a method suited to assess the influence of material chemistry on fungal susceptibility.

The paste test was developed as part of this PhD project and proved to be a useful method to assess the presence of fungicidal compounds in wood and bio-based building materials, as it allows for all bio-based materials to be tested regarding their active ingredients in a similar way.

The paste test is meant to serve as a complementary method to standard natural durability methods to provide more insight into whether a certain wood species or bio-based building product derives its durability from fungicidal compounds, or whether other mechanisms play a role. For future applications, it would be recommendable to also include pH measurements of the pastes, and to develop a method to quantify mycelial density.

Aim 3. Develop a method to assess the influence of RH and material moisture content on fungal decay in the presence of a moisture source.

A test method was proposed to assess the influence of RH on fungal decay in function of time, in the presence of a moisture source. Previous methods either assessed the influence of RH on decay, without a moisture source, or assessed the level of decay in terms of a moisture gradient, at a RH of 100%. An issue that all three types of methods have in common, is that the fungus influences the MC of the mini-blocks when it grows in or on the blocks and when it starts to degrade. This makes it difficult to define critical MCs at which a material is at risk.

While we were able to gather valuable conclusions from the performed experiments, there are several suggestions for improvement. Ventilator settings could be optimised by reducing direct air flow over the specimens and providing ventilation in pulses instead of continuously, and RH should be monitored as well. Also, the number of specimens should be increased to at least five replicates, but preferably ten or more, to guarantee more robust results.

Aim 4. Apply state-of-the-art methods to better understand material moisture dynamics of commonly used wood-based panels and wood fibre insulation products.

Floating test

The floating test (CEN TS 16818 standard, 2018) is a test method for assessing material moisture dynamics. It was initially developed for plywood, since certain plywood types do not contain any active ingredients yet have an adequate service life in outdoor exposure, which could be linked to their moisture dynamics. In this work, the method was applied and found adequate for assessing the moisture dynamics of a wide

selection of bio-based building materials, most of which had not yet been assessed before in this regard. The test also indicated products with water accumulation levels that might be problematic. However, to understand how material structure and chemistry affect these moisture dynamics, other techniques need to be used.

LFNMR

LFNMR provided useful insights into the pore distribution of nine commonly used bio-based building materials in water-saturated state, including cell wall water. LFNMR relaxation time distributions give an indication of how tight the water is bound, which depends on both pore size and the affinity of the water molecules with the pore surface. This makes it often difficult to interpret results. For future experiments, more controlled testing of specific phenomena of interest are needed, to determine, for instance, the influence of changing one step in the production process or by comparing the LFNMR relaxation time distributions of experimentally designed test materials where all components have remained the same, except for pore size.

X-ray CT

X-ray CT was very useful to visualize the internal pore space of the materials in dry state and proved to be valuable to confirm pore distributions of wood-based panels and thermally modified wood. However, for wood-fibre insulation materials, the proposed X-ray CT method was not suited to gain insight into the pore volume in water-saturated state, as fibres stick together and the pore volume changes when becoming wet. Therefore, the X-ray CT pore size distributions of the wood-fibre insulation materials could not be compared with the LFNMR data. For future work, it is recommendable to use X-ray CT to assess the pore space of the dry material before and after water saturation. Nevertheless, for loose, fibrous materials, LFNMR might be the only method to quantify pore distributions in water-saturated state, though MRI visualization and future advancements in development of contrast fluids for X-ray CT analysis might be a solution as well.

ATR-FTIR

When the composition of a bio-based material and its additives are known, ATR-FTIR does not provide much added value. However, it is a valuable technique when used to assess products for which the chemical composition has changed due to a transformation (such as cork and thermally modified wood). ATR-FTIR measurements would be most beneficial to assess the effect of a change in the production process, the amount or type of additives or the degree of modification.

Aim 5. Develop a method to assess the influence of material structure on moisture dynamics and progress of fungal decay.

X-ray CT scanning has proven to be a very useful method to non-destructively analyse decay progress in function of time and was successfully applied to assess the influence of wood structure at submillimetre level. The experimental set-up we developed would

be most useful to improve understanding of decay of wood species that have a distinct macro structure and for wood-based products and bio-based materials, where the effect of glue layers, porosity, strand size and orientation on decay progress still need a lot of unravelling. To gather detailed knowledge on (sub)micron level, the set-up could be adapted to be able to scan at a higher resolution. Another possibility would be to complement the X-ray CT method with light microscopy or SEM to examine certain phenomena at a higher resolution. This would mean that a subset of samples needs to be taken out of the experiment at certain time intervals, as sample preparation for the latter methods is destructive.

All methods in this study were developed and applied complementary to the standard methods, to gain understanding on the influence of material characteristics on the fungal susceptibility and moisture dynamics of bio-based building materials.

6.3 Policy recommendations

Expanding use classes

As material moisture dynamics and structure have a (major) influence on durability and decay risk, there is a need for better-defined use classes. The current use classes go from dry, interior applications (UC1) to applications with permanent or regular immersion in salt water (UC5) (CEN EN 335 standard, 2013). Although the use classes differentiate between different moisture risks, the impact of climate and micro-climate, building design and material properties on Time of Wetness (ToW) is not considered and should be included. This is mainly important for exterior applications exposed to weathering, but not in ground contact (UC3), and also in applications with condensation risk (UC2). For instance, we found that many bio-based building materials, such as most of the assessed wood-fibre insulation boards, have excellent moisture dynamics and are able to dry out completely within a couple of days. Having the ability to dry out fast greatly reduces the risk of fungal decay, as the risk of fungal sporulation decreases. We also found that below fibre saturation point, decay is more limited, confirming literature stating that no decay occurs below 15% MC, although in our set-up even no decay (<1% mass loss) occurred between 15 and 20% MC either. In practice, several bio-based materials, such as wood-fibre insulation materials, are already used with these principles in mind. We showed that most of these products do not contain fungicidal compounds. Nevertheless, some of them are successfully used in applications with a decay risk, such as insulation between the exterior and the cavity wall and as roof insulation (UC2).

Fit-for-purpose

With better-defined use classes comes the need for bio-based products that are tailored to these diversified end uses and moisture conditions. In Section 4.3, we found that hydrophobic additives, wood modification and production process have a major impact on the material moisture dynamics of bio-based building materials. As bio-based materials are tailorable, producers should embrace a fit-for-purpose strategy

when developing and marketing bio-based building products. It is also essential that project designers and architects adopt a fit-for-purpose strategy when renovating or designing new building projects. Like with any class of materials, it takes time and expertise to know how to correctly apply them and how to take advantage of the material properties to optimize building design, even beyond protection by design. It is, for instance, well known that wood insulation materials based on wood fibres have excellent moisture-buffering qualities. There are already architects, contractors and consulting agencies specialized in building with wood and bio-based building materials. However, a transition towards a bio-based building industry will require a broader effort to educate (future) architects, engineers and contractors. The recently started CLICKdesign[3] project is, for instance, responding to this need by developing a software tool that enables users to understand the impact of design choices on product performance of wood, including durability (fungi and insects), moisture, strength, and aesthetics (Suttie *et al.*, 2020).

6.4 Recommendations for future research

The research on fungal degradation in this PhD thesis was limited to two fungal species: *C. puteana*, which is a standard test fungus for investigating brown rot and *T. versicolor*, which is a standard fungus for investigating white rot. Further research could include other brown- and white-rot fungi. There are of course many more organisms that are able to degrade bio-based building materials. It would, therefore, also be interesting to take a similar approach and see how material characteristics affect other wood-degrading organisms, such as soft-rot and insects, which have different colonization patterns and optimum conditions.

Likewise, some parts of the PhD thesis were performed only on solid wood or on a selection of wood-based panels and wood-fibre insulation materials. It would be interesting to use the test methods for other bio-based building materials in future research as well.

In the section on policy recommendations, expansion of the use classes was recommended. An important element in expanding these use classes, will be to have reference values for moisture dynamics that provide an accurate indication of the fungal decay risk in practice. As part of the Plybiotest[4] project, an extensive study was performed on the moisture dynamics of uncoated plywood, linking laboratory tests to actual performance in outdoor exposure conditions (De Windt *et al.*, 2018). A similar approach should be taken to investigate the moisture dynamics of different types of bio-based building materials. Depending on the type of material, outdoor exposure tests might need to be replaced by exposure tests better simulating moisture risk in UC2, as moisture accumulation due to, for instance, condensation is different from exposure to rain.

Research on improving moisture dynamics should be continued as well, both fundamental research on understanding moisture dynamics as well as more applied research on optimizing production processes and additives. Fundamental research is, for instance, recommended to arrive at a better understanding of the moisture-regulating mechanisms in wood species such as *Aucoumea klaineana* and on the fungal decay resistance of modified wood, so that these mechanisms can be better targeted. Also, the influence of material structure on decay and moisture dynamics should be investigated further, as there are many opportunities to alter material structure in engineered wood products and bio-based insulation materials.

[3]CLICKdesign is a ForestValue research Project from a European consortium of eight European organisations, which started in 2019. The CLICKdesign project is developing a performance-based specification protocol to make a software tool for architects, specifiers and the general public to embed service life performance specification for wood. This will increase market confidence in wood as a reliable product and improve performance of timber in the built environment (BRE, 2020).

[4]PLYBIOTEST was a European Research Project in which a total of 60 different kinds of plywood produced by European plywood companies were tested for the biological performance in exterior out of ground application.

7 References

Al-Beldawi, A., Jawad, A., Sheik-Raddy, H. (1982) *Rhizoctonia* seedling disease of hemp and its control. *Crop Protection* 1: 111–113.

Ammer, U. (1963) Investigations on the growth of red-streakiness fungi in dependence of the wood moisture content (In German). *Forstwissenschaftliches Centralblatt* 82: 360–391.

Amusant, N., Arnould, O., Pizzi, A., Depres, A., Mansouris, R.H., Bardet, S., Baudassé, C. (2009) Biological properties of an OSB eco-product manufactured from a mixture of durable and non-durable species and natural resins. *European Journal of Wood and Wood Products* 67: 439–447.

Ancin-Murguzur, F.J., Barbero-López, A., Kontunen-Soppela, S., Haapala, A. (2018) Automated image analysis tool to measure microbial growth on solid cultures. *Computers and Electronics in Agriculture* 151: 426–430.

Andrew, R.M. (2018) Global CO_2 emissions from cement production. *Earth System Science Data* 10: 195.

Anguiz, R., Martin, C. (1989) Anastomosis groups, pathogenicity, and other characteristics of *Rhizoctonia solani* isolated from potatoes in Peru. *Plant Disease* 73: 199–201.

Antwi-Boasiako, C., Atta-Obeng, E. (2009) Vessel-fibre ratio, specific gravity and durability of four Ghanaian hardwoods. *Journal of Science and Technology (Ghana)* 29: 8-23.

APAWOOD (2020) https://www.apawood.org. Accessed on October 29th 2020.

ASTM D1107-96 standard (2013) Standard test method for ethanol–toluene solubility of wood.

Ayerst, G. (1969) The effects of moisture and temperature on growth and spore germination in some fungi. *Journal of Stored Products Research* 5: 127–141.

Baird, R., Carling, D., Mullinix, B. (1996) Characterization and comparison of isolates of *Rhizoctonia solani* AG-7 from Arkansas, Indiana, and Japan, and select AG-4 isolates. *Plant disease* 80: 1421–1424.

Beck, G., Thybring, E.E., Thygesen, L.G., Hill, C. (2018) Characterization of moisture in acetylated and propionylated radiata pine using low-field nuclear magnetic resonance (LFNMR) relaxometry. *Holzforschung* 72: 225–233.

Belt, T., Keplinger, T., Hänninen, T., Rautkari, L. (2017) Cellular level distributions of Scots pine heartwood and knot heartwood extractives revealed by Raman spectroscopy imaging. *Industrial Crops and Products* 108: 327–335.

Benjamini, Y., Hochberg, Y. (1995) Controlling the false discovery rate: a practical and powerful approach to multiple testing. *Journal of the Royal statistical society: series B (Methodological)* 57: 289–300.

Berdy, J. (2005) Bioactive microbial metabolites. *Journal of Antibiotics* 58: 1-26.

Berndt, D., Clifford, J. (1994) Using dynamic time warping to find patterns in time series. In: AAAI-94 workshop on knowledge discovery in databases, AAAIWS'94. AAAI Press, pp. 359–370.

Bilal, M., Khan, K., Thaheem, M., Nasir, A. (2020) Current state and barriers to the circular economy in the building sector: Towards a mitigation framework. *Journal of Cleaner Production* 276: 123250.

Bjurman, J., Wadsö, L. (2000) Microcalorimetric measurements of metabolic activity of six decay fungi on spruce wood as a function of temperature. *Mycologia* 92: 23–28.

Boddy, L. (1983) Effect of temperature and water potential on growth rate of wood-rotting basidiomycetes. *Transactions of the British Mycological Society* 80: 141–149.

Bongers, F., Groenendijk, P., Bekele, T., Birhane, E., Damtew, A., Decuyper, M., Eshete, A., Gezahgne, A., Girma, A., Khamis, M.A., others (2019) Frankincense in peril. *Nature Sustainability* 2: 602–610.

Bonner, J.T. (1948) A study of the temperature and humidity requirements of *Aspergillus niger*. *Mycologia* 40: 728–738.

Bonner, R.D., Fergus, C.L. (1960) The influence of temperature and relative humidity on growth and survival of silage fungi. *Mycologia* 52: 642–647.

Boonstra, M. (2008) A two-stage thermal modification of wood. PhD Thesis, Université Henri Poincaré, France.

Brabant, L., Vlassenbroeck, J., De Witte, Y., Cnudde, V., Boone, M.N., Dewanckele, J., Van Hoorebeke, L. (2011) Three-dimensional analysis of high-resolution X-ray computed tomography data with Morpho+. *Microscopy and Microanalysis* 17:252–263.

Brandner, R. (2013) Production and Technology of Cross Laminated Timber (CLT): A state-of-the-art Report. In: Focus Solid Timber Solutions-European Conference on Cross Laminated Timber (CLT), volume 21. University of Bath, Bath, pp. 3–36.

Bravery, A. (1975) Micromorphology of decay in preservative treated wood. In: Liese, W. (Ed.), Biological Transformation of Wood by Microorganisms: Proceedings of the Sessions on Wood Products Pathology. Springer-Verlag, Berlin, pp. 129–142.

Bravery, A. (1978) A miniaturised wood-block test for the rapid evaluation of wood preservative fungicides. In: Screening techniques for potential wood preservative chemicals, Proceedings of a special seminar held in association with the 10th annual meeting of the IRG. Peebles, pp. 57-65.

BRE (2020) https://www.bregroup.com/services/research/clickdesign. Accessed on November 2nd 2020.

Brischke, C., Alfredsen G. (2020) Wood-water relationships and their role for wood susceptibility to fungal decay. *Applied Microbiology and Biotechnology* 104: 3781–3795.

Brischke, C., Humar, M., Thelandersson, S. (2017) Function. In: Jones, D., Brischke, C. (Eds.), Performance of bio-based building materials. Woodhead Publishing, pp. 250-256.

Brischke, C., Rapp, A.O. (2008) Influence of wood moisture content and wood temperature on fungal decay in the field: observations in different microclimates. *Wood Science and Technology* 42: 663–677.

Brischke, C., Rapp, A.O. (2010) Service life prediction of wooden components - Part 1: Determination of dose-response functions for above ground decay. In: 41st Annual Meeting of the International Research Group on Wood Protection, Biarritz, France.

Brischke, C., Soetbeer, A., Meyer-Veltrup, L. (2017) The minimum moisture threshold for wood decay by basidiomycetes revisited. A review and modified pile experiments with Norway spruce and European beech decayed by *Coniophora puteana* and *Trametes versicolor*. *Holzforschung* 71: 893–903.

Brischke, C., Thelandersson, S. (2014) Modelling the outdoor performance of wood products - A review on existing approaches. *Construction and Building Materials* 66: 384–397.

Brischke, C., Unger, W. (2017) Potential hazards and degrading agents. In: Jones, D., Brischke, C. (Eds.), Performance of bio-based building materials. Woodhead Publishing, p. 188–202.

Broekaert, V., Van Vossel, K. (2019) Invloed van het vochtgehalte op schimmelaantasting van constructiehout: ontwikkeling van een testmethode op laboschaal. Master Thesis, Ghent University, Belgium.

Brunet-Navarro, P., Jochheim, H., Muys, B. (2017) The effect of increasing lifespan and recycling rate on carbon storage in wood products from theoretical model to application for the European wood sector. *Mitigation and adaptation strategies for global change* 22: 1193–1205.

Brunk, M., Sputh, S., Doose, S., van de Linde, S., Terpitz, U. (2018) HyphaTracker: An ImageJ toolbox for time-resolved analysis of spore germination in filamentous fungi. *Scientific reports* 8: 605.

Bucur, V., Garros, S., Navarrete, A., De Troya, M., Guyonnet, R. (1997) Kinetics of wood degradation by fungi with X-ray microdensitometric technique. *Wood Science and Technology* 31: 383–389.

Büttner, G., Pfähler, B., Petersen, J. (2003) Rhizoctonia root rot in Europe-incidence, economic importance and concept for integrated control. In: Proceedings of the 66th IIRB-ASSBT Congress, San Antonio, USA. pp. 897–901.

Cai, C., Javed, M. A., Komulainen, S., Telkki, V. V., Haapala, A., Heräjärvi, H. (2020) Effect of natural weathering on water absorption and pore size distribution in thermally modified wood determined by nuclear magnetic resonance. *Cellulose*, 1-13.

Camenzind, T., Lehmann, A., Ahland, J., Rumpel, S., Rillig, M.C. (2020) Trait-based approaches reveal fungal adaptations to nutrient-limiting conditions. *Environmental microbiology* 22: 3548–3560.

Candelier, K., Thevenon, M.-F., Petrissans, A., Dumarcay, S., Gerardin, P., Petrissans, M. (2016) Control of wood thermal treatment and its effects on decay resistance: a review. *Annals of Forest Science* 73: 571–583.

Carlile, M.J., Watkinson, S.C., Gooday, G.W. (2001) The fungi. Gulf Professional Publishing.

Carmeliet, J., Roels, S. (2001) Determination of the isothermal moisture transport properties of porous building materials. *Journal of Thermal Envelope and Building Science* 24: 183–210.

CEN EN 113 standard (1996) Wood preservatives. Test method for determining the protective effectiveness against wood destroying basidiomycetes. Determination of the toxic values.

CEN EN 252 standard (2014) Field test method for determining the relative protective effectiveness of a wood preservative in ground contact.

CEN EN 335 standard (2013) Durability of wood and wood-based products – Use classes: Definitions, application to solid wood and wood-based products.

CEN EN 350 standard (2016) Durability of wood and wood-based products – Testing and classification of the durability to biological agents of wood and wood-based materials.

CEN EN 460 standard (1992) Durability of wood and wood-based products - Natural durability of solid wood - Guide to the durability requirements for wood to be used in hazard classes.

CEN EN 84 standard (1997) Wood preservatives - Accelerated ageing of treated wood prior to biological testing - Leaching procedure.

CEN ENV 12038 standard (2002) Durability of wood and wood-based products – Wood-based panels - Method for determining the resistance against wood-destroying basidiomycetes.

CEN TS 15083-1 standard (2005) Durability of wood and wood-based products – Determination of the natural durability of solid wood against wood-destroying fungi, Test methods – Part 1: Basidiomycetes.

CEN TS 16818 standard (2018) Durability of wood and wood-based products – moisture dynamics of wood and wood-based products.

Chand, T., Logan, C. (1983) Cultural and pathogenic variation in potato isolates of *Rhizoctonia solani* in Northern Ireland. *Transactions of the British Mycological Society* 81: 585–589.

Chiron, H., Drouet, A., Lieutier, F., Payer, H.-D., Ernst, D., Sandermann, H. (2000) Gene induction of stilbene biosynthesis in Scots pine in response to ozone treatment, wounding, and fungal infection. *Plant Physiology* 124: 865–872.

Churkina, G., Organschi, A., Reyer, C., Vinke, K., Ruff, A., Liu, Z., Reck, B., Graedel, T., Schellnhuber, J. (2020) Buildings as a global carbon sink. *Nature Sustainability* 3: 269-276.

Ciliberti, N., Fermaud, M., Roudet, J., Rossi, V. (2015) Environmental conditions affect *Botrytis cinerea* infection of mature grape berries more than the strain or transposon genotype. *Phytopathology* 105: 1090–1096.

Coggins, C.R. (2008) Trends in timber preservation—a global perspective. *Journal of Tropical Forest Science* 20: 264–272.

Cooke, W.B. (1968) Fungi and Their Environments. In: The American Biology Teacher. pp. 521–526.

Cragg, S.M., Beckham, G.T., Bruce, N.C., Bugg, T.D., Distel, D.L., Dupree, P., Etxabe, A.G., Goodell, B.S., Jellison, J., McGeehan, J.E. (2015) Lignocellulose degradation mechanisms across the Tree of Life. *Current Opinion in Chemical Biology* 29: 108–119.

Curling, S.F., Stefanowski, B.K., Mansour, E., Ormondroyd, G.A. (2015) Applicability of wood durability testing methods to bio-based building materials. In: 46th Annual Meeting of the International Research Group on Wood Protection, Viña del Mar, Chile.

Daniel, G. (2003) Microview of wood under degradation by bacteria and fungi. In: Goodell, B., Nicholas, D.D., Schultz, T.P. (Eds.), Wood deterioration and preservation: Advances in our changing world.. American Chemical Society, Washington, pp. 34–72.

Davidson, F., Sleeman, B., Crawford, J. (1997) Travelling waves in a reaction-diffusion system modelling fungal mycelia. *IMA Journal of Applied Mathematics* 58: 237–257.

Davis, S.J., Lewis, N.S., Shaner, M., Aggarwal, S., Arent, D., Azevedo, I.L., Benson, S.M., Bradley, T., Brouwer, J., Chiang, Y.-M., others (2018) Net-zero emissions energy systems. *Science* 360: eaas9793.

De Angelis, M., Romagnoli, M., Vek, V., Poljansek, I., Oven, P., Thaler, N., Lesar, B., Krzisnik, D., Humar, M. (2018) Chemical composition and resistance of Italian stone pine (*Pinus pinea* L.) wood against fungal decay and wetting. *Industrial Crops and Products* 117: 187–196.

De Blaere, R. (2020) Schimmelgevoeligheid van houtgebaseerde plaat- en isolatiematerialen onder verschillende vochtcondities. Master Thesis, Ghent University, Belgium.

De Ligne, L., Van den Bulcke, J., Baetens, J.M., De Baets, B., Wang, G., Imke De Windt, I., Beeckman, H., Van Acker, J. (2020) Unraveling the natural durability of wood: revealing the impact of decay-influencing characteristics other than fungicidal components. *Holzforschung*.

De Ligne, L., Van den Bulcke, J., De Muynck, A., Baetens, J.M., De Baets, B., Van Hoorebeke, L., Van Acker, J. (2019). Exploring the use of X-ray micro CT as a tool for the monitoring of moisture production and mass loss during lab-based fungal degradation testing. In: Proceedings IRG Annual Meeting 2019 (Quebec City, Canada). IRG/WP 19-20654, 10 pp.

De Muynck, A., Boone, M., Dierick, M., Cambré, I., Louagie, E., Elewaut, D., Van Hoorebeke, L. (2015) Automated processing of series of micro-CT scans. In: 2nd International conference on Tomography of Materials and Structures (ICTMS 2015), pp. 96–99.

de Oliveira, A.C.C., de Souza, P.E., Pozza, E.A., Dornelas, G.A., Monteiro, F.P. (2014) Influence of temperature on the *Rhizoctonia solani* (Kuhn) strains obtained from cotton fields on the Brazilian states. *Bioscience Journal* 30: 119–130.

De Ridder, M., Van den Bulcke, J., Vansteenkiste, D., Van Loo, D., Dierick, M., Masschaele, B., De Witte, Y., Mannes, D., Lehmann, E., Beeckman, H., others (2010) High-resolution proxies for wood density variations in *Terminalia superba*. *Annals of botany* 107: 293–302.

De Vetter, L., Stevens, M., Van Acker, J. (2009) Fungal decay resistance and durability of organosilicon-treated wood. *International Biodeterioration and Biodegradation* 63: 130–134.

De Windt, I., Li, W., Van den Bulcke, J., and Van Acker, J. (2018) Classification of uncoated plywood based on moisture dynamics. *Construction and Building Materials*, 158: 814-822.

Deacon, J.W. (2013) Fungal biology. John Wiley & Sons.

Dean, R., Van Kan, J.A., Pretorius, Z.A., Hammond-Kosack, K.E., Di Pietro, A., Spanu, P.D., Rudd, J.J., Dickman, M., Kahmann, R., Ellis, J., others (2012) The Top 10 fungal pathogens in molecular plant pathology. *Molecular plant pathology* 13: 414–430.

Dederich, L., Wiegand, T., Förster, F., Blau, M., Blum, R., Kranz, B., Stahl, W., Zajonz, R. (2019) Holzfaserdämmstoffe - Eigenschaften, Anforderungen, Anwendungen. Holz, Informationsdienst.

Dedesko, S., Siegel, J.A. (2015) Moisture parameters and fungal communities associated with gypsum drywall in buildings. *Microbiome* 3: 1.

Defoirdt, N., Gardin, S., Van den Bulcke, J., Van Acker, J. (2010) Moisture dynamics of WPC and the impact on fungal testing. *International Biodeterioration and Biodegradation* 64: 65–72.

Deklerck, V., De Ligne, L., Van den Bulcke, J., Espinoza, E., Beeckman, H., Van Acker, J. (2019) IRG/WP 19-10944 Determining the natural durability on xylarium specimens: mini-block test and chemical profiling. In: 50th Conference of the International Research Group on Wood Protection.

Dietsch, P., Gamper, A., Merk, M., Winter, S. (2015) Monitoring building climate and timber moisture gradient in large-span timber structures. *Journal of Civil Structural Health Monitoring* 5: 153–165.

Directive 98/8/EC (1998) Directive 98/8/EC of the European Parliament and of the Council of 16 February 1998 concerning the placing of biocidal products on the market. *Official Journal of the European Communities* L123: 1.

Dixit, M.K., Fernández-Solis, J.L., Lavy, S., Culp, C.H. (2010) Identification of parameters for embodied energy measurement: A literature review. *Energy and buildings* 42: 1238–1247.

Djajadi, D.T., Hansen, A.R., Jensen, A., Thygesen, L.G., Pinelo, M., Meyer, A.S., Jørgensen, H. (2017) Surface properties correlate to the digestibility of hydrothermally pretreated lignocellulosic Poaceae biomass feedstocks. *Biotechnology for biofuels* 10: 49.

Dünisch, O., Richter, H.-G., Koch, G. (2010) Wood properties of juvenile and mature heartwood in *Robinia pseudoacacia* L. *Wood Science and Technology* 44: 301–313.

Dunn, O. (1961) Multiple comparisons among means. *Journal of the American statistical association* 56: 52–64.

Ebes, K. (1937) Vorming van thyllen in geveld beukenhout. PhD Thesis, Wageningen University, The Netherlands.

EEA (2019) The European environment - state and outlook 2020. European Environment Agency, Publications Office of the European Union, Luxembourg.

Eichhorn, S., Erfurt, S., Hofmann, T., Seegmueller, S., Németh, R., Hapla, F. (2017) Determination of the phenolic extractive content in sweet chestnut (*Castanea sativa* Mill.) wood. *Wood Research* 62: 181–196.

Ekeberg, D., Flæte, P.-O., Eikenes, M., Fongen, M., Naess-Andresen, C.F. (2006) Qualitative and quantitative determination of extractives in heartwood of Scots pine (*Pinus sylvestris* L.) by gas chromatography. *Journal of Chromatography A* 1109: 267–272.

Ekesi, S., Maniania, N., Ampong-Nyarko, K. (1999) Effect of temperature on germination, radial growth and virulence of *Metarhizium anisopliae* and *Beauveria bassiana* on *Megalurothrips sjostedti*. Biocontrol *Science and Technology* 9: 177–185.

Erikson, K., Blanchette, R., Ander, P. (1990) Microbial and enzymatic degradation of wood and wood components. Springer Series in Wood Science, Springer-Verlag, Berlin.

Esser, K., Lemke, P.A. (1995) The Mycota. Springer-Verlag, Berlin.

Etheridge, D. (1957) Moisture and temperature relations of heartwood fungi in subalpine spruce. *Canadian Journal of Botany* 35: 935–944.

Feng, S., Shu, C., Wang, C., Jiang, S., Zhou, E. (2017) Survival of *Rhizoctonia solani* AG-1 IA, the causal agent of rice sheath blight, under different environmental conditions. *Journal of Phytopathology* 165: 44–52.

FIEC (2019) Construction in Europe: Key Figures. Activity 2018.

Finch, G., Hubbs, B., Dell, M. J. (2008) Rainscreen walls: Long-term performance and field monitoring in Coastal British Columbia. In: Symposium on Building Envelope Technology.

Floudas, D., Binder, M., Riley, R., Barry, K., Blanchette, R.A., Henrissat, B., Martinez, A.T., Otillar, R., Spatafora, J.W., Yadav, J.S. (2012) The Paleozoic origin of enzymatic lignin decomposition reconstructed from 31 fungal genomes. *Science* 336: 1715–1719.

Fojutowski, A, Kropacz, A, Noskowiak, A (2009): Determination of wood-based panels resistance to wood attacking fungi. *Folia Forestalia Polonica*, 49, 79–88.

Fredriksson, M. (2019) On wood-water interactions in the over-hygroscopic moisture range - mechanisms, methods, and influence of wood modification. *Forests* 10: 779.

Fredriksson, M., Thygesen, L.G. (2017) The states of water in Norway spruce (*Picea abies* (L.) Karst.) studied by low-field nuclear magnetic resonance (LFNMR) relaxometry: assignment of free-water populations based on quantitative wood anatomy. *Holzforschung* 71: 77–90.

Galle, W. (2016) Scenario based life cycle costing. An enhanced method for evaluating the financial feasibility of transformable building. PhD Thesis, Vrije Universiteit Brussel, Belgium.

Gange, A.C., Gange, E.G., Mohammad, A.B., Boddy, L. (2011) Host shifts in fungi caused by climate change? *Fungal Ecology* 4: 184–190.

Ganotopoulou, E. (2014) Biodegradable materials: A research and design handbook; enhancing the use of biodegradable materials on building's envelopes in the Netherlands. Master Thesis, TU Delft, The Netherlands.

Gao, Y., Xu, K., Peng, H., Jiang, J., Zhao, R., Lu, J. (2019) Effect of heat treatment on water absorption of Chinese fir using TD-NMR. *Applied Sciences* 9: 78.

Giama, E., Papadopoulos, A. (2012) Sustainable building management: overview of certification schemes and standards. *Advances in Building Energy Research* 6: 242–258.

Gock, M.A., Hocking, A.D., Pitt, J.I., Poulos, P.G. (2003) Influence of temperature, water activity and pH on growth of some xerophilic fungi. *International Journal of Food Microbiology* 81: 11–19.

Goodell, B., Jellison, J. (1990) Immunological characterization of fungal enzymes and biological chelators involved in lignocellulose degradation. In: Llewellyn, G.C., O'Rear, C.E. (Eds.), Biodeterioration Research. Springer, Boston., pp. 361–375.

Gougouli, M., Koutsoumanis, K.P. (2013) Relation between germination and mycelium growth of individual fungal spores. *International Journal of Food Microbiology* 161: 231–239.

Granger, C.W.J. (1969) Investigating Causal Relations by Econometric Models and Cross-Spectral Methods. *Econometrica* 37: 424–38.

Green III, F., Highley, T.L. (1997) Mechanism of brown-rot decay: paradigm or paradox. *International Biodeterioration and Biodegradation* 39: 113–124.

Grosch, R., Kofoet, A. (2003) Influence of temperature, pH and inoculum density on bottom rot on lettuce caused by *Rhizoctonia solani*. *Journal of Plant Diseases and Protection* 110: 366–378.

Guerreiro, O., Borges, P., Nunes, L. (2016) *Cryptotermes brevis* - a silent earthquake for the wood structures in a World Heritage city in the Azores Islands. Paper prepared for the 47th IRG Annual Meeting Lisbon, Portugal 15-19 May 2016, IRG/WP 16-50316.

Guo, S., Ladroue, C., Feng, J. (2010) Granger causality: theory and applications. In: Feng J., Fu W., Sun F. (Eds.), Frontiers in Computational and Systems Biology. Springer Science and Business Media, London, pp 83–108.

Guo, Y., Zhang, M., Xie, Y., Chen, H., Xiao, Z. (2018) Effect of thermal treatment on the heat of vaporization of bound water by NMR and DSC analysis. *BioResources* 13: 5534-5542.

GWR – Guinness World Record (2019) Tallest wooden building. https://www.guinnessworldrecords.com/world-records/79569-tallest-wooden-building. Accessed on October 29th 2020.

Harikrishnan, R., Yang, X. (2004) Recovery of anastomosis groups of *Rhizoctonia solani* from different latitudinal positions and influence of temperatures on their growth and survival. *Plant Disease* 88: 817–823.

Harju, A.M., Kainulainen, P., Venäläinen, M., Tiitta, M., Viitanen, H. (2002) Differences in resin acid concentration between brown-rot resistant and susceptible Scots pine heartwood. *Holzforschung* 56: 479–486.

Hart, J. (1989) The role of wood exudates and extractives in protecting wood from decay. In: Rowe, J.W. (Ed.), Natural Products of Woody Plants. Springer-Verlag, Berlin, pp. 861–880.

Herczeg, M., McKinnon, D., Milios, L., Bakas, I., Klaassens, E., Svatikova, K., Widerberg, O. (2014) Resource efficiency in the building sector. Final report. Prepared for European Commission by ECORYS and Copenhagen Resource Institute, Rotterdam, The Netherlands.

Hetemäki, L., Hanewinkel, M., Muys, B., Ollikainen, M., Palahi, M., Trasobares, A., Aho, E., Ruiz, C.N., Persson, G., Potocnik, J. (2017) Leading the way to a European circular bioeconomy strategy. From Science to Policy 5. European Forest Institute.

Highley, T.L. (1982) Influence of type and amount of lignin on decay by *Coriolus versicolor*. *Canadian Journal of Forest Research* 12: 435–438.

Hill, C.A. (2007) Wood modification: chemical, thermal and other processes. John Wiley and Sons, Vol. 5.

Hill, C., Altgen, M., Rautkari, L. (2021) Thermal modification of wood - a review: chemical changes and hygroscopicity. *Journal of Materials Science*, 1-34.

Hillis, W.E. (2012) Heartwood and tree exudates. Springer-Verlag, Berlin, Vol. 4.

Hough, P.V. (1962) Method and means for recognizing complex patterns. U.S. Patent No. 3,069,654.

Houtinfobois (2021) https://houtinfobois.be/nl/houtsoort-toepassingen/houtsoort. Accessed on February 12th, 2021.

Huang, Y., Toscano-Underwood, C., Fitt, B.D., Todd, A., West, J.S., Koopmann, B., Balesdent, M.-H. (2001) Effects of temperature on germination and hyphal growth from ascospores of A-group and B-group *Leptosphaeria maculans* (phoma stem canker of oilseed rape). *Annals of Applied Biology* 139: 193–207.

Hughes, M. (2015) Plywood and other veneer-based products. In: Wood Composites. Elsevier, pp. 69–89.

Hurmekoski, E., Jonsson, R., Nord, T. (2015) Context, drivers, and future potential for wood-frame multi-story construction in Europe. *Technological Forecasting and Social Change* 99: 181–196.

Hussein, E., Aly, A., EL-Hawary, O., Mosa, A., Mostafa, M., Asran, A. (2017) Effect of previous crop on susceptibility of flax to *Rhizoctonia solani*. *Journal of Agricultural Chemistry and Biotechnology* 8: 163–165.

Hutchinson, S., Sharma, P., Clarke, K., Macdonald, I. (1980) Control of hyphal orientation in colonies of *Mucor hiemalis*. *Transactions of the British Mycological Society* 75: 177–191.

Ibrahim, M., Rabah, A., Liman, B., Ibrahim, N. (2011) Effect of temperature and relative humidity on the growth of *Helminthosporium fulvum*. *Nigerian Journal of Basic and Applied Sciences* 19: 127-129.

Instratov, A.A., Vyvenko, O.F. (1999) Exponential analysis in physical phenomena. *Review of Scientific Instruments* 70: 1233-1257.

Jankowska, A., Boruszewski, P., Drozdzek, M., Rebkowski, B., Kaczmarczyk, A., Skowronska, A. (2018) The role of extractives and wood anatomy in the wettability and free surface energy of hardwoods. *BioResources* 13: 3082–3097.

Janssens, A., Hens, H. (2003) Interstitial condensation due to air leakage: a sensitivity analysis. *Journal of Thermal Envelope and Building Science*, 27.

Jones, D., Brischke, C. (2017) Performance of bio-based building materials. Woodhead Publishing.

Jones, D., Sandberg, D., Kutnar, A. (2018) A review of wood modification across Europe as part of COST FP1407. In: The 9th European Conference on Wood Modification, Netherlands, Arnhem, pp. 24–31.

Kamel, A.A.-E., Mohamed, A.M., Ali, H.B. (2009) First morpho-molecular identification of *Rhizoctonia solani* AG-7 from potato tuber-borne sclerotium in Saudi Arabia. *African Journal of Microbiology Research* 3: 952–956.

Kauserud, H., Heegaard, E., Semenov, M.A., Boddy, L., Halvorsen, R., Stige, L.C., Sparks, T.H., Gange, A.C., Stenseth, N.C. (2010) Climate change and spring-fruiting fungi. *Proceedings of the Royal Society of London B: Biological Sciences* 277: 1169–1177.

Kebbi-Benkeder, Z., Colin, F., Dumarçay, S., Gérardin, P. (2015) Quantification and characterization of knotwood extractives of 12 European softwood and hardwood species. *Annals of Forest Science* 72: 277–284.

Khanifah, L., Widodo, S., Putra, N.M.D., Satrio, A., others (2018) Characteristics of paraffin shielding of Kartini reactor, Yogyakarta. *ASEAN Journal on Science and Technology for Development* 35: 195–198.

KMI (2021) https://www.meteo.be/nl/klimaat/recente-waarnemingen-in-belgie-en-te-ukkel/klimatologisch-overzicht/2021/januari. Accessed on February 2nd 2021.

Kruskal, W., Wallis, W. (1952) Use of ranks in one-criterion variance analysis. *Journal of the American statistical Association* 47: 583–621.

Kržišnik, D., Lesar, B., Thaler, N., Planinšič, J., Humar, M. (2020) A study on the moisture performance of wood determined in laboratory and field trials. *European Journal of Wood and Wood Products*, 78: 219-235.

Kubo, A.M., Gorup, L.F., Amaral, L.S., Rodrigues-Filho, E., de Camargo, E.R. (2018) Heterogeneous microtubules of self-assembled silver and gold nanoparticles using alive biotemplates. *Materials Research* 21: e20170947.

Kutnik, M., Gabillé, M., Montibus, M. (2020) Performance of European wood species in above ground situations after 10 years of weathering: evidence of a positive impact of proper design. In: International Conference on Durability of Building Materials and Components (DBMC 2020), Barcelona.

Kutnik, M., Suttie, E., Brischke, C. (2014) European standards on durability and performance of wood and wood-based products - Trends and challenges. *Wood Material Science and Engineering* 9: 122–133.

Langmans, J., Klein, R., Roels, S. (2012) Hygrothermal risks of using exterior air barrier systems for highly insulated light weight walls: A laboratory investigation. *Building and Environment* 56: 192–202.

Lew, R.R. (2011) How does a hypha grow? The biophysics of pressurized growth in fungi. *Nature Reviews Microbiology* 9: 509–518.

Li, C., Zhao, X., Wang, A., Huber, G.W., Zhang, T. (2015) Catalytic transformation of lignin for the production of chemicals and fuels. *Chemical Reviews* 115: 11559–11624.

Li, Y., Fazio, P., Rao, J. (2012) An investigation of moisture buffering performance of wood paneling at room level and its buffering effect on a test room. *Building and Environment* 47: 205–216.

Li, Y., Uddin, W., Kaminski, J. (2014) Effects of relative humidity on infection, colonization and conidiation of *Magnaporthe orzyae* on perennial ryegrass. *Plant Pathology* 63: 590–597.

Lindgren, O. (1992) Medical CT-scanners for non-destructive wood density and moisture content measurements. PhD Thesis, Luleå University of Technology, Wood Technology, Skellefteå, Sweden.

Lodge, D. (1987) Nutrient concentrations, percentage moisture and density of field-collected fungal mycelia. *Soil Biology and Biochemistry* 19: 727–733.

Lopez-Molina, C., De Ulzurrun, G.V.-D., Baetens, J.M., Van den Bulcke, J., De Baets, B. (2015) Unsupervised ridge detection using second order anisotropic Gaussian kernels. *Signal Processing* 116: 55–67.

Lozhechnikova, A., Vahtikari, K., Hughes, M., Österberg, M. (2015) Toward energy efficiency through an optimized use of wood: The development of natural hydrophobic coatings that retain moisture-buffering ability. *Energy and Buildings* 105: 37–42.

Lupoi, J.S., Gjersing, E., Davis, M.F. (2015) Evaluating lignocellulosic biomass, its derivatives, and downstream products with Raman spectroscopy. *Frontiers in Bioengineering and Biotechnology* 3: 50.

Macchioni, N., Palanti, S., Rozenberg, P. (2007) Measurements of fungal wood decay on Scots pine and beech by means of X-ray microdensitometry. *Wood Science and Technology* 41: 417–426.

MacNish, G.C., Neate, S.M. (1996) Rhizoctonia bare patch of cereals: An Australian perspective. *Plant Disease* 80: 965–971.

Magan, N., Lacey, J. (1984) Effect of temperature and pH on water relations of field and storage fungi. *Transactions of the British Mycological Society* 82: 71–81.

Mann, H.B., Whitney, D.R. (1947) On a test of whether one of two random variables is stochastically larger than the other. *The Annals of Mathematical Statistics* 18: 50–60.

Mather, R. (2009) The structure of polyolefin fibres. In: Handbook of textile fibre structure. Elsevier, pp. 276–304.

Mazela, B., Popescu, C.-M. (2017) Solid wood. In: Performance of bio-based building materials. Woodhead Publishing, pp. 22-39.

McPartland, J.M., Cubeta, M.A. (1997) New species, combinations, host associations and location records of fungi associated with hemp (*Cannabis sativa*). *Mycological Research* 101: 853–857.

Melchert, L. (2007) The Dutch sustainable building policy: A model for developing countries? *Building and Environment* 42: 893–901.

Meletiadis, J., Meis, J.F., Mouton, J.W., Verweij, P.E. (2001) Analysis of growth characteristics of filamentous fungi in different nutrient media. *Journal of Clinical Microbiology* 39: 478–84.

Mester, T., Varela, E., Tien, M. (2004) Wood degradation by brown-rot and white-rot fungi. In: Kück, U. (Eds.), Genetics and Biotechnology. Springer-Verlag, Berlin, pp. 355–368.

Meyer, L., Brischke, C. (2015) Fungal decay at different moisture levels of selected European-grown wood species. *International Biodeterioration and Biodegradation* 103: 23–29.

Meyer, L., Brischke, C., Treu, A., Larsson-Brelid, P. (2016) Critical moisture conditions for fungal decay of modified wood by basidiomycetes as detected by pile tests. *Holzforschung* 70: 331–339.

Meyer-Veltrup, L., Brischke, C., Alfredsen, G., Humar, M., Flæte, P.-O., Isaksson, T., Brelid, P.L., Westin, M., Jermer, J. (2017) The combined effect of wetting ability and durability on outdoor performance of wood: development and verification of a new prediction approach. *Wood Science and Technology* 51: 615–637.

Michon, L., Siri, O., Hanquet, B., Martin, D. (1996) Qualitative and quantitative functional determination in bitumen acidic fractions by ^{29}Si NMR Spectroscopy. Correlation with Bitumen aging. *Energy and Fuels* 10: 1142–1146.

Miller, E. (2005) Wood substrate - The foundation. *Surface Coatings International Part B: Coatings Transactions* 88: 157–161.

Mislivec, P.B., Tuite, J. (1970) Temperature and relative humidity requirements of species of Penicillium isolated from yellow dent corn kernels. *Mycologia* 61: 75–88.

Montini, R.M. de C., Passos, J.R. de S., Eira, A.F. da (2006) Digital monitoring of mycelium growth kinetics and vigor of shiitake (*Lentinula edodes* (Berk.) Pegler) on agar medium. *Brazilian Journal of Microbiology* 37: 90–95.

Morris, P. (1998) Understanding biodeterioration of wood in structures. Internal report, Forintek Canada Corp., Vancouver, B.C., pp. 16.

Mounguengui, S., Tchinda, J.-B.S., Ndikontar, M.K., Dumarçay, S., Attéké, C., Perrin, D., Gelhaye, E., Gérardin, P. (2016) Total phenolic and lignin contents, phytochemical screening, antioxidant and fungal inhibition properties of the heartwood extractives of ten Congo Basin tree species. *Annals of Forest Science* 73: 287–296.

Murmanis, L. (1975) Formation of tyloses in felled *Quercus rubra* L. *Wood Science and Technology*, 9: 3-14.

Nielsen, K.F., Holm, G., Uttrup, L., Nielsen, P. (2004) Mould growth on building materials under low water activities. Influence of humidity and temperature on fungal growth and secondary metabolism. *International Biodeterioration and Biodegradation* 54: 325–336.

Nishimura, T. (2015) Chipboard, oriented strand board (OSB) and structural composite lumber. In: Wood Composites. Elsevier, pp. 103–121.

Novaes, E., Kirst, M., Chiang, V., Winter-Sederoff, H., Sederoff, R. (2010) Lignin and biomass: a negative correlation for wood formation and lignin content in trees. *Plant Physiology* 154: 555–561.

O'Neill, D.W., Fanning, A.L., Lamb, W.F., Steinberger, J.K. (2018) A good life for all within planetary boundaries. *Nature Sustainability* 1: 88–95.

Okino, E., Alves, M. da S., Teixeira, D.E., de Souza, M.R., Santana, M. (2007) Biodegradation of oriented strandboards of pine, eucalyptus and cypress exposed to four decay fungi. *Scientia Forestalis (Brazil)* 74: 67-74.

Omega (2021) https://www.omega.co.uk/temperature/z/pdf/z103.pdf. Accessed on February 12th, 2021.

Ong, C. (2015) Glue-laminated timber (Glulam). In: Wood Composites. Elsevier, pp. 123–140.

Ormondroyd, G., Spear, M., Curling, S. (2015) Modified wood: review of efficacy and service life testing. *Proceedings of the Institution of Civil Engineers - Construction Materials* 168: 187–203.

Ortiz, O., Castells, F., Sonnemann, G. (2009) Sustainability in the construction industry: A review of recent developments based on LCA. *Construction and Building Materials* 23: 28–39.

Osanyintola, O.F., Simonson, C.J. (2006) Moisture buffering capacity of hygroscopic building materials: Experimental facilities and energy impact. *Energy and Buildings* 38: 1270–1282.

Osono, T. (2015) Effects of litter type, origin of isolate, and temperature on decomposition of leaf litter by macrofungi. *Journal of Forest Research* 20:77–84

Owens, T. (2015) Warm, wet wood means fungi to follow: is your home a mushroom magnet? https://www.fpl.fs.fed.us/labnotes/?cat=14. Accessed on October 29th 2020.

Pardo, E., Marín, S., Sanchis, V., Ramos, A.J. (2005) Impact of relative humidity and temperature on visible fungal growth and OTA production of ochratoxigenic *Aspergillus ochraceus* isolates on grapes. *Food Microbiology* 22: 383–389.

Pasanen, A.-L., Kalliokoski, P., Pasanen, P., Jantunen, M., Nevalainen, A. (1991) Laboratory studies on the relationship between fungal growth and atmospheric temperature and humidity. *Environment International* 17: 225–228.

Peñaloza, D. (2017) The role of biobased building materials in the climate impacts of construction: Effects of increased use of biobased materials in the Swedish building sector.

Pettersen, R.C. (1984) The chemical composition of wood. In: Rowell, R.M. (Ed.), The Chemistry of Solid Wood, Advances in Chemistry, Vol. 207. ACS Publications, pp. 57–126.

Plötze, M., Niemz, P. (2011) Porosity and pore size distribution of different wood types as determined by mercury intrusion porosimetry. *European Journal of Wood and Wood Products* 69: 649–657.

Ramakrishna, N., Lacey, J., Smith, J. (1993) Effects of water activity and temperature on the growth of fungi interacting on barley grain. *Mycological Research* 97: 1393–1402.

Ravcko, V., Cunderlik, I. (2010) Which of the factors do significantly affect beech false heartwood formation? In: Hardwood Science and Technology, The 4th Conference on Hardwood Research and Utilisation in Europe, pp. 94–95.

Rawat, S., Khali, D., Hale, M., Breese, M. (1998) Studies on the moisture adsorption behaviour of brown rot decayed and undecayed wood blocks of *Pinus sylvestris* using the Brunauer-Emmett-Teller theory. *Holzforschung* 52: 463–466.

Rijckaert, V., Van Acker, J., Stevens, M. (1998) Decay resistance of high performance biocomposites based on chemically modified fibres, The International Research Group on Wood Preservation, Document no.: IRG/WP 98–40120, pp. 12.

Riley, R., Salamov, A. A., Brown, D. W., Nagy, L. G., Floudas, D., Held, B. W., Levasseur, A., Lombard, V., Morin, E., Otillar, R., Lindquist, E.A., Sun, H., LaButti, K.M., Schmutz, J., Jabbour, D., Luo, H., Baker, S.E., Pisabarro, A.G., Walton, J.D., Blanchette, R.A., Henrissat, B., Martin, F., Cullen, D., Hibbett, D. S., Grigoriev, I.V. (2014) Extensive sampling of basidiomycete genomes demonstrates inadequacy of the white-rot/brown-rot paradigm for wood decay fungi. *Proceedings of the National Academy of Sciences*, 111: 9923-9928.

Ringman, R., Pilgård, A., Brischke, C., Richter, K. (2014) Mode of action of brown rot decay resistance in modified wood: a review. *Holzforschung* 68: 239–246.

Riquelme, M., Reynaga-Peña, C.G., Gierz, G., Bartnicki-Garcia, S. (1998) What determines growth direction in fungal hyphae? *Fungal Genetics and Biology* 24: 101–109.

Rissanen, K., Hölttä, T., Barreira, L.M., Hyttinen, N., Kurtén, T., Bäck, J. (2019) Temporal and spatial variation in Scots pine resin pressure and composition. *Frontiers in Forests and Global Change* 2: 23.

Ritchie, F., Bain, R., McQuilken, M. (2009) Effects of nutrient status, temperature and pH on mycelial growth, sclerotial production and germination of *Rhizoctonia solani* from potato. *Journal of Plant Pathology* 91: 589–596.

Rockström, J., Steffen, W., Noone, K., Persson, Å., Chapin, F.S., Lambin, E.F., Lenton, T.M., Scheffer, M., Folke, C., Schellnhuber, H.J., Nykvist, B., de Wit, C.A., Hughes, T., van der Leeuw, S., Rodhe, H., Sörlin, S., Snyder, P.K., Costanza, R., Svedin, U., Falkenmark, M., Karlberg, L., Corell, R.W., Fabry, V.J., Hansen, J., Walker, B., Liverman, D., Richardson, K., Crutzen, P., Foley, J.A. (2009) A safe operating space for humanity. *Nature* 461: 472–475.

Rode, C. (Ed.), Peuhkuri, R., Lone, H., Time, B., Gustavsen, A., Ojanen, T., Ahonen, J., Svennberg, K., Harderup, L-E., Arfvidsson, J. (2006). Moisture Buffering of Building Materials. Danmarks Tekniske Universitet. DTU BYG-rapporter, No. R-126.

Rode, C. (Ed.), Peuhkuri, R., Lone, H., Time, B., Gustavsen, A., Ojanen, T., Ahonen, J., Svennberg, K., Harderup, L-E., and Arfvidsson, J. (2006) Moisture Buffering of Building Materials. Danmarks Tekniske Universitet. DTU BYG-rapporter, No. R-126.

Ross, R.J. (2010) Wood handbook: Wood as an engineering material. General Technical Report FPL-GTR-190. USDA Forest Service, Forest Products Laboratory, Madison, WI, U.S.

Rowell, R.M. (2012) Handbook of wood chemistry and wood composites. CRC press.

RStudio Team (2019). RStudio: Integrated Development for R. RStudio, Inc., Boston, MA URL http://www.rstudio.com/.

RVO - Rijksdienst voor Ondernemend Nederland (2020) MilieuPrestatie Gebouwen – MPG. https://www.rvo.nl/onderwerpen/duurzaam-ondernemen/gebouwen/wetten-en-regels/nieuwbouw/milieuprestatie-gebouwen. Accessed on October 27th 2020.

Saito, H., Fukuda, K., Sawachi, T. (2012) Integration model of hygrothermal analysis with decay process for durability assessment of building envelopes. In: Building Simulation, Vol. 5, pp. 315–324.

Samuels, G.J., Dodd, S.L., Lu, B.-S., Petrini, O., Schroers, H.-J., Druzhinina, I.S. (2006) The *Trichoderma koningii* aggregate species. *Studies Mycology* 56: 67–133.

Sandak, A. Sandak, J. (2017) Aesthetics. In: Performance of bio-based building materials. Woodhead Publishing, pp. 285-293.

Sandak, A., Sandak, J., Brzezicki, M., Kutnar, A. (2019) Service Life Performance. In: Bio-based Building Skin. Springer, pp. 127–153.

Sandberg, D., Kutnar, A., Mantanis, G. (2017) Wood modification technologies - a review. *iForest-Biogeosciences and Forestry* 10: 895-908.

Santamouris, M. (2016) Innovating to zero the building sector in Europe: Minimising the energy consumption, eradication of the energy poverty and mitigating the local climate change. *Solar Energy* 128: 61–94.

Sass-Klaassen, U., Sterck, F., den Ouden, J. (2010) Anatomie en morfologie. In: den Ouden, J., Muys, B., Mohren, G.M.J., Verheyen, K. (Eds.), Bosecologie en Bosbeheer. ACCO, Leuven, Belgium, pp. 37–61.

Sathre, R., O'Connor, J. (2010) Meta-analysis of greenhouse gas displacement factors of wood product substitution. *Environmental Science and Policy*, 13: 104-114.

Scalbert, A. (1991) Antimicrobial properties of tannins. *Phytochemistry* 30: 3875–3883.

Scalbert, A. (1992) Tannins in woods and their contribution to microbial decay prevention. In: Laks, P.E., Hemingway, R.W. (Eds.), Plant Polyphenols. Springer, Boston, pp. 935–952.

Schiavoni, S., Bianchi, F., Asdrubali, F., others (2016) Insulation materials for the building sector: A review and comparative analysis. *Renewable and Sustainable Energy Reviews* 62: 988–1011.

Schindelin, J., Arganda-Carreras, I., Frise, E., Kaynig, V., Longair, M., Pietzsch, T., Preibisch, S., Rueden, C., Saalfeld, S., Schmid, B. (2012) Fiji: an open-source platform for biological-image analysis. *Nature Methods* 9: 676-682.

Schmidt, O. (2006) Wood and Tree Fungi: Biology, Damage, Protection, and Use. Springer-Verlag, Berlin.

Schmidt, O. (2007) Indoor wood-decay basidiomycetes: damage, causal fungi, physiology, identification and characterization, prevention and control. Mycological Progress 6: 261–279.

Schmidt, O., Grimm, K., Moreth, U. (2002) Molecular Identity of Species and Isolates of the *Coniphora* Cellar Fungi. *Holzforschung* 56: 563–571.

Schwarze, F.W. (2007) Wood decay under the microscope. *Fungal Biology Reviews* 21: 133–170.

Sèbe, G., Brook, M.A. (2001) Hydrophobization of wood surfaces: covalent grafting of silicone polymers. *Wood Science and Technology* 35: 269–282.

Seehann, G., Riebesell, M. (1988) Zur Variation physiologischer und struktureller Merkmale von Hausfäulepilzen. *Material und Organismen* 23: 241–257.

Shenoy, B.D., Jeewon, R., Hyde, K.D. (2007) Impact of DNA sequence-data on the taxonomy of anamorphic fungi. *Fungal Diversity*.

Silva, S., Sabino, M., Fernandes, E., Correlo, V., Boesel, L., Reis, R. (2005) Cork: properties, capabilities and applications. *International Materials Reviews* 50: 345–365.

Siripatrawan, U., Makino, Y. (2015) Monitoring fungal growth on brown rice grains using rapid and non-destructive hyperspectral imaging. *International Journal of Food Microbiology* 199: 93–100.

Skaar, C. (1988) Hygroexpansion in wood. In: Skaar, C. (Ed.), Wood-water relations. Springer-Verlag, Berlin, pp. 122-176.

Slávik, R., Cekon, M. (2014) Hygrothermal loads of building components in bathroom of dwellings. in: advanced materials research, Vol. 1041, p. 269–272.

Song, K., Yin, Y., Salmén, L., Xiao, F., Jiang, X. (2014) Changes in the properties of wood cell walls during the transformation from sapwood to heartwood. *Journal of Materials Science* 49: 1734–1742.

Speirs, J., McGlade, C., Slade, R. (2015) Uncertainty in the availability of natural resources: Fossil fuels, critical metals and biomass. *Energy Policy* 87: 654–664.

Stienen, T., Schmidt, O., Huckfeldt, T. (2014) Wood decay by indoor basidiomycetes at different moisture and temperature. *Holzforschung* 68: 9–15.

Tchinda, J.-B.S., Ndikontar, M.K., Belinga, A.D.F., Mounguengui, S., Njankouo, J.M., Durmaçay, S., Gerardin, P. (2018) Inhibition of fungi with wood extractives and natural durability of five Cameroonian wood species. *Industrial Crops and Products* 123: 183–191.

Thybring, E.E. (2017) Water relations in untreated and modified wood under brown-rot and white-rot decay. *International Biodeterioration and Biodegradation* 118: 134–142.

Thybring, E.E., Piqueras, S., Tarmian, A., Burgert, I. (2020) Water accessibility to hydroxyls confined in solid wood cell walls. *Cellulose*.

Tommerup, I. (1983) Temperature relations of spore germination and hyphal growth of vesicular-arbuscular mycorrhizal fungi in soil. *Transactions of the British Mycological Society* 81: 381–387.

TOTEM (2020) Tool to optimise the total environmental impact of materials. https://www.totem-building.be. Accessed on October 27th 2020.

Townsend, T.G., Solo-Gabriele, H. (2006) Environmental impacts of treated wood. CRC press.

TRADA (2015) Cross-laminated timber: introduction for specifiers. https://www.trada.co.uk. Accessed on October 29th 2020.

Trinci, A.P. (1969) A kinetic study of the growth of *Aspergillus nidulans* and other fungi. *Journal of General Microbiology* 57: 11–24.

Trinci, A.P. (1974) A study of the kinetics of hyphal extension and branch initiation of fungal mycelia. *Microbiology* 81: 225–236.

Tsror, L. (2010) Biology, epidemiology and management of *Rhizoctonia solani* on potato. *Journal of Phytopathology* 158: 649–658.

Uber, F. M., Goddard, D. R. (1934) Influence of death criteria on the X-ray survival curves of the fungus, *Neurospora*. *Journal of General Physiology*, 17: 577-590.

Uzunovic, A., Byrne, T., Yang, D.-Q., Gignac, M. (2008) Wood discolourations and their prevention: with an emphasis on bluestain. FPInnovations, Canada.

Valik, L., Baranyi, J., Görner, F. (1999) Predicting fungal growth: the effect of water activity on *Penicillium roqueforti*. *International Journal of Food Microbiology* 47: 141–146.

Van Acker, J. Palanti, S. (2017) Durability. In: Performance of bio-based building materials. Woodhead Publishing, pp. 257-276.

Van Acker, J., De Windt, I., Li, W., Van den Bulcke, J. (2014) IRG/WP 14-20555 Critical parameters on moisture dynamics in relation to time of wetness as factor in service life prediction. In: 45th Annual Meeting of the International Research Group on Wood Protection.

Van Acker, J., Jiang, X., Van den Bulcke, J. (2020) Innovative approaches to increase service life of poplar lightweight hardwood construction products. In: International Conference on Durability of Building Materials and Components (DBMC 2020), Barcelona.

Van Beneden, S., Pannecoucque, J., Debode, J., De Backer, G., Höfte, M. (2009) Characterisation of fungal pathogens causing basal rot of lettuce in Belgian greenhouses. *European Journal of Plant Pathology* 124: 9–19.

Van Den Bossche, N., Janssens, A. (2016) Airtightness and watertightness of window frames: Comparison of performance and requirements. *Building and Environment* 110: 129–139.

Van den Bulcke, J., De Windt, I., Defoirdt, N., De Smet, J., Van Acker, J. (2011): Moisture dynamics and fungal susceptibility of plywood. *International Biodeterioration and Biodegradation*, 65: 708-716.

Van den Bulcke, J., Boone, M., Van Acker, J., Van Hoorebeke, L. (2009) Three-dimensional X-ray imaging and analysis of fungi on and in wood. *Microscopy and Microanalysis* 15: 395–402.

van Laarhoven, K.A., Huinink, H.P., Segers, F.J., Dijksterhuis, J., Adan, O.C. (2015) Separate effects of moisture content and water activity on the hyphal extension of *Penicillium rubens* on porous media. *Environmental Microbiology* 17: 5089–5099.

Van Linden, S., Van Den Bossche, N. (2019) On the feasibility of watertight face-sealed window-wall interfaces. In: 4th Central European Symposium on Building Physics (CESBP 2019).

Vanpachtenbeke, M. (2019) Timber frame walls with brick veneer cladding: reliability to fungal decay. PhD Thesis, KU Leuven, Belgium.

Verma, P., Junga, U., Militz, H., Mai, C. (2009). Protection mechanisms of DMDHEU treated wood against white and brown rot fungi. *Holzforschung*, 63: 371-378.

Vicente, G., Bautista, L.F., Rodríguez, R., Gutiérrez, F.J., Sádaba, I., Ruiz-Vázquez, R.M., Torres-Martínez, S., Garre, V. (2009) Biodiesel production from biomass of an oleaginous fungus. *Biochemical Engineering Journal* 48: 22–27.

Vidal-Diez de Ulzurrun, G., Baetens, J., Van den Bulcke, J., Lopez-Molina, C., De Windt, I., De Baets, B. (2015) Automated image-based analysis of spatio-temporal fungal dynamics. *Fungal Genetics and Biology* 84: 12–25.

Viitanen, H., Paajanen, L. (1988) The critical moisture and temperature conditions for the growth of some mould fungi and the brown rot fungus *Coniophora puteana* on wood. International Research Group on Wood Protection, Madrid, Spain.

Vinck, A., Terlou, M., Pestman, W.R., Martens, E.P., Ram, A.F., van den Hondel, C.A., Wösten, H.A. (2005) Hyphal differentiation in the exploring mycelium of *Aspergillus niger*. *Molecular Microbiology* 58: 693–699.

Vlassenbroeck J., Dierick M., Masschaele B., Cnudde V., Van Hoorebeke L., Jacobs P. (2007) Software tools for quantification of X-ray microtomography at the UGCT. *Nuclear Instruments and Methods in Physics Research Section A* 580: 442–445.

Wagenführ, R.S.C. (1974) Holzatlas. Fachbuchverlag, Leipzig, München.

Wälchli, O. (1977) Der Temperatureinfluß auf die Holzzerstörung durch Pilze. *European Journal of Wood and Wood Products* 35: 45–51.

Wang, S., Mahlberg, R., Jämsä, S., Nikkola, J., Mannila, J., Ritschkoff, A.-C., Peltonen, J. (2011) Surface properties and moisture behaviour of pine and heat-treated spruce modified with alkoxysilanes by sol-gel process. *Progress in Organic Coatings* 71: 274–282.

Wang, W., Chen, J., Cao, J. (2019) Using low-field NMR and MRI to characterize water status and distribution in modified wood during water absorption. *Holzforschung* 73: 997–1004.

Watanabe, K., Lazarescu, C., Shida, S., Avramidis, S. (2012) A novel method of measuring moisture content distribution in timber during drying using CT scanning and image processing techniques. *Drying Technology* 30: 256–262.

Welch, B. L. (1938) The significance of the difference between two means when the population variances are unequal. *Biometrika* 29: 350-362.

Wong, M. (2001) Elastic and plastic methods for numerical modelling of steel structures subject to fire. *Journal of Constructional Steel Research* 57: 1–14.

Zabel, R.A., Morrell, J.J. (2012) Wood microbiology: decay and its prevention. Academic press, California.

Zimmer, K. P., Høibø, O. A., Vestøl, G. I., Larnøy, E. (2014) Variation in treatability of Scots pine sapwood: a survey of 25 different northern European locations. *Wood Science and Technology*, 48: 1049-1068.

8 Supplementary information

8.1 Chapter 2

Table 8-1 Workflow for image analysis of fungal growth dynamics developed by Vidal-Diez de Ulzurrun *et al.* (2015)

4-step process to extract fungal growth measures from the initial images

Step 1: Removing noise in the initial images (Figure 8-1a), such as droplets of agar and the initial inoculum (Figure 8-1b).

Step 2: Extracting the fungal network.
A line detection algorithm (Lopez-Molina *et al.*, 2015) is used to extract a thin binary ridge map from each image, which represents the fungal network (Figure 8-1c).

Step 3: Converting the ridge map into a graph. The MorphologicalGraph function of Mathematica (Version 10.0, Wolfram Research Inc., USA) converts images into mathematical graphs (Figure 8-1d): nodes represent junctions (intersections) of hyphae and tips (apices) of the mycelium and the edges represent the hyphal segments connecting them.

Step 4: Extracting fungal measures. Using the information contained in the graphs, we can compute some of the most important fungal growth characteristics: the total number of tips, the area of the mycelium, etc.

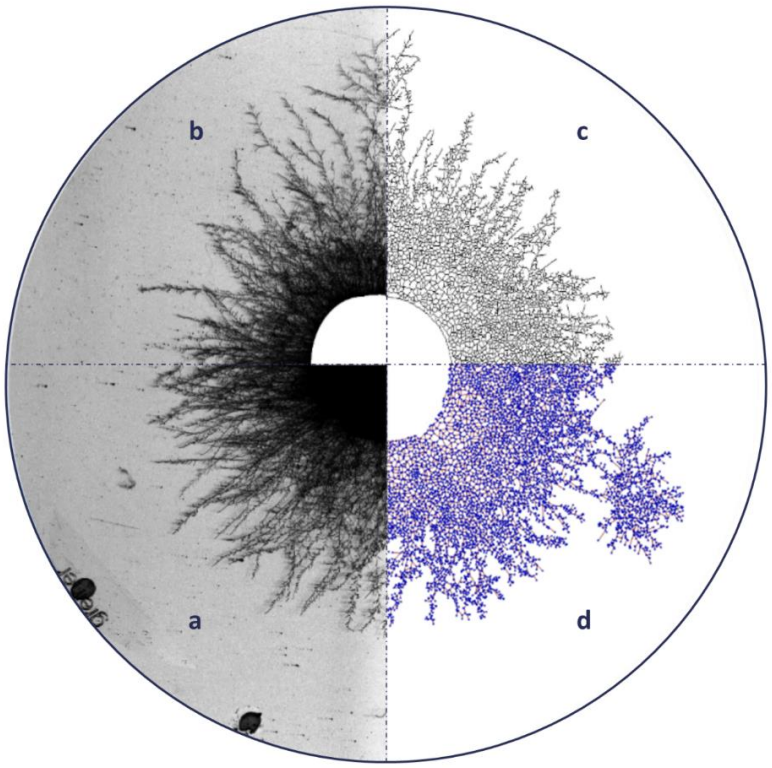

Figure 8-1 Visual representation of the entire process of fungal growth measure extraction from an image of *R. solani*. a) Initial image, b) pre-processed image, c) binary ridge map, d) mathematical graph.

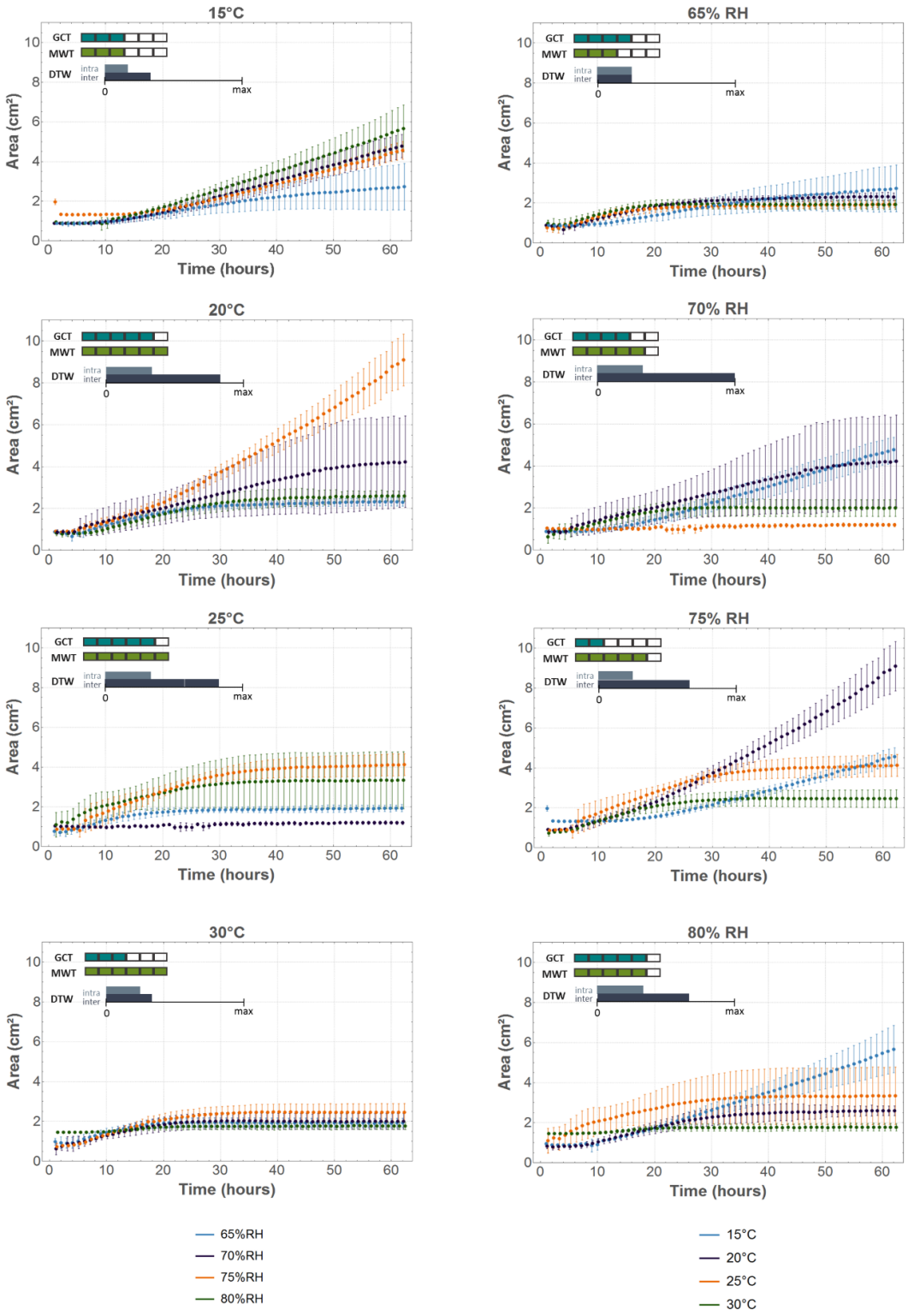

Figure 8-2 Evolution of mycelial area (cm^2) over time for *C. puteana*. On the left, the graphs are grouped by temperature, with one curve per RH at that particular temperature. On the right, the graphs are grouped by RH, with every curve representing one temperature at a given RH. The dots represent the mean values over four replicates, with the bars indicating the standard deviation. For each graph, six pairwise GCT and MWT were performed on the means of each of the four conditions represented in that graph. The two colour scales indicate for how many of those pairwise comparisons a difference was found according to GCT (blue) and MWT (green). The third scale represents the difference between the average DTW distance between the four conditions represented in the graph (inter) and a reference ground value, being the average DTW distance among the replicates of each curve in that graph (intra).

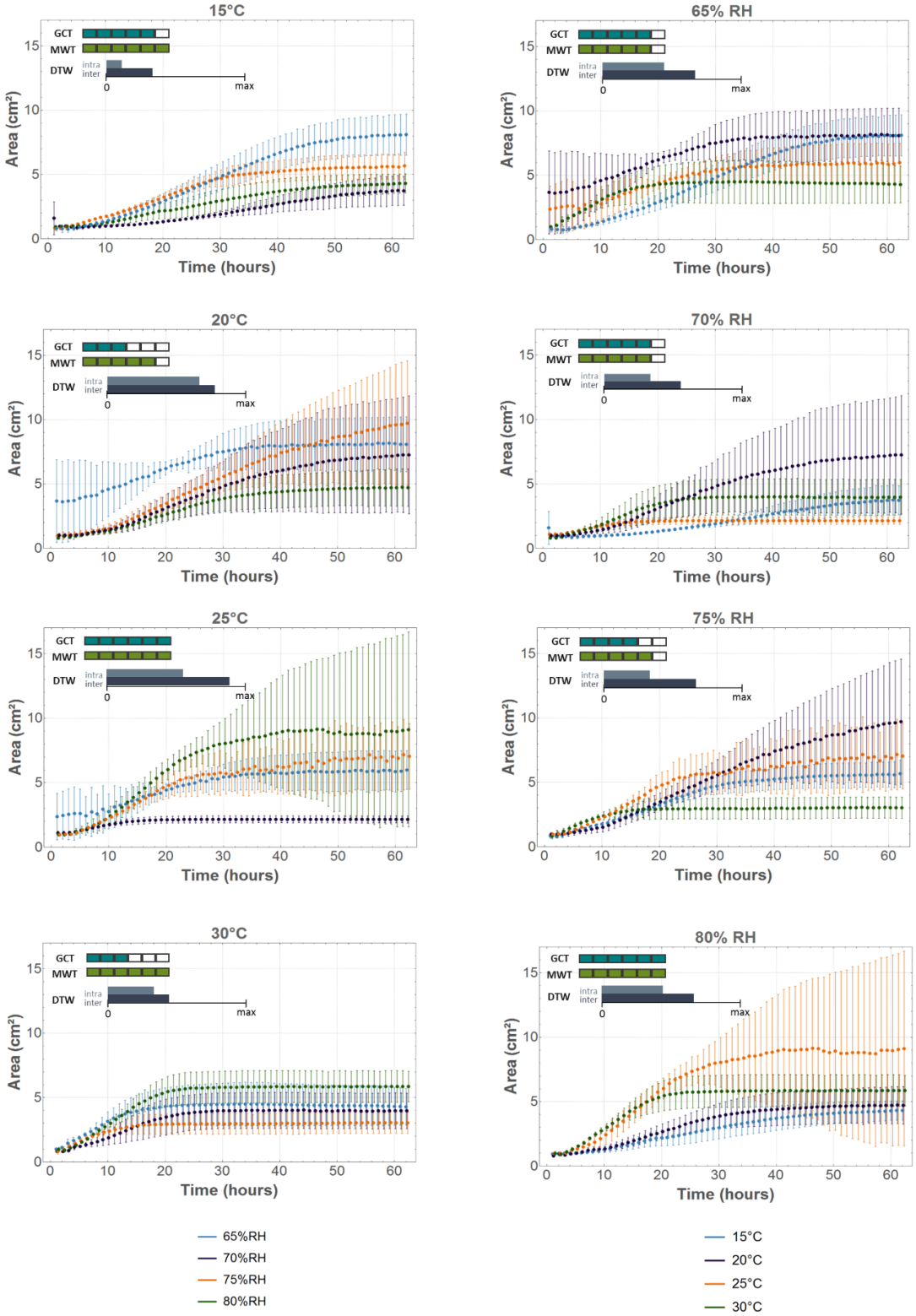

Figure 8-3 Evolution of mycelial area (cm^2) over time for *R. solani*. On the left, the graphs are grouped by temperature, with one curve per RH at that particular temperature. On the right, the graphs are grouped by RH, with every curve representing one temperature at a given RH. The dots represent the mean values over four replicates, with the bars indicating the standard deviation. For each graph, six pairwise GCT and MWT were performed on the means of each of the four conditions represented in that graph. The two colour scales indicate for how many of those pairwise comparisons a difference was found according to GCT (blue) and MWT (green). The third scale represents the difference between the average DTW distance between the four conditions represented in the graph (inter) and a reference ground value, being the average DTW distance among the replicates of each curve in that graph (intra).

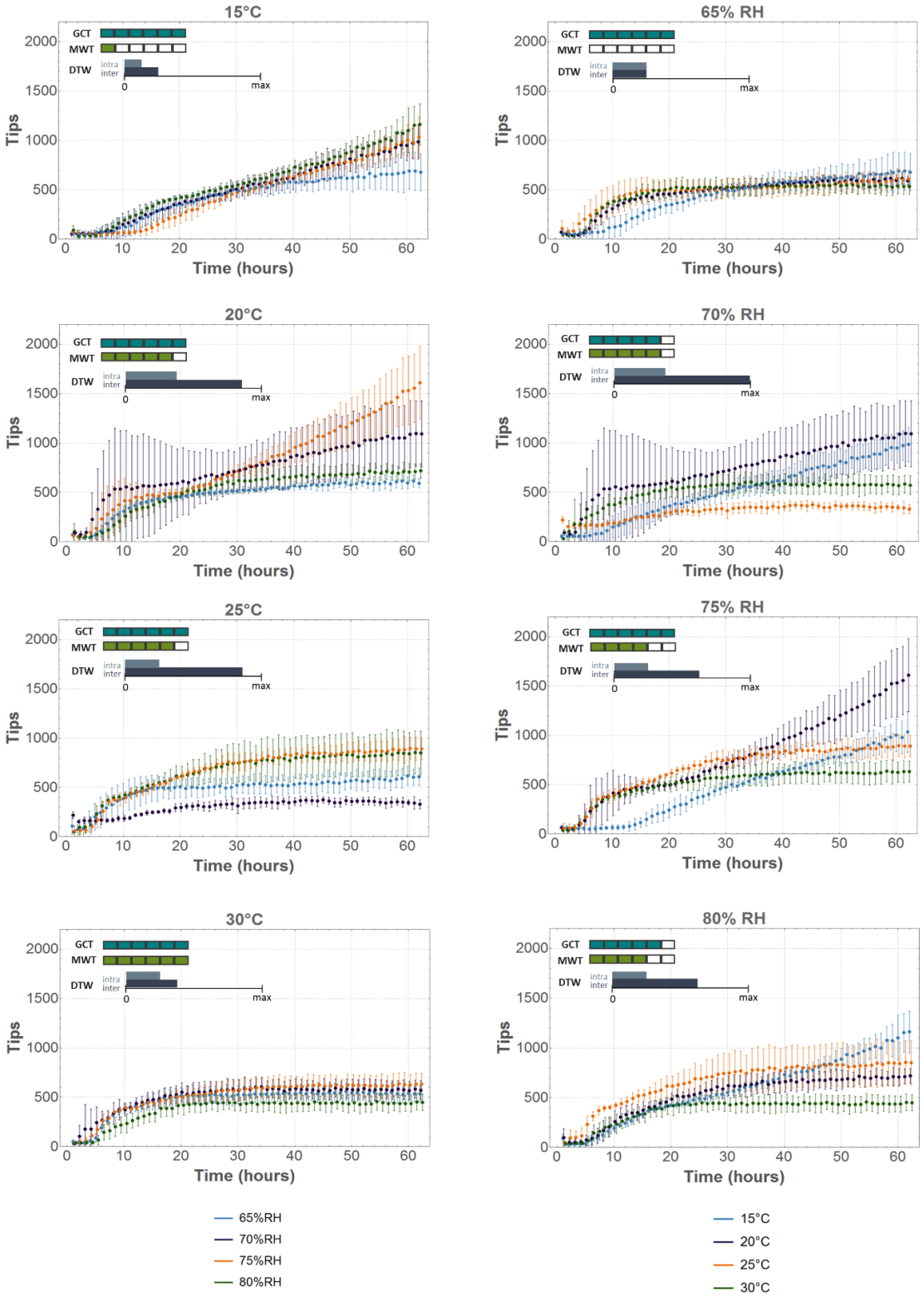

Figure 8-4 Evolution of the number of tips over time for *C. puteana*. On the left, the graphs are grouped by temperature, with one curve per RH at that particular temperature. On the right, the graphs are grouped by RH, with every curve representing one temperature at a given RH. The dots represent the mean values over four replicates, with the bars indicating the standard deviation. For each graph, six pairwise GCT and MWT were performed on the means of each of the four conditions represented in that graph. The two colour scales indicate for how many of those pairwise comparisons a difference was found according to GCT (blue) and MWT (green). The third scale represents the difference between the average DTW distance between the four conditions represented in the graph (inter) and a reference ground value, being the average DTW distance among the replicates of each curve in that graph (intra).

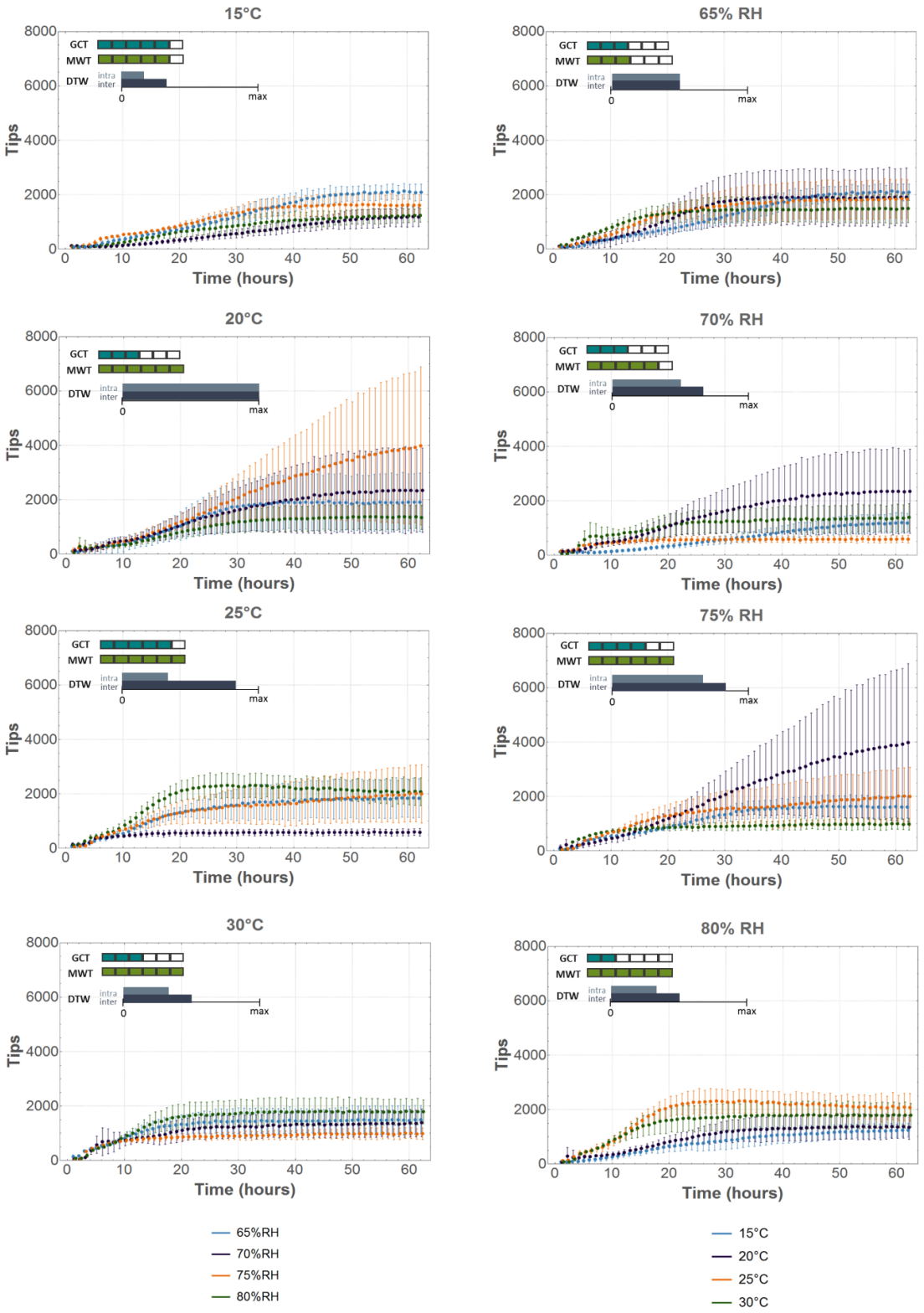

Figure 8-5 Evolution of the number of tips over time for *R. solani*. On the left, the graphs are grouped by temperature, with one curve per RH at that particular temperature. On the right, the graphs are grouped by RH, with every curve representing one temperature at a given RH. The dots represent the mean values over four replicates, with the bars indicating the standard deviation. For each graph, six pairwise GCT and MWT were performed on the means of each of the four conditions represented in that graph. The two colour scales indicate for how many of those pairwise comparisons a difference was found according to GCT (blue) and MWT (green). The third scale represents the difference between the average DTW distance between the four conditions represented in the graph (inter) and a reference ground value, being the average DTW distance among the replicates of each curve in that graph (intra).

8.2 Chapter 4

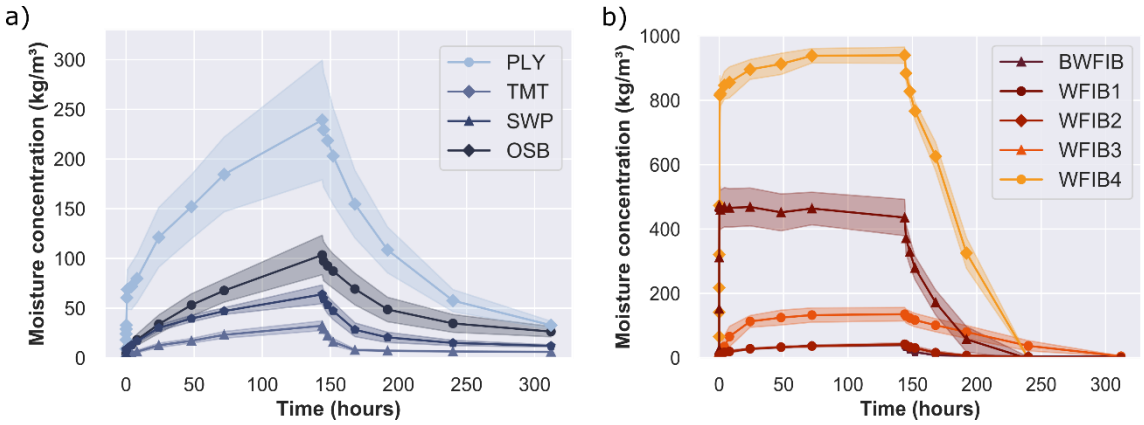

Figure 8-6 Mean moisture concentration (kg/cm^3) with standard deviation over 144 hours of absorption and 168 hours of desorption in a floating test. a) Wood-based panels: radiata pine plywood (PLY), thermally modified spruce (TMT), three-layer spruce binder (SWP) and oriented strand board (OSB). b) Insulation materials: porous bituminised wood fibre board (BWFIB) and wood fibre insulation type 1-4 (WFIB1-4).

8.3 Chapter 5

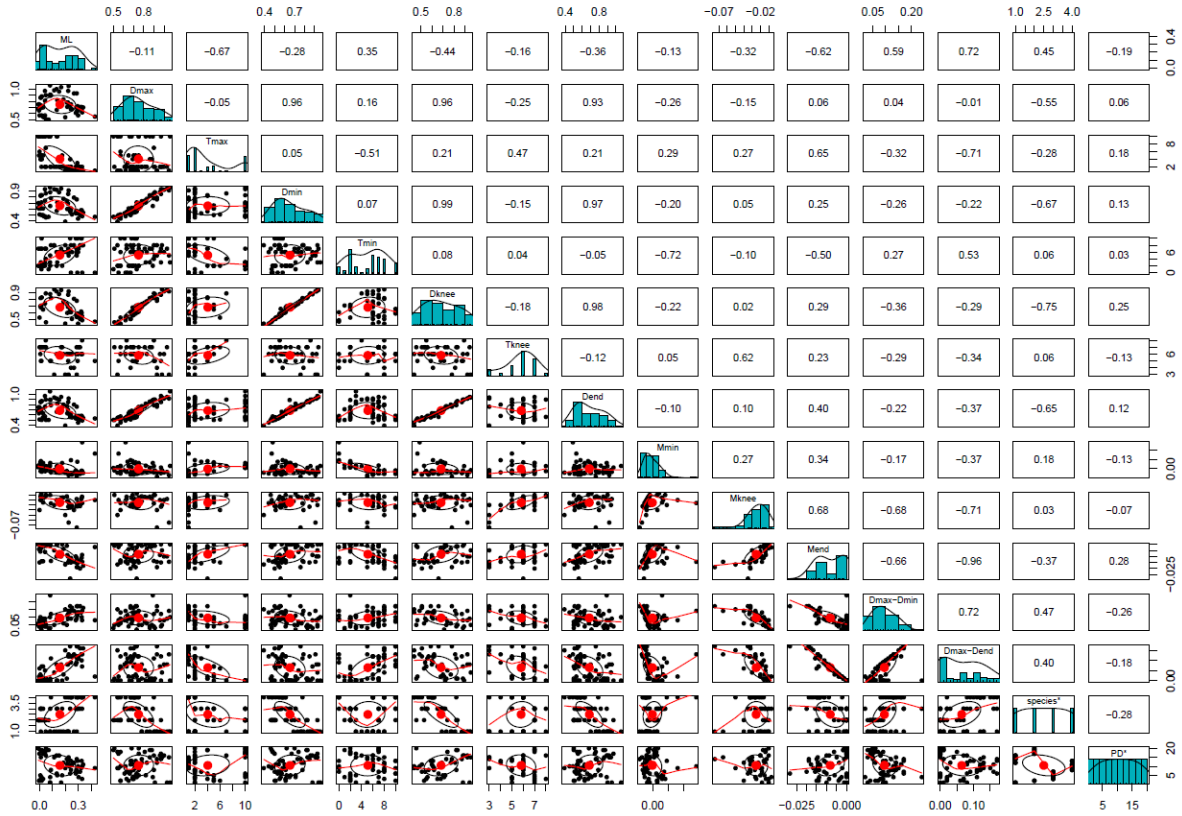

Figure 8-7 Pearson correlation between mass loss (ML) and explanatory variables (top row), and among explanatory variables for all mini-block specimens. For those explanatory variables which had a Pearson correlation of 0.5 or higher, one variable was chosen. The variable histograms and the bivariate scatter plots are given as well.

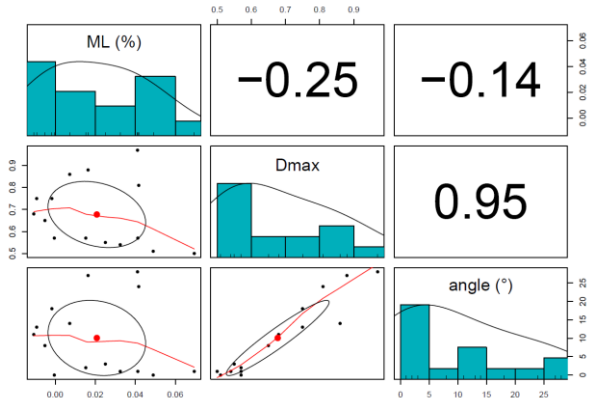

Figure 8-8 Pearson correlation between mass loss (ML), maximal density relative to oven dry density (Dmax) and vessel direction angle (°) for okoumé.

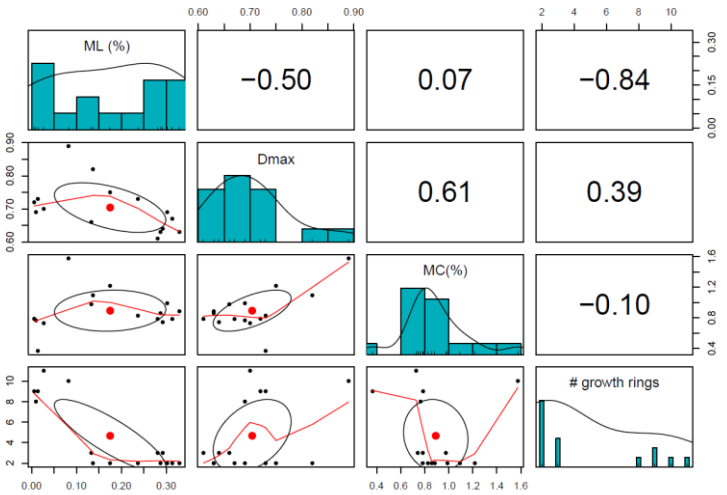

Figure 8-9 Pearson correlation between mass loss (ML), maximal density relative to oven dry density (Dmax), moisture content (%) and number of growth rings for Scots pine.

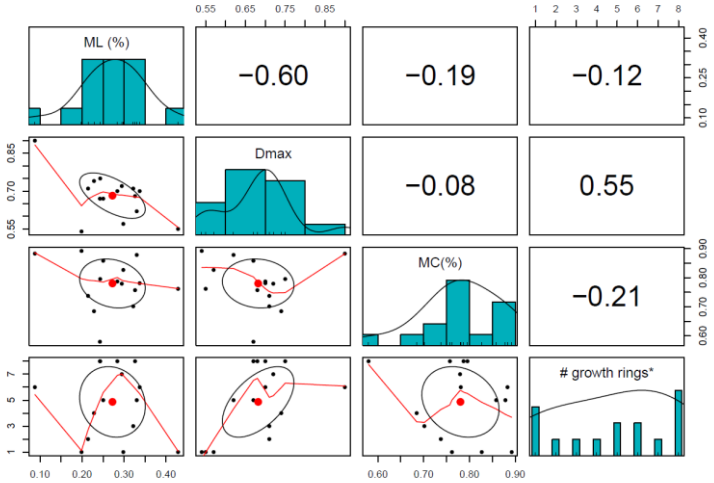

Figure 8-10 Pearson correlation between mass loss (ML), maximal density relative to oven dry density (Dmax), moisture content (%) and number of growth rings for spruce.

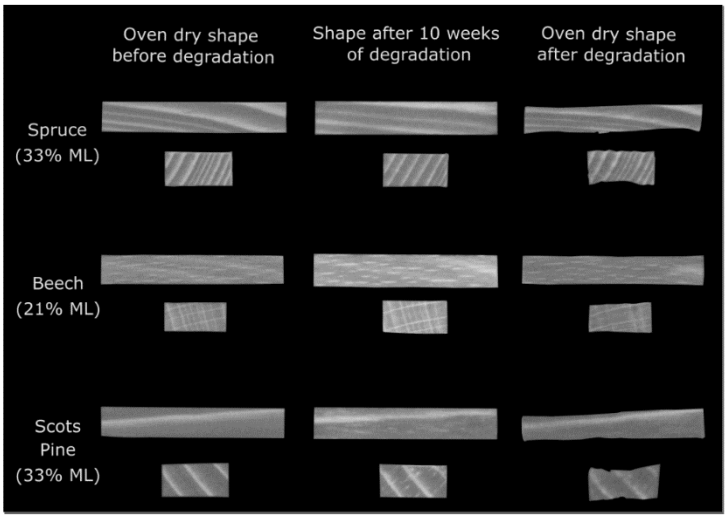

Figure 8-11 Mini-blocks with severe decay (>20% ML) showed clear signs of shrinkage after oven drying.

deligne.liselotte@gmail.be

linkedin.com/in/liselottedl/

researchgate.net/profile/Liselotte_De_Ligne

LISELOTTE DE LIGNE

Wood and bio-based materials researcher specialized in material characterization and fungal decay.

PROFILE

Bioscience engineer and academic researcher, specialized in material characterization and fungal decay of wood and bio-based building materials. After completing my PhD, I want to continue my academic career by further expanding my expertise in material characterization, wood-water relations and state-of-the-art methods for assessment of material moisture dynamics, structure and chemistry in relation to decay. I aim to have a positive impact and help to pave the way towards a fully sustainable building industry.

EDUCATION & RESEARCH EXPERIENCE

2017-current
Dept. of Environment (Ugent-Woodlab) & Dept. of Data Analysis and Mathematical Modelling (Kermit) at Ghent University, Belgium

FWO Fellowship Strategic Basic Research

PhD IN BIOSCIENCE ENGINEERING
PhD thesis: *Fungal susceptibility of bio-based building materials.* Unravelling the influence of a material's chemistry, structure and moisture dynamics on its susceptibility to fungal degradation.
Supervisors: Prof. Joris Van Acker, Prof. Jan Van den Bulcke, Prof. Jan M. Baetens, Prof. Bernard De Baets
Jury members: Prof. Veerle Cnudde, dr. Magdalena Kutnik, Prof. Marijke Steeman, Prof. Lisbeth Garbrecht Thygesen, Prof. Monica Höfte
Key words: bio-based building materials, wood, fungal degradation, moisture dynamics, material structure, material chemistry.
Technical skills acquired: laboratory fungal testing of wood-rot and decay, X-ray micro CT, low-field NMR, FTIR, MRI, DVS, image analysis and programming in Python.
Supervision experience: 7 master theses, 1 bachelor thesis and 4 interns, among which 3 bachelor students via the international DAAD/RISE program.
Teaching experience: Practical exercises differential equations during Biowiskundedagen.
Doctoral training: effective leadership, academic writing skills, writing for non-peers and press.
Other research output:
Semi-automated method for assessing wood degradation with X-ray CT in batch, including an automated set-up, batch reconstruction of the X-ray CT images and semi-automated extraction of the wood volumes in ImageJ.

Jul. – Dec. 2016
Dept. of Environment & Dept. of Data Analysis and Mathematical Modelling at Ghent University, Belgium

RESEARCH ASSISTANT
Designing and performing experiments to assess the influence of environmental conditions on fungal growth for the finalization of an FWO project.
Technical skills acquired: laboratory fungal testing, high-resolution imaging of fungal mycelium and automated image analysis.

2014-2016
Ghent University, Belgium
Erasmus: SupAgro, Montpellier, France
Internship: Oxfam solidarity, Laos (3 months).

MASTER OF SCIENCE IN BIOSCIENCE ENGINEERING
– AGRICULTURAL SCIENCES –
Master thesis: *Participatory value chain analysis of organic tea in Laos.*
Supervisors: Prof. dr. Patrick Van Damme, dr. Wouter Vanhove, dr. Kaat Verzelen.

2011-2014

BACHELOR OF SCIENCE IN BIOSCIENCE ENGINEERING

ADDITIONAL TRAINING & RESEARCH STAYS ABROAD

2019 Research stay (two weeks) at the University of Copenhagen to work with LFNMR and FTIR in collaboration with prof. Emil Thybring and prof. Lisbeth Garbrecht Thygesen.

2018 Research visit (four days) at FCBA Bordeaux to discuss fungal testing and lab protocols.

2017 Workshop "*Chemical imaging of cell walls*" (1 week) organized by the University of Copenhagen.
Workshop COST Action FP1407 (1 week): "*Advanced understanding of the structural influences of bio-based lignocellulosic materials*" in Hamburg.
Workshop COST Action FP1303 (4 days): A technical workshop on "*Design, Application and Aesthetics of biobased building materials*" in Sofia.

PEER-REVIEWED PUBLICATIONS

2020 De Ligne, L., Van den Bulcke, J., Baetens, J.M., De Baets, B., Wang, G., Imke De Windt, I., Beeckman, H., Van Acker, J. (2020) Unraveling the natural durability of wood: revealing the impact of decay-influencing characteristics other than fungicidal components. *Holzforschung*. IF: 1.826

Deklerck, V., De Ligne, L., Espinoza, E., Beeckman, H., Van den Bulcke, J., Van Acker, J. (2020) Assessing the natural durability of xylarium specimens: mini-block testing and chemical fingerprinting for small-sized samples. *Wood Science and Technology* 54:981–1000. IF: 1.912

Vander Mijnsbrugge, K., De Clerck, L., Van der Schueren, N., Moreels, S., Lauwers, A., Steppe, K., De Ligne, L., Campioli, M., Van den Bulcke, J. Counter-Intuitive response to water limitation in a Southern European provenance of *Frangula alnus* Mill. in a common garden experiment (2020). *Forests*, 11, 1186. IF: 2.453

2019 De Ligne, L., Vidal Diez de Ulzurrun, G., Baetens, J.M., Van den Bulcke, J., Van Acker, J., De Baets, B. (2019). Analysis of spatio-temporal fungal growth dynamics under different environmental conditions. *IMA Fungus* 1:7. IF: 4.333

CONFERENCE PRESENTATIONS

2020 De Ligne, L., Van den Bulcke, J., Baetens, J.M., De Baets, B., Van Acker, J. (2020) Bio-based building materials – How to unravel the role of material characteristics on fungal susceptibility? *Proceedings DBMC15* – 15th International Conference on Durability of Building Materials and Components (webinar), 8pp.

De Ligne, L., Caes, J., Omar, S., Van den Bulcke, J. Baetens, J.M., De Baets, B., Van Acker, J. (2020) Performance of bio-based building materials – durability and moisture dynamics. *Proceedings IRG Annual Meeting 2020* (webinar), 16 pp.

2019 De Ligne, L., Van den Bulcke, J., De Muynck, A., Baetens, J.M., De Baets, B., Van Hoorebeke, L., Van Acker, J. (2019). Exploring the use of X-ray micro CT as a tool for the monitoring of moisture production and mass loss during lab-based fungal degradation testing. *Proceedings IRG Annual Meeting 2019* (Quebec City, Canada). IRG/WP 19-20654, 10 pp, Presented in the Scientific Main Session.

Deklerck, V., De Ligne, L., Van den Bulcke, J., Espinoza, E., Beeckman, H., Van Acker, J. (2019). Determining the natural durability on xylarium samples: mini-block test, wood powder and chemical profiling. *Proceedings IRG Annual Meeting 2019* (Quebec City, Canada). IRG/WP 19-10944, 12 pp.

Vanpachtenbeke, M., De Ligne, L., Van den Bulcke, J., Langmans, J., Van Acker, J., Roels, S. (2019) Fungal growth on timber frame houses. *Proceedings AIVC 2019*.

2018 De Ligne, L., Vidal Diez de Ulzurrun, G., Van den Bulcke, J., Baetens, J.M., De Baets, B., Van Acker, J. (2018). Impact of temperature and relative humidity on spatio-temporal fungal growth dynamics of Basidiomycetes. *Proceedings IRG Annual Meeting 2018* (Johannesburg, South-Africa). IRG/WP 18-10905, 15 pp.

2017 De Ligne, L., Vidal Diez de Ulzurrun, G., Baetens, J.M., Van den Bulcke, J., Van Acker, J., De Baets, B. (2017). Assessment of the combined effect of temperature and relative humidity on fungal growth. Presented at the 22nd National symposium for Applied Biological Sciences (Leuven, Belgium).

De Ligne, L., Van den Bulcke, J., Baetens, J.M., De Baets, B., Van Acker, J. (2017). Assessing the nutrient value of bio-based materials in relation to early fungal growth. Presented at the 48th Conference of the International Research Group on Wood Protection (Ghent, Belgium).

CONFERENCE ORGANISATION

Member of organizing committee	24th National Symposium of Applied Biological Sciences (NSABS 2019, Ghent, Belgium). 48th Annual Conference of the International Research group on Wood Protection (IRG48 2017, Ghent, Belgium).
Convenor of working party	Session WP 5.1. Environment & WP 5.2. Sustainability at the 50th Annual Conference of the International Research group on Wood Protection (IRG50 2019, Quebec City, Canada).
Editor (book of abstracts)	Communications in Agricultural and Applied Biological Sciences, Vol 84(1), 1-100 (2019).

MEMBERSHIPS AND INVOLVEMENT

Board member and Support Treasurer of Belgian Women in Science (BeWiSe).
Representative of PhD students and Post-docs at department meetings of the Dept. of Environment (Ghent University).
Actively involved in the organisation of the monthly Science cafés of the Dept. of Environment (Ghent University).
Partner of End-of-Waste platform - a new business platform for valorization of organic by-products from the agro-bio-food sector.
Actively involved in Think Tank Transition UGent - an open innovation network in which knowledge workers, policy makers, dreamers, doers, translators to practice and builders come together to formulate ideas for a sustainable university.
Memberships: International Research Group on Wood Protection (IRG), Society of Wood Science and Technology (SWST).

AWARDS & RECOGNITION

Gareth Williams award
Best oral presentation IRG 2018
Ron Cockcroft award
Travel award IRG 2018
Richard J. Ziobro award
Best poster award IRG 2017
PhD Fellowship Strategic Basic Research
FWO Flanders 2017

LANGUAGES

Dutch (mother tongue)
English
French
Spanish

MISCELLANEOUS

Hiking and travelling.
Co-organising events as part of *Climate Express*, a Belgian climate movement.
Evening courses on fiction writing.
Evening courses on construction with wood and bio-based building materials.

Liselotte De Ligne


moss